

ESSAYS ON EXPLOSIVE TIME SERIES

Nhat Minh Vuong Chu

*A thesis submitted for the degree of
Doctor of Philosophy in Finance*

Essex Business School
University of Essex

July 2023

Abstract

In the first chapter of this thesis, we introduce and explore three prominent research areas related to explosive bubbles. We also establish the link between each chapter in the thesis and consequently, these strands of research.

In Chapter 2, we introduce a novel test that builds upon the existing WLS-based test proposed by [Harvey et al. \(2019\)](#) to identify explosive bubbles in financial data with the presence of time-varying volatility. Our test outperforms both the conventional supremum bubble test of [Phillips and Yu \(2011\)](#) and [Harvey et al. \(2019\)](#)'s test. Our approach involves replacing the kernel-based volatility function estimator used by [Harvey et al. \(2019\)](#) with our own volatility estimator that is based on an iterative cumulative sum of squares algorithm. Similar to [Harvey et al. \(2019\)](#)'s test, we use the estimated volatility to calculate the WLS-based statistic and employ a wild-bootstrap procedure to control the size of the test and make it robust under various time-varying volatility patterns. We suggest using a union of rejections procedure when the volatility pattern is a late upward shift to capture the better power available from the two constituent tests for a given alternative.

Chapter 3 introduces a backward supremum KPSS-based test, which extends the KPSS-based test of [Evrpidou et al. \(2022\)](#) to detect short-lived co-explosive behaviour between a pair of asset prices at the end of the sample period. Finite sample simulations show that our test has well-controlled size under most volatility specifications and has higher power than [Evrpidou et al. \(2022\)](#)'s test in detecting periods without co-bubbles. As with [Evrpidou et al. \(2022\)](#)'s test, our proposed test still employs a wild bootstrap algorithm to deliver a robust test for heteroskedasticity and uses a long-run variance estimate to control the size of the test when serial

correlation exists in innovations. By applying both single and double backward supremum tests to the same dataset as [Evrpidou et al. \(2022\)](#), we show new findings of co-explosive bubbles in pairs of non-ferrous and precious metals in spot and futures markets.

In Chapter 4, we compare the behaviour of common return predictability tests (i.e., IVX, Bonferroni-t, and Bonferroni-Q tests) during bubble periods. Overall, Monte Carlo simulations show that all three tests over-reject the null hypothesis of no predictability. In that regard, the Bonferroni-t test is the least oversized, while the IVX test is badly oversized across different bubble specifications. To conduct the simulations, we introduce a new data generating process that does not require a predetermined variable in the predictive model. Finally, by comparing results obtained from subsamples with and without bubbles, our empirical application shows the over-rejections of the tests to the null using the extended dataset from January 1927 to December 2021 containing 14 financial and macroeconomic predictors of [Welch and Goyal \(2008\)](#).

The last chapter of this thesis provides concluding remarks on the significant findings and limitations, as well as presenting suggestions for future research directions.

Acknowledgements

Throughout my Ph.D. pursuits, I have been the recipient of abundant and invaluable support from many people. Their involvement was crucial to the completion of this thesis. I would like to express my most sincere gratitude to my supervisors, *Prof. Neil Kellard* and *Dr. Sam Astill*, for their unwavering guidance, mentorship, inspiration, and care throughout my studies. It is an immense privilege to have had them as my advisers. Additionally, I extend my gratitude to the University of Essex for awarding me the studentship that facilitated the completion of my Ph.D. thesis.

Additionally, I am grateful to *Prof. Steve Leybourne*, the external examiner, and to *Prof. Simon Price*, the internal examiner, for their time, effort, and expertise in reviewing my thesis and providing valuable feedback during my Ph.D. viva. Special thanks go to *Prof. Jerry Coakley* for his constant encouragement as the chair of the supervisory boards.

Last but not least, I am deeply appreciative of the support and encouragement extended to me by my family. Lastly, I express my profound gratitude to my wife, *Trang Tran*, for her boundless love and unwavering support throughout my academic journey.

Once again, thank you all for being a part of my journey.

Declaration

I affirm that the content of this Ph.D. thesis is entirely my own and has not been used in any previous application for a degree, diploma, or other academic recognition at any other institution. All of the work contained within this thesis, unless noted otherwise through references or acknowledgements, is a result of my own efforts.

Signature: Vuong Chu

Contents

Abstract	I
Acknowledgements	III
Declaration	IV
List of Symbols and Abbreviations	XVI
1 Introduction	1
2 Testing Explosive Bubble With Changes in Innovation Variance	7
2.1 Introduction	8
2.2 Literature Review	12
2.3 Heteroskedastic Bubble Model and Assumptions	18
2.4 Explosive Behaviour Tests	20
2.4.1 An Ordinary Least Squares-based Test	20
2.4.2 A Weighted Least Squares-based Test	22
2.5 Asymptotic Behaviour Of Tests	23
2.5.1 Asymptotic Properties of PWY Test	23
2.5.2 Asymptotic Properties of BZ Test	24
2.6 Feasible Estimator Based Tests	25
2.6.1 Kernel Estimator Based Test	25
2.6.2 ICSS based Test	28
2.7 Wild-Bootstrap Test	33
2.7.1 Wild-Bootstrapped Procedure of HLST	33

2.7.2	Asymptotic Properties of Wild Bootstrap Tests	36
2.7.3	A Union of Rejections Testing Strategy	38
2.8	Finite Sample Properties	40
2.9	Empirical Illustrations	47
2.9.1	Data	47
2.9.2	Testing for Explosive Bubbles	48
2.10	Conclusion	50
3	Testing Co-explosive Behaviour Using Backward Supremum Approach	52
3.1	Introduction and Literature Review	53
3.2	The Bubble Model	59
3.3	The Co-explosive Model	59
3.4	Testing For Co-explosiveness	62
3.4.1	Asymptotic behaviour	64
3.4.2	A wild bootstrap procedure	65
3.4.3	Asymptotic behaviour of wild bootstrap test statistics	66
3.4.4	Accounting for serial correlation	68
3.5	Finite Sample Properties	70
3.5.1	Behaviour under H_0	72
3.5.2	Behaviour under H_1	73
3.5.3	Behaviour of the tests with serially correlated innovations	74
3.5.4	Timing explosive regime migration	78
3.6	Empirical Illustrations	80
3.6.1	Data	80
3.6.2	Testing for explosive autoregression in the individual series	82
3.6.3	Results from tests for co-bubble behaviour	84
3.7	Conclusion	87
4	On the Behavior of Tests for Stock Return Predictability during Bubble Regimes	90

4.1	Introduction	91
4.2	Predictive Regression and Assumptions	97
4.3	Return Predictability Tests	100
4.3.1	IVX Test	100
4.3.2	Bonferroni Based Tests	101
4.3.2.1	The Bonferroni t test	103
4.3.2.2	The Bonferroni Q test	105
4.4	Asymptotic Behaviour Of Tests	107
4.4.1	IVX test	107
4.4.2	Bonferroni Based Tests	108
4.5	Finite Sample Size	109
4.6	Empirical Illustrations	115
4.6.1	Data	115
4.6.2	Evaluating return predictability	118
4.7	Conclusion	122
5	Concluding Remarks	124
5.1	Conclusions	124
5.2	Limitations and Future Research	126
	Appendices	A-1
	Appendix A: Tables and Figures of Chapter 2	A-1
	Appendix B: Tables and Figures of Chapter 3	B-1
	Appendix C: Tables and Figures of Chapter 4	C-1

List of Figures

A-1	Illustration of iterative algorithm in ICSS by Inclán and Tiao (1994)	A-1
A-2	The sample sequences of the sup DF test	A-2
A-3	Finite sample local power curves with $r^* = 0.6, T = 100$	A-4
A-4	Finite sample local power curves with $r^* = 0.8, T = 100$	A-5
A-5	Finite sample local power curves with $r^* = 0.6, T = 200$	A-7
A-6	Finite sample local power curves with $r^* = 0.8, T = 200$	A-8
A-7	Finite sample local power curves with $r^* = 0.6, T = 400$	A-10
A-8	Finite sample local power curves with $r^* = 0.8, T = 400$	A-11
A-9	Finite sample local power curves with $r^* = 0.8$ - Late upward shift in volatility	A-12
A-10	The plots of logarithmic real S&P 500 index from 01/1980 to 03/2000	A-13
A-11	The plots of logarithmic real FTSE 100 index from 01/1985 to 12/1999	A-14
B-1	Finite sample local power curves - Homoskedasticity variance, $T = 200$	B-3
B-2	Finite sample power curves - heteroskedasticity, $T = 200$	B-4
B-3	Finite sample power curves - Homoskedasticity variance, $T = 400$	B-5
B-4	Finite sample power curves - heteroskedasticity, $T = 400$	B-6
B-5	Precious metal spot prices and their squared log returns.	B-14
B-6	Non-precious metal spot prices and their squared log returns.	B-15
B-7	Non-precious metal spot prices and their squared log returns. (Con- tinued)	B-16
B-8	Precious metal futures prices and their squared log returns.	B-17
B-9	Non-precious metal futures prices and their squared log returns.	B-18

B-10 Non-precious metal futures prices and their squared log returns. (Continued)	B-19
B-11 Co-explosive bubble pairs of spot metal prices and full sample estimated residuals	B-23
B-12 Co-explosive bubble pairs of spot metal prices and full sample estimated residuals (Continued)	B-24
B-13 Co-explosive bubble pairs of futures metal prices and full sample estimated residuals	B-25
B-14 Co-explosive bubble pairs of futures metal prices and full sample estimated residuals (Continued)	B-26
C-1 Date-stamping the logarithm of monthly S&P 500 price index from 01/1920 to 12/2021	C-40

List of Tables

A-1	A few results to show the size distortions in sup DF test	A-2
A-2	A few results to show the size distortions in sup BZ test without wild bootstrap	A-3
A-3	Finite-sample sizes under the null hypothesis with $T = 100$	A-3
A-4	Finite-sample sizes under the null hypothesis with $T = 200$	A-6
A-5	Finite-sample sizes with $T = 400$	A-9
A-6	Finite-sample sizes when a late upward shift is in volatility and $r^* = 0.8$	A-12
A-7	The descriptive statistics of S&P 500 and FTSE 100 in different time-frequencies	A-12
A-8	The p-values of sup DF , sup BZ_K , sup BZ_I , \mathcal{U} , \mathcal{U}_K , and \mathcal{U}_I	A-15
B-1	Finite-sample sizes for the co-bubble tests, $T = 200$	B-1
B-2	Finite-sample sizes of the co-bubble tests, $T = 400$	B-2
B-3	Finite-sample powers of the co-bubble tests, $T = 200$	B-3
B-4	Finite-sample powers of the co-bubble tests, $T = 400$	B-5
B-5	Finite-sample sizes of the co-bubble tests without using long-run variance under serial correlation conditions	B-7
B-6	Finite-sample sizes of the co-bubble tests using long-run variance (Bartlett Kernel, $T=200$)	B-8
B-7	Finite-sample sizes of the co-bubble tests using long-run variance (Bartlett Kernel, $T=400$)	B-9
B-8	Finite-sample sizes of the co-bubble tests using long-run variance (Quadratic Spectral Kernel, $T=200$)	B-10

B-9	Finite-sample sizes of the co-bubble tests using long-run variance (Quadratic Spectral Kernel, T=400)	B-11
B-10	Finite-sample powers of the co-bubble tests using long-run variance .	B-12
B-11	Finite-sample rejection rates of the co-bubble tests under different lead/lag values	B-13
B-12	The descriptive statistics of metal prices	B-20
B-13	PSY date-stamping of explosive periods for metal prices	B-20
B-14	Rejection rates of co-bubble tests to metal prices	B-21
B-15	Rejection rates of co-bubble tests to metal prices (Continued)	B-22
C-1	Finite sample size at 5% significance level of one-sided predictability tests: u_t, v_t is N.i.i.d, no bubble in return	C-1
C-2	Finite sample size at 5% significance level of one-sided predictability tests: u_t, v_t is N.i.i.d, bubble in return with $\tau_1 = 0.9, \tau_2 = 1, c_{bub} = 0.01$.	C-2
C-3	Finite sample size at 5% significance level of one-sided predictability tests: u_t, v_t is N.i.i.d, bubble in return with $\tau_1 = 0.9, \tau_2 = 1, c_{bub} = 0.05$.	C-3
C-4	Finite sample size at 5% significance level of one-sided predictability tests: u_t, v_t is N.i.i.d, bubble in return with $\tau_1 = 0.9, \tau_2 = 1, c_{bub} = 0.1$.	C-4
C-5	Finite sample size at 5% significance level of one-sided predictability tests: u_t, v_t is N.i.i.d, bubble in return with $\tau_1 = 0.7, \tau_2 = 1, c_{bub} = 0.01$.	C-5
C-6	Finite sample size at 5% significance level of one-sided predictability tests: u_t, v_t is N.i.i.d, bubble in return with $\tau_1 = 0.7, \tau_2 = 1, c_{bub} = 0.05$.	C-6
C-7	Finite sample size at 5% significance level of one-sided predictability tests: u_t, v_t is N.i.i.d, bubble in return with $\tau_1 = 0.7, \tau_2 = 1, c_{bub} = 0.1$.	C-7
C-8	Finite sample size at 5% significance level of one-sided predictability tests: u_t, v_t is i.i.d from t-distribution with the degree of freedom = 5, no bubble in return	C-8
C-9	Finite sample size at 5% significance level of one-sided predictability tests: u_t, v_t is i.i.d from t-distribution with the degree of freedom = 5, bubble in return with $\tau_1 = 0.9, \tau_2 = 1, c_{bub} = 0.01$	C-9

C-10	Finite sample size at 5% significance level of one-sided predictability tests: u_t, v_t is i.i.d from t-distribution with the degree of freedom = 5, bubble in return with $\tau_1 = 0.9, \tau_2 = 1, c_{bub} = 0.05$	C-10
C-11	Finite sample size at 5% significance level of one-sided predictability tests: u_t, v_t is i.i.d from t-distribution with the degree of freedom = 5, bubble in return with $\tau_1 = 0.9, \tau_2 = 1, c_{bub} = 0.1$	C-11
C-12	Finite sample size at 5% significance level of one-sided predictability tests: u_t, v_t is i.i.d from t-distribution with the degree of freedom = 5, bubble in return with $\tau_1 = 0.7, \tau_2 = 1, c_{bub} = 0.01$	C-12
C-13	Finite sample size at 5% significance level of one-sided predictability tests: u_t, v_t is i.i.d from t-distribution with the degree of freedom = 5, bubble in return with $\tau_1 = 0.7, \tau_2 = 1, c_{bub} = 0.05$	C-13
C-14	Finite sample size at 5% significance level of one-sided predictability tests: u_t, v_t is i.i.d from t-distribution with the degree of freedom = 5, bubble in return with $\tau_1 = 0.7, \tau_2 = 1, c_{bub} = 0.1$	C-14
C-15	Finite sample size at 5% significance level of one-sided predictability tests: u_t, v_t is N.i.i.d, collapsing bubble in return with $\tau_1 = 0.6, \tau_2 =$ $0.9, c_{bub} = 0.01$	C-15
C-16	Finite sample size at 5% significance level of one-sided predictability tests: u_t, v_t is N.i.i.d, collapsing bubble in return with $\tau_1 = 0.6, \tau_2 =$ $0.9, c_{bub} = 0.05$	C-16
C-17	Finite sample size at 5% significance level of one-sided predictability tests: u_t, v_t is N.i.i.d, collapsing bubble in return with $\tau_1 = 0.6, \tau_2 =$ $0.9, c_{bub} = 0.1$	C-17
C-18	Finite sample size at 5% significance level of one-sided predictability tests: u_t, v_t is N.i.i.d, collapsing bubble in return with $\tau_1 = 0.6, \tau_2 =$ $0.9, c_{bub} = 0.2$	C-18

C-19	Finite sample size at 5% significance level of one-sided predictability tests: u_t, v_t is N.i.i.d, collapsing bubble in return with $\tau_1 = 0.4, \tau_2 = 0.7, c_{bub} = 0.01$	C-19
C-20	Finite sample size at 5% significance level of one-sided predictability tests: u_t, v_t is N.i.i.d, collapsing bubble in return with $\tau_1 = 0.4, \tau_2 = 0.7, c_{bub} = 0.05$	C-20
C-21	Finite sample size at 5% significance level of one-sided predictability tests: u_t, v_t is N.i.i.d, collapsing bubble in return with $\tau_1 = 0.4, \tau_2 = 0.7, c_{bub} = 0.1$	C-21
C-22	Finite sample size at 5% significance level of one-sided predictability tests: u_t, v_t is N.i.i.d, collapsing bubble in return with $\tau_1 = 0.4, \tau_2 = 0.7, c_{bub} = 0.2$	C-22
C-23	Finite sample size at 5% significance level of one-sided predictability tests: u_t, v_t is N.i.i.d, collapsing bubble in return with $\tau_1 = 0.1, \tau_2 = 0.4, c_{bub} = 0.01$	C-23
C-24	Finite sample size at 5% significance level of one-sided predictability tests: u_t, v_t is N.i.i.d, collapsing bubble in return with $\tau_1 = 0.1, \tau_2 = 0.4, c_{bub} = 0.05$	C-24
C-25	Finite sample size at 5% significance level of one-sided predictability tests: u_t, v_t is N.i.i.d, collapsing bubble in return with $\tau_1 = 0.1, \tau_2 = 0.4, c_{bub} = 0.1$	C-25
C-26	Finite sample size at 5% significance level of one-sided predictability tests: u_t, v_t is N.i.i.d, collapsing bubble in return with $\tau_1 = 0.1, \tau_2 = 0.4, c_{bub} = 0.2$	C-26
C-27	Finite sample size at 5% significance level of one-sided predictability tests: u_t, v_t is i.i.d from t-distribution with the degree of freedom = 5, collapsing bubble in return with $\tau_1 = 0.6, \tau_2 = 0.9, c_{bub} = 0.01$	C-27

- C-28 Finite sample size at 5% significance level of one-sided predictability
tests: u_t, v_t is i.i.d from t-distribution with the degree of freedom = 5,
collapsing bubble in return with $\tau_1 = 0.6, \tau_2 = 0.9, c_{bub} = 0.05$ C-28
- C-29 Finite sample size at 5% significance level of one-sided predictability
tests: u_t, v_t is i.i.d from t-distribution with the degree of freedom = 5,
collapsing bubble in return with $\tau_1 = 0.6, \tau_2 = 0.9, c_{bub} = 0.1$ C-29
- C-30 Finite sample size at 5% significance level of one-sided predictability
tests: u_t, v_t is i.i.d from t-distribution with the degree of freedom = 5,
collapsing bubble in return with $\tau_1 = 0.6, \tau_2 = 0.9, c_{bub} = 0.2$ C-30
- C-31 Finite sample size at 5% significance level of one-sided predictability
tests: u_t, v_t is i.i.d from t-distribution with the degree of freedom = 5,
collapsing bubble in return with $\tau_1 = 0.4, \tau_2 = 0.7, c_{bub} = 0.01$ C-31
- C-32 Finite sample size at 5% significance level of one-sided predictability
tests: u_t, v_t is i.i.d from t-distribution with the degree of freedom = 5,
collapsing bubble in return with $\tau_1 = 0.4, \tau_2 = 0.7, c_{bub} = 0.05$ C-32
- C-33 Finite sample size at 5% significance level of one-sided predictability
tests: u_t, v_t is i.i.d from t-distribution with the degree of freedom = 5,
collapsing bubble in return with $\tau_1 = 0.4, \tau_2 = 0.7, c_{bub} = 0.1$ C-33
- C-34 Finite sample size at 5% significance level of one-sided predictability
tests: u_t, v_t is i.i.d from t-distribution with the degree of freedom = 5,
collapsing bubble in return with $\tau_1 = 0.4, \tau_2 = 0.7, c_{bub} = 0.2$ C-34
- C-35 Finite sample size at 5% significance level of one-sided predictability
tests: u_t, v_t is i.i.d from t-distribution with the degree of freedom = 5,
collapsing bubble in return with $\tau_1 = 0.1, \tau_2 = 0.4, c_{bub} = 0.01$ C-35
- C-36 Finite sample size at 5% significance level of one-sided predictability
tests: u_t, v_t is i.i.d from t-distribution with the degree of freedom = 5,
collapsing bubble in return with $\tau_1 = 0.1, \tau_2 = 0.4, c_{bub} = 0.05$ C-36

C-37	Finite sample size at 5% significance level of one-sided predictability tests: u_t, v_t is i.i.d from t-distribution with the degree of freedom = 5, collapsing bubble in return with $\tau_1 = 0.1, \tau_2 = 0.4, c_{bub} = 0.1$	C-37
C-38	Finite sample size at 5% significance level of one-sided predictability tests: u_t, v_t is i.i.d from t-distribution with the degree of freedom = 5, collapsing bubble in return with $\tau_1 = 0.1, \tau_2 = 0.4, c_{bub} = 0.2$	C-38
C-39	Unit root tests for regressors	C-39
C-40	Empirical results for the Welch and Goyal (2008) predictive regressions	C-41
C-41	Empirical results for the Welch and Goyal (2008) predictive regressions (continued)	C-42

List of Symbols and Abbreviations

$o(1)$	tends to zero
$o_p(1)$	tends to zero in probability
$O_p(1)$	bounded in probability
$:=$	definitional equality
\in	in or (which) is an element of
\exists	there exists
\forall	for all
\subseteq	(which) is a subset of
$\lim_{n \rightarrow \infty} a_n$	limit as n tends to infinity of a_n
\rightarrow	convergence of a real-valued sequence
\xrightarrow{p}	convergence in probability
\xrightarrow{d}	convergence in distribution
\xrightarrow{w}	weak convergence
\xrightarrow{w}_p	weak convergence in probability
<i>IID</i>	independent and identically distributed
$N(0,1)$	standard normal distribution
$[x]$	integer part of x
\mathbb{E}	mathematical expectation

Σ	sigma (Greek letter used for a sum)
sup	supremum
$X \cup Y$	X union Y
\Rightarrow	(which) implies (that)
\Leftrightarrow	(which) is equivalent to or if and only if
\mathbb{R}	the set of all real numbers
$f : X \rightarrow \mathbb{R}$	function f from X to \mathbb{R}
max	maximum
$[a, b]$	closed interval
(a, b)	open interval
$\{a, b\}$	set containing the elements a and b
∞	infinity
\int	integral

Introduction

The study of speculative bubbles in asset prices has been of interest dating back to the historic tulip market bubble in 1637. These bubbles have been shown to precede economic instability or crises, as demonstrated by recent occurrences such as the Dot-Com bubble, the US housing bubble, and the Chinese stock price bubble (cf. [Allen and Gale, 2000](#)). Economists have examined the concept of price bubbles, both theoretically and empirically, to provide early warning and prevent the unexpected consequences of bubbles. This thesis focuses on several aspects of explosive bubbles that have been actively studied in the recent literature.

Recent advances in econometric techniques have enabled the real-time detection and dating of potential bubbles, attracting increased attention from central banks and regulators. Researchers have proposed a variety of tests and methods to enhance the size and power of bubble identification. The supremum recursive right-tailed unit root tests of [Phillips et al. \(2011\)](#) [[PWY](#) hereafter] is a notable example of these efforts aimed at determining the existence of a bubble. Although the test proposed by [PWY](#) is widely used in practice and empirical research and has also spurred the development of related test procedures, such as those of [Homm and Breitung \(2012\)](#) who consider a collection of supremum CUSUM-based test statistics, and [Phillips et al. \(2015\)](#) [[PSY](#) hereafter] who consider a double supremum of forward and backward recursive Dickey-Fuller statistics, it is relatively simple and not robust to the existence

of non-stationary volatility (e.g., volatility breaks). In that regard, [Harvey et al. \(2016\)](#) [[HLST](#) hereafter] propose a wild-bootstrap version of [PWY](#) test to prevent misleading inferences in the presence of time-varying volatility. Additionally, in the context of non-constant volatility, [Harvey et al. \(2019\)](#) proposed a WLS-based test to improve the power of the [PWY](#) test in detecting explosive autoregressive behaviour at the end of the sample. However, the [Harvey et al. \(2019\)](#) test has lower power in finite samples where the bubble grows quickly at the end of the sample. This is because the estimates of volatilities are either inflated or too dependent on the growth of bubbles.

Building on the principal ideas of [Harvey et al. \(2019\)](#), in the second chapter, we propose a test that uses an alternative approach for estimating volatilities in the WLS-based framework. Specifically, instead of using the smoothing kernel estimator, we employ the algorithm of [Inclán and Tiao \(1994\)](#) to identify volatility breaks using the squared price difference series. Subsequently, we estimate the volatility by using a simple volatility estimator in each regime. In the presence of heteroskedasticity, evidence from asset price simulations reveals the newly proposed test leads to improved size control compared to the test of [PWY](#), while offering significant power gains compared to the test of [Harvey et al. \(2019\)](#) when an end-of-sample explosive episode is present. The results are robust across different bubble and volatility specifications. In the case of a late upward volatility shift, the power of the WLS-based tests, which include the newly proposed test and the test of [Harvey et al. \(2019\)](#), are worse than the conventional [PWY](#) test, as noted by [Harvey et al. \(2019\)](#). To address this, we employ a union strategy to improve the power performance of the WLS-based tests while still maintaining size control. Empirical results show that the proposed test detects explosive behaviour in the S&P 500 stock price index from January 1980 to March 2000, while no evidence of explosive behaviour is found in the FTSE 100 index from December 1985 to December 1999. These results hold for all considered frequencies of data.

While there is much research using statistical methods to identify bubbles in

individual price series, there is substantially less work modelling the relationship between price series that present bubbles. As part of that smaller body of work, the paper of [Evrpidou et al. \(2022\)](#) focuses on identifying the explosive autoregressive characteristics of bubble series and develops a regression-based test to determine whether two series with explosive regimes are co-bubbling. In that context, the test aims to determine whether a linear combination of the two series is integrated of order zero, which is referred to as 'co-explosive behaviour'. The test employs a variant of the stationarity test of [Kwiatkowski et al. \(1992\)](#) [KPSS] to test the null of co-explosive behaviour, allowing for explosive behaviour to be present in subsample regimes. Strikingly, the test can detect both contemporaneous and dynamic correlation between series containing explosive regimes and provides information on the nature of potential explosive regime migration from one price series to another. To overcome the problem of heteroskedasticity present in financial data, the wild bootstrap procedure of [HLST](#) is adopted and, to deal with any serial correlation in innovations, estimates of long-run variance are used.

In the third chapter, we extend the work of [Evrpidou et al. \(2022\)](#) to develop a new test statistic which more effectively detects the co-explosiveness in samples containing short-lived periods where co-bubbles are absent. To accomplish this, we employ the backward recursive procedure of [PWY](#) to run the KPSS-based test of [Evrpidou et al. \(2022\)](#) on recursive subsamples. In addition to demonstrating the robustness of the newly proposed test to the heteroskedastic conditions when using the wild-bootstrap, analogously to [Evrpidou et al. \(2022\)](#), we also investigate the sensitivity of the KPSS-based test to the choice of kernel family and lag parameters in the corresponding kernel. Finite sample simulation results demonstrate that the new backward recursive KPSS-based test has higher power than the test of [Evrpidou et al. \(2022\)](#) in all bubble profiles and across most volatility specifications, but it is oversized in some cases where volatility contains a downward shift or trend patterns. Moreover, although the new test controls the finite sample size well, when using estimates of long-run variance, it is sensitive to different kernel estimators and

corresponding lag parameters. In some simulations, we also show the ability of the tests to identify the timing of explosive regime migration when co-bubbling is present. In an empirical exercise, we employ the same dataset of metal spot and futures prices as [Evrpidou et al. \(2022\)](#). Specifically, since empirical applications require significantly less computing power than Monte Carlo simulations, we employ a general supremum recursive KPSS-based test, where the general recursive procedure is designed as in [PSY](#). The empirical results regarding co-explosivity vary among tests; however, the general recursive test provides more evidence of co-explosivity in metal pairs than the two other tests.

The fourth chapter begins with an introduction to common stock return predictability tests. In practice, detecting the predictive ability of lagged variables is essential in constructing portfolios and risk management. However, as mentioned in the existing literature (e.g., [Cavanagh et al., 1995](#), [Stambaugh, 1999](#), [Campbell and Yogo, 2006](#) [[CY](#) hereafter], [Jansson and Moreira, 2006](#), [Welch and Goyal, 2008](#), [Kostakis et al., 2015](#) [[KMS](#) hereafter], and [Demetrescu et al., 2022a](#)) it is often difficult to determine whether a given predictor can be relied upon for forecasting. This is because the putative predictors used often exhibit high persistence and a significant correlation exists between the predictive regression error and the innovations driving the predictors (see [Cavanagh et al., 1995](#) and [CY](#)). In such circumstances, standard regression estimation and inference methods, including conventional regression t-tests, become invalid.

Criticism of the conventional t-test has led to the development of a number of likelihood-based procedures, such as the Bonferroni-t test by [Cavanagh et al. \(1995\)](#) and the Bonferroni-Q test by [CY](#) for cases where the predictor is endogenous and exhibits strong persistence within the local-to-unity class of processes. However, these approaches may not be valid for weakly persistent predictors, which has motivated the search for alternative methods that are robust to the characteristics of the regressor. [Demetrescu et al. \(2022b\)](#) suggests that, among various approaches, the IVX test proposed by [KMS](#) and its variants are the most prominent. However, it is important

to note that the asymptotic behaviour of IVX predictability test statistics may provide a poor approximation to finite sample behaviour. Later research (e.g., [Demetrescu et al., 2022a](#) and [Demetrescu et al., 2022b](#)) has attempted to improve the IVX and makes it more robust under the stylized facts of financial time series. In any case, the voluminous literature discussed above typically focuses on issues existing on the right-hand side of the linear predictive regression model. There is little literature that deals with issues arising from the returns on the left-hand side of the predictive model. Among the exceptions, [Yang et al. \(2022\)](#) show that when a bubble exists in stock returns, the IVX test is severely over-sized in the univariate predictive model regardless of the degree of endogeneity, especially when the predictive variables are highly persistent.

As a foundation for further research in this area, we introduce a data generating process [DGP] based on [CY's](#) DGP, which we find to be more natural and adaptable than that of [Yang et al. \(2022\)](#). Specifically, we utilize [PSY's](#) explosive price model, which represents the current stock price as the sum of a fundamental price and a bubble component. Our predictive regression model is designed to capture the part of the stock return that can be predicted by the fundamental return, and thus we do not include an unobservable bubble factor in the predictive regression model as in [Yang et al. \(2022\)](#). Additionally, while [Yang et al. \(2022\)](#) focus on the size and power of their extended IVX test with a fixed autoregressive parameter of the bubble, we instead focus on examining the behaviour of Bonferroni-based tests in [CY](#) and the IVX test of [KMS](#) under different bubble specifications incorporating changes in bubble length, position, and magnitude. Monte Carlo simulation exercises show that common predictability tests including the Bonferroni-t, Bonferroni-Q, and IVX test present bad size distortion when the bubble period is at the end of the sample. When bubbles grow quickly and are more long-lasting, over-rejection of the tests also increases accordingly. Among the three tests, the Bonferroni-t has a lower size distortion than the other two. However, when bubbles start and burst in the sample, the behaviour of the tests becomes more complex. Finally, we also apply

the three return predictability tests to the well-known empirical dataset of [Welch and Goyal \(2008\)](#), which includes S&P500 stock index returns and 14 financial and macroeconomic predictors. Unlike previous research (e.g., [Demetrescu et al., 2022a](#) and [Yang et al., 2022](#)), we here carefully separate the full sample into subsamples with and without bubble periods. The empirical results indicate that the tests reject the null hypothesis of no predictability in predictors when bubbles exist in the series.

Testing Explosive Bubble With Changes in Innovation Variance

We propose a novel test for explosive autoregressive behaviour when the innovation volatility is time-varying by extending the forward recursive right-tailed Dickey-Fuller test [sup DF test] of Phillips et al. (2011) [PWY hereafter] and the existing wild bootstrap sup BZ_K test of Harvey et al. (2019). In that regard, we estimate the time-varying volatility using the iterative cumulative sum of squares [ICSS] algorithm of Inclán and Tiao (1994) to detect multiple structural breaks in volatility. Thereafter, we replace the variance estimated by the kernel estimator of Harvey et al. (2019) with our estimated variance. By employing finite sample simulations for various volatility and bubble specifications, we show that the new approach does not cause power reversal (i.e., the power curve is non-monotonic) when the magnitude of the bubble is relatively large compared to the sample size. The proposed test also has a more well-controlled size of the test than the conventional sup DF test, and we reduce the false positive rate significantly. Although the modified test outperforms its counterparts in many bubble and volatility specifications (e.g., the case when the price series contains both a quickly grown bubble and a downward shift in innovations.), analogously to Harvey et al. (2019), a union-rejects strategy avoids losing information about the bubble given a late upward volatility shift. An empirical application to FTSE 100

and S&P 500 indexes indicates the presence of explosive behaviour in the S&P 500, which matches the period supposed to contain the origination of the Dotcom bubble in previous research studies (see e.g., [Ofek and Richardson, 2003](#) and [PWY](#)).

2.1 Introduction

Testing for explosive behaviour is an important contemporary topic in economics and finance ([Gürkaynak, 2008](#) and [PWY](#)). Indeed, determining explosive behaviour in the price of an asset can help us gain information about explosive rational asset price bubbles. Furthermore, by applying explosive behaviour tests to other types of time series data (e.g., public debt or commodity prices), we can characterize abnormal conditions. To limit the economic damage of the collapse of asset bubbles or to make appropriate decisions given abnormal regimes, we ideally need to identify such periods as soon as possible [Phillips et al. \(2015\)](#) [[PSY](#) hereafter]; in these cases, constructing an explosive bubble test that is robust to certain properties of financial time series is an important challenge.

Although the [PWY](#) test is commonly used to detect bubble-like behaviour in financial markets, [Harvey et al. \(2019\)](#) have shown that a Weighted Least Squares [WLS]-based test, which uses a simple nonparametric kernel smoothing estimator to estimate the volatility of innovations, can provide greater asymptotic power in detecting bubbles with various volatility patterns and specifications than the [PWY](#) method. [Harvey et al. \(2019\)](#)'s approach is in line with that of [Boswijk and Zu \(2018\)](#) in which [Boswijk and Zu \(2018\)](#) proposed an adaptive likelihood ratio test to test a full sample unit root against a left-tailed stationary alternative. Both [Boswijk and Zu \(2018\)](#) and [Harvey et al. \(2019\)](#) employ non-parametric estimation of the volatility process to provide more powerful tests. As a result, the asymptotic local powers of their proposed tests are significantly more effective than conventional tests (i.e., the *DF* test and *sup DF* test, respectively) in most of the volatility specifications. However, in finite samples, [Harvey et al. \(2019\)](#) show that with quickly growing bubbles at

the end of the sample, the power of the WLS-based test is appreciably lower and non-monotonic. For this limitation, [Harvey et al. \(2019\)](#) conjecture that the reason causing the power reversals is because the estimated variance is inflated by the quick growth of the bubble. To avoid power loss in cases of quickly grown bubbles, [Harvey et al. \(2019\)](#) used a union-rejection strategy inference from their novel test and the PWY test.

Motivated by the approach of [Harvey et al. \(2019\)](#), it is worth trying another estimator for time-varying volatility besides the kernel-based estimator used by [Harvey et al. \(2019\)](#). We propose to replace the kernel-based estimator with our new estimator. In this sense, the discrete variance breaks are determined by [Inclán and Tiao \(1994\)](#)'s procedure, and then the variances of innovations in the regimes are estimated. We argue that the volatility may change abruptly in intervals, instead of smoothly time-varying, so our estimator will more suitable when dealing with discrete shifts in the volatility. In fact, the assumption of abruptly changing volatility is not new, and it is widely mentioned in work detecting a unit root against the left tail stationary process (see, e.g., [Hamori and Tokihisa, 1997](#), [Kim et al., 2002](#), and [Cavaliere, 2005](#)). Empirical evidence has been found in many financial market indices, including [Inclán and Tiao \(1994\)](#) discovering breaks in the unconditional variance of IBM stock prices, and [Andreou and Ghysels \(2002\)](#) identifying structural breaks in the conditional variance of multiple stock market indices, which also supports this assumption. On the other hand, when the bubble grows quickly, it inflates the estimates of the variance causing power reversals, in which the power of [Harvey et al. \(2019\)](#)'s test is non-monotonic when the bubble size increases. Therefore, we consider whether our proposed variance estimator or any future variance estimators can overcome the limitation of the kernel-based estimator of [Harvey et al. \(2019\)](#).

Along the lines of the approach considered by [Harvey et al. \(2019\)](#), we construct the feasible WLS estimation-based test statistic [$\sup BZ_K$ hereafter] which exploits the ICSS algorithm of [Inclán and Tiao \(1994\)](#), allowing for discrete volatility shifts. In that sense, our new feasible WLS-based test [$\sup BZ_I$ hereafter] employs the *IT* test

statistic and iterative algorithm of [Inclán and Tiao \(1994\)](#) to detect multiple unknown and discrete volatility breaks in the series, employing the standard deviation of the difference of stock price in each regime as a corresponding estimator of the volatility in the price. In other words, this means the variance of innovations is assumed constant in each regime but will change to a different value after a breakpoint. Subsequently, we substitute the estimated volatility into the infeasible WLS-based statistic as in [Harvey et al. \(2019\)](#). By estimating a set of the statistics on forward recursive subsamples, we can obtain a supremum test statistic to compare with its corresponding critical value derived from the bootstrap procedure of [Harvey et al. \(2016\)](#) [[HLST](#) hereafter].

Similar to [Harvey et al. \(2019\)](#), our bubble model portrays normal market behaviour with a unit root process until a specific point in the sample, after which point it displays explosive autoregressive behaviour over the remaining sample. Bubble specifications are versatilely adjusted, in which the bubble may emerge from the middle or near the end of the sample period. In fact, according to [PSY](#), this case has more empirical and practical interest for policymakers (e.g., central banks or regulators) and business decision-makers than the episode when the bubble bursts. If ongoing asset price bubbles are detected early, it will serve as a useful warning system to market participants and stakeholders.

As shown by [Harvey et al. \(2019\)](#), the asymptotic distribution of supremum WLS-based test statistic depends on the specification of volatility. Therefore, following [HLST](#), we also use a wild bootstrap algorithm to control the asymptotic size of the test - detailed steps of the wild bootstrap procedure can be found in Section 2.7 of this chapter. Additionally, we compare the finite-sample power of our test with that of the wild bootstrap [PWY](#) and [Harvey et al. \(2019\)](#) tests. It should be noted that in spite of assuming that both variance estimators of the supremum-based tests, $\sup BZ_K$ and $\sup BZ_I$ are exact and the asymptotic distribution of both tests are the same, the finite sample properties are not analogous. Therefore, we run appropriate simulations and check how test statistics behave across different sample sizes. Lastly, we use a union

of rejections strategy to combine these two tests and examine whether there is any further improvement in power.

Monte Carlo simulations, and the constructed finite sample local curves, show the power of our proposed test is on a par with the **PWY** test, while the $\sup BZ_K$ test of **Harvey et al. (2019)** is non-monotonic and has lower power than the two other tests when the bubble is short-lived at the end of the sample. The union strategy, which combines rejections of $\sup BZ_I$ and $\sup BZ_K$, does not work particularly well because the $\sup BZ_I$ dominates $\sup BZ_K$ and thus reflects its power profile in the local power curve of the union strategy. Notably, when the sample size is small or the magnitude of explosive behaviour is relatively large, in almost all cases, the power of the $\sup BZ_K$ test is worryingly low and reverses, where the power curve presents an inverted U-shape following the increase of bubble magnitude. In other words, in almost all of the volatility specifications with the bubble near the end of the sample, our test is more robust than that of **Harvey et al. (2019)**.

In the case when volatility presents a late upward shift at the end of the sample period, the power of the bootstrap $\sup DF$ test is greater than WLS-based tests; however, the finite sample size of the $\sup DF$ test is seriously oversized. One can therefore suggest that given the $\sup DF$ tends to the over-reject null hypothesis, this is what drives the power performance. Despite this, the underperformance of the WLS-based tests is disappointing, and potentially a result of biased variance estimation. In this situation, and combining rejection decisions from the WLS-based and OLS-based tests, the union of rejections test leads to power improvements.

This chapter is organized along the following lines. In the following section, we review the literature on bubble tests. Section 2.3 discusses the bubble model and its assumptions. Next, in Section 2.4, we will briefly cover the supremum right-tailed unit root test of **PWY**, and discuss the infeasible version of the WLS-based explosive test of **Harvey et al. (2019)**. In Section 2.5, asymptotic properties of the OLS and WLS-based tests are established. Section 2.6 outlines a feasible version of the WLS-based test where the kernel-based estimator of variance will be explained following **Harvey**

et al. (2019), and the ICSS-based estimator of variance is also introduced. For all the test statistics we employ the wild bootstrap procedure to control the size of the test, so we will use Section 2.7 to discuss the wild bootstrap test statistics and a relevant union-rejections strategy. Section 2.8 evaluates the finite sample performance of all tests in this chapter. Section 2.9 provides the empirical results when we apply the conventional sup DF test, sup BZ_K test of Harvey et al. (2019), our proposed test (sup BZ_I), and union strategy-based test (\mathcal{U}) to S&P 500 and FTSE 100 stock prices. The last section concludes this chapter with a summary of the methods, findings, and possible extensions for future research.

2.2 Literature Review

Among different types of bubbles (e.g., rational and irrational bubbles), rational bubbles are the object which is tested in this chapter. According to PWY, the rational bubble model was perhaps the most potential in explaining the explosive behaviour of economic variables.

According to Tirole (1982) and Diba and Grossman (1988), the current price of the asset is determined by the present value of the next period's expected stock price and dividend payoffs:

$$P_t = \mathbb{E}_t \left[\frac{P_{t+1} + D_{t+1}}{1 + R} \right] \quad (2.1)$$

where P_t is the price of the stock at period t , D_t denotes the dividend received from ownership of the stock between $t-1$ and t , and R is the discount rate. Accordingly, we solve the difference Equation (2.1) forward and apply the law of iterated expectations, which yields:

$$P_t = \mathbb{E}_t \left[\sum_{j=1}^k \frac{D_{t+j}}{(1+R)^j} \right] + \lim_{k \rightarrow \infty} \mathbb{E}_t \left[\frac{P_{t+k}}{(1+R)^k} \right] \quad (2.2)$$

The first term on the right-hand side is the standard present value of an asset:

$$P_t^f = \mathbb{E}_t \left[\sum_{j=1}^k \frac{D_{t+j}}{(1+R)^j} \right]$$

in which the fundamental price P_t^f of a stock in any period is equal to the present value of all expected dividend payments from that point onwards. The second term represents the price bubble, B_t :

$$B_t = \lim_{k \rightarrow \infty} \mathbb{E}_t \left[\frac{P_{t+k}}{(1+R)^k} \right] \quad (2.3)$$

If the transversality condition holds, it implies:

$$\lim_{k \rightarrow \infty} \mathbb{E}_t \left[\frac{P_{t+k}}{(1+R)^k} \right] = 0$$

then the current price of the stock, P_t collapses to its fundamental price, P_t^f , and it rules out the existence of a bubble. However, if the condition does not hold, an explosive rational bubble may present itself. Consider a process $\{B_t\}_{t=1}^{\infty}$ satisfying:

$$\mathbb{E}_t[B_{t+1}] = (1+R)B_t \quad (2.4)$$

Adding B_t and P_t^f will yield infinitely many solutions for the current price of the stock in the Equation (2.1), which takes the form:

$$P_t = P_t^f + B_t \quad (2.5)$$

In other phrasing, the presence of a stock price rational bubble is explained by [Homm and Breitung \(2012\)](#) as follows: If a stock price bubble exists, Equation (2.4.2) states that any rational investor interested in buying that stock must anticipate the bubble to expand at a rate R . If this is true and if B_t is positive, it creates the opportunity for speculative investment behaviour: a rational investor is willing to purchase an "overpriced" stock because they believe that the increase in price will compensate for the additional payment B_t . If investors anticipate prices to rise at a rate of R and purchase shares, the stock price will indeed increase, resulting in a self-fulfilling prophecy.

Campbell et al. (1997) define a rational bubble as a rise of asset prices that are driven far higher than could be efficiently explained by fundamentals; however, it is still rational because the rise starts from rational expectations and constant expected returns of investors, who are betting that other investors will pay for the assets higher prices in the future. In the early development (e.g., Garber, 1990 and Hodrick, 1992) of economic theory, the rational bubble hypothesis was considered as lacking empirical support given it is difficult, if not impossible, to both observe expectations and exclude other alternative explanations of asset prices (e.g., completely fundamental, or entirely rational) (Meltzer, 2002); however, the emergence and subsequent collapse of bubbles (e.g., tulip mania in the 18th century and the Mississippi and South Sea bubble) have been well documented by economists for decades.

Given a theory of rational bubbles, many papers have constructed tests to detect bubbles in asset prices. Approaches for detecting and/or dating such bubbles include variance-bound tests (LeRoy and Porter, 1981), West's two-step test (West, 1987), fractionally integrated models (Cuñado et al., 2005 and Frömmel and Kruse, 2012), and integration/cointegration-based test (Diba and Grossman, 1988). In spite of this, these tests show little evidence of the existence of the bubbles (e.g., bubble in Nasdaq) (Campbell et al., 1997). According to Gürkaynak (2008), these tests are partly not suitable or lack power. For example, Blanchard and Watson (1982), Abel et al. (1986), and Tirole (1982) show that the variance bound may be violated because of the bubble and is not well suited. Or, Dezhbakhsh and Demirguc-Kunt (1990) argue that the finite sample size in West's two-step test is distorted (high probability to reject the null when it is true). And, according to Evans (1991), the right-tailed unit root test of Diba and Grossman (1988), using a full sample, lacks power to detect especially periodically collapsing bubbles. In this sense, it is necessary to construct better tests adapted to more complex specifications of bubbles (e.g., multiple periodically collapsing bubbles, end-sample bubbles) and the stylized facts of financial time series (e.g., heteroskedasticity and serial correlation).

Recently there has been a renewed interest in the economics and finance literature

on rational bubble-related topics, where recursive and rolling-recursive bubble tests have become prevalent. For example, PWY and PSY develop causal linear methods which are able to identify and date previous asset price bubbles, responding to the criticism of Evans (1991) regarding the assumptions in the traditional unit root testing methods of Diba and Grossman (1988). Also, to some extent, these tests can capture the existence of empirical bubbles in popular stock indexes and asset prices. Later, several other papers attempt to relax assumptions and improve the supremum-based tests of PWY and PSY. Specifically, newly proposed models can incorporate the stylized facts of financial time series data such as time-varying volatility, serial correlations, and time trend. For instance, HLST use a wild bootstrap algorithm to control the size of the test under heteroskedasticity, Whitehouse (2019) considers the linear trend inside the model of the explosive asset price, Harvey et al. (2019) use a kernel-based estimator and WLS-based test to improve the test of HLST which presents heteroskedasticity in the innovations, and Pedersen and Schütte (2020) consider explosive bubble in the presence of serial correlation.

Together with the development of technical papers on rational bubble testing which aims to improve the power and reduce the size distortion in the current tests, researchers also contribute greatly to the literature on applications of explosive autoregressive behaviour tests. We may name a few papers here: In the exchange rate market, Bettendorf and Chen (2013) found solid evidence of rational explosive bubbles in the Sterling-dollar exchange rate using *GSADF* and *SADF* tests of PWY and PSY, respectively. In the stock market, Phillips and Yu (2011), PWY, PSY, Phillips and Shi (2018), and Phillips and Shi (2019) found evidence of rational explosive processes in the NASDAQ, and S&P 500. Bohl et al. (2013) detected bubbles in German renewable energy stocks using the *SADF* test. Breitung and Kruse (2013) proposed structural break-based test statistics with a monitoring strategy (Chu et al., 1996) to identify bubbles in NASDAQ and Hang Seng indexes. Astill et al. (2017), Astill et al. (2018) developed test statistics to examine bubbles at the end of the sample and real-time monitoring of bubbles employing a wide range of stock indexes (DAX30,

FTSE All Share, Nikkei 225, S&P 500, and Nasdaq Composite Index); moreover, [Harvey et al. \(2019\)](#) used kernel-based test to detect bubbles in S&P 500 and FTSE indexes. In the cryptocurrency market, [Harvey et al. \(2020\)](#) and [Astill et al. \(2021\)](#) showed evidence of a Bitcoin bubble using a signed-based unit root test and CUSUM-based test under assumptions of time-varying volatility, respectively. In addition, several researchers also identify bubbles in the housing market ([Harvey et al., 2020](#) and [Kurozumi, 2021](#)). Finally, in the commodity market, other bubbles are detected ([Etienne et al., 2014](#), [Figueroa-Ferretti et al., 2015](#), [HLST](#), [Tsvetanov et al., 2016](#), and [Evrpidou et al., 2022](#)). Those papers show statistical evidence of rational bubbles, which precede the empirical financial crashes in various markets.

Additionally, different tests for change in persistence can use a recursive algorithm to detect the explosive autoregressive behaviour, such as the sup DF test; however, the sup DF test is still popular and widely used. This is partly because of its simplicity and availability which is built-in various open-source software. Indeed, to conduct sup DF , we only need to run the Dickey-Fuller [DF] test through forward or backward subsamples to obtain a sequence of statistics, then get the maximum value of the sequence to compare with the corresponding critical value. Indeed, [Homm and Breitung \(2012\)](#) also use the same recursive algorithm with other break testing procedures such as the Bhargava statistic, Buseti-Taylor statistic, Kim statistic, and Chow-type unit root statistic. Under assumptions of a single originating phrase of the bubble in [Homm and Breitung \(2012\)](#), the Chow-type based test has the best performance. However, the sup DF test of PWY is still recommended in many research studies because [Homm and Breitung \(2012\)](#) indicate that the Chow-type-based test requires the positions of breakpoints in the mean, which may be estimated by the maximum likelihood estimator of [Bai and Perron \(1998\)](#). Together with that, the sup DF test works more robustly than any other tests in [Homm and Breitung \(2012\)](#) to identify multiple bubbles and bubbles in real-time.

As we have just mentioned, recursive tests of PWY and PSY have had a significant impact on the development of rational bubble tests and applications in testing bubbles

in practice. However, those tests do not account for some stylized facts of financial time series data (e.g., non-constant volatility). In such circumstances, size distortion will occur in the tests, leading to over-rejection of the null hypothesis that the process is a unit root. This is because, in their papers, [PWY](#) and [PSY](#) construct their supremum recursive tests under assumptions of stationary volatility implying the unconditional variance of innovations is unchanged over the whole sample. Indeed, many research papers ([Rapach et al., 2008](#) and [McMillan and Wohar, 2011](#)) have demonstrated that structural breaks in unconditional volatility often coincide with the formation and bursting of stock price bubbles. As [HLST](#) suggest, it is possible that changes in volatility in time series innovations are caused by explosive behaviour, but changes in volatility can also occur without the presence of an explosive period. Therefore, it is important to have a test that is robust to the existence of heteroskedasticity.

According to [HLST](#), using the [PWY](#) test on price series could lead to misrepresentation if there is a significant financial or macroeconomic crisis that results in an increase in unconditional volatility. In line with [Cavaliere and Taylor \(2007\)](#), and employing the wild bootstrap to [PWY](#) tests, [HLST](#) demonstrate that the asymptotic null distribution of the sup DF test depends on the nature of the volatility. If the test is implemented using critical values derived under a homoskedastic volatility assumption, the size of the test will be distorted for nonstationary volatility patterns. Therefore, [HLST](#) combine the sup DF test of [PWY](#) with the wild bootstrap algorithm to reduce the size distortion. Their bootstrap procedure uses direct simulation methods based on a consistent estimate of the variance profile to obtain approximate quantiles from the asymptotic null distributions of the standard test statistics. However, since the sup DF test and its related bootstrap variants use OLS estimation in testing for a unit root against an explosive alternative, in the presence of heteroskedasticity, [Harvey et al. \(2019\)](#) consider whether replacing OLS by WLS estimation, can improve the power of the test but still retain the correct asymptotic size. Applying the non-parametric kernel-based procedure of [Boswijk and Zu \(2018\)](#), [Harvey et al. \(2019\)](#) show that WLS-based tests are more powerful than OLS based

approach (sup *ADF* test) in detecting the presence of a bubble.

2.3 Heteroskedastic Bubble Model and Assumptions

As noted by *PWY*, stock prices must be non-negative and a function of dividend series and unobservable fundamentals (like changes in discount rate). Under the assumption that the fundamental component is either $I(1)$ or $I(0)$, if $B_t = 0$, then the current stock price will follow an $I(1)$ or $I(0)$ process respectively. However, in most of the empirical evidence, the stock price is found to be $I(1)$ (*Fama, 1965* and *Narayan and Smyth, 2005*); therefore, it is natural to assume that the fundamental part will be an $I(1)$ process. On the other hand, if $B_t > 0$, the bubble component will dominate the fundamental price, no matter whether the fundamental component is $I(1)$ or $I(0)$ at any point in time during the sample. In other words, the actual price will increase significantly as the bubble grows because the magnitude of the bubble component is relatively bigger compared to that of the fundamental part. Since rational bubbles burst after exponential growth, there is a subsequent structural break that allows the bubble component to fall back into some arbitrary constant value (see e.g., *HLST* and *Evrpidou et al., 2022*). However, we in this chapter only model the origination phase of bubbles and do not model their collapsing phase. Combined with first-order autoregressive process, an asset price bubble can be modeled by using data generating process [DGP] for y_t of the following form:

$$y_t = \mu + x_t \quad (2.6)$$

$$x_t = \rho_t x_{t-1} + u_t \quad (2.7)$$

$$u_t = \sigma_t \epsilon_t \quad (2.8)$$

$$\rho_t = \begin{cases} 1 & \text{if } t = 2, \dots, [r^*T] \\ 1 + c/T & \text{if } t = [r^*T] + 1, \dots, T \end{cases}$$

where $[\cdot]$ denotes the integer part of its argument. When $c > 0$, y_t follows a unit root process up to time $[r^*T]$, after that point it displays a mildly explosive process over the remaining sample period $t = [r^*T] + 1, \dots, T$. r^* indicates a fraction of the sample where the process switches from a unit root to an explosive process. In the context of testing for explosive autoregressive behaviour, our null hypothesis is $\mathcal{H}_0 : c = 0 \forall t$ (so, $\rho_t = 1 \forall t$), so that the series is a unit root process throughout. The corresponding alternative hypothesis $\mathcal{H}_1 : c > 0$, the series is an explosive process. Since all of the tests in this chapter use a forward recursive algorithm, the alternative hypothesis implies that explosive behaviour exists if it is present in at least one subsample of the data. Therefore, an approach based on the maximum of the sequence of subsample test statistics considered would be appropriate. In line with [Harvey et al. \(2019\)](#), this \mathcal{H}_1 model indicates the asset price follows a random walk till time (r^*T) , then a bubble occurs at the point $(r^*T + 1)$ and grows explosively to the end of the sample period. The model simulates the first phase of the bubble when it starts to grow at the end of the sample and bursts somewhere out of the sample. Hence, our intention is to see how our tests behave in temporary or short-lived bubble episodes.

The model error term, u_t is assumed to be a martingale difference, where ϵ_t is multiplied by a time-varying scale factor, σ_t . In addition, we make two assumptions following [Harvey et al. \(2019\)](#) for ϵ_t and σ_t :

Assumption 2.1 ϵ_t is a vector martingale difference sequence (m.d.s) with respect to \mathcal{F}_t , a natural filtration generated by $\{u_s\}_{s \geq 1}$, and $E[\epsilon_t^4] < \infty$, to which it is satisfying: $E[\epsilon_t | \mathcal{F}_{t-1}] = 0, E[\epsilon_t^2 | \mathcal{F}_{t-1}] = 1$.

Assumption 2.2 $\sigma_t = \sigma(t/T)$ where $\sigma(\cdot)$ is a strictly positive function with $\sigma(\cdot) \in D[0,1]$, the space of right continuous (càd) with left limit (làg) functions on $[0,1]$.

Assumption 2.1 states that ϵ_t is a martingale difference sequence [m.d.s], which is conditionally first-order uncorrelated but may be dependent via higher moments ([Xu and Phillips, 2008](#)). For Assumption 2.2, adopted from [Cavaliere and Taylor \(2007\)](#) and [Cavaliere and Taylor \(2009\)](#), the time-varying scale factor is a time-dependent

continuous or discontinuous function. $\sigma(\cdot)$ is integrable on the interval $(0,1]$ to any finite order. This implies the innovation variance is represented by non-stochastic and bounded models and may contain a countable number of jumps (e.g., single or multiple abrupt volatility shifts, polynomially trending volatility, and smooth transition volatility breaks). Under Assumptions 2.1 and 2.2, the invariance principle holds in the context of both unit root and explosive processes:

$$T^{-1/2} \sum_{t=2}^{[\tau T]} u_t \xrightarrow{w} \int_0^{\tau} \sigma(s) dW(s)$$

where \xrightarrow{w} denotes weak convergence and $W(s)$ is a standard Wiener process.

2.4 Explosive Behaviour Tests

2.4.1 An Ordinary Least Squares-based Test

Existing unit root tests typically have an alternative hypothesis of stationarity, and are left-tailed tests, looking at test statistic on the left of the asymptotic distribution. In that context, [Diba and Grossman \(1988\)](#) conducted left-tailed unit root tests on differences in stock prices or tested for cointegration between the prices and its dividends assuming a time-invariant discount rate. Finding dividends to be nonstationary in levels, a rational bubble is rejected when the price is a unit root in levels but is stationary in differences. This is because they argue that explosive characteristics still exist in the first difference of an explosive process. In addition, they also employ [Bhargava \(1986\)](#) tests to show stock prices and dividends are cointegrated, which supports the evidence of no bubble in the index since there is a long-run relationship between stock price and fundamentals. [Diba and Grossman \(1988\)](#) reject the null hypothesis of a unit root in the real S&P500 stock price index over the period between 1871 and 1986. This means there is insufficient evidence of rational bubbles in the aggregate real stock prices. Although [Diba and Grossman \(1988\)](#) show the usefulness of unit root and cointegration tests in identifying rational

bubbles, [Evans \(1991\)](#) explores the shortcomings of the standard unit root and cointegration tests in detecting the periodically collapsing bubbles, showing that periodically collapsing bubbles in series lowers the power of full sample left-tailed unit root tests.

To handle [Evans \(1991\)](#)'s criticism that full sample tests are not well equipped to identify short-lived bubbles, [PWY](#) proposes a forward recursive right-tailed Dickey-Fuller test [sup DF test] which is capable of distinguishing periodically collapsing bubbles from pure unit root processes:

$$\sup DF := \sup_{\tau \in [\tau_0, 1]} DF_\tau \quad (2.9)$$

$$DF_\tau := \frac{\hat{\rho}_\tau}{\sqrt{\hat{\sigma}_{DF,\tau}^2 / \sum_{t=2}^{\lfloor \tau T \rfloor} (y_{t-1} - \bar{y}_\tau)^2}} \quad (2.10)$$

where DF_τ denotes a standard Dickey-Fuller test statistic with the constant for subsample $t = 1, \dots, \lfloor \tau T \rfloor$, $\hat{\rho}_\tau$ is the estimated coefficient from the OLS regression, $\Delta y_t = \hat{\mu}_\tau + \hat{\rho}_\tau \sum_{i=2}^{\lfloor \tau T \rfloor} y_{t-1} + \hat{u}_{t,\tau}$, $\bar{y}_\tau = (\lfloor \tau T \rfloor - 1)^{-1} \sum_{i=2}^{\lfloor \tau T \rfloor} y_{t-1}$, and $\hat{\sigma}_{DF,\tau}^2 = (\lfloor \tau T \rfloor - 3)^{-1} \sum_{i=2}^{\lfloor \tau T \rfloor} \hat{u}_{t,\tau}^2$. The minimum sample length in the subsample regressions is $\lfloor \tau_0 T \rfloor$.

In the sup DF test, the right-tailed Dickey-Fuller test statistic is estimated repeatedly on subsets of sample data, in which each subset is incremented by one observation at each iteration. The first test statistic is regressed by using a subsample with the minimum sample length $\lfloor \tau_0 T \rfloor$. According to [Harvey et al. \(2016\)](#), caution should be exercised when choosing the value of τ_0 since it requires balancing the need to detect an early and short-lived bubble against incorporating sufficient observations for estimations in the first subsample. The [Figure A-2](#) illustrates the [PWY](#) procedure. As we can see, the supremum test iterates through the series to check whether the series transitions from a unit root process to an explosive process by finding where the maximal test statistic exceeds a relevant critical value. It means the test rejects the null if at least one test statistic is greater than the corresponding critical value of the test.

In addition, the DF test ([Dickey and Fuller, 1979](#)) here is preferred to the aug-

mented DF (ADF test of Said and Dickey, 1984) in the recursive test. Therefore, PSY indicates that the size of the test will be distorted if we try to add fixed transient dynamics to the test statistic. In that case, size distortion increases following the increase in lag length. Even though they use information criteria to choose the lag length, the size of the test is still slightly distorted. Since our innovations are not autocorrelated (see Equation 2.7), we set the lag order to zero. Omitting the lags in the model can help to simplify our test, but it can also be criticised given the model cannot reflect the higher-order autoregressive processes in actual financial time series. Additionally, PSY argue that adding a deterministic time trend under the alternative hypothesis of mildly explosive behaviour seems to be unrealistic, so we also do not add a deterministic trend in the DGP and do not de-trend the process before testing. However, since our DGP in (2.6)-(2.8) still contain a constant mean, we have to account for the intercept in calculating the test statistics or demean the price series before conducting test regression.

According to HLST, although the sup DF has its size well-controlled under the assumption of constant volatility, the test is substantially oversized if the data presents heteroskedasticity. This implies that sup DF tends to over-detect spurious bubbles in data. Using different volatility specifications, HLST shows the size distortion of the sup DF test is caused by the dependency of the limiting null distribution of the test on nuisance parameters derived from the patterns of volatility present in the innovations. This takes them to combine the sup DF test with the wild bootstrap procedure which we will recap in Section 2.7. Nevertheless, the sup DF test after bootstrapped still has its size distorted in many volatility profiles. This causes over-rejections and increases false positives of the presence of explosive bubbles in the series.

2.4.2 A Weighted Least Squares-based Test

In the presence of conditional heteroskedasticity, and in order to improve the power of the conventional PWY test, Harvey et al. (2019) replace OLS-based Dickey-Fuller statistic with a WLS-based equivalent while still employing the wild bootstrap algo-

rithm of **HLST** to guarantee the size of the test well-controlled under the presence of heteroskedasticity. Considering first the underlying x_t process in (2.7), assuming σ_t is known for constructing the infeasible test, the transformed model can be written as:

$$\frac{\Delta x_t}{\sigma_t} = \rho_t \frac{x_{t-1}}{\sigma_t} + \epsilon_t, \quad t = 2, \dots, T$$

From that, they have an infeasible test statistic written as follows:

$$\sup BZ := \sup_{\tau \in [\tau_0, 1]} BZ_\tau \quad (2.11)$$

$$BZ_\tau := \frac{\sum_{t=2}^{\lfloor \tau T \rfloor} \frac{\Delta \tilde{y}_t \tilde{y}_{t-1}}{\sigma_t^2}}{\sqrt{\sum_{t=2}^{\lfloor \tau T \rfloor} \frac{\tilde{y}_{t-2}^2}{\sigma_t^2}}} \quad (2.12)$$

where $\tilde{y}_t := y_t - y_1$ is *GLS* demeaned in the sense of **Elliott et al. (1996)** using $\bar{\alpha} = 1$. Therefore, after demeaning, we will not use an intercept in the test regression. As mentioned in **Elliott et al. (1996)**, compared with OLS demeaning, *GLS* demeaning gives the higher power to the *DF – GLS* test when an unknown mean is present in small samples. BZ_τ is the test statistic calculated on each subsample $[y_1, \dots, y_{\lfloor \tau T \rfloor}]$. $\sup BZ$ test statistic is the maximum value of the sequence of subsample statistics derived from subsamples. As we can see, before calculating the test statistic in (2.11), we have to estimate the volatility because in practice the volatility is unknown. In this case, the **Harvey et al. (2019)**'s test statistic will become feasible when σ_t is replaced by its estimator. Procedures to calculate σ_t estimators will be discussed in Section 2.6.

2.5 Asymptotic Behaviour Of Tests

2.5.1 Asymptotic Properties of **PWY** Test

In this section, we outline the limiting alternative distribution of the $\sup DF$ test statistic, which is constructed from the DGP outlined in (2.6) to (2.8). The corresponding distribution of test under null being obtained as a special case thereof.

Theorem 2.1 Let y_t be generated by Equation (2.6) - (2.8). Under Assumptions 1-2, **HLST** show that:

$$\sup DF := \sup_{\tau \in [\tau_0, 1]} DF_\tau \xrightarrow{w} \sup_{\tau \in [\tau_0, 1]} J_c(\tau) := \mathbb{M}_c^{DF}$$

$$J_c(\tau) = \begin{cases} \frac{\int_0^\tau \tilde{U}_c(r) dU_c(r)}{(\tau^{-1} \int_0^\tau \sigma(r)^2 dr \int_0^\tau \tilde{U}_c(r)^2 dr)^{1/2}}, & \tau \leq \tau^* \\ \frac{\int_0^\tau \tilde{U}_c(r) dU_c(r) + c \int_{\tau^*}^\tau \tilde{U}_c(r)^2 dr}{(\tau^{-1} \int_0^\tau \sigma(r)^2 dr \int_0^\tau \tilde{U}_c(r)^2 dr)^{1/2}}, & \tau > \tau^* \end{cases}$$

where $\tilde{U}_c(r) = U_c(r) - \frac{1}{\tau} \int_0^\tau U_c(s) ds$, and

$$U_c(r) = \begin{cases} \int_0^r \sigma(s) dW(s), & r \leq \tau^* \\ e^{c(r-\tau^*)} \int_0^{\tau^*} \sigma(s) dW(s) + \int_{\tau^*}^r e^{c(r-s)} \sigma(s) dW(s), & r > \tau^* \end{cases}$$

\mathbb{M}_c^{DF} is the limit distribution of $\sup DF$ for each corresponding c in (2.7), DF_τ is the test statistic calculated on a closed interval in (2.10). The limiting null distribution of $\sup DF$ is obtained from the result in Theorem 2.1 simply by setting $c = 0$, so that $\sup DF \xrightarrow{w} \mathbb{M}_0^{DF}$.

As a result, both null and local alternative distributions of this infeasible DF test statistic depend on nuisance parameters derived from the pattern of heteroskedasticity presented in the innovations. Therefore, **HLST** suggest a wild bootstrap algorithm to replicate the pattern of volatility in the original innovations. From that, the modified test of **HLST** is effective in controlling the size of the test.

2.5.2 Asymptotic Properties of BZ Test

In this section, we derive the asymptotic properties of $\sup BZ$ based test statistic in (2.11). The limit distribution of $\sup BZ$ is depicted below.

Theorem 2.2 Let y_t be generated by (2.6) - (2.8); under Assumptions 2.1 and 2.2, **HLST**

and *Boswijk and Zu (2018)* show that:

$$\sup BZ := \sup_{\tau \in [\tau_0, 1]} BZ_{\tau} \xrightarrow{w} \sup_{\tau \in [\tau_0, 1]} L_c(\tau) := \mathbb{M}_c^{BZ}$$

$$L_c(\tau) = \begin{cases} \frac{\int_0^{\tau} V_c(r) dW(r)}{(\int_0^{\tau} V_c(r)^2 dr)^{1/2}}, & \tau \leq \tau^* \\ \frac{\int_0^{\tau} V_c(r) dW(r) + c \int_{\tau^*}^{\tau} V_c(r)^2 dr}{(\int_0^{\tau} V_c(r)^2 dr)^{1/2}}, & \tau > \tau^* \end{cases}$$

with $V_c(r) = U_c(r)/\sigma(r)$, $U_c(r)$ is defined in Section 2.5.1, and BZ_{τ} is the test statistic in (2.12).

Remark 2.1 Analogously to the limit distribution of the infeasible DF test statistic above, the distribution of BZ test statistic also depends on the unknown volatility path. Despite that, as argued in the previous subsection, volatility is typically unknown in practice. Therefore, we also employ the wild bootstrap procedure as in *HLST*.

Remark 2.2 The limiting null distribution of sup DF is derived when $c = 0$, then $\sup BZ \xrightarrow{d} \mathbb{M}_0^{BZ}$.

In their paper, *Harvey et al. (2019)* assume the volatility paths are known and have some common patterns that we will present in Section 2.8, demonstrating that the size-corrected local asymptotic power of the infeasible WLS-based test is higher than that of the sup DF test under the same wild bootstrap procedure.

2.6 Feasible Estimator Based Tests

2.6.1 Kernel Estimator Based Test

Given the volatility path is unknown in practice, the test statistics in (2.10) and (2.12) are infeasible. Therefore, we need to find the estimation of σ_t , $\hat{\sigma}_t$. In that sense, *Harvey et al. (2019)* show the feasible test statistic of sup BZ, that is, $\sup BZ_K$, is as

follows:

$$\sup BZ_K := \sup_{\tau \in [\tau_0, 1]} BZ_{K, \tau} \quad (2.13)$$

$$BZ_{K, \tau} := \frac{\sum_{t=2}^{\tau T} \frac{\Delta \tilde{y}_t \tilde{y}_{t-1}}{\hat{\sigma}_t^2}}{\sqrt{\sum_{t=2}^{\tau T} \frac{\tilde{y}_{t-2}^2}{\hat{\sigma}_t^2}}} \quad (2.14)$$

with $\hat{\sigma}_t$ the time-varying volatility, estimated by using kernel smoothing regression.

[Harvey et al. \(2019\)](#) use a kernel-based variance estimator, σ_t^2 , given by:

$$\hat{\sigma}_t^2 = \frac{\sum_{i=2}^T K_h\left(\frac{i-t}{T}\right) (\Delta y_i)^2}{\sum_{i=2}^T K_h\left(\frac{i-t}{T}\right)}$$

where $K_h(s) = K(s/h)/h$ and $K(\cdot)$ is a kernel function with bandwidth parameter h .

Furthermore, to construct the asymptotic distribution of $\sup BZ_K$, [Harvey et al. \(2019\)](#)

added four more assumptions below:

Assumption 2.3 ϵ_t follows a symmetric distribution, and $E[\epsilon_t^8] < \infty$.

Assumption 2.4 $\sigma(\cdot)$ is a Lipschitz continuous function on $[0, 1]$ except on a finite number of discontinuity points.

Assumption 2.5 $K(\cdot)$ is a bounded non-negative function defined on a real line with an integral, $\int_{-\infty}^{\infty} K(r) dr = 1$.

Assumption 2.6 As $T \rightarrow \infty, h \rightarrow 0$ and $Th^2 \rightarrow \infty$.

Assumption 2.3 as given above, $E[\epsilon_t^8] < \infty$, is a stronger form of Assumption 2.1, and requires the existence of 8^{th} moments of ϵ_t for all t . This moment condition is given by [Xu and Phillips \(2008\)](#) to simplify the proof of the main theorem; therefore, it may be stronger than necessary. Furthermore, [Harvey et al. \(2019\)](#) let ϵ_t have a symmetric distribution for technical reasons and is typically easily satisfied for the type of equity returns examined in this chapter. Assumptions 2.4 and 2.5 are to modify previous assumptions in kernel estimators of [Xu and Phillips \(2008\)](#). Assumption

2.4 presents volatility as a continuous nonparametric function in which the values of σ_t only depend on the relative position of the error in the sample. This is to relax the parametric settings of volatility dynamics and provide suitable models with the wider properties of financial time series. As in [Boswijk and Zu \(2018\)](#), continuity of $\sigma(\cdot)$ is a necessary condition for uniform consistency of the kernel estimator; however, although this non-parametric estimator works well with smooth transition functions like logistic functions, it typically will underperform around abrupt changes. Thus, a condition allowing a finite number of discontinuities as in [Xu and Phillips \(2008\)](#) is enough to keep the volatility estimator converging in probability as the sample size increases. Assumption 2.5 relaxes the conditions on the kinds of kernel used in [Boswijk and Zu \(2018\)](#) and [Xu and Phillips \(2008\)](#). Finally, in accordance with [Harvey et al. \(2019\)](#), we also use the rate condition in Assumption 2.6 as in [Xu and Phillips \(2008\)](#).

In comparison with the sup DF test, the sup BZ_K test of [Harvey et al. \(2019\)](#) presents higher asymptotic local power and is more powerful and has more well-controlled size under finite samples; however, as shown in the simulated results of [Harvey et al. \(2019\)](#), the finite sample power of the sup BZ_K tends to reverse after increases in the magnitude of the bubble after a certain point. In fact, for the same parameter c , the power of the sup BZ test shows a more significant reversal in a small sample size, T . This is due to the fact that the ratio c/T , which represents the relative magnitude of the bubble, is greater when T is smaller. Also, in [Harvey et al. \(2019\)](#), the test power in cases of discrete volatility shifts is worse than with continuous volatility dynamics. Consequently, our proposed tests might be able to deal better with the situation of power reversal since the kernel estimator used previously is more suitable for the continuous volatility models rather than discrete cases. This is part of the rationale motivating the construction of a new test.

Remark 2.3 *According to the proof of Theorem 2 in [Harvey et al. \(2019\)](#), when the variance of the series σ_t^2 is replaced by $\hat{\sigma}_t^2$, the limit distribution of feasible sup BZ (discussed in the Section 2.7.2) will converge to the distribution of the infeasible one. Indeed, we conjecture*

that as long as the volatility estimator is consistent, the asymptotic distribution of infeasible statistic $\sup BZ$ is the same no matter what estimator is used to estimate the volatility. This is the basis for us to propose a second test based on a different variance estimator in Section 2.6.2.

2.6.2 ICSS based Test

It could be the case that, in practice, the path of volatility has one or more discrete shifts. In this case, the kernel estimator would not be well suited, but we could employ the ICSS procedure of [Inclán and Tiao \(1994\)](#) to detect breakpoints in volatility. Then, using the garnered information on the positions of breakpoints, we could estimate the volatility in each interval. Although the ICSS has an improved version to deal with conditional heteroskedasticity while detecting multiple change points (cf. [Sansó et al., 2003](#)), the use of this latter procedure may make it difficult to estimate the volatility later. This is because we would have to make assumptions about conditional volatility models which might be hard to justify or make our proposed test too complex. Therefore, for simplicity, we only use the original ICSS algorithm in this chapter. In the following paragraphs, we will discuss volatility estimation by using ICSS and ICSS-based explosive tests in detail.

In light of the paper of [Harvey et al. \(2019\)](#), our first approach employs the WLS version of the sup DF test procedure; however, we do not calculate the estimates of σ_t^2 using kernel-based estimator, but using an ICSS based estimator. Our approach is to determine breakpoints of volatility, then estimate the volatility in each interval. Then, we replace σ_t in (2.12) by our estimated volatility. We do this to construct a feasible version of the WLS-based test as in [Harvey et al. \(2019\)](#) and assuming that the ICSS algorithm would be a better approach when discrete volatility shifts occur.

To find the breakpoints in variance, we have to use all the information on the series. Consider a series of uncorrelated random variables with mean 0 and variance $\sigma_t^2 = \sigma_1^2 D_t(1/T, \tau_1) + \sigma_2^2 D_t(\tau_1, \tau_2) + \sigma_3^2 D_t(\tau_2, \tau_3) + \dots + \sigma_N^2 D_t(\tau_N, T)$, where $D_t(a, b) = 1(\lfloor aT \rfloor < t \leq \lfloor bT \rfloor)$, N is the number of breakpoints. In this chapter, the series used

as input to detect multiple breakpoints is Δy_t^2 , $t = 1, \dots, T$. Define the following expression:

$$D_k := \frac{C_k}{C_T} - \frac{k}{T}, \quad k = 0, 1, \dots, T$$

D_k is the centered (and normalized) cumulative sum of squares; $C_k = \sum_{t=1}^k \Delta y_t^2$ is the cumulative sum of $k + 1$ uncorrelated random variables Δy_t . Following the formula above, if the series has a homogeneous variance, the plot of D_k against k will oscillate around 0, and the presence of a structural break is somewhere D_k varies away distinguishably from 0. k/T is a scaling factor to center the cumulative sum of squares. Therefore, the **Inclán and Tiao (1994)**'s test [*IT test*] is developed to find the variation of D_k that is statistically significant, which takes the form below:

Theorem 2.3 *Under the Assumption of $\Delta y_t \sim \text{NIID}(0, \sigma^2)$, **Inclán and Tiao (1994)** show:*

$$IT := \sup_k \sqrt{T/2} |D_k| \xrightarrow{d} \sup_r |W(r) - rW(1)|$$

where $r = \frac{k}{T} \in [0, 1]$.

Inclán and Tiao (1994) also derive the asymptotic distribution of the IT test statistics under a more generalized assumption of Δy_t , in which $\Delta y_t \sim \text{IID}(0, \sigma^2)$ as follows:

Proposition 2.1

$$IT = \sup_k \sqrt{T/2} |D_k| \xrightarrow{d} \sqrt{\frac{\eta_4 - \sigma^4}{2\sigma^4}} \sup_r |W(r) - rW(1)|$$

where η_4 denotes the fourth-moment of Δy_t .

Nonetheless, if using the *IT test* on the full sample, we will only find a single point of change, and this single point may not be the true break. Therefore, we have to use *IT test* statistic together with the iteration algorithm of **Inclán and Tiao (1994)**; the so-called ICSS algorithm. Details of the algorithm will be described below in order to estimate multiple changing points of variance.

Step 1: We calculate the IT test statistic on the closed interval $[1, T]$. The test statistic is roughly derived as the maximal point of a set including the cumulative sum of squares from observations 1 through k , C_k , divided by the total sum of squares of the sample, C_T . Then, the fraction is used to calculate $\sqrt{T/2}D_k$, where $\sqrt{T/2}$ is a scaling factor to make the test statistic converge to the Brownian Bridge process. If this test statistic IT on the interval $[1, T]$ has the maximum value at k_1 and is greater than a predetermined critical value, then we find out one break point at k_1 where D_k establishes the largest value on the examined interval. If the break in variance does not exist, we will stop this algorithm and immediately announce that our series has no break in its variance.

Step 2: We will find a set of breakpoints by using a symmetric procedure on two intervals that are separated by k_1 .

- (a) If a breakpoint is determined in step 1, we continue to this next step. Here, we will determine the breaking point $k_{2,a}$ in the interval $[1, k_1]$ in the same manner as step 1. If $k_{2,a}$ is identified, we will repeat this step to find $k_{3,a}$ as the change point between $[1, k_{2,a}]$ and to apply step 2b to find breakpoints between $[k_{2,a}, k_1]$. Then we will have a set of break points $\{k_{n,a}, \dots, k_{3,a}, k_{2,a}, k_1\}$. Indeed, this step will stop only when no more breakpoints are found, or $k_{n,a} = 1$.
- (b) Similarly, if the breakpoint is determined in step 1, we can come to this step. Here, we will determine the breaking point $k_{2,b}$ in the interval $[k_1 + 1, T]$ as the way in step 1. If $k_{2,b}$ presents, we will repeat this step to find $k_{3,b}$ is the change point between $[k_{2,b} + 1, T]$ and step 2a to find break points between $[k_1 + 1, k_{2,b}]$. Then we will have a set of break points $\{k_1, k_{2,b}, k_{3,b}, \dots, k_{n,b}\}$. Indeed, this step will stop only when no more breakpoint is found, or $k_{n,b} = T$.

Step 3: Total breakpoints found from step 2 is a set $\{k_{n,a}, \dots, k_{3,a}, k_{2,a}, k_1, k_{2,b}, k_{3,b}, \dots, k_{n,b}\}$.

We appended 1 and T into these break point set to have a set $\{1, k_{n,a}, \dots, k_{2,a}, k_1, k_{2,b}, \dots, k_{n,b}, T\}$ which will be used to check spurious break points. In this step, we will apply step 1 to find the breaking point between intervals set by nonconsecutive numbers of the set. For example, we find whether $k_{n,a}$ is the break point of the interval $(1, k_{n-1,a})$, $k_{n-1,a}$ is the break point of the interval $(k_{n,a}, k_{n-2,a})$, and so on. It means we have to apply step 1 on the interval $(k_{n,a}, k_{n-2,a})$ to find the test statistic and compare it with the critical value at a significance level of 5%. If the test statistic is still smaller than the critical value, we eliminate the breakpoint $k_{n-1,a}$. If the test statistic is greater than the critical value, we will consider whether the breakpoint is still determined at $k_{n-1,a}$ or not. If the breakpoint is the same as $k_{n-1,a}$, we keep it. If it is different, we replace it with a new point. This step will run iteratively until no other point is changed or removed.

Inclán and Tiao (1994) use an example to illustrate the steps in the ICSS algorithm. Their data sample includes 700 observations ($T = 700$). As in Figure A-1, after the first iteration to calculate the value of maximum test statistic IT at k_1 , which is greater than the critical value, we then obtain the breakpoint at $k_1 = 342$. This is corresponding to step 1 in the algorithm. Next, the procedure keeps running to find the breakpoints in the first part of the sample, $[1, 342]$ as step 2a. As a result, at this time, the iteration stops at Figure 2a when there is no break point in the interval $[1, 342]$. However, the algorithm still continues on the second half of the sample $[343, 700]$. Figure 2b - 2f is to apply step 2b in the algorithm to find as many breakpoints as possible in this second part. Finally, when no more possible breakpoints are found, the algorithm enters step 3 where possible points are verified. Figures 2g - 2l are to reject false points and confirm true ones. As a consequence, the series shows two break points: one is at 376 and another is at 526. In brief, the ICSS algorithm iteratively computes the test statistic to detect all potential additional breakpoints. It searches for unknown breakpoints in each of the subsamples created by newly found breakpoints. If new breakpoints are no longer found, the search stops. This algorithm can help us to test

the null hypothesis of the constant unconditional variance of y_t against the alternative that unknown breaks exist at some points in the series.

Although the ICSS of [Inclán and Tiao \(1994\)](#) is popular because of its straightforward implementation and satisfactory statistical inferences, recent studies ([Andreou and Ghysels, 2002](#), [Sansó et al., 2003](#) and [de Pooter and van Dijk, 2004](#)) argue that the *IT* test can over-detect the number of change points especially when applied to financial time series. In fact, when designing the *IT* test, [Inclán and Tiao \(1994\)](#) assume that the disturbances of the targeted series are independent and normally distributed, which is highly unlikely for financial time series as they evidently show fat-tailed distributions and serial dependence. Therefore, [Sansó et al. \(2003\)](#) modify the *IT* test by taking into consideration the fourth-moment properties of the data series in [Proposition 2.1](#) along with the conditionally heteroskedastic processes which are not properly addressed in ICSS. However, the modified test of [Sansó et al. \(2003\)](#) requires stronger assumptions about the volatility model, reducing the generality of [Assumption 2.2](#) where we do not know the true form of the volatility function.

After finding the breakpoints, we estimate the persistent volatility $\tilde{\sigma}_t$ by using the standard deviation of Δy_t in each regime. As a result, in each interval of the regime, the estimated volatility is a corresponding constant of $\tilde{\sigma}_t$. Under the same WLS estimation, we replace the kernel-based variance estimator $\hat{\sigma}_t^2$ in [Equation \(2.14\)](#) with our proposed estimator, $\tilde{\sigma}_t^2$ above. From that, we have a different feasible test statistic named $\sup BZ_I$. Following feasible $\sup BZ_K$ test statistics derived in [Equation \(2.14\)](#), a similar feasible test statistic using ICSS-based estimator test is expressed in the form:

$$\sup BZ_I = \sup_{\tau \in [\tau_0, 1]} BZ_{I, \tau} \quad (2.15)$$

$$BZ_{I, \tau} = \frac{\sum_{t=2}^{\tau T} \frac{\Delta \tilde{y}_t \tilde{y}_{t-1}}{\tilde{\sigma}_t^2}}{\sqrt{\sum_{t=2}^{\tau T} \frac{\tilde{y}_{t-2}^2}{\tilde{\sigma}_t^2}}} \quad (2.16)$$

where $BZ_{I, \tau}$ is our new statistic which corresponds to subsample from $y_1, \dots, y_{\tau T}$. τ_0

is the minimum length of the subsample. $\sup BZ_I$ is the maximum of the sequence of subsample statistics, $BZ_{I,\tau}$ with $\tau \in [\tau_0, 1]$. When $\tau = \tau_0$, BZ_{I,τ_0} is the test statistic obtained from the initial recursive subsample (i.e., the shortest subsample). Accordingly, $BZ_{I,1}$ is the full sample test statistic in $\sup BZ_I$ test.

As conjectured at the end of Section 2.5.2, if our variance estimator is consistent, our feasible test statistic has the same limiting properties as an infeasible test statistic in 2.12. However, our proposed test statistic may have finite sample properties differing from that of the test statistic, $\sup BZ_K$, of Harvey et al. (2019). Therefore, it is appropriate to examine the finite sample power profiles of both tests.

2.7 Wild-Bootstrap Test

2.7.1 Wild-Bootstrapped Procedure of HLST

From Section 2.5, we can see that the limit distribution of test statistics (i.e., under both null and alternative) depends on the form of variance in the innovations. In this case, the robustness of the tests is not guaranteed when we compare our test statistic with homoskedastic critical values as usual. Indeed, the size of the test is distorted. Therefore, we here employ the wild bootstrap algorithm as in HLST to bring the information of variance in innovations into the critical values. In this way, the size of the test may be controlled at a nominal significance level. Later, in this subsection, we will use simulatory evidence to show wild bootstrap tests are robust with various time-varying volatility patterns in terms of the size of the test. This is because the test statistics are compared with wild bootstrap critical value, which is calculated from the information of volatility in the data itself.

Applying a bootstrap method can reduce bias and increase the accuracy of inference if the sample does not have the same distribution as assumptions in the standard test. Using that idea, HLST combined the wild bootstrap scheme into the PWY test. This wild bootstrap algorithm is employed to replicate the pattern of heteroskedasticity in the original data. The steps of the algorithm to generate critical

values in the tests are constituted as follows:

Step 1: Generate a wild bootstrap sample by constructing innovations, ϵ_t^b as below and cumulatively summing up those innovations.

$$\begin{aligned}\epsilon_t^b &= w_t \Delta y_t, \epsilon_1^b = 0, \text{ where } w_t \sim \text{NIID}(0, 1), t = 2, \dots, T \\ y_t^b &= \sum_{j=1}^t \epsilon_j^b, y_1^b = 0\end{aligned}$$

Step 2: Using wild bootstrap samples to calculate the sup DF and sup BZ_i test statistics with $i \in \{K, I\}$ from Equations (2.10) and (2.12).

Step 3: Repeat the Step 1 and 2 M times to get sets of test statistics, $\{\sup DF_{1,i}^b, \sup BZ_{1,i}^b\}, \dots, \{\sup DF_{M,i}^b, \sup BZ_{M,i}^b\}$.

Step 4: Obtain the wild bootstrap $\xi\%$ level null critical values $q_\xi^{b,DF}$, and $q_\xi^{b,BZ}$ of sup DF and sup BZ tests, respectively by taking $(1 - \xi)$ quantile of a sequence of M realisation of two test statistics generated under null hypothesis $\{\sup DF_{1,i}^b, \sup BZ_{1,i}^b\}, \dots, \{\sup DF_{M,i}^b, \sup BZ_{M,i}^b\}$. In other words, corresponding to the test statistics, the wild bootstrap tests reject the null hypothesis of a unit root, \mathcal{H}_0 if $\sup DF > q_\xi^{b,DF}$, $\sup BZ_K > q_\xi^{b,BZ_K}$, or $\sup BZ_I > q_\xi^{b,BZ_I}$.

In addition, **HLST** propose a few forms of the volatility function to assess the impact of different volatility specifications on the finite sample local power curves. Those, for example, are the single volatility shift, double volatility shift, a logistic smooth transition in volatility, and trending volatility. Additionally, **Harvey et al. (2019)** consider the case of stochastic volatility which is not involved by Assumption 2.2 since this case is common in empirical finance. Analogously to **Harvey et al. (2019)**, we also consider approximately the same volatility specifications as below for evaluating the reliability of the tests:

- (a) Constant volatility: $\sigma(r) = 1, \forall r$.
- (b) Early upward shift: $\sigma(r) = 1 + 5\mathbb{1}(r \geq 0.3)$.

- (c) Mid upward shift: $\sigma(r) = 1 + 5\mathbb{1}(r \geq 0.5)$.
- (d) Late upward shift: $\sigma(r) = 1 + 5\mathbb{1}(r \geq 0.8)$.
- (e) Early downward shift: $\sigma(r) = 1 + 5\mathbb{1}(r < 0.3)$.
- (f) Mid downward shift: $\sigma(r) = 1 + 5\mathbb{1}(r < 0.5)$.
- (g) Late downward shift: $\sigma(r) = 1 + 5\mathbb{1}(r < 0.8)$.
- (h) Uptrend volatility: $\sigma(r) = 1 + 5r$.
- (i) Downtrend volatility: $\sigma(r) = 6 - 5r$.
- (j) Double shift: $\sigma(r) = 1 + 5\mathbb{1}(0.4 < r \leq 0.6)$.
- (k) Logistic smooth transition in volatility: $\sigma(r) = 1 + \frac{5}{1 + \exp\{-50(r-0.5)\}}$.
- (l) Autoregressive volatility: $\sigma_t = 0.5\sigma_{t-1} + \epsilon_t$, $\epsilon_t \sim NIID(0,1)$
- (m) Stochastic volatility: $d\sigma^2(r) = 0.03(0.25 - \sigma^2(r))dr + 0.1\sqrt{\sigma^2(r)}dW(r)$

where $W(r)$ is a standard Brownian motion process and the model to simulate the stochastic volatility above is called the square root process (considered by [Bollerslev and Zhou, 2002](#)). Here, we use $NIID(0,1)$ to approximate the Brownian motion increments. Additionally, $\mathbb{1}(\cdot)$ denotes the indicator function which have value 1 for domain (\cdot) and 0 otherwise. r is the proportion of t/T . Besides volatility specifications proposed by [Harvey et al. \(2019\)](#) (e.g., cases a), b) d), e), g) h), i), j) and m)), we added more forms of volatility functions including: Case (k) to present a smooth volatility with a midpoint transition and transition speed of 50; and Case (l) to show the presence of serial correlation in the variance of the innovations, u_t in (2.8). Despite not being covered by Assumption 2.2, it is worth considering this latter case since serial correlation in volatility is quite common in financial time series. In the case of stochastic volatility, we argue that the tests are still reliable in these cases because of the employment of a wild bootstrap algorithm. In fact, the wild bootstrap method works well to replicate the non-stationary volatility patterns in the data.

Table A-1 illustrates how the size of sup DF tests is distorted under heteroskedasticity (with the sample size, $T = 200$). The distortions are serious without using wild bootstrap. This is due to the critical values not containing information on heteroskedastic variance in the innovations. However, even after we use a wild bootstrap procedure to control the size, the results still show distorted sizes compared with a significance level of 5% in some cases. Specifically, the wild-bootstrap sup DF is under-sized in cases of downward shift, down-trending volatility, and autoregressive volatility and oversized with upward shift, double shift, and logistic smooth transition in volatility.

Although the sup BZ test whitens the series in the WLS estimation, it still needs the wild bootstrap algorithm to control the size of the test, given the null distribution of the test statistic still depends on the pattern of heteroskedasticity. In Table A-2, the size of sup BZ_K is distorted without the wild bootstrap algorithm. However, after using a wild bootstrap, the sup BZ_K test has the corrected size which is well-controlled under a 5% significance level. These results motivate us to keep using the wild bootstrap in our proposed test, sup BZ_I . Although the main motivation for Harvey et al. (2019) is to increase the power of the PSY test by using WLS estimation to replace OLS estimation inside the supremum test, their proposed method indeed outperforms the PSY test in terms of controlling the size of test. Column 2 in Table A-2 shows the size of the test is well-controlled under a nominal significance level of 5%. The results are robust through many different volatility specifications. Finally, although it is not mentioned in Harvey et al. (2019), from Table A-1 and A-2, we can see that sup BZ_K outperforms sup DF test in controlling the size of the test.

2.7.2 Asymptotic Properties of Wild Bootstrap Tests

In Theorem 2.1 and 2.2, the limiting distribution of the sup DF and sup BZ_i tests (where $i \in K, I$) depend on the unknown volatility path in practice. Hence, to address this limitation, we use the wild bootstrap procedure of HLST to generate bootstrap critical values. From now on, all critical values of sup DF and sup BZ_i tests

are calculated under the wild bootstrap algorithm.

Theorem 2.4 *Let y_t be generated by Equations (2.6) - (2.7) under Assumptions 2.1-2.6, HLST and Boswijk and Zu (2018) show that:*

$$\begin{pmatrix} \sup DF_m^b \\ \sup BZ_{m,i}^b \end{pmatrix} \xrightarrow{w,p} \begin{pmatrix} \mathbb{M}_0^{DF} \\ \mathbb{M}_0^{BZ_i} \end{pmatrix}$$

jointly, for $1 \leq m \leq M$, where $\xrightarrow{w,p}$ denotes weak convergence in probability, $i = K, I$ indicates the variances are estimated by kernel or ICSS method.

Theorem 2.4 shows that as $T, N \rightarrow \infty$ empirical distribution functions of $\sup DF_m^b$ and $\sup BZ_m^b$ calculated from M bootstrap replications converge in distribution to the asymptotic null distributions of the $\sup DF$ and $\sup BZ$ statistics under \mathcal{H}_1 (which includes \mathcal{H}_0 as a special case). Note that the asymptotic validity of the marginal bootstrap $\sup DF$ statistic is shown in HLST, while the marginal convergence of the bootstrap $\sup BZ_K$ statistic is derived by Harvey et al. (2019). As also noted by HLST, when the sample size increases to infinity, the first-order null distribution of the wild bootstrap test statistics is as same as that of the conventional one. However, the usefulness of the wild bootstrap procedure is the ability to control the asymptotic size of the test. Asymptotically, it keeps the size of the test correct because the wild bootstrap p-values are a random variable having asymptotically uniform distribution; therefore, the size will be corrected in the existence of conditional heteroskedasticity as Assumptions 2.1-2.2. Although wild bootstrap-based tests have an advantage in preventing size distortion, if the magnitude of the bubble is non-local to zero (fixed magnitude), the wild bootstrap test will not be as powerful as its original test. Using the same arguments, the finding is shown by HLST below:

Theorem 2.5 *Let y_t be generated by (2.6) - (2.7) under Assumptions 2.1-2.2 and with $\rho_t > 0$. Then, when $T \rightarrow \infty$, $\sup DF = O_p(\lfloor r^* T^{1/2} \rfloor (1 + \rho_t)^{(T - \lfloor r^* T \rfloor)})$, $\sup DF^b = O_p(T^{1/2})$.*

2.7.3 A Union of Rejections Testing Strategy

We consider a union of rejections testing approach following that of [Harvey et al. \(2009\)](#), [Harvey et al. \(2012\)](#), and [Harvey et al. \(2019\)](#). In this way, the rejection decision will be a combination of inferences from two tests. Later, in the simulation section, the union strategy-based test is also applied over various volatility and bubble specifications, analogously to the individual $\sup BZ_K$ and $\sup BZ_I$ tests.

Under Assumptions 2.1-2.6, HLST shows the joint convergence of tests in the Theorem 2.4 given those statistics are calculated from the same wild bootstrap sample. Hence, we also consider a similar union of rejections approach in line with that of [Harvey et al. \(2012\)](#) and [Harvey et al. \(2019\)](#) to combine inference from two chosen tests. Simply put, the union of rejections strategy is to reject if either of the individual tests rejects the null hypothesis. In this section, we focus on combining inference from $\sup BZ_K$ and $\sup BZ_I$ tests, but as the same as [Harvey et al. \(2019\)](#) a combination of inference from $\sup BZ_K$ and $\sup DF$, and that from $\sup BZ_I$ and $\sup DF$ can be constructed and reasoned as the same way.

As Subsection 2.7.1, q_ξ^{b,BZ_K} and q_ξ^{b,BZ_I} denote wild bootstrap critical values of corresponding tests at $\xi\%$ level. These critical values are calculated from the empirical distribution functions of $\sup BZ_{m,K}^b$ and $\sup BZ_{m,I}^b$ obtained from M wild-bootstrap replications, respectively. Our proposed union of rejection decision rule is given by:

$$\mathcal{U} : \text{Reject } H_0 \text{ if } \left\{ \sup BZ_I > q_\xi^{b,BZ_I} \text{ or } \sup BZ_K > \psi_\xi^b q_\xi^{b,BZ_K} \right\}$$

where $\psi_\xi^b = \frac{q_\xi^{b,BZ_I}}{q_\xi^{b,BZ_K}}$ is a scaling constant ensuring \mathcal{U} asymptotically correctly sized. It is chosen to ensure the wild bootstrap size of ξ under \mathcal{H}_0 is well-controlled under a nominal ξ level. As in the Theorem 2.4, the wild bootstrap critical value, q_ξ^{b,BZ_i} with $i \in \{K, I\}$ weakly converges in probability to $q_\xi^{BZ_i}$ which is the asymptotic critical value of the $\sup BZ_i$ test.

Decision rule on union statistic can be written as follows:

$$\text{Reject } \mathcal{H}_0 \text{ when } \rho_t = 0 \text{ if } \mathcal{U} > q_\xi^U$$

where q_ξ^U is the critical value for the union statistic at ξ level and \mathcal{U} presents union statistic,

$$\mathcal{U} = \max \left(\sup BZ_I, \frac{q_\xi^{BZ_I}}{q_\xi^{BZ_K}} \sup BZ_K \right)$$

Therefore, the wild bootstrap of union statistic \mathcal{U}_m^b is given by:

$$\mathcal{U}_m^b = \max \left(\sup BZ_{m,I}^b, \frac{q_\xi^{b,BZ_I}}{q_\xi^{b,BZ_K}} \sup BZ_{m,K}^b \right)$$

Consequently, we can prove that $\mathcal{U}_m^b \xrightarrow{p} \max \left(\mathbb{M}_0^{BZ}, \frac{q_\xi^{b,BZ}}{q_\xi^{b,BZ}} \mathbb{M}_0^{BZ} \right) = \mathbb{M}_0^{BZ}$ by using continuous mapping theorem. From that, as in [Harvey et al. \(2019\)](#), a feasible version of \mathcal{U} can be derived when we reject \mathcal{H}_0 when $\mathcal{U} > q_\xi^{b,U}$, where $q_\xi^{b,U}$ is the wild bootstrap critical value of the union test and

$$\mathcal{U} = \max \left(\sup BZ_I, \frac{q_\xi^{b,BZ_I}}{q_\xi^{b,BZ_K}} \sup BZ_K \right) = \max \left(\sup BZ_I, \psi_\xi^b \sup BZ_K \right)$$

Remark 2.4 *In practice, we do not need to calculate the scaling constant and just use the wild bootstrap version of the test to obtain the critical value. In each bootstrap replication, we compute the bootstrap version of $\sup BZ_I$ and $\sup BZ_K$ and take the maximum to give you the value of the \mathcal{U} for that replication. Then, we repeat this M times and take the quantile of your M bootstrap stats to get the critical value. Consequently, the wild bootstrap procedures are size corrected in the limit under \mathcal{H}_0 , and inherit exactly the same asymptotic local power functions under \mathcal{H}_1 .*

Because the limit distribution of the test is identical given our proposed variance estimator is as consistent as the kernel-based estimator of [Harvey et al. \(2019\)](#); we

can compute the scaling factor of the union test, $\frac{q_{\xi}^{b,BZ_I}}{q_{\xi}^{b,BZ_K}} = \psi_{\xi}^b = 1$ in a large sample. In this chapter, we actually run the asymptotic size of the test controlled under 5% and the scaling factor is approximately equal to 1, with $\epsilon > 0$. Furthermore, under conditions of having consistent variance estimators, the limit distribution of $\sup BZ_I$ is as same as that of $\sup BZ_K$. As a result, the power profile of \mathcal{U} is identical to the profile of $\sup BZ$.

Although $\sup BZ_K$ and $\sup BZ_I$ will have the same asymptotic properties under the condition that the estimated variance in WLS estimation has to be unbiased. It is worth establishing a union of rejections strategy of those two to see how it can improve the power of the test by capturing the respective finite sample power advantages of both variants WLS-based test.

2.8 Finite Sample Properties

In this section, we will evaluate the finite sample size and power properties of tests using Monte Carlo simulations. Specifically, our main purpose is to compare two wild bootstrap tests, BZ_K and BZ_I and union strategies, \mathcal{U} , which combine rejection decisions from two $\sup BZ$ tests. In order to do so, data are simulated following the DGPs from (2.6) to (2.8) with the finite volatility function σ_t given one of cases (i.e., a-m) in Subsection 2.7.1. Of course, \mathcal{H}_0 (with $\rho_t = 0$) is used to investigate the size of the test (i.e. falsely rejecting the null hypothesis), and \mathcal{H}_1 (with $\rho_t > 0$) is applied to examine the power properties. All the results are calculated at the nominal asymptotic 0.05 level (i.e., $\xi = 0.05$).

The length of finite sample simulations is chosen as $T \in \{100, 200, 400\}$ and ϵ_t are generated as $NIID(0,1)$. For ease of comparison between our test and those of [Harvey et al. \(2019\)](#), we have chosen the same break fractions (r^*) as in their study: 0.6 for the long explosive in-sample period and 0.8 for the short explosive end-sample period. Volatility specifications used are the same that we present at the end of Section 2.5. Furthermore, we here use a grid of values $c \in [0, 20]$ for both $r^* = 0.6$

and $r^* = 0.8$. This is different from what [Harvey et al. \(2019\)](#), in which a grid of values $c \in [0, 8]$ is used as an x-axis to show the power curve of a long explosive in-sample bubble, and $c \in [0, 20]$ only for short-lived bubble. This is because we intend to show how power reversal, the non-monotonic power curve, occurs in both cases as long as the magnitude of bubbles is relatively large, in which we emphasize the advantage of our proposed test compared to its counterparts. In addition, we use 1,000 Monte Carlo replications to simulate results. Each test uses $M = 499$ wild bootstrap replications to calculate the bootstrap critical value. Although the number of Monte Carlo simulations and wild bootstrap steps seems relatively small, those are sufficient to give robust results according to [Harvey et al. \(2019\)](#). Moreover, following the recommendation of [PWY](#), the minimum window size is selected as $\tau_0 = 0.01 + 1.8/\sqrt{T}$. In this chapter, since the innovations, ϵ_t is unknown, we consider Δy_t^2 as ϵ_t^2 , which is used as a single input to find the breaks in the volatility and estimate the volatility of ϵ_t . Indeed, both the kernel-based volatility estimator of [Harvey et al. \(2019\)](#) and our ICSS-based volatility estimator use Δy_t^2 as approximately ϵ_t^2 .

In terms of kernel-based volatility estimator, there are many different kernel functions (e.g., Gaussian, Uniform, Triangle, Epanechnikov, Biweight, Triweight, etc), which can be used to estimate $\hat{\sigma}_t^2$; however, Gaussian kernel is the most commonly used and is employed by [Harvey et al. \(2019\)](#):

$$K(s) = \frac{1}{\sqrt{2\pi}} \exp\left(-\frac{s^2}{2}\right)$$

The bandwidth h is determined by using a standard leave-one-out cross-validation bandwidth selection procedure:

$$CV(h) = \sum_{t=2}^T ((\Delta y_t)^2 - \hat{\sigma}_{t,-}^2)$$

with $\hat{\sigma}_{t,-}^2$ denotes Gaussian kernel-based variance estimator $\hat{\sigma}_{t,-}^2$ with $K(0) = 0$, the

optimal bandwidth is chosen as below:

$$h_{cv} = \arg \min_{h \in [h_l, h_u]} CV(h)$$

Harvey et al. (2019) set $h_l = 1/(2T)$ and $h_u = 1/6$, ensuring the interval of observations for kernel weights ranges from 3 to T .

After running Monte Carlo simulations on differing specifications of volatility and explosive processes, we construct the size and power of tests. Those results are grouped by the specific finite sample sizes. We can read the results of the size of tests by observing tables or looking at the power curve at 0. The power curves of tests are in figures, in which the y-axis presents the rejection rate and the x-axis shows the magnitude parameter of the bubble, c . When $c = 0$, it implies \mathcal{H}_0 model; otherwise, model of \mathcal{H}_1 .

To begin, note that Table A-3 shows the size of tests with a sample size of 100, while Figures (A-3) and (A-4) show finite sample local power curves with the bubble originating in the sample at $r^* = 0.6$, and 0.8, respectively. Overall, the size of BZ tests is controlled better than $\sup DF$ test, and $\sup BZ_I$ is more stable and has higher power than $\sup BZ_K$.

Looking in more detail, we can see in Table A-3 that the size of $\sup DF$ test is distorted badly in cases of a mid upward shift in volatility - (A-3c), (A-4c), late upward shift in volatility - (A-3d), (A-4d), down-trending volatility - (A-3i), (A-4i), a double shift in volatility - (A-3j), (A-4j), logistic smooth transition - (A-3k), (A-4k), and autoregressive volatility - (A-3l), (A-4l). Despite that, whitening the series may lose partly information on the explosive behaviour as in the case of late upward shift (A-3d and A-4d) and uptrend volatility (see Figures (A-3h) and (A-4h)). In those cases, the $\sup DF$ test has higher power than $\sup BZ$ tests. Potentially, a union strategy between $\sup DF$ and $\sup BZ$ tests can save this case.

In cases a), b), c), e), f), h), i), j), k), l), and m) of both Figures (A-3) and (A-4), the power curves of $\sup BZ_K$ bear close resemblance to $\sup BZ_I$ when the magnitude of the bubble is small. Then, the power of the $\sup BZ_K$ test reduces markedly after

that given the magnitude of the bubble becomes relatively large compared with its sample size. As mentioned by [Harvey et al. \(2019\)](#), the size of the bubble causes the estimated volatility (using non-parametric estimation) to be inflated and significantly biased. When the volatility shift appears later in the sample - Figures ([A-3d](#)) and ([A-4d](#)), the power of $\sup BZ_K$ test is low compared to the two other tests. Similarly to the bubble starting close to the end of the sample, the power curve of $\sup BZ_K$ also has an inverted U-shape; however, this non-monotonic representation in the local power curve is more severe in the case of the short-lived bubble. In such cases, the power reversal appears nearly everywhere in volatility patterns and the power of the $\sup BZ_K$ test is significantly low even when volatility is homoskedastic.

In contrast, in the case of the long-lasting bubble (Figure [A-3](#)), except for case ([A-3e](#)) of early downward shift, the curves of $\sup BZ_I$ test are still monotonic and outperform $\sup DF$ test. Overall, the $\sup BZ_I$ is more robust and powerful than $\sup BZ_K$; therefore, the union strategy \mathcal{U} profile is dominated by $\sup BZ_K$. In that regard, a union strategy combining $\sup BZ_I$ and $\sup BZ_K$ test provides the power curve on par with the $\sup BZ_I$ with the well-controlled size. Only in the case of autoregressive volatility does the union strategy \mathcal{U} becomes useful to improve power. Although both $\sup BZ$ tests have non-monotonic power profiles, the number of cases having power reversals in $\sup BZ_I$ are far less than those of $\sup BZ_K$: 4/13 cases for the former and 13/13 cases for the latter.

Table [A-4](#) presents the size of the tests with a sample size of 200. Overall, the size of $\sup BZ$ tests and union strategy, which combines $\sup BZ_I$ and $\sup BZ_K$ are well-controlled under a nominal significance level of 5%; however, as the size of $\sup DF$ test is still distorted in some volatility specifications (e.g., family of upward shift, double shift, and logistic smooth transition). In these cases, the $\sup DF$ test is easy to detect spurious bubbles in the data. Compared to Table [A-3](#), except for a few mentioned cases of $\sup DF$ test and an under-sized case (in early downward shift) of $\sup BZ_I$, the size of the tests tend to converge closer to the nominal significance level.

In the Figure ([A-5](#)), when bubble originates in the sample at $r^* = 0.6$ and $T = 200$,

we find that the power of bootstrap $\sup BZ_I$ test is always on a par with its counterpart ($\sup BZ_K$) in cases (A-5a), (A-5b), (A-5c), (A-5h), (A-5j), and (A-5k). In cases (A-5d), and (A-5g), our $\sup BZ_I$ test outperforms the $\sup BZ_K$ test. Under several volatility specifications (A-5e, A-5f, A-5i, A-5l, and A-5m) while the power envelope of our proposed test ($\sup BZ_I$) is monotonic, the power of $\sup BZ_K$ tends to be reversed when the magnitude of the bubble is getting larger. (A-5d) and (A-5h) are two cases showing WLS-based tests seem to be slightly less powerful than $\sup DF$ test, but also in the former case, the size of $\sup DF$ test is seriously distorted. For the case (A-5l) where series contains serially correlated volatility, our test ($\sup BZ_I$) is less powerful than the $\sup BZ_K$ test of Harvey et al., (2019) and $\sup DF$ test. A lower power curve occurs when the bubble magnitude parameter c stays from 5 to 20. However, by using the union strategy, we can improve the power of the test $\sup BZ_I$ and also save the power reversal of $\sup BZ_K$ in the case of autoregressive volatility. In comparison with the $\sup DF$ test of HLST, WLS-based tests ($\sup BZ_K$ and $\sup BZ_I$) control the size better. All sizes of BZ tests are controlled at the nominal asymptotic 0.05 level while sizes of $\sup DF$ test are distorted in many cases (e.g., mid upward shift, late upward shift, double shift, and logistic smooth transition).

Figure (A-6) demonstrates that while the power of the wild bootstrap $\sup BZ_K$ test is non-monotonic in all cases, the $\sup BZ_I$ test is still robust across different magnitudes of the short bubbles living at the end of the sample ($r^* = 0.8$). Harvey et al. (2019) explain that the estimates of σ^2 are inflated when c/T is large. For small c , the power of $\sup BZ_K$ test is significantly better than that of $\sup DF$ test in scenarios of downward shifts in volatility (Figures (A-6e), and (A-6f)), down-trending volatility (A-6i) and double shift in volatility (A-6j); however, in the same cases, the power of $\sup BZ_K$ test reverse for large c .

As we can see, although the union strategy increases the power of the $\sup BZ_K$ and $\sup BZ_I$ tests when volatility is autoregressive, in almost all of the other cases the union profiles are identical to the $\sup BZ_I$ test. The case of (A-6d) shows the significant outperformance of the $\sup DF$ test compared with the WLS-based tests,

but in this case, the sup DF test is the most oversized. Overall, when the bubble exists at the end of the sample, the sup BZ_I and \mathcal{Z} tests are robust and have higher power than sup DF in most cases, but under finite sample size, sup BZ_K seems unsuitable in this type of bubble.

From Table A-5, we can see WLS-based tests (sup BZ_K and sup BZ_I) keep the size well close to the normal 0.05 level of significance. Similarly, the size of the \mathcal{Z} test is also well-controlled. However, the size distortion of the sup DF test still obviously occurs in scenarios of upward shift and double shift in volatility.

In Figure (A-7), we examine the powers and sizes of the tests with the presence of a bubble in the sample ($r^* = 0.6$) as simulations in Figures (A-5) and (A-3), but now we use the larger sample size ($T = 400$). Under homoskedastic volatility, none of the tests is significantly better than the others. In terms of heteroskedastic volatility, similar to the profiles in (A-5), for relatively small c , the sup DF test has less power than sup BZ_K and sup BZ_I in almost all cases (A-7b), (A-7c), (A-7e), (A-7f), (A-7g), (A-7i), (A-7j), and (A-7k). Although in case (A-7l), sup BZ_K test outperforms sup BZ_I test, in the case of late upward shift (A-7d) and late downward shift (A-7g) in volatility, sup BZ_I test is more powerful. In addition, power reversals of the sup BZ_K test still appear in two first cases of downward shift (A-7e and A-7f). These cases show the obvious drawbacks of the sup BZ_K when the magnitude of the bubble is large. Finally, while profiles of \mathcal{Z} test are dominated by sup BZ_I in almost all cases, it is good to use to boost the power of the test in the case of autoregressive volatility.

In terms of the short-lived bubble at the near end of sample (A-8), the power reversals of sup BZ_K tend to improve when the sample size doubly increases. Yet the power is still very much lower than its counterparts when the magnitude of the bubble is large. Many cases show the size distortion of sup DF , but the case of a late upward shift in volatility is the most obvious. Also, this upward shift case and uptrend volatility provide solid evidence of outperformance of sup DF compared with WLS based tests, where the power of sup DF is significantly higher than sup BZ

tests. That is the reason [Harvey et al. \(2019\)](#) still keep $\sup DF$ and combine it with $\sup BZ_K$ tests to create the union of rejection strategies. In all cases, (A-8e) and (A-8f) the power curves of $\sup BZ_I$ are monotonic and do not reverse when c is large.

Since the power of $\sup DF$ test is higher than $\sup BZ$ tests, we may construct union rejection strategies between $\sup DF$ and each $\sup BZ$ test. Similar to the strategy of \mathcal{U} test in Subsection 2.7.3, our new strategies will have the decision rules as follows:

$$\begin{aligned}\mathcal{U}_K : & \quad \text{Reject } H_0 \text{ if } \left\{ \sup BZ_K > q_\xi^{b,BZ_K} \text{ or } \sup DF > \psi_{\xi,K}^b q_\xi^{b,DF} \right\} \\ \mathcal{U}_I : & \quad \text{Reject } H_0 \text{ if } \left\{ \sup BZ_I > q_\xi^{b,BZ_I} \text{ or } \sup DF > \psi_{\xi,I}^b q_\xi^{b,DF} \right\}\end{aligned}$$

where $\psi_{\xi,K}^b$ and $\psi_{\xi,I}^b$ are constant scaling factors which respectively make \mathcal{U}_K and \mathcal{U}_I asymptotically correctly sized. $q_\xi^{b,DF}$ is wild-bootstrap critical value of $\sup DF$ test. Based on the same arguments in Subsection 2.7.3, union statistics are given accordingly,

$$\begin{aligned}\mathcal{U}_K &= \max \left(\sup BZ_K, \psi_{\xi,K}^b \sup DF \right) \\ \mathcal{U}_I &= \max \left(\sup BZ_I, \psi_{\xi,I}^b \sup DF \right)\end{aligned}$$

Figure A-9 illustrates how \mathcal{U}_K and \mathcal{U}_I union tests boost the power of the $\sup BZ$ tests in the case of a late upward shift in volatility and the bubble is short-lived near the end of the sample. The new union strategy tests, which combined rejection decisions of $\sup DF$ and $\sup BZ$ tests, are slightly oversized as in Table A-6. The union strategy indeed improves the power of $\sup BZ$ tests. The results from the figures are not surprising when the power curve of \mathcal{U}_K seems matched with \mathcal{U}_I although the power of $\sup BZ_K$ test is significantly lower than $\sup BZ_I$ test. This is because the power profiles of \mathcal{U}_K and \mathcal{U}_I are dominated by the profile of the $\sup DF$ test. Despite those results, we do not recommend using the union strategy in every scenario, this is because we always have to trade off a little bit of size distortion for a higher power.

2.9 Empirical Illustrations

2.9.1 Data

In this section, we apply the mentioned wild bootstrap test statistics as introduced in Section 2.8 (i.e., $\sup DF$, $\sup BZ_K$, $\sup BZ_I$, \mathcal{U} , \mathcal{U}_K , and \mathcal{U}_I) to two datasets with three different sampling frequencies (i.e., daily, weekly, and monthly). The datasets include (the logarithms of) the inflation-adjusted S&P 500 index from January 1980 to March 2000 and FTSE 100 index from December 1985 to December 1999. These two series are in the same sample periods with the data used by [Homm and Breitung \(2012\)](#) and [Harvey et al. \(2019\)](#). Series adjusted for stock splits and dividend distributions are obtained from Yahoo Finance while the Core Consumer Price Index (CPI¹) is retrieved from the Federal Reserve Bank of St. Louis database to compute the real indexes. Since the CPI data is collected at a monthly frequency, we cannot adjust inflation directly in weekly and daily indexes; therefore, as [Homm and Breitung \(2012\)](#) we linearly interpolate the CPI data. After interpolation, we subtract from all the data the initial value. In this manner, we are using the *GLS* demeaning method on the series, with all the series starting from zero. Descriptive statistics of series by their frequencies can be found in Table A-7. The last column shows a number of breaks in volatility which are found by using the ICSS algorithm.

Figures A-10 and A-11 show graphically the series for (the logarithm of) the real S&P 500 index and real FTSE 100 index. respectively. Unsurprisingly, the figures show that the higher frequency of the sample, the more each series varies in terms of price and return. As we can see in Figures a), b) and c) below, the series is supposed to show the origination phase of the bubble only since visually the prices increase during the period considered and reach their peaks at the sample endpoints. In fact, the sample period coincides with the timeline during which the Dotcom bubble existed as discussed and analyzed by [Homm and Breitung \(2012\)](#). In the considered

¹Consumer Price Index for All Urban Consumers: All Items Less Food and Energy in U.S. Monthly, Seasonally Adjusted

period, we can see a flash crash - Black Monday 1987. This may or may not affect our test results; however, so the sample periods and data match with those in [Homm and Breitung \(2012\)](#) and [Harvey et al. \(2019\)](#), we do not remove the crash. In addition, since we estimate the volatility for sup BZ tests, Figures [A-10g-l](#) and [A-11g-l](#) show how our estimates approximate clustering volatility and generalize the shape of squared log returns.

Overall, when estimating the variance of the stock price, while the estimated variances based on the kernel estimator display a smooth line that follows the fluctuation of the squared log return, the ICSS-based estimates of variances are represented as a step function. It means the former will vary in each time step, but the latter will only change after an interval of time. Both kinds of volatility estimators depend on the frequency of the data. This can be seen when we observe their shape in each frequency. For instance, at a monthly frequency, the kernel-based estimated variances tend to be very smooth, and the variance also changes less under the ICSS-based estimator. In S&P 500 index, the ICSS algorithm detects 4 break points in the monthly volatility, 9 breaks in the weekly volatility, and 11 breaks in the daily volatility. Similarly, in the FTSE 100 index, when the frequency of data increases, the number of detected breaks also increases. The monthly FTSE 100 data has 2 breaks, there are 4 breaks in the weekly data, and 16 breaks in daily data (see [Table A-7](#)).

2.9.2 Testing for Explosive Bubbles

We apply six tests including sup DF , sup BZ_K , sup BZ_I , \mathcal{U} , \mathcal{U}_K , and \mathcal{U}_I to six series i.e., the two indexes with three time frames for each. The results are presented in [Table A-8](#).

Examining the S&P 500 index, we can see sup BZ_K and sup BZ_I have the same conclusion; the existence of a bubble in the sample at all frequencies at the 0.05 level of significance. Strikingly, the sup DF fails to reject the null hypothesis in all cases given sup DF test has relatively little power to detect the explosiveness in the series. The conclusions from sup DF and sup BZ_K also match with those shown by [Harvey](#)

et al. (2019). Under the union of rejection strategy, the combined sup BZ tests, \mathcal{U} , confirm the results obtained from sup BZ_K and sup BZ_I tests. \mathcal{U}_K and \mathcal{U}_I also provide the same conclusion of a bubble in S&P 500; however, the p-value shows slightly weaker evidence compared with those of sup BZ tests and \mathcal{U} . In fact, \mathcal{U}_K rejects the null hypothesis of no bubble at a significance level of 10% instead of 5%. From that we may argue that BZ tests are a bit oversized but the power is still dominated by sup BZ tests, meaning the union strategies \mathcal{U}_K and \mathcal{U}_I have slightly lower power than a single sup BZ test.

Examining the FTSE 100 index, the higher frequency of the data, the smaller the p-values of sup BZ and \mathcal{U} strategy-based test. This means the BZ -based tests and corresponding \mathcal{U} tests tend to reject the null hypothesis of a non-existing explosive process at a higher level of frequency. Our proposed test, the sup BZ_K test, and \mathcal{U} test cannot reject the null hypothesis in favor of the existing explosive bubble at weekly and monthly frequencies at the 5% significance level, while the results of the sup DF tests fail to reject the null hypothesis in all frequencies at a significance level of 10%. While sup BZ_I finds weak evidence of the bubble in the daily FTSE 100 index, the sup BZ_K test rejects the null hypothesis of no bubble in the price series at a 5% significance level. The results of \mathcal{U}_I fail to reject the null hypothesis of the unit root process and are consistent under all frequencies. Finally, although \mathcal{U} and \mathcal{U}_K tests fail to reject the presence of unit root process under monthly data, those tests reject when data is at a daily frequency.

In conclusion in Harvey et al. (2019), the sup BZ_K test and its union strategy-based test actually work better than the sup DF test in detecting the bubble in stock price. However, the results are mixed over different frequencies. If we choose the daily data as the norm, then our proposed test sup BZ_I and sup BZ_K provide the same conclusion about the existence of a bubble in both S&P 500 and FTSE 100 series. However, empirical results in our test are more robust to different frequency levels of the data. Historically, it confirms that those tests can early detect the bubble in the origination phase before it bursts.

2.10 Conclusion

In this chapter we propose a wild bootstrap WLS-based variant of the sup DF test, which is different from the sup BZ_K test of [Harvey et al. \(2019\)](#), for explosive bubbles in a financial time series. In particular, the new test aims to be suitable when volatility shifts are discrete. In line with [Harvey et al. \(2019\)](#), we estimate the volatility and scale them out from the price series before testing for explosiveness; however, instead of using a kernel-based estimator, we estimate the volatility in each regime where those regimes are divided by breakpoints found from the ICSS algorithm. In that regard, our test aims to improve the power of the test of [Harvey et al. \(2019\)](#) in the case of small sample sizes and when the magnitude of the bubble is relatively large. Although the new test employs a WLS-based estimator, robust to heteroskedasticity inside a forward recursive mechanism, we still employ the wild bootstrap algorithm, proposed by [HLST](#), to control the size of the test under time-varying volatility.

In comparison to the wild bootstrap sup DF test, our proposed test (the sup BZ_I) controls the size of the test better and in most cases, our test has better power. Additionally, when compared to the sup BZ_K test of [Harvey et al. \(2019\)](#), the new test better handles power reversals when the magnitude of the bubble is large and the bubble exists in a small sample. From this perspective, our proposed test has the monotonic power curve under finite-sample simulations, especially when the bubble is short-lived near the end of the sample. Nonetheless, the power profile of our test is slightly behind compared with sup BZ_K of [Harvey et al. \(2019\)](#) in the case of autoregressive volatility but a union of rejections strategy (combined sup BZ tests) helps us to improve the power. Moreover, although WLS-based estimators have significant advantages compared with sup DF test in retaining correct asymptotic size when volatility has a late upward shift we have to use another union strategy combining rejection decisions between sup DF and sup BZ test to improve the power of sup BZ test. Finally, by applying the tests to logarithmic real FTSE 100 and S&P 500 stock price data, we show the ability to detect explosive autoregressive behaviour in

practice. Since the sup BZ tests, including the new test, reject the null hypothesis of the unit root process when the sup DF test does not, we show the relatively improved ability of such tests to detect bubbles during the origination phase.

There are several directions in which to conduct new research conditional on the findings in this chapter. For example, we could replace the forward recursive supremum by backward recursive or double supremum mechanism as in [PSY](#) to conduct the explosive test in the presence of multiple collapsing bubbles. Moreover, the bubble test using CUSUM test statistics in [Homm and Breitung \(2012\)](#) can be modified to consider heteroskedasticity using volatility estimators. We will discuss these in more detail in [Chapter 5](#).

Testing Co-explosive Behaviour Using Backward Supremum Approach

In the work of [Evrpidou et al. \(2022\)](#) co-explosive behaviour, also termed co-bubbling, occurs when a linear combination of two explosive price series is stationary across all sub-regimes. To detect co-explosive behaviour in pairs of asset prices, in this third chapter, we propose a backward supremum KPSS-based test, which is an extension of the test proposed in [Evrpidou et al. \(2022\)](#). Unlike the approach used by [Evrpidou et al. \(2022\)](#) where they compute their test statistic on the full sample data, our method involves calculating the supremum value of a series of [Evrpidou et al. \(2022\)](#)'s test statistics, where each test statistic is computed on a subsample of the data. Notably, the new test has advantages over the test of [Evrpidou et al. \(2022\)](#) in capturing short-lived periods where co-bubbles are absent. This is essential because, in practice, policymakers usually require a quick and accurate evaluation of the market (e.g., co-bubble in two asset prices) based on the available data. Analogously to [Evrpidou et al. \(2022\)](#), the new test employs a wild bootstrap algorithm to control the size of the test under heteroskedasticity and uses a long-run variance estimate to deal with over-rejections caused by serial correlation. We demonstrate through finite sample simulations that the new test exhibits superior power properties to the test proposed by [Evrpidou et al. \(2022\)](#) in almost all bubble and innovation

specifications. However, the proposed approach is still oversized in a few cases of heteroskedasticity where the variance of the innovations exhibits a downward shift, downward trend, or double shift.

In this chapter, we also conduct an empirical application using the same dataset of precious and non-ferrous metal spot and futures prices as [Evripidou et al. \(2022\)](#). In contrast to the simulation section, here can run both single and double supremum-based tests to compare with the full sample KPSS-based test without much concern about computational power. In fact, a double supremum test is a series of recursive tests that examine a range of flexible windows by changing the starting points. This enables the test to cover a larger number of ranges, but it also results in significant time complexity. As a result, we find evidence of co-bubbles in pairs of metal prices such as Lead/Tin, Tin/Silver, Silver/Lead, Copper/Tin, Copper/Silver, Copper/Lead, Gold/Tin, Lead/Gold, Copper/Gold, Palladium/Nickel, and Platinum/Gold, but reject the co-bubbling of Nickel/Zinc and Copper/Platinum, which were reported by [Evripidou et al. \(2022\)](#). Additionally, with the same method as in [Evripidou et al. \(2022\)](#), we demonstrate how to identify the timing of explosive behaviour migration by using estimated regression residuals.

3.1 Introduction and Literature Review

Detecting asset price bubbles at a particular point in time is a widely studied topic. In the past, well-documented bubbles such as the Dot-Com bubble, the US housing market bubble, the US stock price bubble, and the Asian exchange rate bubble have caused significant economic damage. Therefore, it is of interest to many economists and researchers to detect these bubbles as early as possible to minimize the harm caused by their subsequent collapse.

The study of explosive behaviour in asset prices has led to various explanations and models of their existence in the literature, such as rational bubbles, irrational exuberance, and herd behaviour. However, rational bubbles, as described by [Phillips](#)

et al. (2011) [PWY hereafter], perhaps are the most prominent. The concept of rational bubbles was first mentioned in early research papers by *inter alia* Tirole (1982), Diba and Grossman (1988), Flood and Hodrick (1990), and Garber (1990). According to Homm and Breitung (2012), these papers describe rational bubbles as a discrepancy between the actual market price of an asset and the price that would be expected based on rational expectations. This discrepancy occurs because the fundamental price model does not account for arbitrary and self-fulfilling elements in expectations.

A natural approach to identifying rational bubbles is to determine a structural change from a random walk to an explosive process. In light of this, a number of econometric methods for asset price bubble detection have been proposed; for instance, variance bounds tests (LeRoy and Porter, 1981 and Shiller, 1981), West (1987)'s two-step test, applications of full sample left-tailed unit root and cointegration tests Diba and Grossman (1988), fractionally integrated models (Cuñado et al., 2005 and Frömmel and Kruse, 2012). Gürkaynak (2008)'s review revealed that such bubble tests are not effective in distinguishing between misinterpreted fundamentals and bubbles. In fact, Gürkaynak (2008) argues for every bubble test above that there is a counterargument disputing the bubble interpretation. Thus, these tests do not provide clear evidence of the existence of bubbles. Nonetheless, these tests help us understand important stylized facts regarding the areas in which the present value model of stock prices fails.

Subsequently, PWY as well as Phillips et al. (2015) [PSY hereafter] introduced an autoregressive approach to bubble testing and proposed recursive tests that determine the presence of bubbles in a price series by examining whether it contains an explosive autoregressive component that the corresponding fundamentals series does not exhibit. These tests have gained significant popularity in empirical studies. Accordingly, the PWY and PSY procedures and their variants that use the recursive procedure are applied to detect bubbles in various kinds of assets such as commodity prices (Gilbert, 2010; Homm and Breitung, 2012; Gutierrez, 2012; Etienne et al., 2014;

Figuerola-Ferretti et al., 2015; Figuerola-Ferretti and McCrorie, 2016; Harvey et al., 2016 [HLST hereafter]), housing prices (Yiu et al., 2013; Jiang et al., 2015; Pavlidis et al., 2016; Engsted et al., 2016; Shi et al., 2016; Greenaway-McGrevy and Phillips, 2016, Shi, 2017; Gomez-Gonzalez et al., 2018), energy markets (Bohl et al., 2013; Sharma and Escobari, 2018, Caspi et al., 2018), stock prices (PWY, PSY, Escobari et al., 2017; Deng et al., 2017; Astill et al., 2017), and cryptocurrency markets (Hafner, 2018 and Corbet et al., 2018).

According to Evripidou et al. (2022), despite a large amount of research on bubble detection in individual price series, there is relatively little literature on modelling the relationship between explosive price series. It is crucial for those in charge of managing risks, portfolios, and monetary policies to comprehend the potential connection between bubbles in various markets. An essential question to consider is whether bubbles in one market have a likelihood of spreading to another market, as this would increase their systemic risk to the financial sector as a whole compared to if they remained isolated. In recent research, Phillips and Yu (2011) used PWY's procedure to estimate the origination and collapse dates of bubbles in the housing, oil, and bond markets. By placing the estimated dates on a timeline, the results of Phillips and Yu (2011) suggest that the subprime crisis spread to the oil and bond markets. In another study, Pavlidis et al. (2016) used the tests proposed by PSY to detect multiple bubbles in the housing market indicators of the OECD (Organisation for Economic Co-operation and Development) countries. They demonstrated that the synchronization of the origination and collapsing of the bubbles are related to global macro and financial factors by using macroeconomic variables to predict the probability of a rational bubble in a probit model. Engsted and Nielsen (2012) and Engsted et al. (2016) show that the hypothesis of a rational bubble can be tested in the context of a co-explosive and cointegrated vector autoregression. By capturing that idea to provide a new framework for testing bubble migration across markets, Evripidou et al. (2022) developed a KPSS-based test to determine co-bubble behaviour and extended it to lead/lag cases to understand the bubble migration of

paired asset prices. They argued that if two series exhibit co-bubble behaviour, there exists a linear combination of the series integrated of order zero, $I(0)$. Therefore, applying a stationary test, such as the KPSS test, on the residuals obtained from a linear regression of the two corresponding series will reveal the co-bubble behaviour of the series. Additionally, the test can provide information on bubble migration between asset prices if we test the co-bubble behaviour on residuals obtained by regressing a price series (y_t) on lags/leads of another price series (x_t). To elaborate, if we fail to reject the stationarity of the residuals from regressing y_t on the lag of x_t , we can conclude that the explosive behaviour migrates from x_t to y_t . Similarly, if we fail to reject the stationarity of the residuals from regressing y_t on the lead of x_t , we can infer that the explosive behaviour migrates from y_t to x_t . Furthermore, the lead and lag values provide an estimate of the time it takes for migration to occur between the two series.

In this chapter, we extend the work of [Evripidou et al. \(2022\)](#) to test the co-bubble behaviour of asset price series. However, we focus on the case when the co-bubble is short-lived at the end of the sample; therefore, the mechanism of our co-bubble test developed here allows for backward recursive regressions on the subsamples of the data as proposed by [PSY](#). In this regard, our method should have more power to detect a short-lived departure from the co-bubble hypothesis at the end of the sample than the full sample test of [Evripidou et al. \(2022\)](#). This is because recursive tests that run through subsamples are more flexible and informative about the points where the observations change from a unit root behaviour to explosive behaviour. In particular, backward recursive tests are more powerful than forward recursive tests to detect bubbles at the end of the sample. To evaluate the size and power of the tests, we perform simulations of both our new test and the Evripidou test on a modified co-bubble model. Our null hypothesis (H_0) model is the same as in [Evripidou et al. \(2022\)](#), which assumes the presence of a co-bubble in two series. In contrast, under our alternative hypothesis (H_1) model, instead of assuming no co-bubbling throughout the entire sample, we only assume no co-bubbling near the

end of the sample. Since financial data is known to exhibit non-constant volatility and serial correlation in the innovations, we also apply the wild bootstrap procedure of [HLST](#) to reduce size distortions when volatility is non-constant and use a long-run variance estimator to control for possible serial correlation in the innovations as in [Evrpidou et al. \(2022\)](#).

Through Monte Carlo simulations, we evaluate the size and power performance of our tests on bubbles that start at the end of the sample under various volatility specifications. As in [Evrpidou et al. \(2022\)](#), we also use a wild bootstrap procedure to generate critical values for the tests because we cannot depend on the homoskedastic critical values of KPSS to ensure the robustness of the test in subsamples under heteroskedastic cases. Overall, our finite sample simulation results show that our test has greater finite sample power than that of [Evrpidou et al. \(2022\)](#) with relatively well-controlled size in almost all cases. The results show that our proposed test outperforms the tests of [Evrpidou et al. \(2022\)](#) for all scenarios where there is no short-lived co-bubbling at the end of the sample. These results hold under most of the heteroskedastic volatility specifications, but the size of the test is slightly distorted in a few scenarios where the patterns of variance in the innovations exhibit an abrupt downward shift, two abrupt shifts or is trending downward. In the context of serial correlation in innovations, simulation results demonstrate that employing a long-run variance estimator is effective in controlling size. We also compare the finite sample power profiles of our proposed test with those of the KPSS-based test of [Evrpidou et al. \(2022\)](#) using different kernel-based long-run variance estimators (Bartlett and quadratic spectral [QS]). Results show that with suitable lag selection parameters (i.e., lag selection parameter is a parameter which is used in [Newey and West \(1994\)](#)'s optimal choice of bandwidth procedure), the test of [Evrpidou et al. \(2022\)](#) is more robust and has a well-controlled size under the QS kernel while our test has better-controlled size than [Evrpidou et al. \(2022\)](#)'s test under the Bartlett kernel. Furthermore, our Monte Carlo simulations demonstrate that our tests are capable of detecting the co-movements between pairs of series by employing the co-bubble

test on a range of lead/lag predictors. As with the test proposed by [Evrpidou et al. \(2022\)](#), our test may be invalid if we select the wrong lead/lag of the series. Therefore, we suggest using a broad range of lead and lag values to locate the co-bubble and track the bubble migration between the two series having co-explosive relationship.

An empirical application of these methodologies is conducted to the commodity market in order to investigate whether bubbles in metal prices migrate to other kinds of precious and non-ferrous metal prices in the same market. Accordingly, this chapter first uses the wild-bootstrap generalized supremum ADF [GSADF] test of [PSY](#) to test whether explosive bubbles exist in asset prices. After that, we employ our new method to identify co-explosive behaviour in the lag/lead of pairs of different metals spot and futures prices. Our results confirm the presence of co-movements in six pairs of metal prices (including Silver/Lead, Tin/Silver, Copper/Tin, Copper/Gold, Palladium/Nickel, and Platinum/Gold) while failing to confirm such co-movements in two pairs of Zinc/Nickel and Copper/Platinum identified in the co-explosivity analysis conducted by [Evrpidou et al. \(2022\)](#).

The rest of this chapter is organized as follows. In section [3.2](#), we present the data generating process [DGP] of bubble models for individual series. In Section [3.3](#), we model the linear relationship between series, which is used to derive the null of the presence of co-explosivity between the series, and the alternative hypothesis of no co-explosivity at the end of the sample. Section [3.4](#) outlines the test of [Evrpidou et al. \(2022\)](#) and our new extended test procedure. In this Section, we also present the asymptotic behaviour of the test statistic and outline the wild bootstrap procedure used to generate critical values for the tests. In Section [3.5](#) we report results from a Monte Carlo simulation exercise examining the finite sample size and power of the tests for various parameterizations of our DGP as well as exploring the capability of the tests to correctly determine the timing of bubble migration. Section [3.6](#) reports the results of the bubble migration test and the timing of bubble migration when applied to empirical data. Section [3.7](#) concludes.

3.2 The Bubble Model

We consider the following DGP for a generic series x_t , observed from $t = 1, \dots, T$.

$$x_t = \mu_x + u_{x,t} \quad (3.1)$$

$$u_{x,t} = \begin{cases} u_{x,t-1} + \epsilon_{x,t}, & t = 2, \dots, \lfloor \tau_x T \rfloor \\ (1 + \delta_x)u_{x,t-1} + \epsilon_{x,t}, & t = \lfloor \tau_x T \rfloor + 1, \dots, T \end{cases} \quad (3.2)$$

where x_t behaves is assumed to be an $I(1)$ unit root process up until time $t = \lfloor \tau_x T \rfloor$ before exhibiting mildly explosive behaviour which persists until the end of the sample at time $t = T$. The initial condition $u_{x,1}$ is assumed to be $o_p(T^{1/2})$. $\delta_x = c_x T^{-\alpha_x}$ with $\alpha_x \in (0,1)$. $c_x > 0$ is a constant controlling the magnitude of the bubble, T is the sample size, the parameter α_x is a localizing coefficient as $T \rightarrow \infty$, and $\epsilon_{x,t}$ is an innovation process with mean equal to zero and is stationary. As we mentioned in Section 3.1, we only focus on the bubble originating at the end of the sample. For this reason, our bubble model here only includes model (1) of [Evrpidou et al. \(2022\)](#) who also allows for bubble collapse and the reversion to unit root behaviour in other model specifications. In that regard, the bubble phase starts at $\lfloor \tau_x T + 1 \rfloor$ and runs up to the sample end; however, while [Evrpidou et al. \(2022\)](#) examines various $0 < \tau_x < 1$, here we only consider $\tau_x \geq 0.8$ to indicate the explosive regime emerges somewhere near the end of the sample. This is because practitioners are usually concerned more with early bubble detection, and so would also likely be more interested in departures from the co-bubble null at the sample end.

3.3 The Co-explosive Model

As in [Evrpidou et al. \(2022\)](#), let y_t and x_t be two observed series where x_t exhibits explosive behaviour as generated from (3.1) - (3.2). Additionally, let z_t be a latent process generated from the same DGP like x_t , but with the symbols of x replaced by corresponding ones of z . In that regard, τ_z denotes the fraction of data sample when

the bubble in z_t begins and c_z indicates the factor that used to set the magnitude of the bubble. From that, we construct a DGP for y_t as given below,

$$y_t = \mu_y + \beta_{x,t}x_{t-i} + \beta_{z,t}z_t + \epsilon_{y,t} \quad (3.3)$$

where $\epsilon_{y,t}$ is a mean-zero and stationary error term, $\beta_{x,t}, \beta_{z,t}$ denote the coefficients in linear combination between y_t and x_t, z_t , respectively. Here, y_t is an explosive process which is driven by x_{t-i} if $\beta_{x,t} > 0$, or by z_t if $\beta_{z,t} > 0$. In Equation (3.3), if $\beta_z = 0$ and $\beta_x > 0$, it can be assumed that y_t and x_{t-i} are co-bubbling, which means that a linear combination of these processes, namely $y_t - \mu_y - \beta_{x,t}x_{t-i}$, is stationary across all sub-regimes. In other words, it means under our co-explosive bubble model, co-explosivity between y_t and x_{t-i} involves cointegration in the unit root regime as well as co-explosivity in the explosive regime. On the other hand, if $\beta_z > 0$ and $\beta_x = 0$, then y_t includes an explosive episode that is influenced by the unobserved process z_t , and the observed process x_t is not relevant as a co-explosive variate for y_t . Therefore, the two series are not co-exploding. In Equation (3.3), the delay parameter i determines the direction of migration. Specifically, if $i > 0$, the series x_t is lagged relative to y_t , whereas if $i < 0$, x_t is leading. When $i = 0$, co-bubbling occurs simultaneously. In the case of $i > 0$, the bubble is delayed by i periods before migrating from x_t to y_t , and vice versa for $i < 0$. Finally, similar to the $\epsilon_{x,t}$ term in Equation (3.2), we have $\epsilon_{y,t}$ to indicate the innovations of y_t , and implicitly, $\epsilon_{z,t}$ are the innovations of z_t . Correlations among the innovation terms, $\epsilon_{x,t}, \epsilon_{y,t}$, and $\epsilon_{z,t}$, are allowed.

With regard to testing co-bubble between observed series, y_t and x_t , our hypotheses can be given by,

$$H_0 : \beta_{x,t} > 0, \beta_{z,t} = 0, \forall t \in [0, T] \quad (3.4)$$

$$H_1 : \begin{cases} \beta_{x,t} > 0, \beta_{z,t} = 0, t \in [0, \tau T] \\ \beta_{x,t} = 0, \beta_{z,t} > 0, \text{ otherwise} \end{cases} \quad (3.5)$$

Regardless of the migration direction if $\beta_{z,t} = 0$ and $\beta_{x,t} > 0 \forall t$, then y_t and x_t are

said to be co-bubbling. Under the alternative hypothesis, the series y_t is co-explosive with x_t from the beginning until time $\lfloor \tau T \rfloor$. However, the explosive behaviour in y_t is driven by z_t instead of x_t for the remainder of the sample, indicating that $\beta_{z,t} > 0$ and $\beta_{x,t} = 0$. Our bubble model differs from that of [Evrupidou et al. \(2022\)](#) in that it aims to capture departures from the co-bubble null for a small number of observations at the end of the sample instead of the full sample. In summary, the null hypothesis states that two series are co-integrated and co-explode throughout the entire sample period. On the other hand, the alternative hypothesis suggests that the two series share a long-run relationship only for some proportion of the sample. We only consider positive co-explosivity $\beta_{x,t} > 0$ here, in line with [Evrupidou et al. \(2022\)](#); however, both their and our procedures can be applied when $\beta_{x,t} < 0$ also.

Similar to [Evrupidou et al. \(2022\)](#), following [Cavaliere and Taylor \(2007\)](#) we make the following assumption for the innovation series, $\epsilon_{y,t}$.

Assumption 3.1 *Let $\epsilon_{y,t} = \sigma_t v_t$ where $v_t \sim \text{IID}(0,1)$ with $\mathbb{E}|v_t|^r < K < \infty$ for some $r \geq 4$, where K is some constant depending only upon r . The volatility σ_t satisfies $\sigma_t = \omega(t/T)$, where $\omega(\cdot)$ is a non-stochastic and strictly positive function.*

Remark 3.1 *Under Assumption 3.1, the innovation variance is non-stochastic and bounded with a countable number of jumps. The test allows for variance profiles that include single or multiple variance shifts, smooth transition variance shifts, or shifts in trend. For example, the model of a single abrupt change in volatility of [Hamori and Tokihisa \(1997\)](#), [Kim et al. \(2002\)](#), [Buseti and Taylor \(2003\)](#), and [Cavaliere \(2005\)](#) also falls under this assumption, which corresponds to the function $\omega(t/T) := \sigma_0 + (\sigma_1 - \sigma_0)\mathbb{1}(t/T \geq \tau)$, $0 < \tau < 1$. This function shows the volatility shift from σ_0 to σ_1 at time $\lfloor \tau T \rfloor$.*

In later sections, we make use of the variance profile of the process,

$$\eta(s) = \left(\int_0^1 \omega(h)^2 dh \right)^{-1} \int_0^s \omega(h)^2 dh$$

This variance profile is homoskedastic when $\eta(s) = s$, and is heteroskedastic otherwise.

$\bar{\omega}^2 = \int_0^1 \omega(h)^2 dh$ is an asymptotic average error variance, which is equivalent to the limit of $T^{-1} \sum_{t=1}^T \sigma_t^2$.

Also, under Assumption 3.1, we make use of the invariance principle from Theorem 1(i) of [Cavaliere and Taylor \(2009\)](#) which establishes that:

$$T^{-1/2} \sum_{t=1}^{\lfloor rT \rfloor} \epsilon_{y,t} \xrightarrow{w} \bar{\omega} W^\eta(r)$$

where $W^\eta(r) = \int_0^r dW(\eta(s))$ with $W(r)$ denoting a standard Brownian motion on $[0, 1]$, is known as a variance-transformed Brownian motion.

3.4 Testing For Co-explosiveness

As mentioned in previous sections, [Evrpidou et al. \(2022\)](#) define co-explosivity as a linear combination that is stationary across all sub-regimes. Therefore, to test H_0 against H_1 , [Evrpidou et al. \(2022\)](#) suggest the KPSS-type statistic, which is the Lagrange multiplier (LM) or score statistic, for testing the full sample OLS residuals from model (3.3) is stationary around a mean against the alternative of non-stationary due to a unit root given by:

$$R := R_0^1 \tag{3.6}$$

where

$$R_{r_1}^1 = \hat{\sigma}(r_1)_y^{-2} (T - \lfloor r_1 T \rfloor - |i|)^{-2} \sum_{t=i\mathbb{1}(i>0)+\lfloor r_1 T \rfloor+1}^{T+i\mathbb{1}(i<0)} \left(\sum_{s=i\mathbb{1}(i>0)+\lfloor r_1 T \rfloor+1}^t \hat{e}(r_1)_{y,s,i} \right)^2$$

with $\hat{e}(r_1)_{y,t,i} = y_t - \hat{\mu}_y - \hat{\beta}_{x,t} x_{t-i}$ with $\lfloor r_1 T \rfloor + i\mathbb{1}(i > 0) + 1 \leq t \leq T + i\mathbb{1}(i < 0)$ are OLS residuals from regressing $y_{\lfloor r_1 T \rfloor + i\mathbb{1}(i>0)+1 \leq t \leq T + i\mathbb{1}(i<0)}$ on $x_{\lfloor r_1 T \rfloor + i\mathbb{1}(i>0)+1 \leq t \leq T + i\mathbb{1}(i<0)-i}$ and a constant, and $\hat{\sigma}(r_1)_y^2 = (T - \lfloor r_1 T \rfloor - |i|)^{-1} \sum_{t=i\mathbb{1}(i>0)+\lfloor r_1 T \rfloor+1}^{T+i\mathbb{1}(i<0)} \hat{e}(r_1)_{y,t,i}^2$ is the short run variance estimator. $r_1 = 0$ implies the test statistic is calculated on the full sample of data. Although the original purpose of KPSS test statistic is to distinguish between

model errors being $I(0)$ and $I(1)$ under the context that x_t is $I(1)$, [Evripidou et al. \(2022\)](#) argue that the KPSS-based test statistic in Equation (3.6) is able to distinguish between the stationary linear combination between y_t and x_t and no co-explosive processes. On that point, we also construct a modified version of the test statistic, R , with the hope that our new test can improve the ability to detect the (lack of) co-explosivity between two series at the end of the sample.

To evaluate whether current data indicate the presence of co-bubbling, regulators and central banks require an assessment of whether any observation near the end of the sample belongs to a co-explosive phase in the overall trajectory. The backward supremum procedure proposed by [PSY](#) is the approach we use in order to improve the power of the full sample test of [Evripidou et al. \(2022\)](#) when the co-explosive relationship potentially breaks down at the end of the sample. Our backward supremum KPSS-based test, S test, involves recursively re-estimating the OLS model for each subsample to obtain different residuals. Consequently, different residuals enter into each test statistic, R , in the sequence. S test statistic is the largest value of the series of R test statistics we calculated. Since we use the backward procedure of [PSY](#), we perform a sequence of KPSS-based tests on a backward expanding sample sequence, where the endpoint of each sample is fixed at T and the start point for each sample varies for $t \in [1, \lfloor (1 - r_0)T \rfloor]$ where r_0 denotes the minimum fraction of the dataset used for testing. In other words, the corresponding R statistic sequence is $\{R_{r_1}^1\}_{r_1 \in [0, 1 - r_0]}$, where $R_{r_1}^1$ denotes the R statistic performed on subsample data of y_t and x_{t-i} with $t \in [\lfloor r_1 T \rfloor + 1, T]$. In this regard, the full sample test of [Evripidou et al. \(2022\)](#) is R_0^1 that means R statistic performed on full sample of y_t and x_{t-i} with $t = [2, T]$. Our statistic S is defined as the largest value of the sequence of R statistics calculated over all subsamples ending at the end of the sample subject to a minimum window size $T - \lfloor r_0 T \rfloor$, so that

$$S := \sup_{r_1 \in [0, 1 - r_0]} R_{r_1}^1 \quad (3.7)$$

3.4.1 Asymptotic behaviour

Theorem 3.1 *According to the proof of [Evrpidou et al. \(2022\)](#), let Assumption 3.1 hold, then under the null hypothesis, H_0 ,*

$$R \xrightarrow{w} \int_0^1 V^\eta(r)^2 dr \quad (3.8)$$

where $V^\eta(r) = W^\eta(r) - rW^\eta(1)$. Applying continuous mapping theorem to our test statistics (3.7), the large sample behaviour of S under the null hypothesis is given as below:

$$S \xrightarrow{w} \sup_{r_1 \in [0, 1-r_0]} \left\{ \int_{r_1}^1 V^\eta(r)^2 dr \right\} \quad (3.9)$$

On the other hand, under H_1 , the test statistic $R = S = O_p(T^{2\alpha_z+1})$.

The limiting null distributions of R and S under the null depend on the volatility path of $\epsilon_{y,t}$. According to [Evrpidou et al. \(2022\)](#), the limit critical values coincide with those of KPSS (the demeaned case) in the homoskedastic case where $W^\eta(r) = \int_0^r dW(s) = W(r)$. However, in cases where heteroskedasticity is present, the critical values of KPSS are inappropriate as they are affected by the heteroskedasticity. Under the alternative, if the localizing coefficient, $\alpha_{z,1}$, in the unobservable series z_t belongs to the half-open interval $(0, 1/2]$, then the R and S tests do not diverge. If $\alpha_{z,1}$ falls within the range of $(1/2, 1)$, Theorem 3.1 suggests that comparing R or S with any finite critical values will lead to a consistent test under the alternative hypothesis. However, [Evrpidou et al. \(2022\)](#) proved that, by using wild-bootstrap critical values, the R test will be consistent on the whole range of $\alpha_{z,1} \in (0, 1)$. We conjecture that the same is also true for the S test. To perform large sample size-controlled inference, comparison of $\sup_{r_1 \in [0, 1-r_0]} R_{r_1}^1$ with the upper-tail critical values from $\sup_{r_1 \in [0, 1-r_0]} \left\{ \int_{r_1}^1 V^\eta(r_1)^2 dr_1 \right\}$ makes it possible to test for a stationary process against a unit root, given a known pattern of heteroskedasticity. However, in practice, it is infeasible to determine the pattern of heteroskedasticity required to calculate the limiting distribution under both the null hypothesis and the alternative hypothesis. For this reason, in the next

subsection, we propose a bootstrap procedure, as in [Evrividou et al. \(2022\)](#), to ensure the large sample size robustness of the R and S tests to heteroskedasticity.

Also, according to [Evrividou et al. \(2022\)](#) the partial sum process of $\hat{\epsilon}_{y,t}$ can be denoted as follows:

$$T^{-1/2} \sum_{t=1}^{\lfloor rT \rfloor} \hat{\epsilon}_{y,t} = T^{-1/2} \sum_{t=1}^{\lfloor rT \rfloor} (\epsilon_{y,t} - \bar{\epsilon}_y) + O_p(T^{\alpha(x,1-1)/2}) \quad (3.10)$$

Remark 3.2 *From the Equation (3.10), the effect of x_t is asymptotically negligible when x_t is a mildly explosive process with $\alpha_{x,1} \in (0, 1)$. Because of the asymptotic negligibility of x_t , [Evrividou et al. \(2022\)](#) show that we can allow $\epsilon_{x,t}$ to be an $I(0)$ process and be correlated to $\epsilon_{y,t}$. In the case that $\epsilon_{x,t}$ is heteroskedastic, the Theorem 3.1 still holds.*

The results of Theorem 3.1 above hold under Assumption 3.1. In the case, $\epsilon_{y,t}$ are serially dependent, we can estimate $\hat{\sigma}(r_1)_y^2$ by using a long-run variance estimator with suitable kernel functions. In that case, assuming that the estimator is consistent, our test statistics are consistent, and the limiting null distribution of tests continues to hold.

3.4.2 A wild bootstrap procedure

We now outline how bootstrap implementation of our proposed S test can be achieved, where we follow [Evrividou et al. \(2022\)](#) and utilise the wild bootstrap algorithm of **HLST**, recalling that we cannot use asymptotic critical values due to the limiting null distribution of the tests depending on the pattern of heteroskedasticity in the data. In fact, via finite sample simulations, [Evrividou et al. \(2022\)](#) show that the size of their test is distorted significantly when heteroskedasticity exists in the co-explosivity model if using the standard homoskedastic critical values of KPSS.

The bootstrap algorithm below is used to replicate the pattern of heteroskedasticity in the original data. Using this method, the distribution of test statistics computed from the bootstrap data will replicate their asymptotic null distribution under the forms of heteroskedasticity allowed for in Assumption 3.1. The steps of the algorithm

to generate critical values for the tests is as follows:

Step 1: Generate a wild-bootstrap samples, $y_{t,b}$.

$$y_{t,b} = w_t \hat{e}_{y,t}, \text{ where } w_t \sim NIID(0,1), t = i\mathbb{1}(i > 0) + 1, \dots, T + i\mathbb{1}(i < 0)$$

Step 2: Regress $y_{t,b}$ on a constant and x_{t-i} to obtain OLS residuals, $\hat{e}_{t,b}$. Then, calculate the bootstrap analogues of R and S , denoted R_b and S_b , according to:

$$R_b = R_{0,b}^1 \quad (3.11)$$

$$S_b = \sup_{r_1 \in [0, 1-r_0]} R_{r_1,b}^1 \quad (3.12)$$

where

$$R_{r_1,b}^1 = \hat{\sigma}(r_1)_b^{-2} (T - \lfloor r_1 T \rfloor - |i|)^{-2} \sum_{t=i\mathbb{1}(i>0)+\lfloor r_1 T \rfloor+1}^{T+i\mathbb{1}(i<0)} \left(\sum_{s=i\mathbb{1}(i>0)+\lfloor r_1 T \rfloor+1}^t \hat{e}(r_1)_{b,s,i} \right)^2$$

with $\hat{e}(r_1)_{b,t,i} = y_{t,b} - \hat{\mu}_b - \hat{\beta}_{x,t} x_{t-i}$ with $\lfloor r_1 T \rfloor + i\mathbb{1}(i > 0) + 1 \leq t \leq T + i\mathbb{1}(i < 0)$ are OLS residuals from regressing $y_{\lfloor r_1 T \rfloor + i\mathbb{1}(i > 0) + 1 \leq t \leq T + i\mathbb{1}(i < 0), b}$ on $x_{\lfloor r_1 T \rfloor + i\mathbb{1}(i > 0) + 1 \leq t \leq T + i\mathbb{1}(i < 0) - i}$ and a constant, and $\hat{\sigma}(r_1)_b^2 = (T - \lfloor r_1 T \rfloor - |i|)^{-1} \sum_{t=i\mathbb{1}(i>0)+\lfloor r_1 T \rfloor+1}^{T+i\mathbb{1}(i<0)} \hat{e}(r_1)_{b,t,i}^2$.

Step 3: Repeat step 1 and step 2 M times to obtain pairs of statistics $\{R_{b,1}, S_{b,1}\}, \dots, \{R_{b,M}, S_{b,M}\}$ and calculate the (upper tail) π -level critical value, $c_{\pi,M}^R$ and $c_{\pi,M}^S$ say, of the empirical CDF of R_b and S_b , respectively.

Step 4: Rejection rule: Reject H_0 in favour of H_1 if $R > c_{\pi,M}^R$ in the test of [Evripidou et al. \(2022\)](#) and $S > c_{\pi,M}^S$ in our supremum test.

3.4.3 Asymptotic behaviour of wild bootstrap test statistics

Theorem 3.2 *As provided by [Evripidou et al. \(2022\)](#), under Assumption 3.1 and null hypothesis, H_0 ,*

$$R_b \xrightarrow{w} \int_0^1 V^\eta(r)^2 dr \quad (3.13)$$

Also, under H_1

$$R_b = O_p(T^{\alpha_{z,1}-1}) \quad (3.14)$$

Similarly, using continuous mapping theorem, under H_0 we obtain the asymptotic distribution for backward sup KPSS test as given:

$$S_b \xrightarrow{w} \sup_{r_1 \in [0, 1-r_0]} \left\{ \int_{r_1}^1 V^\eta(r)^2 dr \right\} \quad (3.15)$$

Using the same arguments as in [Evrpidou et al. \(2022\)](#), when the null hypothesis H_0 is true, the distribution of R_b coincides with that of R . Similarly, the result also holds for S_b . As a result, if the number of bootstrap replications M is large, the empirical cumulative distribution function (CDF) of R_b ensures that $Pr(R > c_{\pi, M}^R) = \pi$, which means that the size of R is asymptotically controlled. This robustness is achieved because the heteroskedasticity pattern present in the original errors $\epsilon_{y,t}$ is replicated in the bootstrap data $y_{t,b} = w_t \hat{\epsilon}_{y,t}$.

Remark 3.3 According to Remark 2 in [Evrpidou et al. \(2022\)](#), it is possible to construct the bootstrap residuals $\hat{\epsilon}(r_1)_{b,t,i}$ without including the regressor x_{t-i} . This is because the limiting null distribution of R_b does not involve x_t . However, the impact of the regression effect of x_t on R might still be significant in finite samples when $\alpha_{x,1}$ is close to 1. Therefore, excluding x_{t-i} when constructing $\hat{\epsilon}(r_1)_{b,t,i}$ could result in the finite sample distributions of R_b and R being less similar compared to when x_{t-i} is included. Based on simulation evidence that has not been reported, the [Evrpidou et al. \(2022\)](#) recommend including x_{t-i} in the bootstrap regressions. We conjecture that the arguments above also hold for S_b .

According to [Evrpidou et al. \(2022\)](#), under alternative hypotheses, theorems 3.2 and 3.1 indicate that when $\alpha_{z,1}$ falls in the range of $(1/2, 1)$, R tends to infinity while R_b converges to zero. When $\alpha_{z,1}$ is equal to $1/2$, R is $O_p(1)$, and S_b tends to zero. Conversely, when $\alpha_{z,1}$ falls in the range of $(0, 1/2)$, R tends to zero, but R_b tends to zero at a faster rate than R . Consequently, under the alternative hypothesis H_1 , the

ratio of $R/R_b = O_p(T^{\alpha_{z,1}})$, which implies that $R/c_{\tau,M}^R = O_p(T^{\alpha_{z,1}})$. This further suggests that $\lim_{T \rightarrow \infty} Pr(R > c_{\tau,M}^R) = 1$. Hence the bootstrap-based test is consistent for the entire range of $\alpha_{z,1} \in (0,1)$. We conjecture that the same is also true for our S test.

Remark 3.4 *Evripidou et al. (2022) also noted that the testing method we use does not require us to have detailed information about x_t , only that it includes some form of explosive component. We do not need to know which specific model generated x_t or z_t , nor do we need to know the specific attributes of x_t . Additionally, the procedure will remain valid even if there are multiple explosive episodes in x_t (or z_t).*

When there is a possibility of serial dependence in $\epsilon_{y,t}$, R_b and S_b can be constructed without using a long-run variance estimator because there is no serial dependence in the wild bootstrap sample $y_{t,b}$. Although we do not use the long-run variance estimator in the wild bootstrap, we still employ it in the original test statistics that are used to compare with the bootstrapped critical values.

3.4.4 Accounting for serial correlation

Although Assumption 3.1 implies that the innovations $\epsilon_{y,t}$ are not serially dependent, we can relax this assumption to allow the serial correlation in the innovations. By running a few preliminary simulations on series with innovations following AR(1) with $\epsilon_{y,t} = 0.5\epsilon_{y,t-1} + v_t$, and MA(1) with $\epsilon_{y,t} = 0.5v_{t-1} + v_t$, results in Table B-5 show that the finite sample size of our proposed test and Evripidou et al. (2022)'s test are seriously distorted. Therefore, we propose utilising a long-run variance estimator to replace the short-run variance estimator $\hat{\sigma}_y^2$ in the same manner as Evripidou et al. (2022). In this way, the asymptotic behaviour of Evripidou et al. (2022)'s test and our proposed test still hold, as stated in Theorem 3.1 under the condition of serial correlation in the model errors.

The innovation of $\epsilon_{y,t}$ can be taken to satisfy the assumption of Said and Dickey (1984), Zivot and Andrews (1992), Phillips and Solo (1992), Chang and Park (2002), and Whitehouse (2019) as follows:

Assumption 3.2 Let $\epsilon_{y,t} = \zeta(L)e_t$, $\zeta(L) = \sum_{i=0}^{\infty} \zeta_i L^i$, $C_0 = 1$ with $\zeta(z) \neq 0$ for all $|z| \leq 1$ and $\sum_{i=0}^{\infty} i|\zeta_i| < \infty$, where $\zeta(L)$ is the lag polynomial and e_t is a martingale difference sequence that follows Assumption 3.1.

When $\zeta_i = 0$ for $i \geq 1$ in Assumption 3.2 this implies the no serial correlation setting considered in Assumption 3.1. Furthermore, the conditions around $\zeta(L)$ are standard conditions of summability and invertibility.

Let $\gamma_j = \text{cov}(\epsilon_{y,t}, \epsilon_{y,t-j})$ where $\sum_{j=0}^{\infty} |\gamma_j| < \infty$ under the Assumption 3.2, and $j > 0$ indicates lag parameter. Then, in line with Newey and West (1987), Andrews (1991), and Newey and West (1994), the long-run variance estimator for the full sample has a form of

$$\hat{\sigma}(0)_{y,lr}^2 = \hat{\gamma}_0 + 2 \sum_{j=0}^{\hat{m}} k(j/\hat{m}(T)) \hat{\gamma}_j. \quad (3.16)$$

where $k(j/\hat{m}(T))$ denotes kernel function - a smooth function of a ratio of j to the bandwidth $m + 1$, $\hat{\gamma}_j := \text{cov}(\hat{e}_{y,t}, \hat{e}_{y,t-j})$ is an estimated value of γ_j calculated from the data sample, $\hat{\sigma}(r_1)_{y,lr}^2$ is the long-run variance for a subsample of y_t with $\lfloor r_1 T \rfloor + i \mathbb{1}(i > 0) + 1 \leq t \leq T + i \mathbb{1}(i < 0)$. Since we estimate the long-run variance for the full sample of y_t , $r_1 = 0$.

By replacing $\hat{\sigma}(r_1)_{y,lr}^2$ by $\hat{\sigma}(r_1)_{y,lr}^2$ (an estimate of long run variance in the subsample determined by r_1), the test statistics in (3.6) and (3.7) take a different form to handle the serial correlation inside the innovations $\epsilon_{y,t}$. That is,

$$\tilde{R} := \tilde{R}_0^1 \quad (3.17)$$

where

$$\tilde{R}_{r_1}^1 = \hat{\sigma}(r_1)_{y,lr}^{-2} (T - \lfloor r_1 T \rfloor - |i|)^{-2} \sum_{t=i \mathbb{1}(i>0) + \lfloor r_1 T \rfloor + 1}^{T+i \mathbb{1}(i<0)} \left(\sum_{s=i \mathbb{1}(i>0) + \lfloor r_1 T \rfloor + 1}^t \hat{e}(r_1)_{s,i} \right)^2$$

with $\hat{e}(r_1)_{t,i} = y_t - \hat{\mu}_t - \hat{\beta}_{x,t} x_{t-i}$ with $\lfloor r_1 T \rfloor + i \mathbb{1}(i > 0) + 1 \leq t \leq T + i \mathbb{1}(i < 0)$ are OLS residuals from regressing $y_{\lfloor r_1 T \rfloor + i \mathbb{1}(i > 0) + 1 \leq t \leq T + i \mathbb{1}(i < 0)}$ on $x_{\lfloor r_1 T \rfloor + i \mathbb{1}(i > 0) + 1 \leq t \leq T + i \mathbb{1}(i < 0) - i}$ and a

constant. Similarly, our new proposed backward supremum test statistic will be as below:

$$\tilde{S} := \sup_{r_1 \in [0, 1-r_0]} \tilde{R}_{r_1}^1 \quad (3.18)$$

where r_0 is the minimum recursive window.

In line with [Evrpidou et al. \(2022\)](#), when $\epsilon_{y,t}$ is serially correlated, we only use the long-run estimator in calculating the test statistics of interest, but not in the bootstrapped statistics. This is because the wild bootstrap samples, y_t^b do not contain serial correlation.

3.5 Finite Sample Properties

In this section, we examine the size and power properties of our proposed wild-bootstrap S test compared to the wild-bootstrap R test of [Evrpidou et al. \(2022\)](#) at a significance level of 0.05 (i.e. $\pi = 0.05$). In other words, all simulations are conducted at the nominal 0.05 level. To do so, we generate data according to (3.1) - (3.3) with sample sizes of $T = 200$ and 400 , respectively. The DGPs in (3.1) and (3.2) are used to construct x_t and z_t with innovations $\epsilon_{x,t}$ and $\epsilon_{z,t}$, a sequence of $NIID(0,1)$ variates, while model (3.3) is used to simulate the co-explosive relationship between the processes. We select these two sample sizes so we can observe how the properties of the tests behave as the sample size increases. To evaluate the finite sample profiles of the tests, we use 2,000 Monte Carlo simulations and $M = 499$ bootstrap replications. For all simulations in this section except for Section 3.5.4, we assume that $i = 0$ so that we do not need to run the tests under the pre-chosen lag/lead values.

For the bubble specification, we have chosen fixed localizing coefficients, namely $\alpha_x = \alpha_z = 0.5$. We have followed the same approach as [Evrpidou et al. \(2022\)](#) and set $\mu_x = \mu_y = \mu_z = 0$, without loss of generality. In contrast to x_t and z_t , where we always set the innovations to be homoskedastic, the series y_t is generated with either homoskedastic or heteroskedastic innovations. As mentioned in Assumption

3.1, $\epsilon_{y,t} = \sigma_t v_t$ with $t \in [1, T]$, where $\sigma_t = \omega(t/T)$ is the discrete-time analogues of the volatility functions given by cases a) – k), and $v_t \sim NIID(0,1)$. We have set $\sigma_t = 1$ for all t in the homoskedastic case and have considered eleven heteroskedastic specifications, which are listed below:

- a) Downward shift (Coincidence): $\sigma(r) = 5\mathbb{1}(r \leq \tau_x) + \mathbb{1}(r > \tau_x)$
- b) Upward shift (Coincidence): $\sigma(r) = \mathbb{1}(r \leq \tau_x) + 5\mathbb{1}(r > \tau_x)$
- c) Upward trend volatility: $\sigma(r) = 1 + 5r$
- d) Downward trend volatility: $\sigma(r) = 6 - 5r$
- e) Early upward shift: $\sigma(r) = 1 + 5\mathbb{1}(r \geq 0.3)$.
- f) Mid upward shift: $\sigma(r) = 1 + 5\mathbb{1}(r \geq 0.5)$.
- g) Late upward shift: $\sigma(r) = 1 + 5\mathbb{1}(r \geq 0.8)$.
- h) Early downward shift: $\sigma(r) = 1 + 5\mathbb{1}(r < 0.3)$.
- i) Mid downward shift: $\sigma(r) = 1 + 5\mathbb{1}(r < 0.5)$.
- j) Late downward shift: $\sigma(r) = 1 + 5\mathbb{1}(r < 0.8)$.
- k) Double shift: $\sigma(r) = 1 + 5\mathbb{1}(0.4 < r \leq 0.6)$.

The first two cases are scenarios where volatility break coincides with the potential start date of the bubbles in y_t and x_t . In other cases, the volatility break varies and is independent of the break of the bubble model. All these volatility specifications satisfy Assumption 3.2 in Section 3.4. To correct the size of the test from being distorted by the impact of heteroskedasticity, we use the wild bootstrap algorithm as suggested in HLST. Finally, we set the minimum window length for our backward supremum test as the recommendation of PSY, $r_0 = 0.01 + 1.8/\sqrt{T}$.

3.5.1 Behaviour under H_0

Under the null hypothesis, we quantify the size of the wild bootstrap tests for homoskedastic, heteroskedastic, and serially correlated innovations. In this subsection, all the finite sample sizes that are reported are calculated from tests without long-run variance correction. We only use tests with a long-run variance to assess the test size in cases where there is serial correlation in innovations, as described in the next Subsection 3.5.3. The DGP we consider for x_t is as Equations (3.1) and (3.2) with settings of parameters as follows:

$$c_x \in \{0.2, 0.4, 0.8\}$$

$$\tau_x \in \{0.8, 0.85, 0.9\}$$

The DGP to create y_t is as Equations (3.3) and (3.4) with the finite sample volatility functions σ_t being the discrete time analogs of those given in the cases (i.e., a–k) at the beginning of Section 3.5. In regard to the finite sample size, in Table B-1, under the null hypothesis when the innovations are homoskedastic the size of the R test is well-controlled at a significance level of 5%, while our backward supremum test is slightly oversized. However, when the sample size increases from $T = 200$ to $T = 400$ in Table B-2, our proposed test is shown to have well-controlled when conducted at a nominal 0.05 level of significance. Similarly, the results with the presence of upward shifts and upward trends in volatility lie within two percentage points from the nominal size for $T = 200$ and have well-controlled sizes for $T = 400$. Although the finite sample size of the S test tends to slowly converge to the true nominal rejection rate when the sample size increases to 400 in all cases, it is still oversized in cases of downward shift, downward trend, and double shift in volatility. Additionally, the size of the test is robust with the magnitude and position of co-bubbling. In other words, there are small differences among the finite sample sizes across different magnitudes and positions of bubbles with the same heteroskedastic profile.

3.5.2 Behaviour under H_1

Finite sample simulations in this subsection are used to quantify the power of the bootstrap procedure under H_1 . Our series z_t is generated using DGPs as in (3.1) and (3.2) in the same way as we create the series x_t . The innovations of x_t and z_t , $\epsilon_{x,t}$ and $\epsilon_{z,t}$ respectively, are independent and uncorrelated. We construct y_t as Equations (3.3) and (3.5), where we can set $\tau = \tau_z$ for convenience. Here, τ represents the point in time when the series y_t begins to co-bubble with series z_t in Equation 3.5, while τ_z denotes the time when the bubble in z_t begins. Similar to the model under H_0 , we can set $\beta_{x,t} = 0$ because using x_t or not, in this case, does not impair the generality of the model since $\epsilon_{y,t}$ is invariant to $\beta_{x,t}$. Also, σ_t is given by one of the homoskedastic and heteroskedastic cases at the beginning of Section 3.5. To compare the finite sample powers of R and S tests, we let the magnitude of the linear coefficient between y_t and z_t change, and the magnitude of the bubble in the unobserved series, z_t , change as well. z_t is constructed from the combined sets below:

$$c_z \in \{0.2, 0.4, 0.8\}$$

$$\tau_z \in \{0.8, 0.85, 0.9\}$$

The series y_t is generated as (3.3) with $\beta_{z,t} = \{0.025, 0.050, 0.075\}$. This coefficient is to control the magnitude of the linear relationship between y_t and latent series z_t . In that sense, we expect that the larger this coefficient is, the higher chance we reject the null hypothesis of the existence of co-bubble.

Table B-3 and B-4 provide the finite sample power of the tests under sample sizes of 200 and 400 when the innovations to y_t are homoskedastic. Across all the bubble magnitude settings, our proposed test and [Evripidou et al. \(2022\)](#)'s test has power that rises monotonically with c_z . To elaborate further, as the magnitude of the bubble increases in the unobserved series, the rejection rate of both tests also increases. On the other hand, if the bubble in z_t appears later in the sample, our rejection rate tends to decrease. Likewise, if the bubble begins closer to the end of the

sample, then the probability of rejecting the null hypothesis regarding the presence of a co-explosive bubble is higher for both tests. Additionally, we can see that our test marginally outperforms the KPSS-type test of [Evrividou et al. \(2022\)](#) in various settings of magnitude and origination time of co-bubbles. When the sample size is increased to 400 (Table [B-4](#)), the rejection rates of both tests are higher than they are in Table [B-3](#). Similarly, the S test is still more powerful than the R test.

Looking at the results under Figures [B-1](#) and [B-3](#) in which the x-axis is the different values of β_z and the y-axis indicates the rejection rate from Monte Carlo simulations, we find again our proposed test is slightly more powerful than the test of [Evrividou et al. \(2022\)](#) and this result is robust throughout the range of different values of $\beta_z \in [0, 0.12]$. The results hold if we change the magnitude of the bubble $c_z \in \{0.2, 0.4, 0.8\}$.

In the context of non-constant volatility, finite sample power curves of both tests are relatively the same under upward patterns of heteroskedasticity of innovations, $\epsilon_{y,t}$; however, our test is oversized when volatility exhibits downward patterns and double shift, (see [b](#)), [d](#)), [h](#)), [i](#)), [j](#)) and [k](#)) in Figures [B-3](#) and [B-4](#)). Although the finite sample size reduces when the sample size T increases from 200 to 400, the false positive rate is still high. For that reason, we run the simulation with a massive sample size. Simulated results show the sizes of the test all ended up around 5%; therefore, we conjecture the limitation of our proposed test is that its finite sample distribution converges slowly to the limiting null distribution when downward shift patterns of volatility are present.

3.5.3 Behaviour of the tests with serially correlated innovations

To investigate how co-explosivity tests behave under serially correlated innovations, we generate data according to [\(3.1\)](#) and [\(3.2\)](#) adopting the same parameter settings as Subsections [3.5.1](#) and [3.5.2](#) to construct series x_t and z_t . However, there is a bit of change to construct y_t , for considering scenarios where serial correlation exists in the innovations of y_t , the model adopts two settings for innovation terms as follows:

1. Serial correlation - AR(1): $\epsilon_{y,t} = 0.5\epsilon_{y,t-1} + v_t$

2. Serial correlation - MA(1): $\epsilon_{y,t} = 0.5v_{t-1} + v_t$

where $\epsilon_{y,t}$ denotes the innovation term of the series y_t , and v_t is $NIID(0,1)$, $\sigma_t = 1 \forall t$.

A feasible long-run variance estimator is given by:

$$\hat{\sigma}(r_1)_{y,lr}^2 = \tilde{\gamma}_0 + 2 \sum_{j=0}^{\tilde{m}} k(j/\tilde{m}(T^*)) \tilde{\gamma}_j.$$

where $\tilde{\gamma}_j := cov(\hat{\epsilon}_{y,t}, \hat{\epsilon}_{y,t-j})$ with $\lfloor r_1 T \rfloor + i\mathbb{1}(i > 0) + 1 \leq t \leq T + i\mathbb{1}(i < 0)$, where T^* is the sample length of subsample.

In terms of serial correlation in innovations, normally in practice, it is to use quadratic spectral (QS) kernel to estimate long-run variance for innovations as below:

$$k(j) = \begin{cases} \frac{25\tilde{m}^2}{12\pi^2 j^2} \left(\frac{5\tilde{m}}{6\pi j} \sin \frac{6\pi j}{5\tilde{m}} - \cos \frac{6\pi j}{5\tilde{m}} \right) & \text{for } 0 \leq j \leq \tilde{m} \\ 0, & \text{otherwise} \end{cases}$$

where $\tilde{m} = \lfloor n(T^*/100)^{2/25} \rfloor$ is the optimal choice of bandwidth parameter (or lag length) following recommendations of [Newey and West \(1994\)](#). n is the lag selection parameter.

To sum up, the test statistics in (3.17) and (3.18) can be re-written as below to handle the serial correlation inside the innovations $\epsilon_{y,t}$.

$$\begin{aligned} \tilde{R} &:= \tilde{R}_0^1 \\ \tilde{S} &:= \sup_{r_1 \in [0, 1-r_0]} \tilde{R}_{r_1}^1 \end{aligned}$$

where

$$\tilde{R}_{r_1}^1 = \hat{\sigma}(r_1)_{y,lr}^{-2} (T - \lfloor r_1 T \rfloor - |i|)^{-2} \sum_{t=i\mathbb{1}(i>0)+\lfloor r_1 T \rfloor+1}^{T+i\mathbb{1}(i<0)} \left(\sum_{s=i\mathbb{1}(i>0)+\lfloor r_1 T \rfloor+1}^t \hat{\epsilon}(r_1)_{s,i} \right)^2$$

It is due to the fact that the Bartlett kernel is another function commonly used to estimate long-run variance. We would like to run simulations to compare and choose

between both. For that, a weighting scheme employs Bartlett kernel as given by:

$$k(j) = \begin{cases} 1 - \frac{j}{\tilde{m}+1} & \text{for } 0 \leq j \leq \tilde{m} \\ 0, & \text{otherwise} \end{cases}$$

where $\tilde{m} = \lfloor n(T^*/100)^{2/9} \rfloor$ indicates another optimal choice of bandwidth parameter (or lag length) following recommendations of [Newey and West \(1994\)](#).

In our simulations, we use the wild-bootstrap algorithm to control the size of the tests, similar to [Evrpidou et al. \(2022\)](#). However, we replace the short-run estimators of variance $\hat{\sigma}(r_1)_y^2$ of y_t with the Bartlett or QS long-run variances in calculating test statistic (3.6). We do not use the long-run variance to construct the bootstrap statistics as mentioned in Subsection 3.4.4, because [Harvey et al. \(2016\)](#) demonstrate that the wild bootstrap procedure eliminates any weak dependence present in the innovations, $\epsilon_{y,t}$. We investigate the size and power performance of two co-explosive tests (e.g., R and S) employing the long-run variance estimator obtained from kernel estimates under finite sample simulations. For that reason, we use notations of \tilde{R} and \tilde{S} to denote R and S tests using the long-run variance estimation, respectively. Simultaneously, we use two types of kernel functions in each test to evaluate the properties of each kernel function for that test. We select the appropriate kernel and optimal lag length for each test. To recommend the optimal lag length, we vary the lag selection parameters, n , because the choice of n can help control the finite sample size of the tests under a nominal significance level and ensure robustness under different patterns of serial correlation. For simulations related to the performance of the test using long-run variance, we set $n \in \{2, 4, 6\}$ for the Bartlett kernel and $n \in \{5, 10, 15\}$ for the QS kernel.

In terms of serial correlation in innovations, as shown in Table B-5, the R and S tests are significantly oversized, with rejection rates ranging from 20 to 60% when a standard short-run variance estimator is employed. This poses a serious problem, as high false positive rates render the test unreliable in practice. Since serial correlation

is a common feature of financial time series data, over-rejection of co-bubbling may occur even when the serial correlation is present in the innovations to y_t . To address this issue, we follow the suggestions of [Evrpidou et al. \(2022\)](#) and replace the test statistic in Equations (3.6) and (3.7) with an improved statistic of Equations (3.17) and (3.18), in which the simple estimate of $\hat{\sigma}(r_1)_y^2$ is replaced with the long-run variance estimate $\hat{\sigma}(r_1)_{y,lr}^2$.

By employing the Bartlett kernel and its optimal choice of bandwidth parameter as described in [Newey and West \(1994\)](#), we present the results in Table B-6. In this table, we observe that the size of the tests is significantly better compared to the finite sample size of the tests when not using a long-run variance estimator. Despite this improvement, the results still vary depending on the lag selection parameter and across different serial correlation specifications. Specifically, when $T = 200$ and the innovations are not serially correlated (i.e., $NIID(0,1)$) almost all finite sample sizes lie within one percentage point above or below the nominal level of 0.05, except for the \tilde{S} test with a lag parameter of 4 or 6, which is undersized. In fact, for these independent cases, the \tilde{R} test controls the size better than the \tilde{S} test over the range of the lag parameters. When the innovations follow an AR(1) and MA(1) process, the size of the tests is oversized in almost all cases, except for the \tilde{S} test with a lag parameter of 6. With the lag selection parameter of 6, the \tilde{S} test is undersized in the case of MA(1) innovations, but it has a well-controlled size under AR(1) innovations. Under a sample size of $T = 400$, results in Table B-7 shows the \tilde{S} test using a Bartlett kernel-based long-run variance estimator with a lag parameter of 6 is well controlled at a 5% significance level in all co-explosivity settings.

In Table B-8, when using the QS kernel for estimating the long-run variance on a small sample size of $T = 200$, we find that the \tilde{S} test is oversized when the lag parameter is large and undersized when the lag parameter is small. The finite sample sizes of the \tilde{R} test are well-controlled at a nominal level of 5%, except for the case where we use a lag parameter of 5 when the innovations follow an AR(1) process. In other cases, the results are more robust and less sensitive to the choice of lag

parameter for the \tilde{R} test. In Table B-9 when $T = 400$, the finite sample size of \tilde{R} test tends to be corrected towards the nominal significance level. In summary, to control for the size of the test, both tests require different numbers of lag parameters and types of kernel estimators. However, our \tilde{S} test tends to be more sensitive to the choice of kernel types and corresponding lag parameters. Based on the simulated results, if we manually choose the lag length for the kernel estimations, we suggest using the Bartlett kernel with a lag parameter of 6 (i.e., lag length $\tilde{m} = \lfloor 6(T^*/100)^{2/9} \rfloor$) in the \tilde{S} test and the QS kernel with a lag selection parameter of 10 (i.e., lag length $\tilde{m} = \lfloor 10(T^*/100)^{2/25} \rfloor$) in the \tilde{R} test for empirical applications, after comparing their power performance. This is because under this choice of lag parameter here, \tilde{S} test and \tilde{R} test are the most robust to the different patterns of serially correlated innovations.

We also examine the finite sample power profiles of the tests under the existence of serial correlation in innovation terms. Here, we use the suggestions for the type of kernel and the value of the lag parameter as mentioned above. In all cases, when the innovation terms are not serially correlated, the innovation terms follow the first-order autoregressive process, and the first-order moving average process, \tilde{S} test still outperforms the \tilde{R} , as shown in Table B-10. The results are robust in all settings of the co-bubble model. When the position of the bubble in the latent series z_t is near the end of the sample, \tilde{S} test has significantly more power than the \tilde{R} test. As with other tables mentioned before, the power increases as the bubble of latent variable, z_t is long-lasting in the data sample, and its magnitude is more significant. Hence, the \tilde{S} test indeed improves the power to detect the co-bubbles starting nearly at the end of the sample. Additionally, the conclusions continue to hold in the case of no serially correlated volatility.

3.5.4 Timing explosive regime migration

In this section, we introduce the method of [Evrpidou et al. \(2022\)](#) to estimate the lag/lead variables. Additionally, we will use finite sample simulations to demonstrate

how the co-explosive tests behave under lag/lead parameter selections.

The value of the lead/lag parameter, i is unknown under the null hypothesis of co-bubbling. Therefore, to estimate full sample residuals in R , R_b , and \tilde{R} , or subsample residuals in S , S_b , and \tilde{S} , we all have to use a subjectively chosen value, j , to replace for i . According to [Evripidou et al. \(2022\)](#), we have the fitted full sample residuals as $\hat{e}_{y,t,j} = y_t - \hat{\mu}_y - \hat{\beta}_{x,t}x_{t-j}$. When $j \neq i$, $\hat{e}_{y,t,j}$ can be decomposed by replacing y_t in equation of residuals by $y_t = \mu_y + \beta_{x,t}x_{t-i} + \epsilon_{y,t}$ as below:

$$\begin{aligned}\hat{e}_{y,t,j} &= \beta_{x,t}(\mu_y/\beta_{x,t} + x_{t-i} - x_{t-j}) + \epsilon_{y,t} - \hat{\mu}_y - (\hat{\beta}_{x,t} - \beta_{x,t})x_{t-j} \\ \Leftrightarrow \hat{e}_{y,t,j} &= \beta_{x,t}r_{1,t,i,j} + r_{2,t,j}\end{aligned}$$

where $r_{1,t,i,j}$ is a residual from a regression of $x_{t-i} - x_{t-j}$ on a intercept and x_{t-j} , while $r_{2,t,j}$ is a residual from a regression of $\epsilon_{y,t}$ on an intercept and x_{t-j} . When $i = j$, $\hat{e}_{y,t,j} \approx r_{2,t,j}$. Therefore, in line with [Evripidou et al. \(2022\)](#), we can estimate i by minimizing $\hat{\sigma}_{y,t}^2 = (T - |j|)^{-1} \sum_{t=j+1}^{T+j\mathbb{1}(j<0)} \hat{e}_{y,t,j}^2$ with respect to j across a range of values of j . In other words, let \hat{i} is the estimate of i , we have $\hat{i} = \arg \min_{j \in J} \hat{\sigma}_{y,t}^2$, where J is a set of predetermined j and it implies $i \in J$. When a pair of prices is co-explosive, all subsample linear combinations of the pair must be stationary. In this way, we conjecture that the estimated lag \hat{i} proposed by [Evripidou et al. \(2022\)](#) still holds in the S test and its variants.

To measure the ability to detect co-bubble behaviour with different lead/lag values, we use the same DGP as in (3.3) with a wide range of $j \in \{-6, -2, -1, 0, 1, 2, 6\}$. At this stage, we generate two series, x_t and y_t , using Equations (3.1), (3.2), and (3.3) under the null hypothesis with $c_x = 0.4$; however, we apply the test on the error term obtained from regressing y_t on the lag/lead of x_t and a constant. Like [Evripidou et al. \(2022\)](#), we set the true lead/lag i to zero and expect the rejection rate to increase as the absolute distance from j to 0 increases. In this case, the co-bubble occurs contemporaneously. Furthermore, the leads/lags of the independent variable indicate the direction of migration from one market to another. For instance, if we

determine that the residual of the regression of y_t on the lead (lag) of x_t is stationary, then the bubble is more likely to migrate from (to) y_t to (from) x_t . Moreover, the value of i indicates the length of time a bubble existing in one asset price migrates to another price, in the case of a co-bubble relationship between them.

The results are presented in Table B-11. As anticipated, both tests reject more frequently when the lead/lag value is farther away from the actual point of co-bubbling. The rejection rates for the S test tend to be slightly higher than those for the R test. Similar to the results of [Evrupidou et al. \(2022\)](#), these rejection rates also increase notably with $\beta_{x,t}$ which is in line with expectations. This indicates that the negative effects of selecting the wrong lag length could be exacerbated by the impact of co-bubbling. These outcomes remain robust across sample sizes of 200 and 400. Lastly, the rejection rate using estimated values of i , which are shown in the last two columns of the table. The rejection rates obtained by using the R and S tests with the estimated value of i , represented by \hat{i} , are almost identical to those obtained using $j = 0$, indicating that the estimator reliably selects the correct value of $i = 0$. Similar with findings of [Evrupidou et al. \(2022\)](#) in the context of R test, our findings also suggest that the estimator \hat{i} performs well, and we, therefore, recommend using it as standard practice for S test. However, it is important to note that in practice, users must determine the search set j and exercise discretion.

3.6 Empirical Illustrations

3.6.1 Data

In recent research studies, [Figuerola-Ferretti et al. \(2015\)](#), [Figuerola-Ferretti and McCrorie \(2016\)](#), [HLST](#), and [Pan \(2018\)](#) have shown significant evidence of the existence of explosive autoregressive behaviour in precious metals and non-ferrous metals during financial crises. These findings all use the recursive autoregressive-based test of [PWY](#) and its variants. Furthermore, [Escribano and Granger \(1998\)](#) show the long-run (cointegration) relationship of precious metals (i.e., Gold and Silver)

mainly due to a specific bubble and post-bubble period. Even when using a very long monthly sample period from 1970 to 2011 (40 years), [Baur and Tran \(2014\)](#) model shows the same conclusions as [Escribano and Granger \(1998\)](#) did. These empirical studies taken together possibly imply a co-bubble relationship or bubble migration. Therefore, in this section, we focus on detecting co-bubble behaviour, including bubble migration, between pairs of metal prices.

Besides the reasons for focusing on metal prices mentioned above, we use the same dataset of metal prices as [Evripidou et al. \(2022\)](#)'s to highlight the differences between [Evripidou et al. \(2022\)](#)'s full sample test and our backward recursive KPSS-based test. In their paper, [Evripidou et al. \(2022\)](#) show evidence of co-bubbles using a wild bootstrap form of the KPSS-based test on pairs of spot and futures metal prices. As a result, we use similar procedures to theirs to come to our results. In that sense, after detecting explosive behaviour in the individual metal prices using a wild bootstrap generalized right-tailed recursive test of [PSY](#), we employ our supremum recursive tests with a wild bootstrap algorithm and long-run variance estimation to identify the co-bubbles.

[Evripidou et al. \(2022\)](#) use a dataset of spot and futures metal prices to examine the possibility of co-bubbles between these prices using a wild bootstrap version of the KPSS-based test on pairs of metal prices. Therefore, to compare our backward recursive KPSS-based test with the full sample test of [Evripidou et al. \(2022\)](#), we use the same dataset of [Evripidou et al. \(2022\)](#), which includes monthly spot and futures prices for four precious metals (Gold, Palladium, Platinum, and Silver) and six non-ferrous metals (Aluminium, Copper, Lead, Nickel, Tin, and Zinc), obtained from Datastream. We also computed the real metal prices using Core CPI, which was obtained from the Federal Reserve Bank of St. Louis database. The entire dataset comprises 311 monthly observations covering the period from July 1993 to May 2019.

Subsequently, we employ an identical procedure to their study to come to our results. Specifically, after detecting explosive behaviour in individual metal prices using [PSY](#) test, we use our proposed test with a wild bootstrap algorithm and long-

run variance estimation to identify co-bubbles. For that reason, the notations of the R and S tests in this section are presented as \tilde{R} and \tilde{S} , respectively. Also, in this section, we can use a general supremum version of \tilde{S} test (denoted \tilde{GS}) to identify the co-explosive behaviour in the pairs of metal prices. As we mentioned in previous sections, the general supremum algorithm of **PSY** is very computing-consuming particularly when used with a wild bootstrap procedure and long-run variance estimation, as we are doing here.

Figures **B-5 - B-10** graphs the trajectories of real metal prices and their squared log returns. Overall, all the metal prices fluctuate throughout the sample range reflecting their different primary roles as investment assets and manufacturing inputs (see [Evripidou et al., 2022](#)). For instance, demand for non-ferrous metals in BRICS countries¹ drove the prices of these metals up significantly in the early- and mid-2000s. Similarly, after the global financial crisis in 2007-2008, there was a decline in global demand and production of manufactured goods, leading to a significant decrease in the prices of all metals, including non-ferrous and precious metals. As a result, the volatilities of these metals are also high during potential bubbles and crashes.

3.6.2 Testing for explosive autoregression in the individual series

We first test for the presence of explosive autoregressive behaviour in individual series before applying the co-bubble test. Although the explosive autoregressive process may link with the existence of a rational bubble in the prices, it still may be the case when the explosive behaviour is driven by fundamentals consisting of the prices. Despite these considerations, in this study, we use the term "bubble" interchangeably with the presence of explosive autoregressive features in prices and avoid considering the case of explosive behaviour in fundamental prices as it is difficult to determine fundamental prices in practice. In summary, there is no need

¹BRICS is a term created by Jim O'Neill, an economist at Goldman Sachs, in 2001 to refer to five prominent economies - Brazil, Russia, India, China, and South Africa. The term is used to describe these rapidly developing economies that are expected to have significant global influence by 2050.

to decompose the price into bubble and fundamental parts in this study, and we can directly apply the **PSY** test to the price series.

In our empirical analysis, we utilize the GSADF test proposed by **PSY**, which has been shown to be effective in identifying single and multiple bubbles in asset prices. To determine the appropriate lag length, we use Bayesian Information Criteria (BIC), with a maximum of six lags. Additionally, we employ the wild bootstrap procedure introduced by **HLST** with 1,999 bootstrap replications to control for any heteroskedasticity in the data. This enables us to use the resulting p-values to test the null hypothesis of a unit root against the alternative of explosivity.

As shown in Table **B-12**, the last two columns present p-values obtained from the *IID* bootstrap and wild bootstrap tests proposed by **PSY**. Since we use the same dataset of **Evripidou et al. (2022)**, for convenience, the results of **PSY** tests are taken from Table 4 of **Evripidou et al. (2022)**. Here, the results showed that all metal prices, except for Aluminium spot and futures prices, exhibit explosive behaviour. The wild bootstrap test results are not as strong as those from the *IID* bootstrap test, but they lead to the same conclusion of explosive behaviour in metal prices at a significance level of 10%. These findings are consistent with those of **HLST** and **Figuerola-Ferretti and McCrorie (2016)**, who also employed wild bootstrap **PWY/PSY** critical values in their empirical applications.

Furthermore, we examine the date-stamping results in **Evripidou et al. (2022)** to identify the time periods where bubbles are likely to occur in the prices. Once again, we have extracted these results from Table 5 of **Evripidou et al. (2022)**. As we can see in our Table **B-13**, which corresponds to Table 5 of **Evripidou et al. (2022)**, the findings for spot and futures prices are fairly similar. Although the explosive periods vary across prices, most of them exhibit a bubble during 2007-2008 (e.g., Gold, Platinum, Silver, Lead, Nickel, Tin, and Zinc). Additionally, Palladium and Zinc show explosive periods that may be linked to the Dotcom bubble in the 1990s. Some metal prices, including Gold, Platinum, Copper, Lead, and Tin, experience a bubble around 2003-2004.

3.6.3 Results from tests for co-bubble behaviour

According to Barsky et al. (2021), gold plays a very important role in the global economy as a hedge against inflation and a reserve to protect against recessions. Therefore, a bubble in gold may migrate to other metals. However, the causal relationship between pairs of metals is unknown in practice. Therefore, estimating the true lead/lag of the co-explosive model is necessary to determine the direction of migration. Indeed, the migration direction can only be revealed when the lead/lag values show the true direction. Therefore, in this section, we will follow Evripidou et al. (2022) and apply the test on a combination of metal prices to determine whether a bubble in one metal price drives the bubble of another metal price or not.

After testing individual series in Subsection 3.6.2, we will exclude Aluminum from testing co-bubble behaviour with other metals as for this metal the *GSADF* test finds no evidence of explosivity. To test co-bubble behaviour in pairs of metals, we will calculate the \tilde{R} and \tilde{S} (Equations 3.17 and 3.18) and compare them to their corresponding wild-bootstrap critical values. If the tests fail to reject the null hypothesis, we can conclude that a co-explosive bubble is present in the two tested series.

Additionally, as mentioned above, we do not know exactly when the co-explosive bubble of two series will occur and the direction of bubble migration in practice. The estimated lead/lag value will help us determine the direction of bubble migration. Therefore, to estimate the true lead/lag value and identify the timing and direction of bubble migration between pairs of metals, we will consider a range of user-chosen lead/lag values on the independent variable, as discussed in Subsection 3.5.4. Following Evripidou et al. (2022), we will consider lead/lag values up to 1 year, with $j = \{-12, -11, \dots, -1, 0, 1, \dots, 11, 12\}$. This range of lead/lag values is reasonable because the explosive periods of almost all bubbles are around one year (see Table B-13).

As in Evripidou et al. (2022), based on the p-values² of the tests in Tables B-14 and B-15, going through the columns from left to right, when the p-value is less than 2.5%,

²A p-value is defined as the probability of obtaining observed results given that the null hypothesis is true. Here, it is calculated by one subtracts rejection rate, which shows how many the percentages of bootstrap critical values are smaller than our test statistic.

we reject the null hypothesis of the presence of co-explosivity against the alternative hypothesis of no co-explosivity. In other words, we fail to reject the null hypothesis of the stationary linear combination of two price series when the p-value is greater than 2.5%. While the \tilde{R} test shows evidence of a co-explosive bubble in the paired prices of Copper/Lead, Platinum/Copper, Copper/Silver, Lead/Gold, Lead/Tin, Gold/Tin, and Zinc/Nickel, the \tilde{S} test rejects the null hypothesis of co-bubbling in half of these cases except for Lead/Gold, Gold/Tin, Copper/Lead, and Gold-Zinc. However, our proposed test finds another case of co-bubbling: Silver/Lead. Subsection 3.5.2 shows that our proposed test, \tilde{S} , has higher power than the full sample KPSS-based test of Evripidou et al. (2022) to reject the null hypothesis when it is false; therefore, it is unsurprising that we find fewer co-bubble pairs in our results. Furthermore, our findings on the co-explosivity of spot prices are relatively identical to those of futures prices.

As we can see in Table B-13, which shows the bubble periods of spot and futures prices of metals, we may conjecture that the explosive bubbles in metals are in-sample bubbles. In PSY, evidence is shown of the drawbacks of the single supremum test to detect in-sample bubbles compared to the generalized supremum test. In that sense, it is arguable that our backward supremum test may not be powerful enough compared to the double supremum test for detecting bubbles that exist and collapse inside the sample periodically. Therefore, using a double supremum co-bubble test, the GS test, is necessary to test co-bubbles that may occur in-sample. Although we cannot run thousands of simulations of the generalized supremum KPSS-based test (GS) because of intensive computing power requirements, we can still employ the test here on pairs of metal prices where we only need to run on a sample path for each pair. Since we employ long-run variance estimation to address serial correlation in the test, \tilde{GS} , a variant of GS with long-run variance estimator, is used throughout this section. In fact, from the results in the sixth column of Tables B-14 and B-15, besides co-bubbles detected by the S test, we can see that compared with the GS test, the backward sup KPSS test is missing a few other co-bubbles such as

Platinum/Gold, Copper/Gold, Copper/Silver, Silver/Lead, Tin/Silver, Copper/Tin, and Palladium/Nickel. Similar to the \tilde{R} and \tilde{S} tests, the results of the $\tilde{G}\tilde{S}$ test on futures prices are the same as those on spot prices.

Using the estimated lead and lag values \hat{i} in Tables B-14 and B-15, we can determine the migration direction of metal pairs. To keep our discussion brief, we focus on presenting new findings from \tilde{S} and $\tilde{G}\tilde{S}$ that do not match the co-bubbling results reported by [Evrpidou et al. \(2022\)](#). Since the results of the \tilde{R} test have already been reported in [Evrpidou et al. \(2022\)](#), we do not repeat them here. Additionally, because the $\tilde{G}\tilde{S}$ test uses a more general algorithm than that of the \tilde{S} test, all the bubbles detected by the \tilde{S} test are also covered in the findings of the $\tilde{G}\tilde{S}$ test (e.g., Lead/Tin, Gold/Tin, Lead/Gold, Silver/Lead, and Copper/Lead), but not the converse. Furthermore, [Evrpidou et al. \(2022\)](#) discussed the migration direction of their detected pairs under the \tilde{R} test carefully in their paper. While the $\tilde{G}\tilde{S}$ test detects co-explosivity in pairs of Silver/Lead, Tin/Silver, Copper/Tin, Copper/Gold, Palladium/Nickel, and Platinum/Gold, it is unable to identify co-bubbles in pairs of Zinc/Nickel and Copper/Platinum, as the \tilde{S} test of [Evrpidou et al. \(2022\)](#) did. The estimated lead/lag values of pairs that are reported in the third column of Tables B-14 and B-15 show the migration direction of pairs. For example, $\hat{i} = 0$ in the pairs of Silver/Lead, Tin/Silver, indicating contemporaneous co-explosive relationships in those pairs. The explosive behaviour in the Nickel price is found to lead to explosive behaviour in the Palladium price by 12 months. Similarly, the bubble in Platinum is led by the bubble in Gold by 12 months. The explosive behaviour in Copper lags behind Tin by 1 month. Additionally, the results also show that the explosive bubble in Gold leads that in Copper by 12 months. As [Evrpidou et al. \(2022\)](#) noted, we confirm that the Lead price leads the Gold price by 7 months. This finding also matches the results of the bubble in [Figuerola-Ferretti et al. \(2015\)](#) and [Figuerola-Ferretti and McCrorie \(2016\)](#), where bubbles in non-ferrous metals occurred in the period 2003-2007, and precious metals like Gold appeared in and after 2007-2009. In addition, the $\tilde{G}\tilde{S}$ test supports the evidence of explosive behaviour in the Tin price, lagging that of Lead

by 2 months. Furthermore, via the $\tilde{G}\tilde{S}$ test, we find that the Copper lead bubble occurs in Gold 8 months later. This information matches our data-stamping Table B-13 and the conclusions in [Figuerola-Ferretti et al. \(2015\)](#), [Zhao et al. \(2015\)](#), and [Figuerola-Ferretti and McCrorie \(2016\)](#). For the results of the Copper/Tin pair, we can say that it takes one month for the explosive behaviour in the Copper price to migrate to the Tin price. Finally, we find an explosive bubble in Platinum leading that in Gold and a bubble in Nickel leading that in Palladium by 12 months via the $\tilde{G}\tilde{S}$ test. Although the results are statistically significant, the migration point may not be accurate because we cannot ensure that the true lead/lag can be outside of a pre-chosen set of lead/lag J or not. Finally, the results of futures prices of metals are relatively similar to those of the spot prices.

The results of co-explosivity in the empirical application section are illustrated by figures from Figure B-11 to Figure B-14. In these graphs, the metal prices are normalized and shifted vertically before plotting them with normalized residuals from corresponding regressions on the same graph. Additionally, the series is trimmed to match the dependent variable with the estimated lead/lag of the independent variable in Figures B-14 and B-15. In these figures, we can observe instances in time where pairs of metals move up together. The reported residuals are estimated on a full sample. Here, we only report non-overlapped pairs for both spot and futures metal markets. While Figures B-11 and B-12 show co-explosive pairs on the spot market, futures market are presented in Figures B-13 and B-14.

3.7 Conclusion

This chapter contributes to the literature on modelling the relationship of explosive series at the end of the sample by introducing a modified KPSS-based test for testing co-explosive behaviour. Specifically, our test combines the test of [Evripidou et al. \(2022\)](#) and the backward recursive procedure of [PSY](#). In the context of heteroskedasticity, [Evripidou et al. \(2022\)](#) prove that the limiting null distribution of test statistics

still depends on the pattern of heteroscedasticity; therefore, we, in this chapter, still use the wild bootstrap algorithm of [HLST](#) to provide a size-robust test under various volatility specifications. On the other hand, when the co-explosive model contains serial correlation, as suggested by [Evrpidou et al. \(2022\)](#), we use long-run variance estimator to correct the finite sample size of the test. As shown in finite sample simulation results, these treatments are highly effective to guarantee the size of the test controlled.

Together with that, Monte Carlo simulations demonstrate that our backward recursive test generally outperforms the full sample test of [Evrpidou et al. \(2022\)](#) in rejecting the spurious co-explosivity. In fact, the results are robust across almost all different specifications of bubble, heteroskedasticity, serial correlation, and co-bubble settings. Although our test is more powerful than [Evrpidou et al. \(2022\)](#)'s test in homoskedastic and upward patterns of volatility, the finite sample size of our test is oversized in some heteroskedastic scenarios (i.e., downward shifts, downward trend, and double shift). Under serial correlation, our simulated results show the competence of different kernels with different co-explosive tests, where our test works better under the Bartlett kernel at a suitable lag parameter. Because the R and S test are very sensitive to the choice of kernel and lag parameter, we recommend using the quadratic spectral kernel for the R test and the Bartlett kernel for the S test.

Applying our proposed test with long-run variance estimator to empirical data on various metal prices with explosive behaviour, the results demonstrate the presence of co-explosivity, indicating that bubbles migrate from one metal price to another. The results of co-bubbles from single backward supremum test are reasonable and consistent with those using double supremum recursive test. The single backward supremum test detects the same co-explosivity of metal pairs as the generalized supremum test, but the latter detects more co-bubbles than the former. In addition, the supremum tests detect a few more co-bubbles in pairs of metals, but they also reject some co-bubbles detected by [Evrpidou et al. \(2022\)](#) full sample test. The results show the presence of co-bubbles under both spot and futures prices are relatively

similar.

Finally, although we could not draw finite sample power curves for the double supremum test to compare with our test due to limitations in computing power, we still highly recommend the use of the double supremum test (GS) over the S test in practice. This is because the double supremum test is a generalized supremum test in which a supremum test is repeatedly implemented on moving windows, which has advantages in capturing in-sample co-bubbling.

On the Behavior of Tests for Stock Return Predictability during Bubble Regimes

The predictability of asset returns is a significant and contentious issue in the fields of economics and finance. The fourth chapter makes three key contributions to this topic. Firstly, we introduce a more versatile data generating process [DGP hereafter] compared to the one described in [Yang et al. \(2022\)](#). Both DGPs aim to incorporate in the price series from which returns are generated in the period during which the return predictability test is conducted, however, the more versatile DGP allows us to adjust the bubble specifications in an uncorrelated manner with the fundamental asset return. This approach helps to avoid the inclusion of an indirectly observable variable in our return predictive model. Secondly, based on the proposed DGP, we investigate the finite sample performance of two widely used predictability tests (i.e., the IVX test, Bonferroni-t, and Bonferroni-Q tests) through simulations. The results show that these tests tend to over-reject the null hypothesis of no predictability when the bubble is large and long-lasting, although the Bonferroni-t test appears to have more well-controlled size across a majority of bubble and predictive model specifications. Lastly, using the updated dataset from [Welch and Goyal \(2008\)](#) covering the period from January 1927 to December 2021, we re-assess the return predictability of 14 financial and macroeconomic predictors. The results of our simulations are further

validated by our empirical findings in which the predictability tests provide more rejections during bubble regimes.

4.1 Introduction

The predictability of lagged financial variables over future stock returns is one of the fundamental topics in finance. This is because understanding return predictability in practice is very important to select crucial predictors in portfolio management and risk analysis. In fact, many different predictor variables are used in predictive models to answer the question: "Can future returns be predicted by specific independent variables?". Early empirical studies, including [Fama \(1970\)](#), [Fama \(1990a\)](#), [Keim and Stambaugh \(1986\)](#), [Campbell and Shiller \(1988a\)](#), [Campbell and Shiller \(1988b\)](#), [Fama and French \(1988b\)](#), [Fama and French \(1989\)](#), [Fama \(1990b\)](#), [Campbell \(1991\)](#) and [Cochrane \(1992\)](#) often show evidence of in-sample predictability of U.S. stock index returns over a relatively long time horizon.

Despite a large amount of research supporting the existence of return predictability, findings are still controversial because the return predictability test might provide spurious results about the predictability of predictors, in which the predictability tests tend to over-reject the null hypothesis of no return predictability and those results are not held through time. For instance, [Cavanagh et al. \(1995\)](#) show that a standard t-test, which is used in testing a null hypothesis of no predictability, suffers from severe size distortions when the predictor is both persistent and endogenous, [Ang and Bekaert \(2007\)](#) show evidence of short-horizon return predictability with interest rates or the three-month T-bill rate and the presence of predictability is not robust across countries and different sample periods. Together with that, by using various prominent variables from previous research, [Welch and Goyal \(2008\)](#) show poor predictability of models using those variables both in-sample and out-of-sample. Moreover, when testing for long-horizon predictability, research has shown that there is a degree of predictability in stock returns over long periods (cf. [Fama and French,](#)

1988a), but it disappears when adjustments are made for heteroskedasticity and serial correlation in the error terms induced by cumulative returns (see e.g., [Richardson and Smith, 1991](#) and [Hodrick, 1992](#)). [Boudoukh et al. \(2006\)](#), for example, demonstrated that when returns cannot be predicted, the estimated return forecasting coefficients may increase with the horizon due to sampling variation alone.

Besides the expansion of empirical studies to find good predictors for stock returns, theoretical research has provided several new candidate tests for predictability. [Gregory Mankiw and Shapiro \(1986\)](#), [Nelson and Kim \(1993\)](#), [Elliott and Stock \(1994\)](#), [Stambaugh \(1999\)](#), [Lanne \(2002\)](#), and [Torous et al. \(2004\)](#) show that strongly persistent predictors and the correlation between innovations in the predictors and in returns lead to the asymptotic distribution of the standard t-statistic to depend on nuisance parameters. Accordingly, the standard t-test over-rejects the null hypothesis if we compare the test statistic with conventional critical values (see [Cavanagh et al., 1995](#), [Campbell and Yogo, 2006](#) [CY hereafter], [Jansson and Moreira, 2006](#) and [Phillips and Magdalinos, 2008](#)). According to [Lewellen \(2004\)](#), the presence of highly persistent and endogenous predictors is very common in practice since endogeneity and high persistence are typical characteristics of commonly used predictors (e.g., price-scaled ratios). This finding has motivated researchers to construct improved tests for the predictability that allow for both strong persistence and endogeneity in the predictor series. For instance, likelihood-based tests that are robust to a strongly persistent predictor and endogenous innovations have been proposed (e.g., Bonferroni t-test of [Cavanagh et al. \(1995\)](#), sup-bound Q-test of [Lewellen \(2004\)](#), [Jansson and Moreira \(2006\)](#)'s conditional test and Bonferroni-Q test of [CY](#)). To account for highly persistent regressors, these tests assume the regressors have the form of a first-order autoregression with a local-to-unit root $\rho = 1 + c/T$, approaching a random walk as the sample size T increases to infinity.

Among likelihood-based tests, the Bonferroni type tests of [Cavanagh et al. \(1995\)](#) and [CY](#) are the most prominent. For a while, before the IVX test come into light, a great deal of empirical research applied the Bonferroni Q test of [CY](#) to examine

return predictability. Therefore, in this chapter, we will evaluate the behaviour of these three tests under the presence of a bubble in return. Although Bonferroni-based tests are prevalent in practice and empirical research, these procedures are excessively intricate and have limitations. Indeed, while the Bonferroni-Q test of [CY](#) is quite successful for testing predictability in the cases where endogenous and highly persistent regressors exist, [Ang and Bekaert \(2007\)](#) show it is oversized if the persistence of predictors are weak (i.e predictors are stationary or near-stationary) or the sample size is relatively small. Likewise, [CY](#) show that the Bonferroni-t test of [Cavanagh et al. \(1995\)](#) and sup-bound Q-test of [Lewellen \(2004\)](#) lack power to detect return predictability relative to the Bonferroni-Q test when the predictor is strongly persistent and endogenous. Furthermore, because the joint predictability by combinations of financial predictors cannot be tested, the Bonferroni-based tests are restricted to the case of univariate regression.

Consequently, various alternative tests have been developed to be robust to the characteristics of the predictor. In fact, [Phillips and Magdalinos \(2008\)](#) proposed a new instrumental variable (IV) method, known as the IVX regression, which allows for robust chi-square inference across a broader range of values near unity than previous studies that have typically focused solely on the case of a single regressor with near integration (local to unity). Later, works of [Gonzalo and Pitarakis \(2012\)](#), [Phillips and Lee \(2013\)](#), [Breitung and Demetrescu \(2015\)](#), [Kostakis et al. \(2015\)](#) [[KMS](#) hereafter], [Lee \(2016\)](#), [Demetrescu and Hillmann \(2022\)](#), [Demetrescu et al. \(2022a\)](#), and [Demetrescu et al. \(2022b\)](#) extended the instrumental variable [IVX hereafter] approach of [Phillips and Magdalinos \(2008\)](#) to tests for predictability. In that sense, the IVX based-tests are improved to be robust to stylized facts of financial time series data (e.g., heteroskedasticity or serial correlation).

According to [Demetrescu et al. \(2022a\)](#), the IVX test of [KMS](#) is the most prominent return predictability test. In their research, [KMS](#) use the extended instrumental variable [IVX] procedure of [Phillips and Magdalinos \(2008\)](#) to estimate the predictive regression. For each predictor, they construct a corresponding mildly-integrated

instrument formed from the first differences of the predictor. Because the IVX instrument has lower persistence than the near-integrated regressors, predictability statistics have asymptotically pivotal limiting null distributions robust to the persistence of the predictor. Although IVX-based predictability statistics possess standard (pivotal) limiting null distributions, regardless of whether the predictor is local-to-unity or weakly dependent (stationary), it provides a very poor approximation to their finite sample behaviour, particularly for highly persistent and endogenous predictors. Therefore, [KMS](#) suggest a finite sample correction for the standard error in the IVX test statistic. However, [Demetrescu et al. \(2022a\)](#) show that the correction only works well on the two-sided test and the one-sided IVX test suffers from severe size distortions. Together with that, by simulations, [Demetrescu et al. \(2022a\)](#) show although the IVX works well for tests against two-sided alternatives, the tests against one-sided alternatives are badly size-distorted compared to Bonferroni-based tests. Additionally, under the context of multivariate regression, [Xu and Guo \(2022\)](#) show that the IVX test tends to discover spurious predictability as the number of predictors increases. Despite this drawback of the IVX test, for simplicity, we will use it to look into the behaviour of tests under the existence of a rational bubble.

As we mentioned above, while most papers focus on issues relating to predictors (e.g., high persistence, endogeneity, heteroskedasticity, and serial correlation), there is little literature discussing potential issues of predicted variables (i.e., return). By letting a rational bubble appear in the log price of the asset, [Yang et al. \(2022\)](#) show that the IVX test is badly size-distorted. This is because the return of a stock price containing the bubble still has explosive behaviour. Thus, [Yang et al. \(2022\)](#) argue that estimated coefficients in the predictive regression are biased since two persistent variables, a variable of bubble effect and an instrumental variable, cause spurious correlation.

[Yang et al. \(2022\)](#) utilise a log-linear bubble model derived by [Campbell et al. \(1997\)](#) and [Phillips et al. \(2011\)](#). Because the explosiveness in stock price is driven by the bubble component, in line with [Phillips et al. \(2015\)](#) [[PSY](#) hereafter], log price

p_t is assumed to follow an explosive autoregressive process with two regimes as $p_t = \rho_b p_{t-1} + \epsilon_t$, where $\rho_b > 1$ when a bubble emerges at time t and otherwise when $\rho_b = 1$, it means the prices is a unit root process.

As in [Yang et al. \(2022\)](#), during the bubble period, the logarithmic excess stock returns, r_t depend on $b_{t-1} = (\rho_b - 1)p_{t-1}$ constituted by a pre-determined component the logarithm of lag one of stock price, and an indirectly observable explosive root in the bubble model. In that regard, [Yang et al. \(2022\)](#) filter the bubble component out from the returns. In more detail, they employ the bubble date-stamping algorithm of [PSY](#) to estimate the autoregressive parameter ρ_b in the bubble model, then construct the estimator of the variable b_{t-1} from the estimated autoregressive value of $\hat{\rho}_b$. Consequently, after removing the fitted values, which were constructed from the estimator, from the corresponding predicted variable (i.e., returns) and predictors, they provide an extended IVX test statistic robust to the bubble effect.

In this chapter, we also consider the predictability tests under bubble period as [Yang et al. \(2022\)](#); however, we focus more on analyzing how different predictability tests behave rather than constructing a test statistic robust to the bubble effect as the way [Yang et al. \(2022\)](#) have done. On the way to do that, we construct a DGP based on the DGP of [CY](#) which is more natural and flexible than that of [Yang et al. \(2022\)](#). In fact, we employ the price model of [PSY](#) where the current stock price, P_t is equal to the sum of the fundamental price, P_t^f and bubble component, B_t . We assume that the part of the stock return that can be predicted by predictors is the fundamental return; therefore, the original form of the predictive regression model of [CY](#) does not contain the pre-determinant bubble factor as in [Yang et al. \(2022\)](#). Secondly, while [Yang et al. \(2022\)](#) focus on the size and power of their extended IVX test by letting the autoregressive parameter of the bubble be fixed, we in this chapter emphasize examining how the finite sample size of Bonferoni-based tests in [CY](#) and IVX test of [KMS](#) behave with various changes in the specification of bubbles (e.g., length, position, and magnitude of the bubble). Furthermore, in empirical applications, we will demonstrate the changes in the predictability of a large number of different

predictors through return predictability tests in subsamples with and without a bubble. In fact, while [Yang et al. \(2022\)](#) only applied their test to the full sample, we employ the test on the subsamples to investigate how common predictability tests behave in practice under the bubble effect. This is another novel aspect of this chapter.

By using finite sample simulations, we examine the behaviour of the predictability tests against one-sided alternatives under various specifications of bubbles and predictors. Overall, the tests over-reject the null hypothesis of no predictability when a bubble exists in the stock price. In that sense, the tests will be affected more strongly if the bubbles are large and long-lasting. The results show that the Bonferroni-t test has better size control than IVX and Bonferroni-Q test when the bubble exists at the end of the price series. The Bonferroni-Q test is very sensitive to the presence of bubbles. When the bubble is large and long-lasting in the sample, the Bonferroni-Q test exhibits more severe size distortions than the other two tests. The behaviour of tests becomes complex when an in-sample bubble exists. In other words, when the bubble starts and bursts in the sample, the finite sample size of the tests is not monotonically increasing when the bubble length or the growth rate of the bubble increase. The reason may come from the effect of the large negative jump in return caused by the in-sample bubble.

Besides evaluating the behaviour of the predictability tests on simulated data, we also examine an empirical application that reinforces our numerical results on the well-known dataset of [Welch and Goyal \(2008\)](#). To predict stock returns, most researchers often focus on relevant financial variables such as dividend price ratio or dividend yield ratio, earning price ratio, and common interest rate-related variables (e.g., treasury-bill rates and long-term rates). [Fama \(1990a\)](#), for instance, examines the predictability of stock returns using various candidate predictors including interest rates, industrial production, GNP, and capital stock and expenditure, while [CY](#) considers candidate predictors that include the dividend-price ratio, the earning-price ratio, the three-month T-bill rate, and the long-short yield spread. We here use

similar financial and macroeconomic predictors as previous researchers which are collected and updated up to December 2021 by Welch and Goyal (2008) in order to re-evaluate the return predictability of regressors. Therefore, in the empirical application section, on the one hand, we still investigate the return predictability of predictors on the full sample as in previous research studies. On the other hand, we divide the data sample into subsamples with and without the Dot-com bubble period, which is determined by applying the PSY test to date-stamp the start and end dates of bubbles in stock prices. Our empirical results actually confirm that commonly used predictability tests are more likely to reject in the presence of a bubble.

The remainder of this chapter is organized as follows. In Section 4.2 we introduce our predictive regression model that allows for a potential bubble in the stock price. Section 4.3 describes IVX and Bonferroni-based test procedures and their limitations. Section 4.4 presents the asymptotic properties of the tests. Section 4.5 provides simulation results illustrating how return predictability tests behave both with and without bubbles in the stock price. In Section 4.6, we report empirical results from re-evaluating the return predictability of fourteen popular financial and macroeconomic variables in full sample and subsamples with and without bubble. Section 4.7 provides a brief conclusion.

4.2 Predictive Regression and Assumptions

In this chapter, we consider the following predictive regression model.

$$r_t^f = \mu_r + \beta x_{t-1} + u_t, \quad t = 1, \dots, T \quad (4.1)$$

$$x_t = \mu_x + \xi_t \quad (4.2)$$

$$\xi_t = \rho \xi_{t-1} + v_t \quad (4.3)$$

where T is the sample size, r_t^f is the logarithmic fundamental (excess) return. x_{t-1} denotes a putative predictor. u_t denotes innovations forming a martingale difference sequence (MDS). β is the slope coefficient of the predictive model. μ_r and μ_x are

intercepts of r_f^f and x_t , respectively.

Although the predictive regression model can be formed in a general set-up that includes multiple regressors, we here only focus on the univariate form of the model. In that regard, we can compare the behaviour of the Bonferroni-based tests and the IVX test since the former is designed to test the return predictability of only a single variable at one time. Following **CY**, we make the assumptions as below:

Assumption 4.1 *Let L be the lag operator, we assume $\psi(L)v_t = e_t$, where $\psi(L) = \sum_{i=0}^{p-1} \psi_i L^i$ with $\psi_0 = 1$ and $\psi(1) \neq 0$ with the roots of $\psi(L)$ assumed to be less than one in absolute value. The initial condition, ξ_0 , is a mean zero $o_p(T^{1/2})$ variate. The autoregressive parameter ρ is given by $\rho := 1 + c/T$ for a fixed c . This allows for unit root regressors ($c = 0$), mildly stationary regressors ($c < 0$), and mildly explosive regressors ($c > 0$).*

Remark 4.1 *Innovations, u_t , is serially uncorrelated. This condition is appropriate to empirical evidence of serial correlation of the unpredictable component of returns. Furthermore, Assumption 4.1 permits the dynamics of the predictor variable to be represented by an AR(p) model, with the persistence of the predictor (strong or weak) being determined by the parameter ρ .*

Assumption 4.2 *The conditional homoskedasticity in **CY** and **KMS**,*

$$\begin{aligned} (i) \quad & \mathbb{E}[(u_t, e_t)', (u_t, e_t)] := \begin{pmatrix} \sigma_u^2 & \sigma_u \sigma_e \\ \sigma_u \sigma_e & \sigma_e^2 \end{pmatrix} \\ (ii) \quad & \sup_t \mathbb{E}[u_t^4] < \infty \\ (iii) \quad & \sup_t \mathbb{E}[e_t^4] < \infty \end{aligned}$$

We define $\delta := \frac{\sigma_{eu}}{\sigma_e \sigma_u}$ is the correlation between the innovations $\{u_t\}$ and $\{e_t\}$. For future reference, we define $\omega_v^2 := \lim_{T \rightarrow \infty} \mathbb{E}(\sum_{t=1}^T v_t)^2 = \sigma_e^2 / \psi(1)^2$ as the long-run variance of $\{v_t\}$.

Remark 4.2 *The conditions in Assumption 4.1 are largely similar to those of Assumption 1 presented in **CY**. These conditions allow for conditional heteroscedasticity in the sequence of innovations, while imposing unconditional homoscedasticity.*

Assumption 4.3

$$P_t = P_t^f + B_t \quad (4.4)$$

$$P_t^f = P_{t-1}^f \exp(r_t^f) \iff r_t^f = p_t^f - p_{t-1}^f \quad (4.5)$$

$$B_t = \begin{cases} \rho_b B_{t-1} + v_t, & t = \lfloor \tau_1 T \rfloor + 1, \dots, \lfloor \tau_2 T \rfloor \\ 0, & \text{otherwise} \end{cases} \quad (4.6)$$

$$r_t = \begin{cases} r_t^f, & B_t = 0 \\ p_t - p_{t-1}, & \text{otherwise} \end{cases} \quad (4.7)$$

The bubble in return is created following rational bubble-generating mechanisms of [Blanchard and Watson \(1982\)](#); [Diba and Grossman \(1988\)](#); therefore, P_t is the price of the asset, which can be decomposed into a market fundamental, P_t^f and a bubble component, B_t with $B_0 = o_p(T^{1/2})$. p_t and p_t^f are the logarithmic price and logarithmic fundamental price, respectively. In that, $v_t \sim NIID(0, 1)$ and $\rho_b = 1 + c_{bub}/T$ presents the autoregressive parameter (or the magnitude of the bubble component), which displays locally explosive autoregressive behaviour. $\lfloor \tau_1 T \rfloor + 1$ is the position where the bubble starts from and $\lfloor \tau_2 T \rfloor$ is a position where the bubble ends. It means when $\tau_2 = 1$, then we can say the bubble starts from the time, $t = \lfloor \tau_1 T \rfloor + 1$, exists till the end of the sample, and bursts somewhere out of the sample; however, if $0 < \tau_2 < 1$ we have a bubble that starts at $t = \lfloor \tau_1 T \rfloor + 1$ and bursts at $t = \lfloor \tau_2 T \rfloor$ before the sample ends. B_t only exists in bubble regime from $t = \lfloor \tau_1 T \rfloor + 1$ to $t = \lfloor \tau_2 T \rfloor$, it receives value of zero outside its bubble period. Here, we assume the bubble is rational and follows a positive explosive autoregressive process. [Tirole \(1982\)](#) and [Diba and Grossman \(1988\)](#) argue that rational bubbles cannot be negative. In this chapter, we also ensure this condition when constructing an explosive process in stock returns. All detailed procedures will be stated in Section [4.5](#).

4.3 Return Predictability Tests

In this section, we outline feasible versions of the IVX test statistic of **KMS** and the Bonferroni type tests of **Cavanagh et al. (1995)**, and **CY** which are used to detect predictability in practice. All tests are designed to test the null hypothesis $H_0 : \beta = 0$, which means the return is not predictable by the predictor.

4.3.1 IVX Test

The basic idea underlying the IVX procedure of **Phillips and Magdalinos (2008)** is to instrument the regressor x_{t-1} by a variable of controlled persistence, constructed as

$$z_0 = 0 \text{ and } z_t = (1 - \rho L)_+^{-1} \Delta x_t := \sum_{j=0}^{t-1} \rho^j \Delta x_{t-j}, t = 1, \dots, T. \quad (4.8)$$

where $\rho := 1 - \zeta T^{-\eta}$ with $\zeta > 0$ and $0 < \eta < 1$. The IVX scale and exponent parameters, ζ and η respectively, are tuning parameters set by the practitioner. In that sense, since ρ converges slowly to 1, one can adjust these two parameters (i.e., ζ and η) for a trade-off between the size and power of the test. By employing the instrument variable, **KMS** propose the full sample IVX-based t-ratio statistic for testing the return predictability of a single regressor as given below:

$$t_{zx} := \frac{\hat{\beta}_{zx}}{s.e.(\hat{\beta}_{zx})}, s.e.(\hat{\beta}_{zx}) := \frac{\sqrt{\hat{\sigma}_u^2 \sum_{t=1}^T z_{t-1}^2 - \Xi}}{\sum_{t=1}^T z_{t-1} (x_{t-1} - \bar{x}_{-1})} \quad (4.9)$$

$$\hat{\beta}_{zx} := \frac{\sum_{t=1}^T z_{t-1} (r_t - \bar{r})}{\sum_{t=1}^T z_{t-1} (x_{t-1} - \bar{x}_{-1})} \quad (4.10)$$

where, $\bar{r}_t = T^{-1} \sum_{t=1}^T r_t$, $\bar{x}_{-1} := T^{-1} \sum_{t=1}^T x_{t-1}$ is the de-meaned value of x_{t-1} , $\Xi := T \bar{z}_{-1}^2 (\hat{\sigma}_u^2 - \hat{\sigma}_{lr,ue}^2 \hat{\sigma}_{lr,e}^{-2})$ is the finite-sample correction term which is suggested by **KMS** to control the finite-sample size. $\bar{z}_{-1}^2 := T^{-1} \sum_{t=1}^T z_{t-1}^2$. $\hat{\sigma}_u^2$, $\hat{\sigma}_{lr,e}^2$ and $\hat{\sigma}_{lr,ue}^2$ are estimates of the short-run variance of u_t , the long-run variance of e_t and of the long-run covariance between u_t and e_t , respectively.

We can calculate $\hat{\sigma}_u^2 := \sum_{t=1}^T \hat{u}_t^2$. \hat{u}_t is residuals that can be computed in many ways. In one way, under the null hypothesis, someone can employ $\hat{u}_t := r_t - \bar{r}$. However, in another way, which is used by [Phillips and Magdalinos \(2008\)](#), [Breitung and Demetrescu \(2015\)](#), and [KMS](#), residuals, \hat{u}_t , can be obtained from regressing r_t on x_{t-1} and a constant as in (4.1). With Assumptions 4.1-4.2, under the local alternative hypothesis that $\beta > 0$, residuals from these two methods are asymptotic equivalent; therefore, choosing one over the other does not affect the asymptotic properties of the IVX test statistic. Besides these two ways to estimate \hat{u}_t , it is feasible to use corresponding IV residuals, $\hat{u}_t := r_t - \hat{\beta}_{iv,0} - \hat{\beta}_{iv,1}x_{t-1}$ where $\hat{\beta}_{iv,j}, j \in \{0,1\}$ represents two-stage least square (2SLS) estimator of α and β in (4.1); however, according to [Demetrescu et al. \(2022b\)](#), IV residuals converge slower than the residuals from two previous methods, and their finite-sample behaviour is less stable than those of two other ways for estimating the residuals \hat{u}_t .

4.3.2 Bonferroni Based Tests

In this section, first of all, we will discuss the t-test statistic and Q-test statistic, both of which are infeasible due to the dependence of their limit distribution on the unknown non-centrality parameter, c . Together with that, in subsections, we will show how the Bonferroni method can be used to implement feasible versions of these tests in practice.

Regressing r_t on constant and x_{t-1} , t test statistic is given as below:

$$t := \frac{\hat{\beta}}{s.e.(\hat{\beta})}, s.e.(\hat{\beta}) := \sqrt{\frac{\hat{\sigma}_u^2}{\sum_{t=1}^T (x_{t-1} - \bar{x}_{-1})^2}} \quad (4.11)$$

$$\hat{\beta} := \frac{\sum_{t=1}^T (x_{t-1} - \bar{x}_{-1})(r_t - \bar{r}_t)}{\sum_{t=1}^T (x_{t-1} - \bar{x}_{-1})^2} \quad (4.12)$$

Q test statistic of [CY](#) is as follows.

$$Q(\rho) = \frac{\sum_{t=1}^T (x_{t-1} - \bar{x}_{-1}) \left[r_t - \frac{\sigma_{ue}}{\sigma_e \omega_v} (x_t - \rho x_{t-1}) \right] + \frac{T}{2} \frac{\sigma_{ue}}{\sigma_e \omega_v} (\omega_v^2 - \sigma_v^2)}{\sigma_u (1 - \delta^2)^{1/2} \left[\sum_{t=1}^T (\bar{x}_{t-1}^\mu)^2 \right]^{1/2}} \quad (4.13)$$

where σ_v^2 is the short-run variance of the error process v_t . Under the null hypothesis when $\delta = 0$, or when $\delta \neq 0$ and the true value of ρ is known, the Q-test statistic can be shown to follow a standard normal limiting distribution. However, tests based on $Q(\rho)$ are infeasible because the computation of $Q(\rho)$ requires knowledge of ρ , where c , and hence ρ , is unknown and cannot be estimated consistently. Therefore, **CY** propose constructing a confidence interval for c as in **Stock (1991)** and **Cavanagh et al. (1995)**, by using the known distribution of some unit root test statistic and using Bonferroni methods to deliver a confidence interval for β based on this initial confidence interval for c .

Cavanagh et al. (1995) show that the asymptotic distribution of the t-statistic depends on the nuisance parameter c causing over-rejection of the null hypothesis of no predictability when testing in the right tail both asymptotically and in finite samples if using standard normal critical values. Therefore, **Cavanagh et al. (1995)** constructs a confidence region for β that does not depend on c by employing the Bonferroni method. As noted by **Elliott and Stock (2001)**, a more powerful unit root test leads to a more precise confidence interval for c . As such, **CY** replace the DF-OLS test used by **Cavanagh et al. (1995)** with the DF-GLS unit root test proposed by **Elliott et al. (1996)** when constructing their initial confidence interval for c . Similar to the t-test, Q-test is infeasible and is required to know the information of a nuisance parameter ρ (or equivalently c). The Q statistics in Equation (4.13) can be computed using values of c from the confidence interval for c obtained by inverting the DF-GLS unit root test statistic. In other words, by utilizing a confidence interval of the unknown c parameter a Bonferroni-based test can provide a feasible confidence interval for β .

Both **CY** and **Cavanagh et al. (1995)** use Bonferroni-based methods to implement test procedures based on these statistics for an unknown value of c . The procedure to construct Bonferroni confidence interval for β is given:

Step 1: Construct a $100(1 - \alpha_1)\%$ confidence interval for ρ , denoted $C_\rho(\alpha_1)$.

Step 2: Construct a $100(1 - \alpha_2)\%$ confidence interval for β given ρ , denoted $C_{\beta|\rho}(\alpha_2)$.

It means for each value of ρ in $C_\rho(\alpha_1)$, we obtain a confidence interval $C_{\beta|\rho}(\alpha_2)$.

Step 3: Construct a confidence interval independent of ρ , denoted $C_\beta(\alpha)$, where

$$C_\beta(\alpha) = \bigcup_{\rho \in C_\rho(\alpha_1)} C_{\beta|\rho}(\alpha_2)$$

By Bonferroni's inequality, the confidence interval, $C_\beta(\alpha)$, has coverage of at least $100(1 - \alpha)\%$ where $\alpha = \alpha_1 + \alpha_2$.

Although both Bonferroni-t and Bonferroni-Q tests use the same procedures to construct the Bonferroni confidence interval for β , there are many different features between them. In the next subsections, we will present the detailed procedures of these two Bonferroni-based tests.

4.3.2.1 The Bonferroni t test

Following the paper of [Cavanagh et al. \(1995\)](#), the Bonferroni-t test procedure is performed as follows:

Step 1: Obtain $\hat{\beta}$, residuals \hat{u}_t and the standard error for $\hat{\beta}$, $SE(\hat{\beta})$ by run regression of r_t on x_{t-1} and a constant.

Step 2: Run ADF regression with the intercept below to obtain $DF - OLS$ statistic.

$$\Delta x_t = \mu_{\Delta x} + \theta_O x_{t-1} + \sum_{i=1}^{p-1} \psi_i \Delta x_{t-i} + e_t$$

where Δ denotes the first difference operator, where $\Delta x_t = x_t - x_{t-1}$ and t -statistic for θ_O is $DF - OLS$ statistic.

Step 3: Given the $DF - OLS$ statistic from step 2, invert the $DF - OLS$ statistic to construct a $100(1 - \alpha_1)\%$ (asymptotic) confidence interval $[\underline{c}, \bar{c}]$ for c using pre-defined confidence belts and the associated confidence interval for ρ by $[\underline{\rho}, \bar{\rho}] = [1 + \underline{c}/T, 1 + \bar{c}/T]$.

Step 4: Let $d_{c,\eta}$ be the η -level critical value of null distribution of t for a given value of c . [Cavanagh et al. \(1995\)](#) show that a $100(1 - \alpha_2)\%$ asymptotic confidence belt for β can be constructed as $[\underline{\beta}^t(\alpha_1, \alpha_2), \bar{\beta}^t(\alpha_1, \alpha_2)]$ where

$$\begin{aligned}\underline{\beta}^t(\alpha_1, \alpha_2) &:= \hat{\beta} - \bar{d}(\alpha_1, \alpha_2)SE(\hat{\beta}) \\ \bar{\beta}^t(\alpha_1, \alpha_2) &:= \hat{\beta} - \underline{d}(\alpha_1, \alpha_2)SE(\hat{\beta})\end{aligned}$$

with

$$(\underline{d}(\alpha_1, \alpha_2), \bar{d}(\alpha_1, \alpha_2)) = \left(\min_{\underline{c} \leq c \leq \bar{c}} d_{c, \alpha_2/2}, \max_{\underline{c} \leq c \leq \bar{c}} d_{c, 1-\alpha_2/2} \right)$$

For a right-tailed test, the null of no return predictability is rejected if $\underline{\beta}^t(\alpha_1, \alpha_2) > 0$, whereas, for a left-tailed test, the null is rejected if $\bar{\beta}^t(\alpha_1, \alpha_2) < 0$. The (asymptotic) coverage of confidence interval for β is at least $100(1 - \alpha)\%$ with $\alpha = \alpha_1 + \alpha_2$.

[Cavanagh et al. \(1995\)](#) show that the Bonferroni interval may be very conservative in practice. In that sense, the actual coverage probability is greater than the nominal confidence level $100(1 - \alpha)\%$, which may cause more false negatives, or the test is under-sized. In regard to one-sided tests, the asymptotic size of one-sided tests is smaller than $100(\alpha/2)\%$ for all values of c . Therefore, [Cavanagh et al. \(1995\)](#) propose a refinement of the Bonferroni method to make the test less conservative by shrinking the confidence interval for ρ until the asymptotic size of the Bonferroni test is maximised at the desired significance level, $\tilde{\alpha}$, across a grid of values of c . To do so they fix $\alpha_2 = 0.10$ and choose $\bar{\alpha}_1^t$ and $\underline{\alpha}_1^t$, for each δ such that

$$Pr(\underline{\beta}^t(\bar{\alpha}_1^t, \alpha_2) > \beta) \leq \tilde{\alpha}/2 \text{ and } Pr(\bar{\beta}^t(\underline{\alpha}_1^t, \alpha_2) > \beta) \leq \tilde{\alpha}/2 \quad (4.14)$$

holds across a grid of values of $c \in [-5, 50]$, with equality at some point on the grid. Consequently, for chosen values of δ , the one-sided tests for predictability constructed in this manner will have an asymptotic size of exactly $\tilde{\alpha}/2$ for some permissible value of c while remaining slightly under-sized for all other values

of c . We denote the confidence interval of β from this refined Bonferroni t-test as $[\underline{\beta}^{tOLS}(\bar{\alpha}_1^t, \alpha_2), \bar{\beta}^{tOLS}(\underline{\alpha}_1^t, \alpha_2)]$ and denote the predictability test based on this confidence interval as *Bonf.t.*

4.3.2.2 The Bonferroni Q test

In detail, following **CY**'s discussion in their online appendix, the Bonferroni Q test is conducted as follows:

Step 1: Obtain $\hat{\beta}$, residuals \hat{u}_t and the standard error for $\hat{\beta}$, $SE(\hat{\beta})$ by run regression of r_t on x_{t-1} and a constant.

Step 2: Run regression $\Delta x_t = \mu_{\Delta x} + \theta x_{t-1} + \sum_{i=1}^{p-1} \psi_i \Delta x_{t-i} + e_t$ to obtain the coefficients $\hat{\psi}_i$, ($i = 1, \dots, p-1$), where the lag length can be set manually or chosen automatically by using BIC and the residuals \hat{e}_t . Additionally, an OLS is used to estimate $x_t = \pi + \rho x_{t-1} + v_t$ and obtain $\hat{\rho}$, the residuals \hat{v}_t , and the standard error for $\hat{\rho}$, denoted $SE(\hat{\rho})$.

Step 3: Calculate the *DF – GLS* statistic of **Elliott et al. (1996)** by regressing $(x_0, x_1 - \rho_{GLS}x_0, \dots, x_T - \rho_{GLS}x_{T-1})'$ on $(1, 1 - \rho_{GLS}, \dots, 1 - \rho_{GLS})'$ where $\rho_{GLS} = 1 - 7/T$ to obtain the coefficient μ_{GLS} . Run the regression without the intercept below:

$$\Delta \tilde{x}_t = \theta_G \tilde{x}_{t-1} + \sum_{i=1}^{p-1} \psi_i \Delta \tilde{x}_{t-i} + e_t \quad (4.15)$$

where Δ denotes the first difference operator, where $\Delta x_t = x_t - x_{t-1}$, $\tilde{x}_t = x_t - \mu_{GLS}$, and t-statistic for θ_G is *DF – GLS* statistic.

Step 4: By using, residuals \hat{u}_t , \hat{v}_t , \hat{e}_t , and $\hat{\psi}_i$ from steps 1-2, we compute

$$\begin{aligned} \hat{\sigma}_u &= \frac{1}{T-2} \sum_{t=1}^T \hat{u}_t^2, & \hat{\sigma}_e &= \frac{1}{T-2} \sum_{t=1}^T \hat{e}_t^2, \\ \hat{\sigma}_{ue} &= \frac{1}{T-2} \sum_{t=1}^T \hat{u}_t \hat{e}_t, & \hat{\sigma}_v &= \frac{1}{T-2} \sum_{t=1}^T \hat{v}_t^2, \\ \hat{\delta} &= \frac{\hat{\sigma}_{ue}}{\hat{\sigma}_u \hat{\sigma}_e}, & \hat{\omega}_v^2 &= \frac{\hat{\sigma}_e^2}{(1 - \sum_{i=1}^{p-1} \hat{\psi}_i)^2} \end{aligned}$$

Step 5: Given the $DF-GLS$ statistic from step 3 and $\hat{\delta}$, we can compute a $100(1-\alpha_1)\%$ (asymptotic) confidence interval for c , $[\underline{c}, \bar{c}]$ using pre-computed confidence belts in Table 2-11 of **CY**. As a result, we can obtain an associated $100(1-\alpha_1)\%$ confidence interval for ρ , called $C_\rho(\alpha_1)$ as $[\underline{\rho}, \bar{\rho}] = [1 + \underline{c}/T, 1 + \bar{c}/T]$.

Step 6: Run regression of $r_t - \hat{\sigma}_{ue}(\hat{\sigma}_e \hat{\omega}_v)^{-1}(x_t - \rho x_{t-1})$ on x_{t-1} and a constant, where $\rho = \{\underline{\rho}, \bar{\rho}\}$. Let $\hat{\beta}(\rho) = \{\hat{\beta}(\underline{\rho}), \hat{\beta}(\bar{\rho})\}$ denote the estimated coefficient on x_{t-1} in this regression. A $100(1-\alpha_2)\%$ confidence interval for β (called Bonferroni interval) is constructed by $C_\beta(\alpha_2) := [\underline{\beta}^Q(\bar{\rho}, \alpha_2), \bar{\beta}^Q(\underline{\rho}, \alpha_2)]$ where

$$\begin{aligned}\underline{\beta}^Q(\bar{\rho}, \alpha_2) &:= \hat{\beta}(\bar{\rho}) + \frac{T-2}{2} \frac{\hat{\sigma}_{ue}}{\hat{\sigma}_e \hat{\omega}_v} \left(\frac{\hat{\omega}_v^2}{\hat{\sigma}_v^2} - 1 \right) SE(\hat{\rho})^2 - z_{\alpha_2/2} (1 - \hat{\delta}^2)^{1/2} SE(\hat{\beta}) \\ \bar{\beta}^Q(\underline{\rho}, \alpha_2) &:= \hat{\beta}(\underline{\rho}) + \frac{T-2}{2} \frac{\hat{\sigma}_{ue}}{\hat{\sigma}_e \hat{\omega}_v} \left(\frac{\hat{\omega}_v^2}{\hat{\sigma}_v^2} - 1 \right) SE(\hat{\rho})^2 + z_{\alpha_2/2} (1 - \hat{\delta}^2)^{1/2} SE(\hat{\beta})\end{aligned}$$

and in which $z_{\alpha_2/2}$ indicates the $1 - \alpha_2/2$ quantile of the standard normal distribution.

Similar to Bonferroni-t test, the confidence interval for β has (asymptotic) coverage rate of at least $100(1-\alpha)\%$ (rather than exactly $100(1-\alpha)\%$) with $\alpha = \alpha_1 + \alpha_2$. For a right-tailed test, the null hypothesis of no predictability is rejected if $\underline{\beta}^Q(\bar{\rho}, \alpha_2) > 0$ whereas the null is rejected if $\bar{\beta}^Q(\underline{\rho}, \alpha_2) > 0$, for a left tailed test. Since **CY** uses the Bonferroni method to construct the confidence interval for β , the Bonferroni-Q test also has to use a refinement to shrink the confidence interval for ρ such that a test for β with a given (asymptotic) significance level is achieved as **Cavanagh et al. (1995)** suggest. In that sense, **CY** fix α_2 and numerically iterate through a grid of values of $c \in [-5, 50]$ and δ to find $\bar{\alpha}_1^Q$ and $\underline{\alpha}_1^Q$, for each δ such that

$$Pr(\underline{\beta}^Q(\bar{\rho}(\bar{\alpha}_1^Q), \alpha_2) > \beta) \leq \bar{\alpha}/2 \text{ and } Pr(\bar{\beta}^Q(\underline{\rho}(\underline{\alpha}_1^Q), \alpha_2) > \beta) \leq \bar{\alpha}/2 \quad (4.16)$$

All refinements are performed on asymptotic sizes, with the asymptotic distribution outlined in the next section. Consequently, for given values of δ , the one-sided tests for predictability constructed in this approach will have an asymptotic size

of exactly $\tilde{\alpha}/2$ for some value of c while remaining slightly undersized for all other values of c . Also, to refine the Bonferroni method to make the size of the one-sided test have asymptotic size well-controlled under a nominal significance level of 5%, **CY** calibrate this procedure as same as what **Cavanagh et al. (1995)** did by fixing $\tilde{\alpha} = \alpha_2 = 0.1$ (equivalently, a 5% one-sided Q-test for predictability). The confidence interval for β in the Bonferroni Q-test after refinement is represented by $[\underline{\beta}^{Q^{GLS}}(\bar{\rho}(\bar{\alpha}_1^Q), \alpha_2), \bar{\beta}^{Q^{GLS}}(\underline{\rho}(\underline{\alpha}_1^Q), \alpha_2)]$. We denote this test henceforth as *Bonf.Q*.

4.4 Asymptotic Behaviour Of Tests

Given the local-to-zero alternative hypothesis $H_b : \beta = T^{-1}b$, where b is a finite constant; and the null hypothesis $H_0 : \beta = 0$, in this section we will provide limiting distribution theory for the t, Q, and IVX statistics from Section 4.3, under Assumption 4.1-4.2.

4.4.1 IVX test

We will present the limit distributions of the IVX statistic from Section 4.3 as below. Proofs for the theorem below are in **KMS** and **Demetrescu et al. (2022a)**. For simplicity, we do not show details of the theorem in different assumptions of the persistence of predictors.

Theorem 4.1 *Following **KMS** and **Demetrescu et al. (2022a)**, consider the model in (4.1)-(4.3) and let Assumptions (4.1)-(4.2) hold, then under the null hypothesis, H_0 : IVX test statistic (t_{zx}) has a normal distribution.*

Because the limiting distribution under the null hypothesis of IVX is standard normal, the decision rule of the right-tailed IVX test is as follows: *Reject H_0 if t_{zx} is greater than $1 - \alpha$ quantile of the standard normal distribution.*

4.4.2 Bonferroni Based Tests

According to [Cavanagh et al. \(1995\)](#), the limiting distribution of the t statistic in the local-to-unity setting is a function of the unknown nuisance parameter c ; however, a confidence interval for β based on the t test can be constructed by making use of a confidence interval for c obtained from the inversion of a unit root test. Similarly, because the computation of $Q(c)$ requires information of ρ which is constructed from an unknown parameter c . Therefore, [CY](#) compute $Q(c)$ statistic for some value of c, \tilde{c} , where an initial confidence interval for c is based on inverting a unit root test.

Theorem 4.2 *Let data be generated according to (4.1) - (4.3). Let $(W_u(s), W_e(s))$ be a two dimensional Wiener process with correlation parameter δ , and let $W_{e,c}(s)$ be the Ornstein-Uhlenbeck process defined by the stochastic differential equation $dW_{e,c}(s) = -cW_{e,c}(s)ds + dW_e(s)$ with initial condition $W_{e,c}(0) = 0$. If Assumption 4.1 and 4.2 holds, then under local alternative $H_b : \beta = T^{-1}b$*

$$t \xrightarrow{w} \frac{b\omega_v\kappa_c}{\sigma_u} + \delta \frac{\tau_c}{\kappa_c} + (1 - \delta^2)^{1/2}Z \quad (4.17)$$

$$Q(\tilde{c}) \xrightarrow{w} \frac{b\omega_v\kappa_c}{\sigma_u(1-\delta^2)^{1/2}} + \frac{\delta(\tilde{c}-c)\kappa_c}{(1-\delta^2)^{1/2}} + Z \quad (4.18)$$

where $\kappa_c := (\int_0^1 W_{e,c}^\mu(s)^2 ds)^{1/2}$ and $\tau_c := \int_0^1 W_{e,c}^\mu(s) dW_e(s)$ with $W_{e,c}^\mu(s) := W_{e,c}(s) - \int_0^1 W_{e,c}(r) dr$ where integration is over $[0, 1]$ unless otherwise noted, and Z is a standard normal random variable independent of $W_e(s)$.

The limiting null distributions of the t and $Q(\tilde{c})$ statistics are obtained by setting $b = 0$ in the expressions in (4.17) and (4.18), respectively.

The limiting distribution of t depends on both c through the random variable τ_c/κ_c and δ ; however, according to [Cavanagh et al. \(1995\)](#), δ is consistently estimated by the sample correlation between \hat{e}_t , and \hat{u}_t , so we can treat δ as known for the purposes of the asymptotic theory. Similarly, the Q -test is also infeasible since it requires ρ (or c) and nuisance parameters of variance and covariance of innovations to compute test statistic; however, we can obtain consistent estimators for the latter. Therefore, in the

next sections, we will show how to estimate the nuisance parameters following **CY**.

In this chapter, we focus on the right-tailed test only; therefore, the decision rules for the Bonferroni-based test ($\delta < 0$) are as below:

- For Bonferroni t-test: Reject H_0 if lower bound of confidence interval for β constructed from *Bonf.t* test, $\underline{\beta}^{tOLS}(\bar{\alpha}_1^t, \alpha_2) > 0$.
- For Bonferroni Q-test: Reject H_0 if lower bound of confidence interval for β constructed from *Bonf.Q* test, $\underline{\beta}^{tGLS}(\bar{\rho}(\bar{\alpha}_1^Q), \alpha_2) > 0$.

The appropriate value of $\bar{\alpha}_1^Q$ leads to the right-tailed Bonferroni Q-test with the maximum asymptotic size of 5% for $c \in [-5, 50]$ when using the DF-OLS test to obtain the confidence interval for ρ are provided in the pre-computed tables of **CY**. Similar, the pre-computed tables of **Cavanagh et al. (1995)** provide the suitable value for $\bar{\alpha}_1^t$ that results in a Bonferroni t-test with a maximum asymptotic size of 5% in the right tail for $c \in [-5, 50]$ when using the DF-GLS test to derive the confidence interval for ρ . Under Assumptions 4.1 and 4.2, the values of $\bar{\alpha}_1^t$ and $\bar{\alpha}_1^Q$ are pre-computed by **Cavanagh et al. (1995)** and **CY**, respectively, which involve the limiting null distributions of the t and $Q(\bar{c})$ statistics stated in Theorem 4.2 (with $b = 0$), along with the standard limit distributions of DF-OLS and DF-GLS (as described in **Elliott et al., 1996**)

4.5 Finite Sample Size

In this section, we will examine the finite-sample performance of the IVX test procedure of **KMS**, the Bonferroni-t test of **Cavanagh et al. (1995)**, and the Bonferroni-Q test of **CY**. We perform right-tailed tests at a nominal significance level of 5%. The null hypothesis of no predictability ($H_0 : \beta = 0$) is tested against the alternative hypothesis $H_1 : \beta > 0$. To determine rejection rates, we utilize 10,000 Monte Carlo simulations to draw finite sample paths generated from the DGPs described in Equations from

(4.1) to (4.7), which are restated below:

$$\begin{aligned}
r_t^f &= \mu_r + \beta x_{t-1} + u_t, \quad t = 1, \dots, T \\
x_t &= \mu_x + \xi_t \\
\xi_t &= \rho \xi_{t-1} + v_t \\
P_t &= P_t^f + B_t \\
P_t^f &= P_{t-1}^f \exp(r_t^f) \iff r_t^f = p_t^f - p_{t-1}^f \\
B_t &= \begin{cases} \rho_b B_{t-1} + v_t, & t = \lfloor \tau_1 T \rfloor + 1, \dots, \lfloor \tau_2 T \rfloor \\ 0, & \text{otherwise} \end{cases} \\
r_t &= \begin{cases} r_t^f, & B_t = 0 \\ p_t - p_{t-1}, & \text{otherwise} \end{cases}
\end{aligned}$$

where $\rho = 1 + c/T$, $p_t = \ln(P_t)$. τ_b and τ_p are parameters controlling where the bubble will originate and terminate, respectively. $\beta = 0$, T is sample size, (u_t, e_t) are homoskedastic, $v_t = e_t$, $(u_t, e_t)' \sim Niid(0, \Sigma)$, with $\Sigma = [1 \ \sigma_{ue}; \sigma_{eu} \ 1]$.

The initial condition of innovations $x_0 = 0$, $\xi_0 = 0$, $P_0^f = 100$ and $B_0 = 0$. We focus only on the positively explosive behaviour of bubbles; therefore, if the last value of the bubble is negative, we multiply the bubble path, B_t , by minus one to ensure our bubble is always positive. The nuisance parameters are normalized as $\alpha = \gamma = 0$ and $\sigma_u^2 = \sigma_e^2 = 1$. The innovations have correlation $\delta := \sigma_{eu}/(\sigma_e \sigma_u) \in \{-0.95, -0.5, 0, 0.5, 0.95\}$ and are drawn from a bivariate normal distribution. We set $\mu_r = \mu_x = 0$ without loss of generality. We report results for six levels of persistence in predictor $c \in \{0, -2, -20, -50, -100\}$. We consider finite sample sizes, $T \in \{100, 250, 500, 1000\}$. To the instrument predictor, following [KMS](#) recommendations, we choose $\zeta = 1$ and $\eta = 0.95$. Together with that, we use three parameters to adjust the specification of bubbles including c_{bub} controlling the magnitude of the bubble, $\lfloor \tau_1 T \rfloor + 1$ setting up where the bubble originates, and $\lfloor \tau_2 T \rfloor$ for where the bubble terminates. Although our DGP is very flexible, for simplicity, we only construct series with a single bubble

period. Also, when constructing the long-run quantities we will follow **KMS** and use the Bartlett kernel with bandwidth $T^{1/3}$.

The simulations are designed to evaluate the finite sample size of three tests in various bubble specifications. However, overall, we can classify them into three groups below:

- There is no bubble present in the price series, $c_{bub} = 0$. This case will serve as the benchmark for comparison with cases where a bubble exists in the price.
- The bubble starts within the sample and lasts until the end of the sample. As defined in Section 4.2, $\tau_2 = 1$ is set to ensure that the bubble lasts until the end. The origination of the bubble is determined by setting $\tau_1 = \{0.9, 0.7\}$. The magnitude of the bubble, c_{bub} , is set to $\{0.01, 0.05, 0.1\}$.
- The bubble starts and ends within the sample. At the end of the bubble period, r_t reverts directly to a unit root dynamics at the same level as before the bubble started. The beginning position of the bubble is determined by the parameter $\tau_1 \in \{0.6, 0.4, 0.1\}$ with a bubble length held constant at $\lfloor 0.3T \rfloor$, the corresponding ending points of the bubble are $\tau_2 \in \{0.9, 0.7, 0.4\}$, respectively. As with the previous group, the magnitude of the bubble, c_{bub} , is set to $\{0.01, 0.05, 0.1, 0.2\}$.

Together with that, for each group, we run the simulations with innovation vectors $[u_t, e_t]'$ drawn from a bivariate Student's t-distribution besides those from a bivariate Gaussian distribution.

Table C-1 shows the size of three right-tailed predictability tests (i.e., IVX, Bonferroni-t [Bonf.t], and Bonferroni-Q [Bonf.Q] tests) without a bubble period. This table of results is different from Table C-8 since the pairs of innovations, (u_t, v_t) , in Table C-8 are drawn from an i.i.d. bivariate fat-tailed distribution (t-distribution) instead of Gaussian distribution as in C-1. As we can see, in terms of the endogeneity correlation parameter, δ , the IVX test is significantly oversized when the correlation parameter is negative and is severely undersized for the positive parameter. In that sense, the test works fairly well (i.e the size is well-controlled under a nominal significance

level of 5%) when there is no endogeneity in the predictive model. Surprisingly, the size distortion decrease when the predictor becomes a stationary process. In other words, the IVX test has its size well-controlled under 5% of the significance level. The findings related to the size of the IVX test match those of Demetrescu et al. (2022a). Although the Bonf.t is more undersized when the correlation of innovations is strongly positive, it has a well-control size of the test when the correlation parameter is negative. Similar to the IVX test, the size distortion is diminishing when the predictor is stationary. For the Bonf.Q test, it is slightly oversized when the sample size is small ($T = 100$) and the correlation parameter is negative. As in the same two previous tests, Bonf.Q test is undersized when the δ are positive but still lightly better than the two formers. However, in contrast to the first two tests, when the autoregressive roots in the predictor are away from unity, the Bonf.Q test tends to be badly oversized but IVX and Bonf.t test has a well-controlled size. Across the different sample sizes, the finite-sample rejection rates are relatively the same with the same level of endogeneity, δ , and level of persistence, c . In addition, there is an exception for when the predictor is near stationary ($c = -100$) and the correlation coefficient δ is negative or equal to zero. In that scenario, the finite sample size of Bonf.Q test is badly oversized which exceeds those of the simulations using a large sample size. The simulation results are held and very similar in the case of innovations has the fat-tailed distribution of Table C-8.

Subsequently, we monitor the finite-sample size of three tests with the presence of a bubble. Tables C-2-C-7 and C-9-C-14 report the empirical rejection frequencies at a 5% significance level of predictability tests for cases when bubble emerges in-sample and exists until the end of sample. The bubble specifications are mainly controlled by the magnitude parameter c_{bub} and the starting point of the bubble τ_1 . The ending point of the bubble will be set constantly at 1. While the results reported from Tables C-2-C-7 show simulated results when the bubble starts and lives till the end of the sample with u_t and v_t have Gaussian distribution, the results in Tables C-9-C-14 are with innovations drawn from a Student's t-distribution. Overall, all tests tend

to be oversized when the magnitude of the bubble and/or the time bubble lives in the sample increase. Among the three tests, Bonf.Q is the most sensitive with the existence of a bubble in the return, while the IVX test and Bonf.t are ranked behind, respectively.

When the bubble is near the end of the sample with $\tau_1 = 0.9$ and $c_{bub} = 0.01$ (Table C-2), the Bonf.t test is still very robust and has its finite sample size well-controlled in almost all cases except when the sample sizes are large (e.g., $T = 500$ and $1,000$) and $c = 0$. However, all three tests are still undersized when $c = 0$ and innovations are positively correlated. Even at the small magnitude of bubble ($c_{bub} = 0.01$), the empirical sizes of the IVX and Bonf.Q tests are further distorted in cases they used to be oversized. When the bubble is adjusted to be larger in Tables C-3-C-4, the size distortion in tests becomes worse. For instance, the cases of IVX test when $\delta < 0$ and predictor is close to the unity. At $c_{bub} = 0.1$, the Bonf.t test still has well-controlled sizes in nearly all scenarios of $T = 100$ except for the case of $T = 100$, $c = 0$ and $\delta > 0$, in which the test is undersized. The sizes of IVX tests become more well-controlled in a few cases (e.g., $\delta > 0$ and $T = 250$) and tend to be oversized in most of the cases where $\delta > 0$. However, the Bonf.Q test is size-distorted in nearly every scenario.

When the bubble starts earlier at $\tau_1 = 0.7$ in Tables C-5-C-7, the signs of size distortion in tests are obvious across all three tests, even when the magnitude of the bubble is relatively small ($c_{bub} = 0.01$). Fortunately, the finite sample sizes of the Bonf.t test are still well-controlled in cases of small sample sizes or when the regressor is stationary. Only a few results show that the Bonf.Q and IVX tests have well-controlled sizes. When the predictor is non-stationary, $\delta > 0$ and $c_{bub} = 0.01$, the size of the Bonf.Q test is distorted in nearly all cases. When the magnitude of the bubble increases from 0.01 to 0.1, the size of all tests in all scenarios of $c = 0$ is badly distorted. The Bonf.t test and IVX tests still have well-controlled sizes at the 5% significance level when the sample size is small ($T = 100$) and the predictor is stationary with $c < -50$. The conclusions are relatively similar in corresponding cases when Gaussian innovations are replaced by innovations generated from the

t-distribution (see Tables C-9-C-14).

Finally, Tables C-15-C-26 report rejection rates from three predictability tests in the case the bubble bursts inside the sample. In this context, at the point of the bubble burst in-sample, there is a huge negative jump in return. Overall, the in-sample bubble makes our tests behave differently than what we saw in the context of a bubble existing until the end of the sample. When the magnitude of the bubble is small ($c_{bub} = 0.01$), the presence of a bubble period does not have a strong effect on finite sample size when compared to the results in Table C-1. The effect of the bubble becomes more apparent when $c_{bub} = 0.05$, where the empirical rejection rates decrease for small sample sizes ($T < 250$) and increase for large sample sizes ($T > 500$). However, the decrease is not consistent across the tests as the magnitude of the bubble increases (see Tables C-16-C-18).

We used simulations to investigate the behavior of the tests when bubbles start and burst at different positions in the sample. When $\tau_1 = 0.6$, $\tau_2 = 0.9$, and $T = 100$, the size of the IVX test is well-controlled at a nominal significance level of 5% for all c values. However, the Bonf.t and Bonf.Q tests are undersized when $c = 0$, and the Bonf.Q test is oversized when $c = -100$. As the magnitude of the bubble increases, the size distortion in large samples becomes worse. The results in Tables C-19-C-22, where the bubble starts at $\tau_1 = 0.4$ and bursts at $\tau_2 = 0.7$, and in Tables C-23-C-26, where the bubble starts at $\tau_1 = 0.1$ and bursts at $\tau_2 = 0.4$, lead to similar conclusions.

Tables C-27-C-38 investigate the behaviour of the size of tests with the same bubble specification and predictive model but the innovations have fat-tailed distribution. Under the presence of an in-sample bubble, the simulated results, in which innovations are drawn from the t-distribution, are not significantly different from the previous cases when innovations are generated by the Gaussian distribution.

4.6 Empirical Illustrations

4.6.1 Data

In this chapter, we re-evaluate the return predictability of regressors in the empirical research of [Welch and Goyal \(2008\)](#) by using a one-sided IVX test and Bonferroni 90% confidence intervals. The dataset is monthly data which is collected from January 1927 and updated to December 2021¹ (i.e., sample size, $T = 1,140$). The short versions of this dataset are also used in the papers of [KMS, Demetrescu et al. \(2022a\)](#), [Demetrescu et al. \(2022b\)](#), and [Yang et al. \(2022\)](#) to illustrate the application of the tests in practice. On the other hand, [Goyal et al. \(2021\)](#) updated their original paper to evaluate the return predictability on 29 variables from 26 well-known papers² published after [Welch and Goyal \(2008\)](#) in the top finance journals besides the original 14 variables. Similar to the findings in the original paper by [Welch and Goyal \(2008\)](#), [Goyal et al. \(2021\)](#) present empirical results indicating that a majority of the variables exhibited poor predictability both in-sample and out-of-sample. Despite the availability of more diverse predictors, the data used in [Goyal et al. \(2021\)](#) study is not currently accessible and would require replication to extend the time period. As a result, for the sake of simplicity in this chapter, we will continue to employ the dataset from the original paper by [Welch and Goyal \(2008\)](#).

A stylized method in the literature of stock return predictability is to obtain the predicted variable as a log of excess stock return (including dividends). As noted in [Welch and Goyal \(2008\)](#), this regressand is obtained as the difference of the log value of monthly return on the value-weighted S&P 500 price index and the log of the risk-free rate. Also, lag one of 14 financial and macroeconomic independent variables are obtained by [Welch and Goyal \(2008\)](#) as follows:

- Dividend payout ratio (d/e) is computed as the log dividends minus the log of

¹The dataset can be downloaded directly from Professor Amit Goyal's webpage: <https://sites.google.com/view/agoyal145>.

²All the details of papers and their variables can be found in Table 1 of [Goyal et al. \(2021\)](#)

earnings.

- Long-term yield (lty) is the US yield on long-term US government bonds series collected from NBER's Macrohistory database.
- Dividend yield (d/y) is the difference between the log of dividends and the log of lag one price.
- Dividend Price Ratio (d/p) is the difference between the log of dividends and the log of prices.
- Treasury bills (tbl) is 3 monthly treasury series obtained from sources of NBER's Macrohistory database and Federal Reserve Bank at St. Louis (FRED).
- Earning price ratio (e/p) is obtained by subtracting the log of earnings from the log of prices.
- Book-to-market ratio (b/m) is the ratio of book value to market value for the Dow Jones Industrial Average.
- Default yield spread (dfy) is calculated by subtracting AAA-rated corporate bond yields from BAA-rated ones.
- Net equity expansion ($ntis$) is computed by dividing 12-month moving sums of net issues by NYSE listed stock for the total end-of-year market capitalization of NYSE stocks.
- Term spread (tms) is the difference between the long-term yield on US government bond series (lty) and treasury bill rates (tbl).
- Inflation (inf) is represented by Consumer Price Index (All Urban Consumers) from the Bureau of Labour Statistics.
- Stock variance ($svar$) is the sum of squared monthly returns on the S&P500.
- Long-term rate of return (ltr) is collected from Ibbotson's Stock, Bonds, Bills, and Inflation Yearbook.

- Default return spread (dfr) is the difference between long-term corporate bond and long-term government bond rates.

Table C-39 reports the results from unit root tests on predictors using their monthly data. This is because the IVX test has the advantage to control the size of the test better than Bonferroni-based tests when the predictors are stationary or nearly stationary. Overall, because our dataset is an extension of KMS and Yang et al. (2022)'s one, our results from pretests are similar to theirs. The second column, ADF, exhibits the test statistic and rejection level of the Augmented Dickey-Fuller test. In this case, the test fails to reject statical evidence of the existence of unit root process in long-term yield (lty), dividend yield (d/y), dividend-price ratio (d/p), and T-bill rate (tbl). The evidence is reinforced by the DF-GLS test and Phillips-Perron test in the third and fourth columns, respectively.

Prior to applying the return predictability tests, it is important to formally test whether explosive autoregressive regimes are present in the stock price or not since this is a precondition for us to examine how the tests behave during bubble periods. Similar to Yang et al. (2022), we use a new version of the real-time bubble detection method of PSY to identify all episodes of bubble over the period from Jan-1920 to Dec-2021. The new test, proposed by Phillips and Shi (2020), is a combination of the PSY test and a new wild-bootstrap algorithm (called the composite bootstrap). The improved test allows the presence of heteroskedasticity in the series as suggested by Harvey et al. (2016) [HLST hereafter] and to address multiplicity issues referred to the increase in the probability of over-rejection to the null hypothesis when the number of hypotheses tested rises. Instead of using bootstrapped price series at a full sample length, Phillips and Shi (2020) suggest using a part of it, T_b , to prevent the family-wise size control or multiplicity issue in testing. In this way, the method not only has a well-controlled size but also lessens the computational complexity in the wild-bootstrap algorithm. As Yang et al. (2022), we use an empirical size controlled over a 3.5-year period ($T_b = 3.5 \times 12 = 42$) in the wild bootstrap procedure. Additionally, as suggestions of PSY and Phillips and Shi (2020), we use the smallest

window size in PSY test, $r_0 = 0.01 + 1.8/\sqrt{T}$; therefore, we have the minimum window width of $\lfloor r_0 T \rfloor = 75$ with $T = 1,225$ ³. The PSY test rejects the null hypothesis of no bubble if its test statistic exceeds 95% bootstrapped critical value generated from 2,000 bootstrap replications. As in PSY, we select optimal lags by using the Bayesian information criterion (BIC) with a maximum lag length of 6 in each subsample.

Figure C-1 shows the origin and conclusion of explosive behaviour in the monthly S&P 500 price index. In the figure, the shaded areas represent periods of explosive behaviour that have been detected. Seven bubble periods have been identified, of which the first six align with the findings in Yang et al. (2022). The seventh bubble period spans from April 2021 to December 2021. The periods from December 1954 to February 1955 and April 1955 to August 1956 are so close together that, following the findings of Yang et al. (2022), we can consider them as a recurring bubble. Historically, financial crises are often followed by a bubble crash Allen and Gale (2000), so, as noted by PSY and Yang et al. (2022), the first bubbles have been named after the catastrophic financial events they correspond to: the Great Crash (July 1927 to September 1929), the Great Depression (May 1932 to June 1932), the Post-Korean War Recession (December 1954 to August 1956), Black Monday (June 1987 to September 1987), and the Dotcom bubble (November 1996 to July 2001). The last bubble we detected is from April 2021 to December 2021 and may have been caused by the COVID-19 crisis.

By identifying the bubble periods, we can create a strategy for dividing our full dataset into subsamples. This allows us to investigate whether the results of IVX and Bonferroni-based tests are impacted by the presence of bubbles.

4.6.2 Evaluating return predictability

In this subsection, we re-examine the return predictability of financial and macroeconomic variables mentioned in the empirical paper of Welch and Goyal (2008) using

³Because PSY test requires an additional subsample for training, we run it on a longer period of time from January 1920 to December 2021. This ensures that the sample size tested for the bubble matches the sample size of our dataset.

return predictability tests against one-sided alternatives. Specifically, on one hand, we run the tests on the full dataset from Jan-1927 to December 2021. On the other hand, we also perform testing on subsamples around the Dot-com bubble, which was detected in the previous subsection. This choice was made because the Dot-com period, which started in Nov-1996 and ended in Jul-2001, is the longest-lasting bubble (see Figure C-1). Hence, based on evidence from our finite sample simulations, the behaviour of predictability tests during bubble periods will be most pronounced in our analysis. To this end, we choose a subsample from Oct-1987 to Oct-1996 ($T = 109$) as a benchmark, which is the period just before the Dot-com period and does not contain a bubble. Another subsample, from Oct-1987 to Jul-2001 ($T = 166$), is selected to proxy a sample containing the short-lived bubble at the end of the sample. The last subsample, from Oct-1987 to Mar-2021 ($T = 402$), includes an in-sample collapsed Dot-com bubble. These three subsamples correspond to the three forms of data generated in Section 4.5.

As shown in Table C-40 and Table C-41, the results from the return predictability tests, including the IVX test of KMS, the Bonferroni-t (Bonf.t) test of Cavanagh et al. (1995), and the Bonf.Q test of CY, are presented. The tests are applied to the full sample periods and subsamples as follows: Panel A in the tables presents the p-values for one-sided predictability tests on the full sample. Panels B, C, and D show the p-values for the following subsamples: Oct-1987 to Oct-1996, Oct-1987 to Jul-2001, and Oct-1987 to Mar-2021, respectively.

Overall, most of the evidence of predictability is identified when we employ the tests on full sample data and on subsamples containing bubble periods. Using the IVX test statistic, we find that the null hypothesis of no predictability can only be rejected at the 5% level when the lagged e/p is used as a predictor in the subsample without bubbles. For the Bonf.Q test, the null hypothesis is rejected when ltr is the predictor, but the Bonf.t test does not reject the null for any predictor. This may be because the Bonf.t test has lower power than the Bonf.Q test. Additionally, despite no rejection in either the subsample with or without bubbles, the confidence intervals of

the Bonferroni-based test are shrunk in the subsample with bubbles, indicating that the tests tend to over-reject in the sample with bubbles. These findings are consistent with our simulation results regarding the size properties of the predictability tests.

Dividend Payout Ratio (d/e)

The ratio does not exhibit any predictability across all tested samples and different tests at the 5% level. This evidence is consistent with the empirical findings on the full sample by KMS, Yang et al. (2022), and Demetrescu et al. (2022a).

Long-term Yield (lty)

On the full sample from Jan-1927 to Dec-2021, one-sided IVX and Bonf.t tests show weak predictability at the 5% level. The full sample result of the one-sided IVX test matches that of Demetrescu et al. (2022a). However, in the short samples from Jan-1927 to Dec-2012 in KMS and from Jan-1927 to Dec-2016 in Yang et al. (2022), their two-sided tests do not indicate that the long-term yield has no predictability. Therefore, it appears that the one-sided IVX test over-rejects the null hypothesis of no predictability when the correlation of innovations is negative.

Dividend Yield Ratio (d/y)

All three tests demonstrate the predictability of the dividend yield ratio in the full sample and in the sample containing a collapsing bubble. This may be due to the effects of the sharp negative jump in returns, as we mentioned in Section 4.5. No predictability was detected in the sample that had a bubble existing until the end of the sample. The full sample result of the IVX test matches those of KMS, Yang et al. (2022), and Demetrescu et al. (2022a).

Dividend Price Ratio (d/p)

No predictability was detected across different tests and samples. The result from the IVX test is consistent with the empirical findings from the one-sided IVX test in Demetrescu et al. (2022a). However, it does not agree with the evidence from the two-sided tests of KMS and Yang et al. (2022). This is because the one-sided IVX test is undersized when the correlation of innovations is positive.

Treasury-bill Rate (tbl)

Predictability exists in the full sample only and for all three tests at the 5% level. The result from the IVX test is the same as those of [Yang et al. \(2022\)](#), and [Demetrescu et al. \(2022a\)](#).

Earnings Price Ratio (e/p)

IVX test shows weak predictability at 5% in all of the samples except for the one with an in-sample collapsing bubble. Under the Bonferroni-based tests, we fail to reject the null hypothesis of no predictability.

Book-to-Market Ratio (b/m)

Predictability is reported in the full sample under the IVX test and Bonferroni-Q test. Even we failed to reject the null hypothesis of no predictability, if we look carefully into the confidence interval of Bonferroni-tests, it is easy to realize that the confidence intervals of subsamples with bubbles are shrunk compared to those in the subsample without bubbles. It indicates bubble effect increases the rejection rate.

Default Yield Spread (dfy)

Results in Table C-41 do not show any statistical evidence of return predictability in default yield spread across all samples. The result is similar to those reported in the papers of [KMS](#), [Yang et al. \(2022\)](#), and [Demetrescu et al. \(2022a\)](#).

Net Equity Expansion Ratio ($ntis$)

The IVX test rejects the null hypothesis of no predictability at a significance level of 2.5% in the full sample. The Bonferroni-t test also concludes that there is statistically significant evidence of predictive ability for the net equity expansion ratio in the full sample. The result of the IVX test on the full sample is consistent with the results reported in [KMS](#), [Yang et al. \(2022\)](#), and [Demetrescu et al. \(2022a\)](#).

Term Spread (tms)

With the term spread predictor, there is no predictability in all forms of the sample at any significance levels. The result matches papers using the same dataset (e.g., [KMS](#), [Yang et al. \(2022\)](#), and [Demetrescu et al. \(2022a\)](#).)

Inflation (inf)

IVX test shows weak predictability (at a significance level of 5%) of inflation rate

in the sample containing a bubble that lives till the end of the sample. This result matches that of the one-sided IVX test in [Demetrescu et al. \(2022a\)](#). This indicates the over-rejection of IVX in the case of a negative correlation between innovations and during bubble periods.

Stock Variance (svar)

The Bonferroni-based test provides evidence of predictability in the subsamples containing bubbles. In these subsamples, the confidence interval of the Bonferroni-Q test shows more rejection of the null hypothesis than the Bonferroni-t test. This is because the Bonferroni-t test has better size control than the Bonferroni-Q test in the presence of a bubble period.

Long-term Rate of Returns (ltr)

The Bonferroni-Q test shows return predictability of the long-term rate of return in all sample forms except for the period with an in-sample collapsing bubble. The results show that the confidence intervals of the Bonferroni-Q test are narrower in subsamples containing bubbles, indicating a higher rejection rate during bubble periods.

Default Return Spread (dfr)

Bonferroni-Q test and IVX test provide evidence of predictability in only the full sample. In fact, as we mentioned, the size of the Bonferroni-t test is better controlled than the two other tests during the bubble period; therefore, they are less likely to reject the null hypothesis under the bubble effect. In addition, the result of the one-sided IVX test is different from that of [Demetrescu et al. \(2022a\)](#).

4.7 Conclusion

In this study, we examine the finite sample behaviour of two widely used types of return predictability tests, the IVX test and Bonferroni-based tests, in the presence of a bubble in returns. While previous research such as [Yang et al. \(2022\)](#) has investigated the impact of bubbles on predictive models, our aim is to compare the behaviour of

these tests from different perspectives. Unlike [Yang et al. \(2022\)](#), our data generating process is more flexible and natural, allowing us to independently adjust the bubble specifications from the predictive model.

Our finite sample simulations, based on the proposed data generating process, indicate that IVX and Bonferroni-based tests tend to over-reject the null hypothesis of no predictability during bubble periods. This over-rejection is observed for both positive and negative correlations in innovations, particularly when the bubble is large or long-lasting. The Bonferroni-t test appears to be more robust to the bubble effect than other tests, as it better controls the finite sample size under the nominal significance level in various scenarios. The results remain valid when innovations are drawn from a fat-tailed distribution.

In addition, by re-applying these predictability tests to a recent dataset of fourteen financial and macroeconomic variables from [Welch and Goyal \(2008\)](#), we provide further empirical evidence that the bubble effect can lead to significant over-rejection of the null hypothesis. This is because the predictability of predictors appears more frequently in subsamples where bubbles are present than in subsamples without bubble periods. The shrinking of confidence intervals of Bonferroni-based tests also implies the size distortion of the Bonferroni-based tests during bubble regimes.

This study opens up several avenues for further research. For example, it would be interesting to evaluate the proposed test statistic of [Yang et al. \(2022\)](#) using our data generating process or to develop an improved version of the Bonferroni-based test using the methodology of [Yang et al. \(2022\)](#). Additionally, it would be valuable to explore the robustness of proposed tests for the bubble effect under conditions of heteroskedasticity and serial correlation in the innovations.

Concluding Remarks

5.1 Conclusions

Bubbles have been a crucial subject in finance and economics for a long time because they are considered the germs of economic and financial instability. Testing for explosive behaviour in the price of an asset can provide us with information about the existence of an explosive rational asset price bubble. In practice, it is essential to identify such explosive behaviour in asset prices as quickly as possible to help policymakers make informed decisions and limit the economic damage from the collapse of asset bubbles. Therefore, this thesis contributes to the rational bubble literature by improving econometric testing for detecting the existence of explosive and co-explosive behaviour. It also examines the behaviour of stock predictability tests during bubble regimes.

In the second chapter of this thesis, we contribute to the literature on bubble testing by proposing a WLS-based test that is more robust than the WLS-based test of [Harvey et al. \(2019\)](#) to different heteroskedastic patterns. The main idea of the new test is to use a different estimator to estimate volatility. Specifically, instead of using a kernel-based estimator as in [Harvey et al. \(2019\)](#), we propose to use the ICSS algorithm of [Inclán and Tiao \(1994\)](#) to detect unknown and discrete volatility breaks in the series and then employ the standard deviation of the difference of

stock prices in each regime as the corresponding estimator of persistent volatility. Simulations show that the finite sample power curve of the newly proposed test is monotonic, while that of [Harvey et al. \(2019\)](#) is not when the bubble grows quickly. Finite sample simulation results indicate that the procedure should work well in practice. In empirical applications, the new test finds explosive behaviour in the S&P500 price index over a period from January 1980 to March 2000 but not in the FTSE 100 index from December 1985 to December 1999. The results are robust across different data frequencies.

In the third chapter, we employ the backward recursive procedure of [PWY](#) to the KPSS-based test of [Evrupidou et al. \(2022\)](#) to detect the co-explosivity of two explosive series. Simulation results show that the new test has higher power than the test of [Evrupidou et al. \(2022\)](#); in particular, to detect co-explosivity in the absence of short-lived co-bubbling at the end of the sample. Other simulation results show how the KPSS-based test is sensitive to the choice of kernel estimators and their corresponding lag parameters. As in [Evrupidou et al. \(2022\)](#), we also show how the new test can efficiently work in timing the migration from one series to another. Since the empirical application consumes less computing power than the simulation section, we can use the general supremum recursive procedure of [PSY](#) to detect co-explosivity that may originate and collapse before the sample ends. Using the same dataset of metal prices over a period from July 1993 to May 2019, our test results are more varied than those of [Evrupidou et al. \(2022\)](#); however, all tests still agree about the co-explosivity of a few metal pairs - specifically, Lead-Tin, Gold-Tin, Lead-Gold, and Copper-Lead.

Finally, Chapter 4 demonstrates how predictability tests, including Bonferroni-based tests and IVX tests, behave during bubble periods. Among other things, Monte Carlo simulations reveal that these tests are significantly size-distorted when a bubble exists at the end of the sample. The finite sample size of the tests behaves in a complex manner when a bubble occurs and bursts within the sample. When applying these tests to the dataset of [Welch and Goyal \(2008\)](#) over a period between January 1927

and December 2021, the results indicate that the null hypothesis of no predictability is rejected more frequently during the bubble regimes.

The results of this thesis suggest that policymakers can use a more powerful econometric test, the $\sup BZ_t$ test, which is robust to changes in volatility, to detect the existence of bubbles. With this test, policymakers can quickly detect bubbles and provide early warnings to the market, thus preventing economic crashes. Additionally, policymakers and practitioners can track the migration of a bubble from one market to another by employing our backward recursive KPSS-based test (or even the double recursive test), in addition to the full sample KPSS-based test of [Evripidou et al. \(2022\)](#). This helps to avoid systemic risk resulting from the contagion of bubbles across different markets. Finally, understanding the effect of bubbles on return predictability tests is necessary for portfolio managers to make cautious decisions. This is because when bubbles exist in stock returns, the false positive rate of return predictability tests significantly increases.

5.2 Limitations and Future Research

As with similar work, a limitation of this thesis is that it could, within the many simulations, always employ more replications and other examples of bubble and heteroskedastic patterns. Of course, employing an even larger number of replications would be preferable to obtain more accurate results and using a greater variety of profiles for bubbles and volatility, would aid in better understanding the finite sample size and power of the tests. As an example, we could extend the data generating process to include cases where a single bubble terminates in-sample with various forms of adjustments in price level after the bubble bursts (see [Harvey et al., 2019](#), [Whitehouse, 2019](#), [HLST](#), [PSY](#), and [PWY](#)).

Moving on, in the empirical applications presented throughout this thesis, we present the outcomes based solely on asset price data, acknowledging that the identification of explosive autoregressive behaviour does not necessarily indicate the

existence of explosive bubbles if only the price series are considered. Therefore, future research could attempt to employ reliable methods to decompose price series into a fundamental component and a bubble component, employing the bubble tests on the latter to assess the presence of bubbles.

When considering further possible extensions to the work in this thesis note that in Chapter 2, we utilize the union of rejections strategy by combining WLS-based and OLS-based tests to enhance the power of the WLS-based tests in certain scenarios where the WLS-based test exhibits lower power than the OLS-based test. However, we must exercise caution in using this approach, as we need to balance the trade-off between a slight size distortion and the increase in the power of the WLS-based test in finite samples.

Under the existence of multiple episodes of exuberance and collapse, the backward recursive procedure of PWY may suffer reduced power and can be inconsistent in revealing the existence of a bubble. To overcome this weakness, one could employ the general supremum recursive procedure of PSY in WLS based test. In such a way, we may have a test that is robust to multiple bubbles and heteroskedasticity. Of course, in the context of explosive bubbles, bubble testing procedures often go along with bubble dating strategies, allowing, policymakers to monitor the origination and collapse of bubbles closely. We can use the general supremum recursive WLS-based test to date-stamp bubbles.

In addition, Xu (2015) has shown that CUSUM tests, in general, are not robust to nonstationary volatility. To address this issue, as suggested by Harvey et al. (2019), we can modify the CUSUM-based test of Homm and Breitung (2012) using our estimated volatility. With this modification, we anticipate that a CUSUM-based test can be developed that delivers a robust approach to bubble detection and dating in this more general setting.

Chapter 3 could be extended by replacing the KPSS test with any kind of unit root and stationary test, such as the left-tailed ADF test. In this way, we could detect the co-explosivity between two series by testing the stationarity of the linear combination

of two separate explosive series. To compare the finite sample power profiles of the tests, we will use the same data generating processes that were used in Chapter 3 to conduct simulations.

For simplicity, in Chapter 3, we focused on detecting the presence of co-bubbles at the end of the sample. However, we can further examine the behaviour of the co-explosive tests in cases where co-bubbles start and collapse within the sample, similar to the data generating processes used by [Evripidou et al. \(2022\)](#). This would allow us to evaluate the robustness of co-bubble tests across a wider range of co-bubble profiles.

Finally, in Chapter 4, analogously to [Yang et al. \(2022\)](#), who attempted to improve the IVX test to make it more robust to the bubble effect, we can extend the research to find ways to control the size of the Bonferroni-based predictability test during bubble periods. After ensuring that the finite sample size of the test is well-controlled under a nominal significance level, we can evaluate the finite sample power profiles of the tests to determine which tests are more powerful for different bubble profiles.

Similar to Chapters 2 and 3, once we have ensured that the size of the return predictability tests is well-controlled under the bubble effect, we can extend our analysis to cases where heteroskedasticity exists in the returns. In such cases, we can use wild-bootstrap based tests, as in [Demetrescu et al. \(2022a\)](#), to make the well-controlled size of the test robust to different patterns of heteroskedasticity.

Appendices

Appendix A: Tables and Figures of Chapter 2

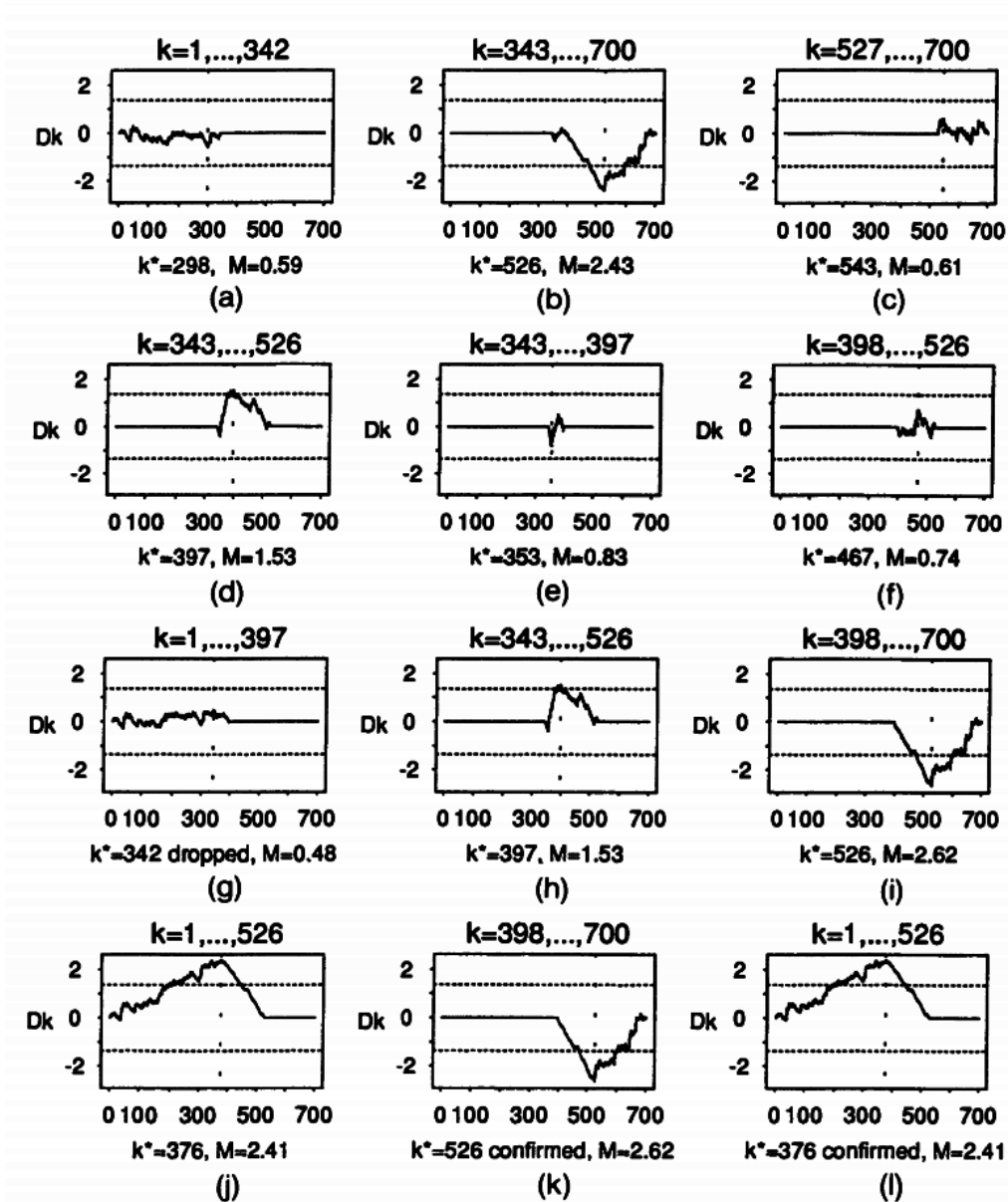
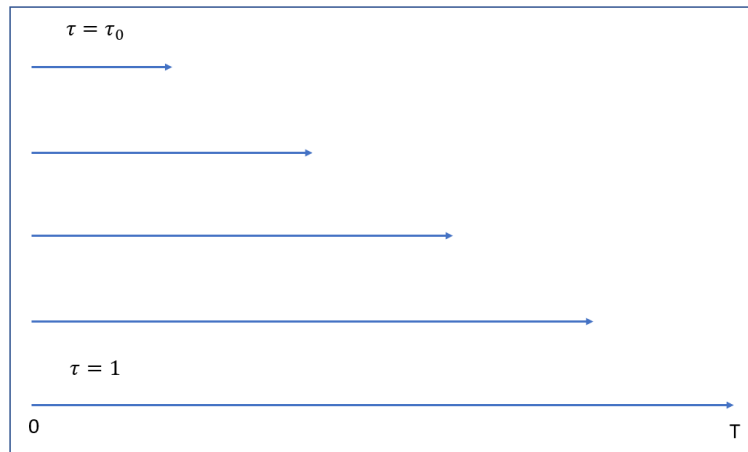


Figure A-1: Illustration of iterative algorithm in ICSS by Inclán and Tiao (1994)

Figure A-2: The sample sequences of the sup DF test

Volatility profiles ¹	sup DF without wild bootstrap	sup DF with wild bootstrap
Early upward shift	0.584	0.075
Mid upward shift	0.593	0.085
Late upward shift	0.481	0.077
Early downward shift	0.016	0.035
Mid downward shift	0.025	0.030
Late downward shift	0.035	0.037
Uptrend volatility	0.324	0.056
Downtrend volatility	0.011	0.029
Double shift	0.528	0.082
Logistic smooth transition	0.600	0.079
Autoregressive volatility	0.089	0.034
Stochastic volatility	0.059	0.048

Table A-1: A few results to show the size distortions in sup DF test

¹Details of these volatility specifications will be shown in Section 7.

Volatility profiles ²	sup BZ_K without wild bootstrap	sup BZ_K with wild bootstrap
Early upward shift	0.330	0.051
Mid upward shift	0.042	0.045
Late upward shift	0.022	0.046
Early downward shift	0.088	0.039
Mid downward shift	0.098	0.036
Late downward shift	0.585	0.043
Uptrend volatility	0.444	0.042
Downtrend volatility	0.592	0.039
Double shift	0.015	0.045
Logistic smooth transition	0.065	0.048
Autoregressive volatility	0.011	0.044
Stochastic volatility	0.000	0.032

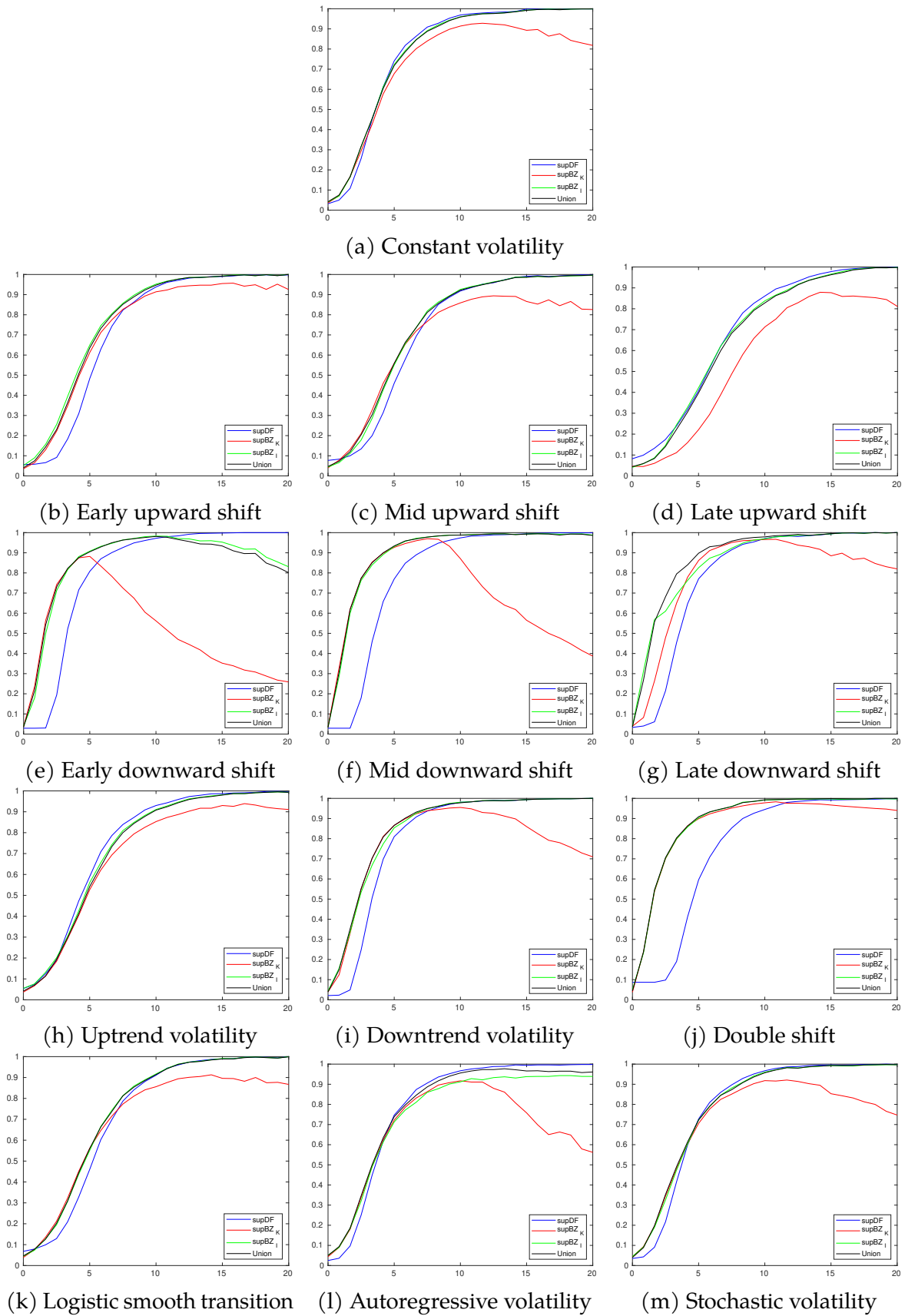
Table A-2: A few results to show the size distortions in sup BZ test without wild bootstrap

Volatility profiles	sup DF	sup BZ_K	sup BZ_I	\mathcal{U}
a) Constant volatility	0.029	0.039	0.041	0.043
b) Early upward shift	0.062	0.039	0.051	0.042
c) Mid upward shift	0.067	0.039	0.048	0.050
d) Late upward shift	0.086	0.048	0.042	0.044
e) Early downward shift	0.029	0.041	0.042	0.036
f) Mid downward shift	0.033	0.039	0.035	0.034
g) Late downward shift	0.032	0.045	0.038	0.034
h) Uptrend volatility	0.054	0.040	0.058	0.047
i) Downtrend volatility	0.024	0.043	0.046	0.039
j) Double shift	0.072	0.042	0.050	0.046
k) Logistic smooth transition	0.031	0.044	0.050	0.045
l) Autoregressive volatility	0.024	0.047	0.048	0.048
m) Stochastic volatility	0.081	0.039	0.049	0.040

Table A-3: Finite-sample sizes under the null hypothesis with $T = 100$

NOTES: Nominal 5% significance level. DGP with $c = 0$.

²Details of these volatility specifications will be shown in Section 7.

Figure A-3: Finite sample local power curves with $r^* = 0.6$, $T = 100$

supDF: —; supBZ_K: —; supBZ_I: —; \mathcal{U} : —

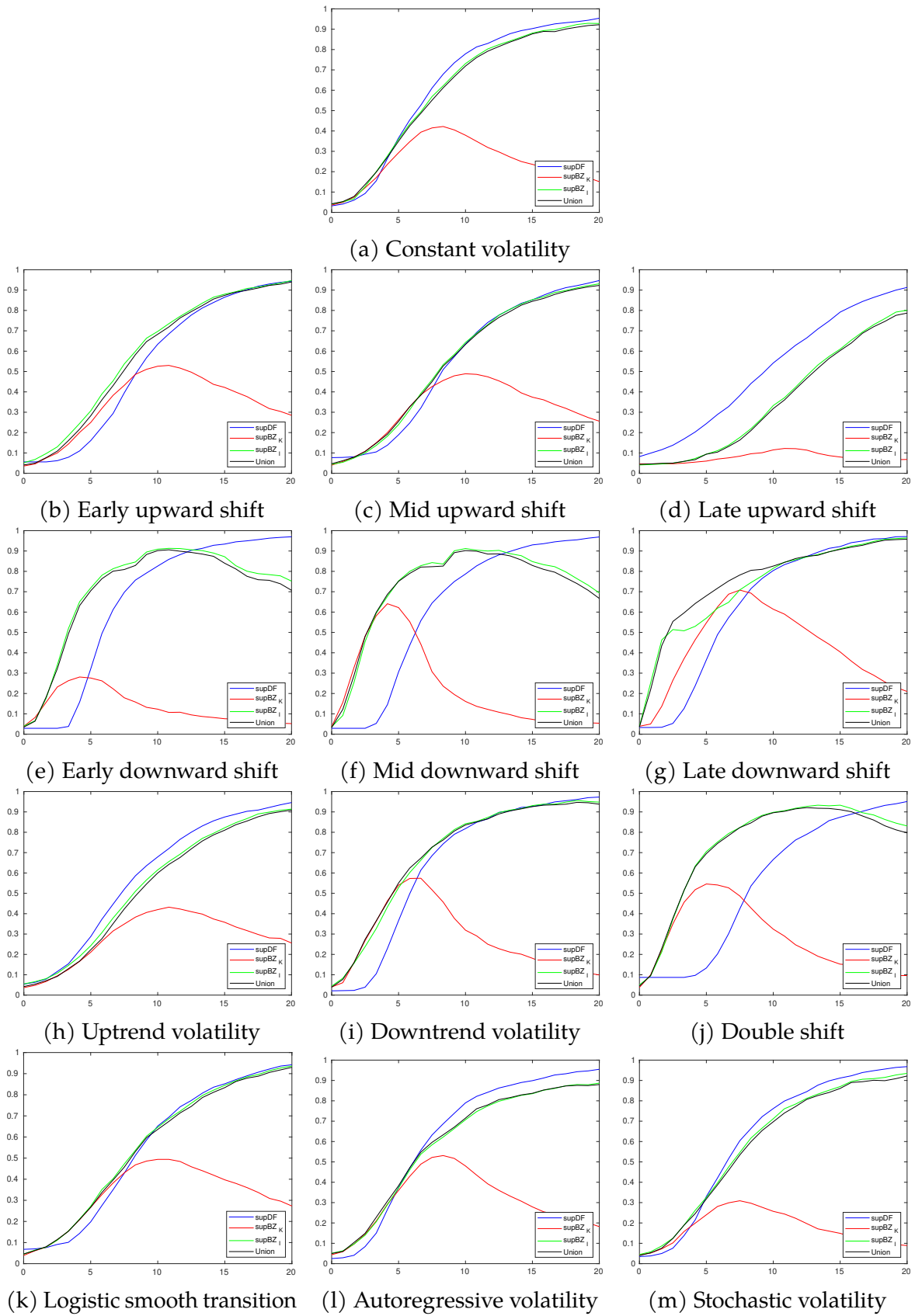


Figure A-4: Finite sample local power curves with $r^* = 0.8$, $T = 100$

NOTES: supDF: —; supBZ_K: —; supBZ_I: —; \mathcal{U} : —

Volatility profiles	sup DF	sup BZ_K	sup BZ_I	\mathcal{U}
a) Constant volatility	0.035	0.044	0.043	0.048
b) Early upward shift	0.078	0.052	0.048	0.046
c) Mid upward shift	0.086	0.049	0.040	0.045
d) Late upward shift	0.073	0.050	0.042	0.044
e) Early downward shift	0.040	0.042	0.025	0.032
f) Mid downward shift	0.036	0.039	0.042	0.037
g) Late downward shift	0.041	0.049	0.035	0.039
h) Uptrend volatility	0.055	0.044	0.052	0.047
i) Downtrend volatility	0.035	0.043	0.046	0.042
j) Double shift	0.090	0.042	0.046	0.049
k) Logistic smooth transition	0.079	0.048	0.046	0.046
l) Autoregressive volatility	0.035	0.048	0.055	0.056
m) Stochastic volatility	0.056	0.048	0.051	0.049

Table A-4: Finite-sample sizes under the null hypothesis with $T = 200$

NOTES: Nominal 5% significance level. DGP with $c = 0$.

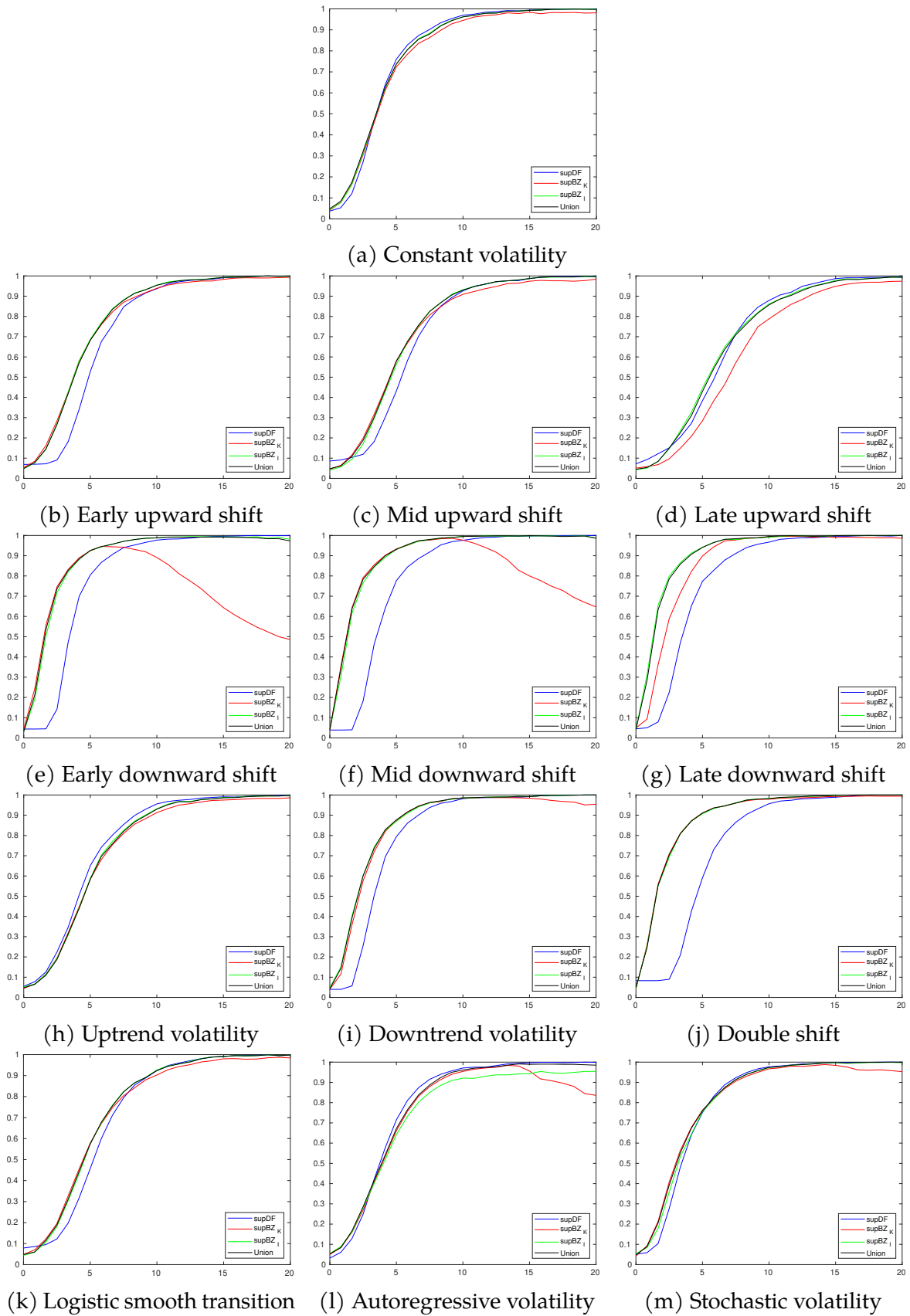
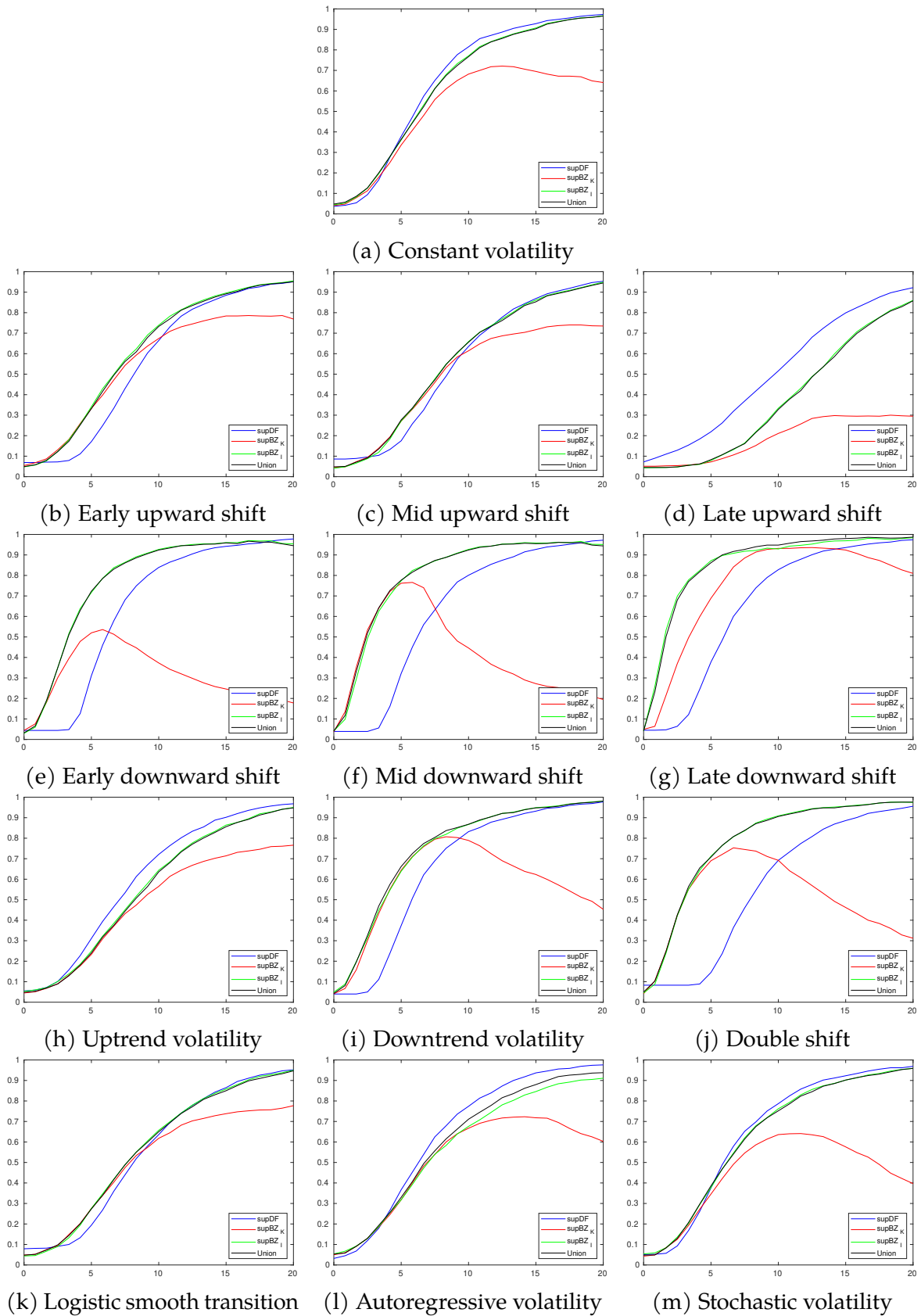


Figure A-5: Finite sample local power curves with $r^* = 0.6$, $T = 200$

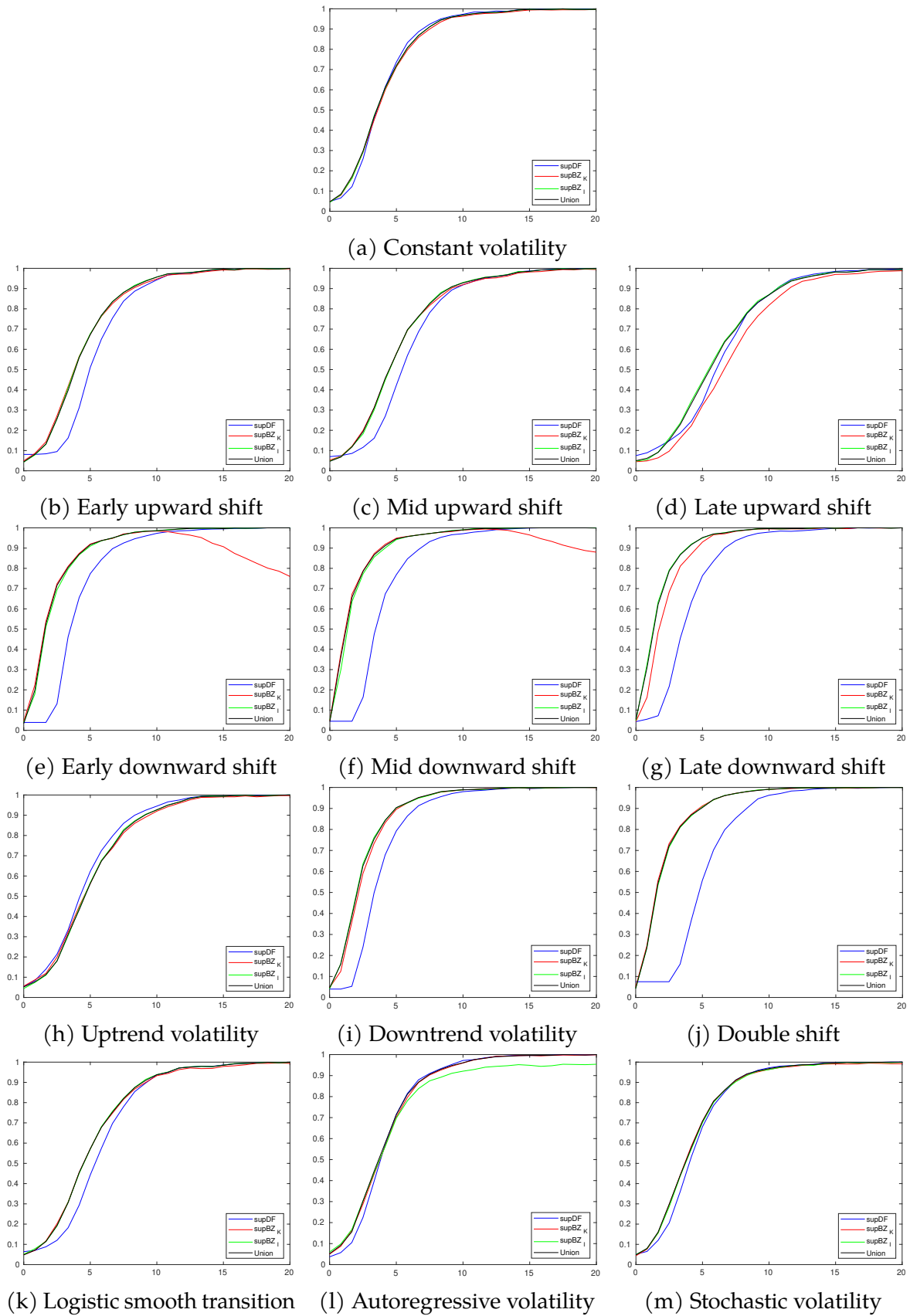
NOTES: supDF: —; supBZ_K: —; supBZ_I: —; \mathcal{U} : —

Figure A-6: Finite sample local power curves with $r^* = 0.8$, $T = 200$

NOTES: supDF: —; supBZ_K: —; supBZ_L: —; \mathcal{U} : —

Volatility profiles	sup DF	sup BZ_K	sup BZ_I	\mathcal{U}
a) Constant volatility	0.046	0.047	0.044	0.047
b) Early upward shift	0.077	0.049	0.043	0.044
c) Mid upward shift	0.070	0.053	0.048	0.047
d) Late upward shift	0.077	0.045	0.048	0.050
e) Early downward shift	0.039	0.045	0.039	0.034
f) Mid downward shift	0.046	0.048	0.051	0.043
g) Late downward shift	0.041	0.044	0.048	0.054
h) Uptrend volatility	0.053	0.056	0.044	0.052
i) Downtrend volatility	0.039	0.047	0.041	0.046
j) Double shift	0.076	0.051	0.043	0.043
k) Logistic smooth transition	0.064	0.049	0.051	0.048
l) Autoregressive volatility	0.038	0.050	0.060	0.052
m) Stochastic volatility	0.052	0.044	0.050	0.048

Table A-5: Finite-sample sizes with $T = 400$ NOTES: Nominal 5% significance level. DGP with $c = 0$.

Figure A-7: Finite sample local power curves with $r^* = 0.6$, $T = 400$ NOTES: supDF: —; supBZ_K: —; supBZ_I: —; \mathcal{U} : —

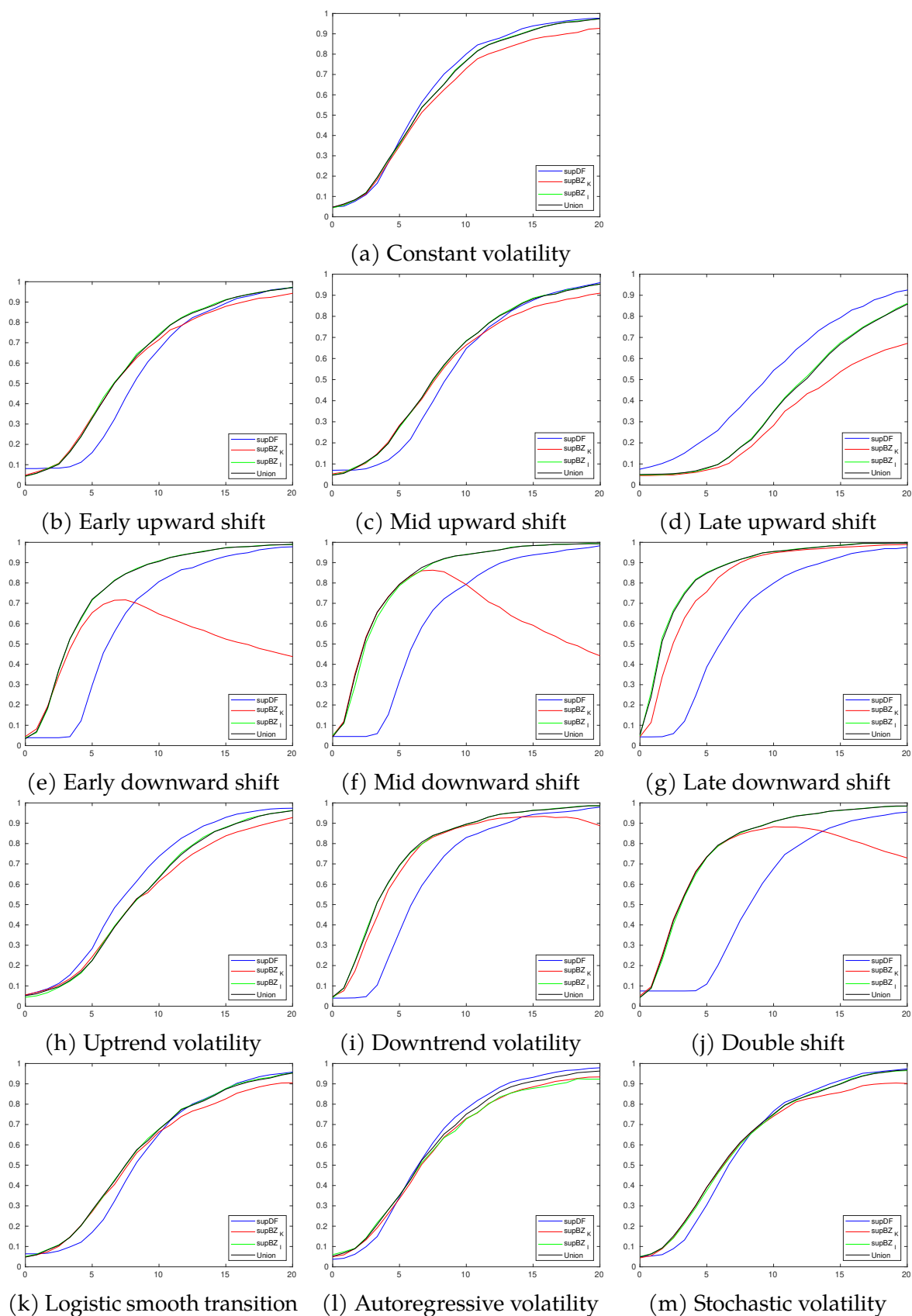
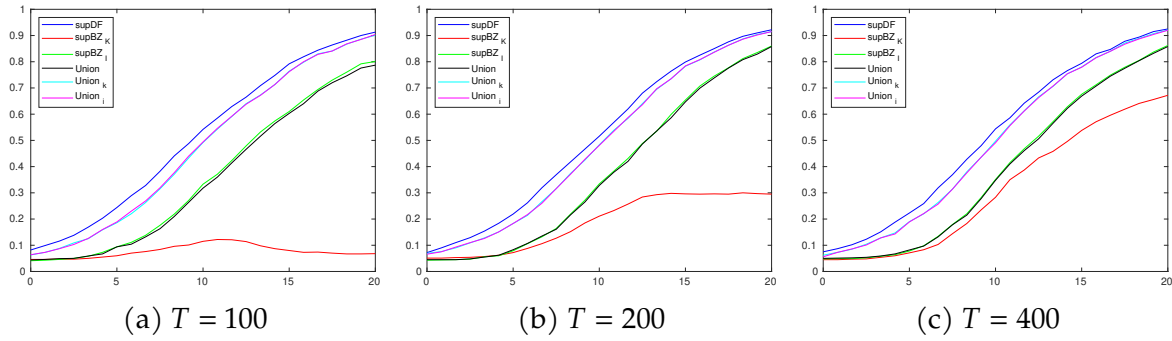


Figure A-8: Finite sample local power curves with $r^* = 0.8$, $T = 400$

NOTES: sup DF: —; sup BZ_K: —; sup BZ_I: —; \mathcal{U} : —

Sample size (T)	sup DF	sup BZ_K	sup BZ_I	\mathcal{U}	\mathcal{U}_K	\mathcal{U}_I
100	0.086	0.048	0.042	0.044	0.058	0.059
200	0.073	0.050	0.042	0.044	0.063	0.061
400	0.077	0.045	0.048	0.050	0.059	0.057

Table A-6: Finite-sample sizes when a late upward shift is in volatility and $r^* = 0.8$ Figure A-9: Finite sample local power curves with $r^* = 0.8$ - Late upward shift in volatility

NOTES: sup DF : —; sup BZ_K : —; sup BZ_I : —; \mathcal{U} : —; \mathcal{U}_K : —; \mathcal{U}_I : —

Data Sample	Obs	Mean	Median	Max	Min	S.D	No of vol breaks
S&P 500 daily	5118	0.634	0.626	1.816	-0.268	0.499	11
S&P 500 weekly	1057	0.625	0.616	1.804	-0.271	0.500	9
S&P 500 monthly	243	0.563	0.559	1.722	-0.296	0.499	4
FTSE 100 daily	3626	0.448	0.386	1.111	-0.040	0.281	16
FTSE 100 weekly	735	0.471	0.406	1.130	-0.015	0.284	4
FTSE 100 monthly	169	0.460	0.395	1.118	0.000	0.283	2

Table A-7: The descriptive statistics of S&P 500 and FTSE 100 in different time-frequencies

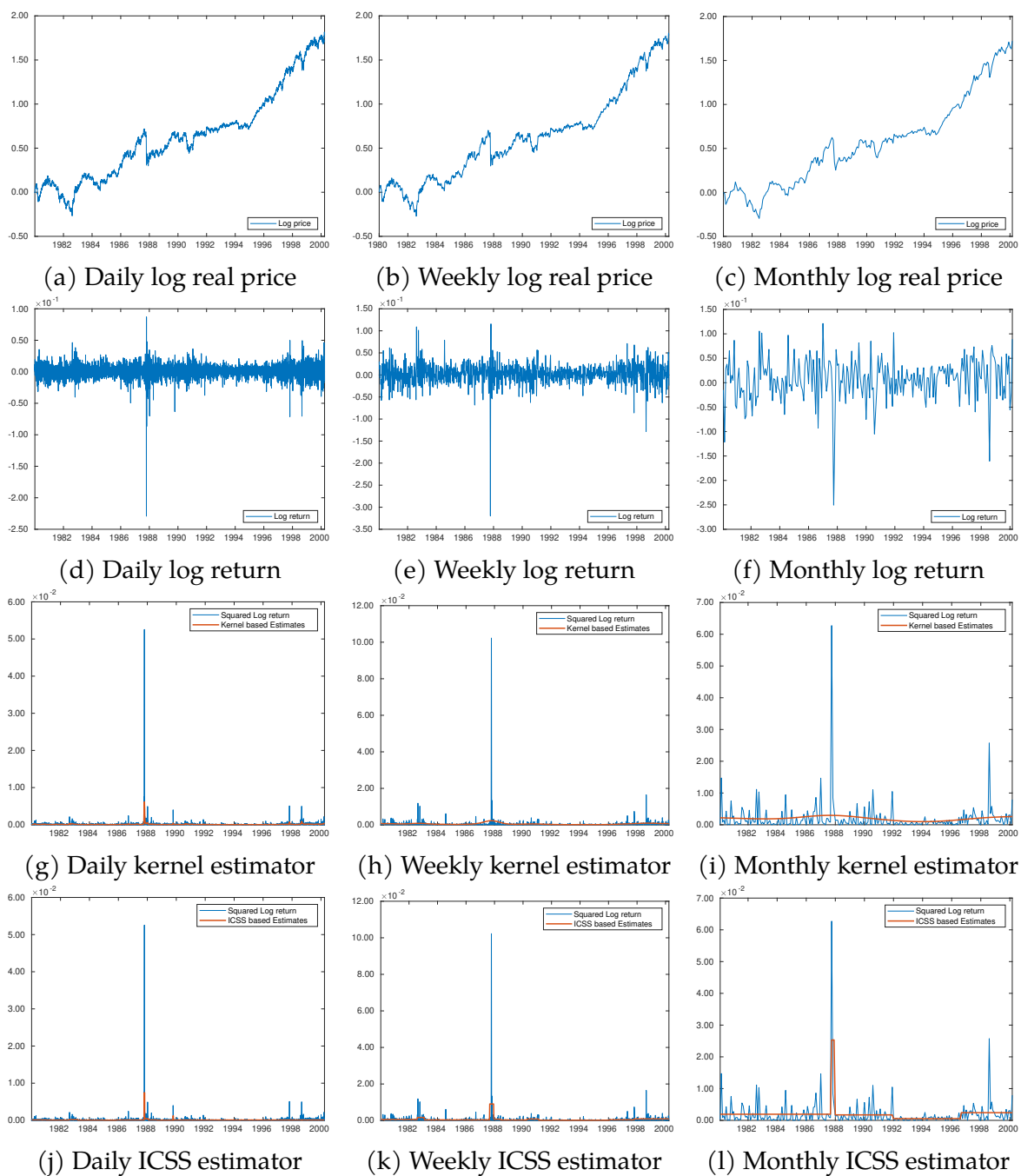


Figure A-10: The plots of logarithmic real S&P 500 index from 01/1980 to 03/2000

NOTES: Time on x-axis and values on the y-axis.

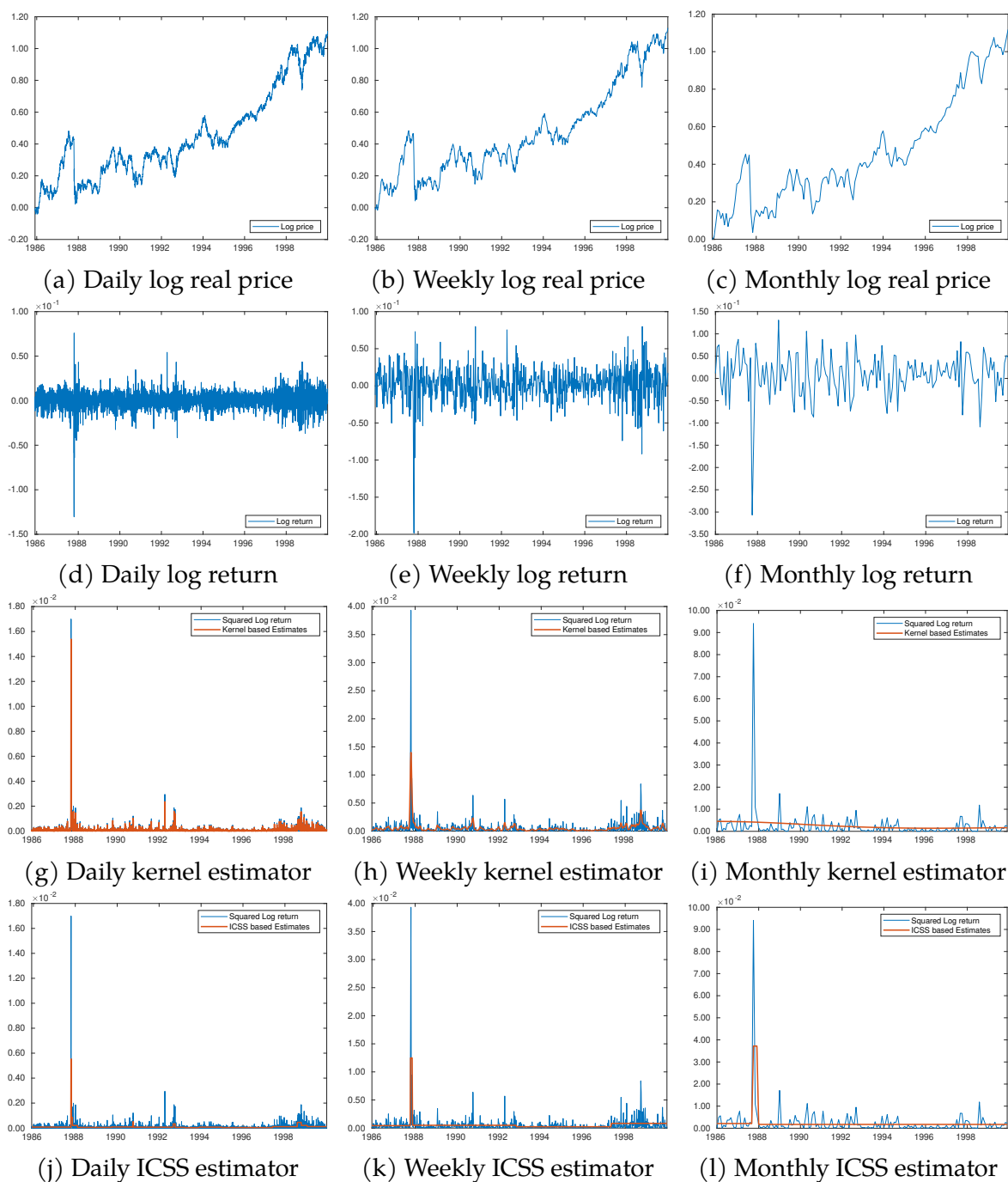


Figure A-11: The plots of logarithmic real FTSE 100 index from 01/1985 to 12/1999

NOTES: Time on x-axis and values on the y-axis.

Data Sample	sup DF	sup BZ_K	sup BZ_I	\mathcal{U}	\mathcal{U}_K	\mathcal{U}_I
S&P500 daily	0.386	0.000	0.018	0.000	0.002	0.049
S&P500 weekly	0.309	0.032	0.014	0.023	0.065	0.044
S&P500 monthly	0.144	0.046	0.018	0.028	0.073	0.044
FTSE100 daily	0.319	0.012	0.061	0.025	0.044	0.112
FTSE100 weekly	0.436	0.063	0.121	0.096	0.113	0.191
FTSE100 monthly	0.620	0.157	0.171	0.218	0.188	0.210

Table A-8: The p-values of sup DF , sup BZ_K , sup BZ_I , \mathcal{U} , \mathcal{U}_K , and \mathcal{U}_I

Appendix B: Tables and Figures of Chapter 3

Table B-1: Finite-sample sizes for the co-bubble tests, $T = 200$

Heteroskedasticity Specs	$T = 200$						
	τ_x	$c_x = 0.2$		$c_x = 0.4$		$c_x = 0.8$	
		R	S	R	S	R	S
0. Homoskedasticity	0.8	0.046	0.056	0.049	0.059	0.051	0.056
	0.85	0.049	0.056	0.049	0.058	0.054	0.057
	0.9	0.049	0.055	0.048	0.054	0.049	0.061
a. Upward shift (Coincidence)	0.8	0.055	0.056	0.049	0.052	0.052	0.055
	0.85	0.060	0.057	0.059	0.054	0.056	0.057
	0.9	0.063	0.065	0.062	0.061	0.067	0.056
b. Downward shift (Coincidence)	0.8	0.05	0.076	0.051	0.077	0.049	0.067
	0.85	0.050	0.083	0.050	0.079	0.052	0.074
	0.9	0.046	0.086	0.047	0.080	0.047	0.076
c. Upward trend volatility	0.8	0.055	0.055	0.055	0.057	0.060	0.060
	0.85	0.057	0.053	0.060	0.055	0.055	0.054
	0.9	0.054	0.053	0.058	0.056	0.062	0.058
d. Downward trend volatility	0.8	0.051	0.070	0.053	0.070	0.055	0.070
	0.85	0.051	0.073	0.051	0.071	0.052	0.074
	0.9	0.052	0.071	0.051	0.073	0.050	0.077
e. Early upward shift	0.8	0.051	0.057	0.055	0.056	0.060	0.063
	0.85	0.054	0.057	0.057	0.060	0.054	0.062
	0.9	0.057	0.058	0.056	0.058	0.055	0.063
f. Mid upward shift	0.8	0.052	0.056	0.057	0.060	0.061	0.063
	0.85	0.053	0.055	0.055	0.060	0.058	0.060
	0.9	0.055	0.058	0.054	0.057	0.055	0.061
g. Late upward shift	0.8	0.056	0.055	0.059	0.056	0.062	0.061
	0.85	0.055	0.055	0.057	0.056	0.059	0.060
	0.9	0.058	0.056	0.056	0.054	0.055	0.059
h. Early downward shift	0.8	0.056	0.088	0.052	0.088	0.057	0.082
	0.85	0.058	0.082	0.055	0.084	0.056	0.083
	0.9	0.055	0.080	0.057	0.080	0.051	0.082
i. Mid downward shift	0.8	0.046	0.082	0.050	0.089	0.055	0.096
	0.85	0.050	0.085	0.048	0.084	0.054	0.093
	0.9	0.047	0.085	0.049	0.088	0.052	0.089
j. Late downward shift	0.8	0.048	0.089	0.047	0.091	0.050	0.094
	0.85	0.048	0.092	0.050	0.096	0.048	0.096
	0.9	0.047	0.090	0.049	0.093	0.048	0.096
k. Double shift	0.8	0.060	0.096	0.059	0.094	0.056	0.092
	0.85	0.059	0.094	0.059	0.094	0.058	0.094
	0.9	0.056	0.093	0.057	0.097	0.058	0.097

NOTES: The data generating process is from (3.1) to (3.3) with sample size 200 ($r_0 = 0.01 + 1.8/\sqrt{T}$). Power calculations are based on 2,000 replications. Empirical probabilities of rejection at nominal 5% significance level.

Table B-2: Finite-sample sizes of the co-bubble tests, $T = 400$

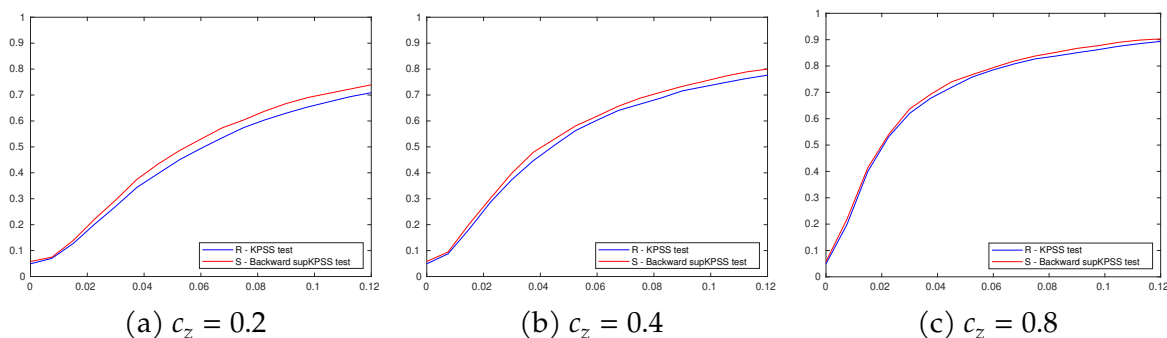
Heteroskedasticity Specs	$T = 400$						
	τ_x	$c_x = 0.2$		$c_x = 0.4$		$c_x = 0.8$	
		R	S	R	S	R	S
0. Homoskedasticity	0.8	0.046	0.047	0.045	0.047	0.046	0.046
	0.85	0.045	0.044	0.046	0.047	0.046	0.049
	0.9	0.044	0.050	0.045	0.046	0.048	0.049
a. Upward shift (Coincidence)	0.8	0.049	0.052	0.048	0.051	0.049	0.050
	0.85	0.047	0.048	0.051	0.049	0.048	0.047
	0.9	0.058	0.056	0.058	0.051	0.058	0.054
b. Downward shift (Coincidence)	0.8	0.042	0.068	0.045	0.071	0.044	0.074
	0.85	0.040	0.066	0.041	0.075	0.047	0.065
	0.9	0.045	0.067	0.044	0.061	0.045	0.058
c. Upward trend volatility	0.8	0.043	0.044	0.043	0.047	0.042	0.050
	0.85	0.043	0.044	0.044	0.045	0.044	0.050
	0.9	0.042	0.043	0.043	0.043	0.048	0.052
d. Downward trend volatility	0.8	0.041	0.054	0.046	0.054	0.048	0.050
	0.85	0.043	0.054	0.042	0.055	0.047	0.053
	0.9	0.042	0.061	0.043	0.059	0.044	0.057
e. Early upward shift	0.8	0.043	0.048	0.044	0.052	0.041	0.053
	0.85	0.041	0.042	0.041	0.046	0.040	0.054
	0.9	0.038	0.049	0.042	0.046	0.045	0.050
f. Mid upward shift	0.8	0.045	0.047	0.047	0.049	0.047	0.053
	0.85	0.044	0.041	0.044	0.049	0.042	0.053
	0.9	0.043	0.044	0.043	0.047	0.045	0.054
g. Late upward shift	0.8	0.047	0.050	0.044	0.047	0.048	0.046
	0.85	0.05	0.047	0.049	0.048	0.048	0.051
	0.9	0.046	0.048	0.048	0.048	0.05	0.053
h. Early downward shift	0.8	0.050	0.073	0.047	0.075	0.053	0.069
	0.85	0.049	0.070	0.048	0.070	0.051	0.066
	0.9	0.045	0.068	0.049	0.069	0.046	0.066
i. Mid downward shift	0.8	0.045	0.069	0.047	0.073	0.046	0.070
	0.85	0.047	0.066	0.045	0.070	0.045	0.072
	0.9	0.049	0.067	0.045	0.071	0.046	0.073
j. Late downward shift	0.8	0.043	0.069	0.044	0.067	0.044	0.076
	0.85	0.048	0.070	0.042	0.075	0.041	0.076
	0.9	0.049	0.070	0.048	0.076	0.042	0.080
k. Double shift	0.8	0.047	0.080	0.050	0.081	0.049	0.081
	0.85	0.051	0.077	0.048	0.077	0.046	0.085
	0.9	0.051	0.072	0.050	0.077	0.047	0.079

NOTES: The data generating process is from (3.1) to (3.3) with sample size 400 ($r_0 = 0.01 + 1.8/\sqrt{T}$). Power calculations are based on 2,000 replications. Empirical probabilities of rejection at nominal 5% significance level.

Table B-3: Finite-sample powers of the co-bubble tests, $T = 200$

		$T = 200$					
$\beta_{z,t}$	τ_z	$c_z = 0.2$		$c_z = 0.4$		$c_z = 0.8$	
		R	S	R	S	R	S
0.025	0.8	0.226	0.248	0.320	0.336	0.566	0.580
	0.85	0.169	0.194	0.225	0.248	0.387	0.412
	0.9	0.110	0.135	0.135	0.161	0.201	0.234
0.050	0.8	0.430	0.468	0.550	0.565	0.748	0.758
	0.85	0.357	0.380	0.433	0.461	0.614	0.635
	0.9	0.248	0.288	0.302	0.333	0.418	0.465
0.075	0.8	0.574	0.604	0.665	0.688	0.827	0.839
	0.85	0.486	0.524	0.572	0.594	0.725	0.736
	0.9	0.383	0.418	0.444	0.483	0.553	0.601

NOTES: The data generating process is from (3.1) to (3.3) with sample size 200 ($r_0 = 0.01 + 1.8/\sqrt{T}$). Power calculations are based on 2,000 replications. Empirical probabilities of rejection at nominal 5% significance level.

Figure B-1: Finite sample local power curves - Homoskedasticity variance, $T = 200$

NOTES: x-axis represents different values of $\beta_{z,t}$ and y-axis indicates simulated rejection rates. $t_z = 0.8$

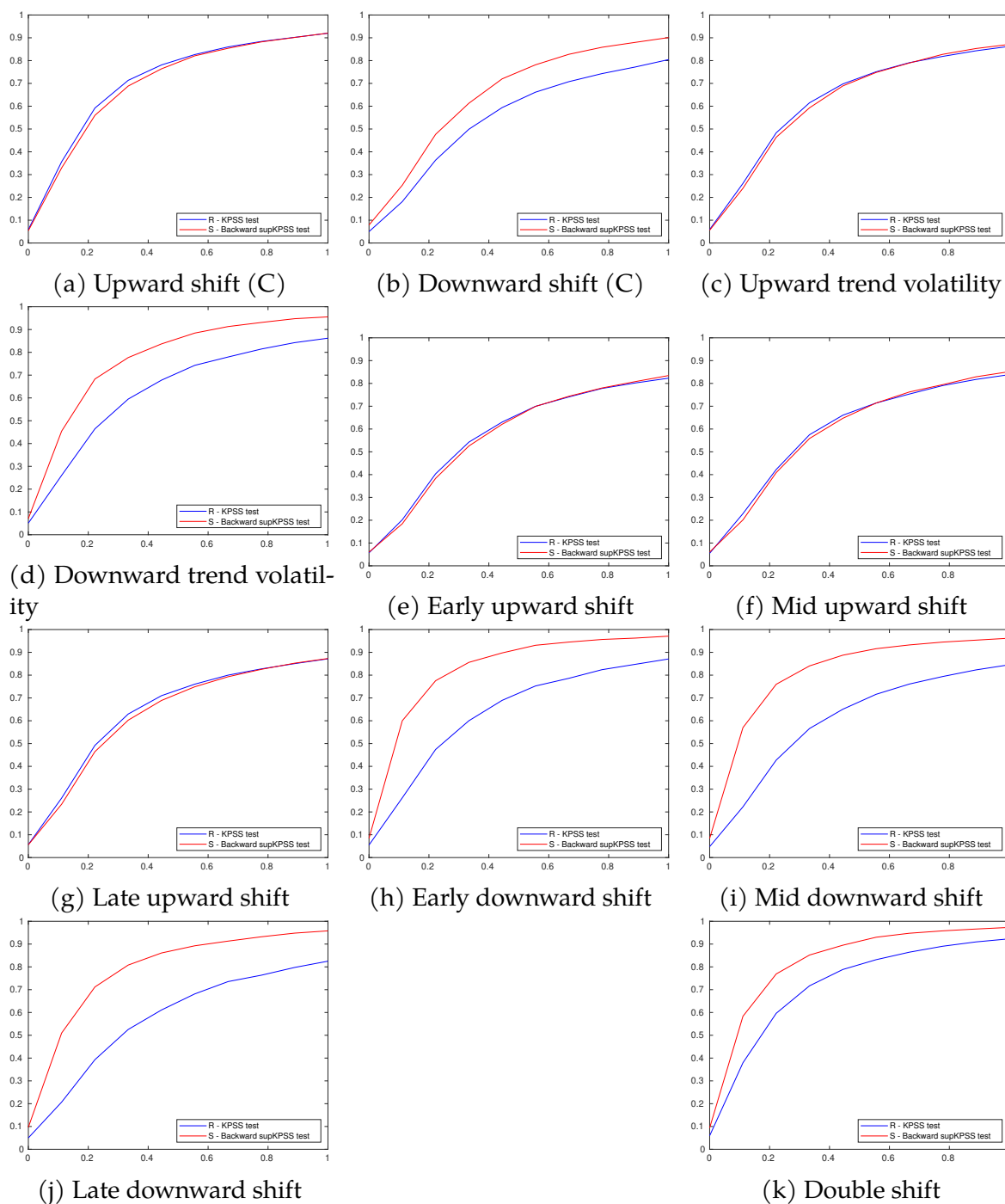


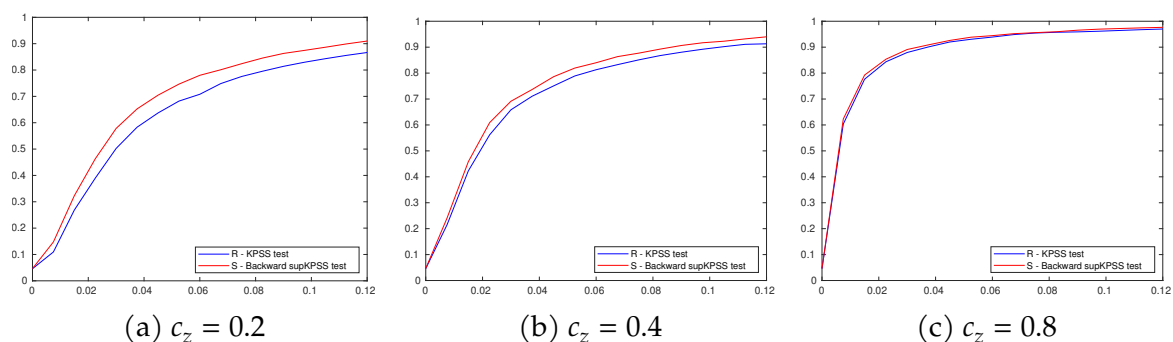
Figure B-2: Finite sample power curves - heteroskedasticity, $T = 200$

NOTES: x-axis represents different values of $\beta_{z,t}$ and y-axis indicates simulated rejection rates. $t_z = 0.8$. $c_z = 0.2$. (C) indicates that the break in volatility is coincident with the starting point of the bubble.

Table B-4: Finite-sample powers of the co-bubble tests, $T = 400$

		$T = 400$					
$\beta_{z,t}$	τ_z	$c_z = 0.2$		$c_z = 0.4$		$c_z = 0.8$	
		R	S	R	S	R	S
0.025	0.8	0.433	0.500	0.602	0.645	0.855	0.868
	0.85	0.335	0.379	0.461	0.505	0.733	0.750
	0.9	0.232	0.261	0.317	0.348	0.504	0.536
0.050	0.8	0.673	0.731	0.776	0.808	0.927	0.934
	0.85	0.572	0.639	0.683	0.707	0.854	0.871
	0.9	0.466	0.502	0.551	0.583	0.713	0.753
0.075	0.8	0.776	0.824	0.851	0.878	0.955	0.956
	0.85	0.695	0.746	0.776	0.807	0.901	0.910
	0.9	0.601	0.636	0.675	0.712	0.812	0.820

NOTES: The data generating process is from (3.1) to (3.3) with sample size 200 ($r_0 = 0.01 + 1.8/\sqrt{T}$). Power calculations are based on 2,000 replications. Empirical probabilities of rejection at nominal 5% significance level.

Figure B-3: Finite sample power curves - Homoskedasticity variance, $T = 400$

NOTES: x-axis represents different values of $\beta_{z,t}$ and y-axis indicates simulated rejection rates. $t_z = 0.8$.

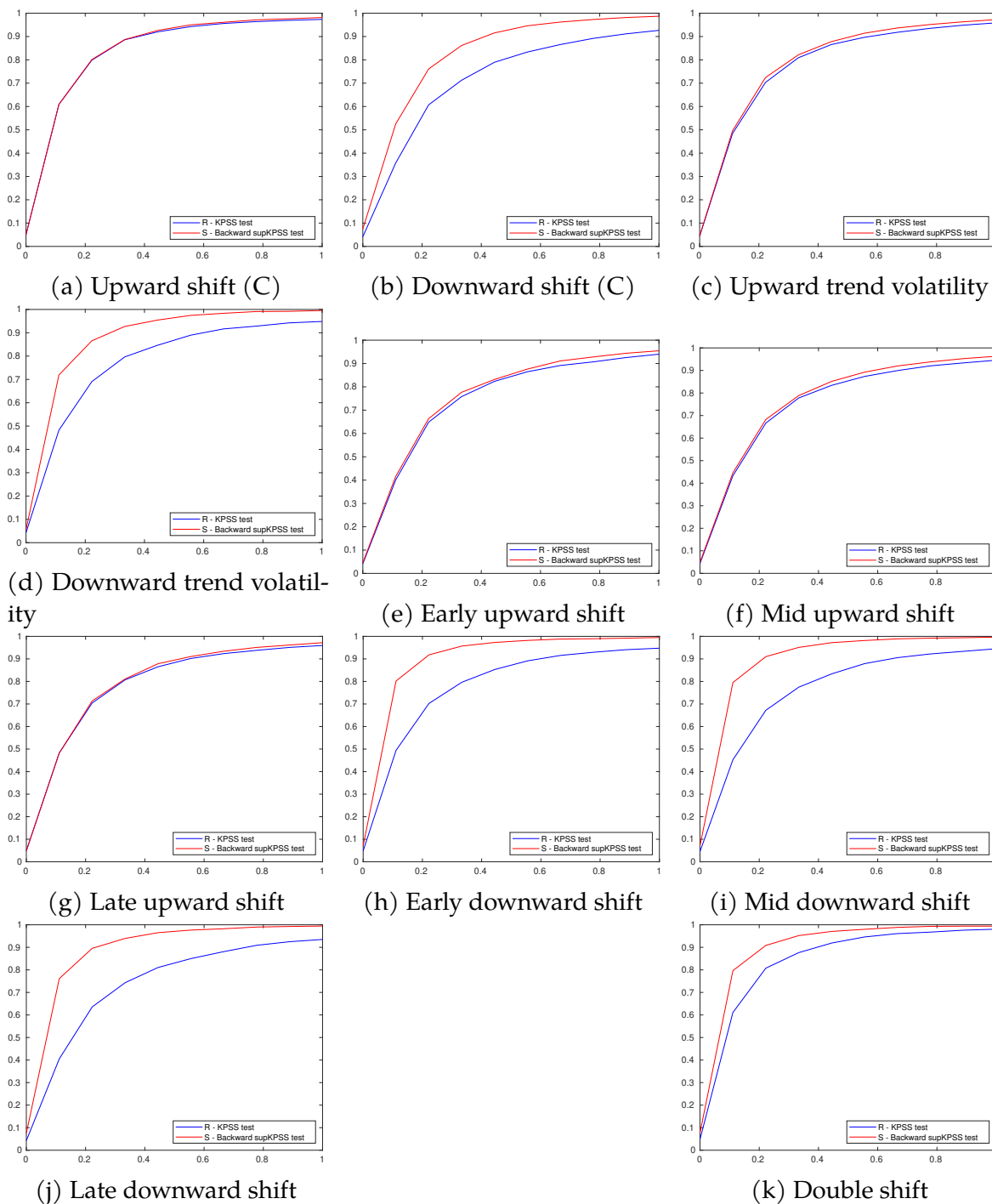


Figure B-4: Finite sample power curves - heteroskedasticity, $T = 400$

NOTES: x-axis represents different values of $\beta_{z,t}$ and y-axis indicates simulated rejection rates. $t_z = 0.8$. $c_z = 0.2$. (C) indicates that the break in volatility is coincident with the starting point of the bubble.

Table B-5: Finite-sample sizes of the co-bubble tests without using long-run variance under serial correlation conditions

$T = 200$							
σ_t	τ_x	$c_x = 0.2$		$c_x = 0.4$		$c_x = 0.8$	
		R	S	R	S	R	S
AR(1)	0.8	0.432	0.641	0.433	0.641	0.402	0.634
	0.85	0.428	0.621	0.428	0.632	0.411	0.632
	0.9	0.433	0.625	0.430	0.631	0.425	0.634
MA(1)	0.8	0.214	0.321	0.210	0.309	0.195	0.304
	0.85	0.208	0.321	0.210	0.305	0.208	0.297
	0.9	0.208	0.306	0.210	0.314	0.207	0.312

NOTES: The data generating process is from (3.1) to (3.3) with sample size 200 ($r_0 = 0.01 + 1.8/\sqrt{T}$). Power calculations are based on 2,000 replications. Empirical probabilities of rejection at nominal 5% significance level.

Table B-6: Finite-sample sizes of the co-bubble tests using long-run variance (Bartlett Kernel, T=200)

			Bartlett Kernel					
			T = 200					
			\tilde{R}			\tilde{S}		
$\epsilon_{y,t}$	c_x	τ_x	n=2	n=4	n=6	n=2	n=4	n=6
NIID	0.2	0.80	0.053	0.053	0.046	0.048	0.034	0.031
		0.85	0.056	0.054	0.047	0.044	0.033	0.029
		0.90	0.055	0.054	0.049	0.049	0.038	0.030
NIID	0.4	0.80	0.052	0.050	0.047	0.050	0.041	0.033
		0.85	0.051	0.053	0.047	0.049	0.037	0.032
		0.90	0.054	0.053	0.048	0.046	0.035	0.031
NIID	0.8	0.80	0.052	0.050	0.049	0.053	0.042	0.035
		0.85	0.055	0.055	0.051	0.053	0.044	0.032
		0.90	0.051	0.054	0.049	0.052	0.038	0.033
AR(1)	0.2	0.80	0.150	0.096	0.079	0.226	0.081	0.043
		0.85	0.151	0.095	0.077	0.242	0.076	0.044
		0.90	0.147	0.088	0.076	0.241	0.089	0.043
AR(1)	0.4	0.80	0.156	0.106	0.088	0.230	0.084	0.048
		0.85	0.152	0.104	0.082	0.237	0.081	0.043
		0.90	0.156	0.099	0.079	0.244	0.084	0.045
AR(1)	0.8	0.80	0.154	0.106	0.088	0.234	0.100	0.056
		0.85	0.160	0.113	0.095	0.242	0.094	0.052
		0.90	0.152	0.112	0.084	0.245	0.089	0.042
MA(1)	0.2	0.80	0.076	0.065	0.056	0.079	0.035	0.024
		0.85	0.070	0.060	0.056	0.084	0.041	0.027
		0.90	0.067	0.060	0.055	0.092	0.041	0.030
MA(1)	0.4	0.80	0.085	0.075	0.067	0.083	0.042	0.027
		0.85	0.084	0.067	0.059	0.086	0.037	0.026
		0.90	0.071	0.060	0.055	0.092	0.039	0.023
MA(1)	0.8	0.80	0.082	0.072	0.069	0.088	0.055	0.037
		0.85	0.087	0.071	0.068	0.085	0.044	0.032
		0.90	0.083	0.068	0.061	0.084	0.038	0.023

NOTES: The data generating process is from (3.1), (3.2), and (3.3) with sample size of 200 and $r_0 = 0.01 + 1.8/\sqrt{T}$. Power calculations are based on 2,000 replications. Empirical probabilities of rejection at nominal 5% significance level.

Table B-7: Finite-sample sizes of the co-bubble tests using long-run variance (Bartlett Kernel, T=400)

			Bartlett Kernel					
			T = 400					
			\tilde{R}			$\tilde{\xi}$		
$\epsilon_{y,t}$	c_x	τ_x	n=2	n=4	n=6	n=2	n=4	n=6
NIID	0.2	0.80	0.050	0.050	0.048	0.052	0.044	0.043
		0.85	0.058	0.057	0.054	0.060	0.047	0.045
		0.90	0.065	0.067	0.060	0.059	0.049	0.045
NIID	0.4	0.80	0.049	0.053	0.053	0.050	0.038	0.040
		0.85	0.052	0.049	0.050	0.052	0.044	0.045
		0.90	0.058	0.061	0.054	0.055	0.043	0.040
NIID	0.8	0.80	0.043	0.045	0.051	0.054	0.047	0.041
		0.85	0.045	0.049	0.051	0.055	0.042	0.039
		0.90	0.053	0.049	0.050	0.051	0.044	0.045
AR(1)	0.2	0.80	0.171	0.093	0.073	0.248	0.094	0.055
		0.85	0.157	0.093	0.075	0.255	0.100	0.058
		0.90	0.154	0.091	0.079	0.241	0.098	0.054
AR(1)	0.4	0.80	0.178	0.100	0.077	0.220	0.089	0.059
		0.85	0.185	0.094	0.073	0.227	0.090	0.053
		0.90	0.155	0.091	0.072	0.247	0.106	0.054
AR(1)	0.8	0.80	0.159	0.097	0.080	0.210	0.093	0.062
		0.85	0.169	0.102	0.078	0.234	0.108	0.061
		0.90	0.169	0.097	0.078	0.225	0.107	0.051
MA(1)	0.2	0.80	0.072	0.059	0.056	0.094	0.053	0.043
		0.85	0.076	0.061	0.060	0.092	0.058	0.036
		0.90	0.077	0.058	0.054	0.093	0.054	0.038
MA(1)	0.4	0.80	0.077	0.058	0.054	0.084	0.053	0.044
		0.85	0.071	0.057	0.055	0.078	0.047	0.038
		0.90	0.067	0.056	0.055	0.092	0.052	0.037
MA(1)	0.8	0.80	0.076	0.062	0.057	0.081	0.056	0.042
		0.85	0.080	0.062	0.058	0.086	0.053	0.037
		0.90	0.074	0.055	0.054	0.088	0.046	0.038

NOTES: The data generating process is from (3.1), (3.2), and (3.3) with sample size of 400 and $r_0 = 0.01 + 1.8/\sqrt{T}$. Power calculations are based on 2,000 replications. Empirical probabilities of rejection at nominal 5% significance level.

Table B-8: Finite-sample sizes of the co-bubble tests using long-run variance (Quadratic Spectral Kernel, T=200)

			Quadratic Spectral Kernel					
			T = 200					
			\tilde{R}			$\tilde{\xi}$		
$\epsilon_{y,t}$	c_x	τ_x	n=5	n=10	n=15	n=5	n=10	n=15
		0.80	0.056	0.054	0.055	0.032	0.170	0.476
NIID	0.2	0.85	0.055	0.056	0.059	0.032	0.160	0.446
		0.90	0.054	0.057	0.063	0.030	0.152	0.428
		0.80	0.051	0.057	0.052	0.037	0.182	0.521
NIID	0.4	0.85	0.056	0.055	0.059	0.035	0.167	0.490
		0.90	0.053	0.057	0.060	0.031	0.150	0.455
		0.80	0.054	0.056	0.056	0.038	0.152	0.495
NIID	0.8	0.85	0.059	0.059	0.059	0.037	0.145	0.472
		0.90	0.059	0.057	0.059	0.038	0.138	0.465
		0.80	0.068	0.048	0.040	0.034	0.071	0.308
AR(1)	0.2	0.85	0.070	0.044	0.044	0.040	0.070	0.279
		0.90	0.071	0.049	0.046	0.043	0.070	0.268
		0.80	0.083	0.058	0.053	0.039	0.084	0.322
AR(1)	0.4	0.85	0.075	0.049	0.049	0.037	0.078	0.301
		0.90	0.069	0.049	0.047	0.040	0.075	0.285
		0.80	0.078	0.059	0.053	0.052	0.078	0.325
AR(1)	0.8	0.85	0.086	0.056	0.057	0.051	0.069	0.305
		0.90	0.074	0.051	0.050	0.041	0.075	0.296
		0.80	0.052	0.048	0.046	0.021	0.123	0.393
MA(1)	0.2	0.85	0.049	0.046	0.049	0.024	0.110	0.368
		0.90	0.050	0.046	0.049	0.026	0.101	0.340
		0.80	0.058	0.057	0.059	0.025	0.122	0.412
MA(1)	0.4	0.85	0.051	0.050	0.053	0.024	0.117	0.379
		0.90	0.049	0.047	0.053	0.024	0.111	0.362
		0.80	0.063	0.058	0.057	0.031	0.119	0.416
MA(1)	0.8	0.85	0.061	0.062	0.059	0.027	0.113	0.389
		0.90	0.054	0.051	0.055	0.019	0.105	0.362

NOTES: The data generating process is from (3.1), (3.2), and (3.3) with sample size of 200 and $r_0 = 0.01 + 1.8/\sqrt{T}$. Power calculations are based on 2,000 replications. Empirical probabilities of rejection at nominal 5% significance level.

Table B-9: Finite-sample sizes of the co-bubble tests using long-run variance (Quadratic Spectral Kernel, T=400)

			Quadratic Spectral Kernel					
			T = 400					
			\tilde{R}			$\tilde{\xi}$		
$\epsilon_{y,t}$	c_x	τ_x	n=5	n=10	n=15	n=5	n=10	n=15
		0.80	0.053	0.047	0.048	0.048	0.058	0.199
NIID	0.2	0.85	0.060	0.054	0.056	0.046	0.056	0.191
		0.90	0.069	0.057	0.057	0.050	0.054	0.175
		0.80	0.053	0.054	0.054	0.044	0.055	0.196
NIID	0.4	0.85	0.051	0.054	0.052	0.045	0.052	0.186
		0.90	0.061	0.052	0.056	0.045	0.044	0.172
		0.80	0.050	0.054	0.056	0.046	0.046	0.179
NIID	0.8	0.85	0.050	0.053	0.057	0.042	0.041	0.171
		0.90	0.054	0.053	0.058	0.045	0.041	0.161
		0.80	0.069	0.054	0.051	0.054	0.020	0.119
AR(1)	0.2	0.85	0.074	0.056	0.053	0.056	0.022	0.107
		0.90	0.074	0.057	0.048	0.055	0.022	0.103
		0.80	0.084	0.049	0.044	0.059	0.030	0.120
AR(1)	0.4	0.85	0.069	0.050	0.048	0.052	0.026	0.111
		0.90	0.070	0.055	0.048	0.049	0.020	0.106
		0.80	0.082	0.054	0.052	0.064	0.031	0.119
AR(1)	0.8	0.85	0.082	0.054	0.049	0.065	0.028	0.109
		0.90	0.080	0.048	0.046	0.053	0.025	0.102
		0.80	0.050	0.046	0.052	0.038	0.037	0.172
MA(1)	0.2	0.85	0.051	0.047	0.051	0.037	0.030	0.156
		0.90	0.047	0.048	0.046	0.031	0.033	0.140
		0.80	0.050	0.047	0.043	0.040	0.044	0.174
MA(1)	0.4	0.85	0.050	0.043	0.046	0.034	0.039	0.168
		0.90	0.050	0.046	0.049	0.037	0.033	0.150
		0.80	0.051	0.051	0.050	0.037	0.042	0.165
MA(1)	0.8	0.85	0.052	0.049	0.053	0.031	0.039	0.151
		0.90	0.046	0.048	0.046	0.031	0.029	0.145

NOTES: The data generating process is from (3.1), (3.2), and (3.3) with sample size of 400 and $r_0 = 0.01 + 1.8/\sqrt{T}$. Power calculations are based on 2,000 replications. Empirical probabilities of rejection at nominal 5% significance level.

Table B-10: Finite-sample powers of the co-bubble tests using long-run variance

		$T = 200$						
$\epsilon_{y,t}$	$\beta_{z,t}$	τ_z	$c_z = 0.2$		$c_z = 0.4$		$c_z = 0.8$	
			\tilde{R}	\tilde{S}	\tilde{R}	\tilde{S}	\tilde{R}	\tilde{S}
NIID	0.25	0.80	0.593	0.707	0.640	0.772	0.549	0.846
		0.85	0.458	0.634	0.481	0.703	0.434	0.787
		0.90	0.289	0.484	0.299	0.515	0.291	0.561
NIID	0.50	0.80	0.610	0.764	0.642	0.817	0.531	0.879
		0.85	0.450	0.715	0.469	0.771	0.406	0.828
		0.90	0.292	0.569	0.299	0.610	0.280	0.637
NIID	0.75	0.80	0.600	0.782	0.634	0.830	0.526	0.883
		0.85	0.428	0.735	0.447	0.794	0.397	0.838
		0.90	0.295	0.605	0.297	0.641	0.271	0.650
AR(1)	0.25	0.80	0.478	0.619	0.535	0.683	0.503	0.784
		0.85	0.345	0.510	0.372	0.582	0.356	0.684
		0.90	0.196	0.339	0.221	0.389	0.222	0.459
AR(1)	0.50	0.80	0.561	0.730	0.587	0.783	0.507	0.846
		0.85	0.390	0.637	0.398	0.699	0.368	0.771
		0.90	0.249	0.504	0.259	0.522	0.244	0.542
AR(1)	0.75	0.80	0.566	0.763	0.596	0.805	0.503	0.855
		0.85	0.390	0.671	0.405	0.743	0.370	0.796
		0.90	0.261	0.539	0.267	0.561	0.241	0.591
MA(1)	0.25	0.80	0.526	0.656	0.583	0.724	0.510	0.810
		0.85	0.400	0.536	0.437	0.620	0.406	0.719
		0.90	0.246	0.381	0.260	0.433	0.256	0.480
MA(1)	0.50	0.80	0.581	0.752	0.609	0.795	0.519	0.852
		0.85	0.425	0.649	0.450	0.718	0.397	0.783
		0.90	0.277	0.524	0.282	0.542	0.262	0.573
MA(1)	0.75	0.80	0.580	0.772	0.613	0.816	0.520	0.864
		0.85	0.413	0.682	0.432	0.759	0.395	0.809
		0.90	0.275	0.556	0.283	0.576	0.260	0.606

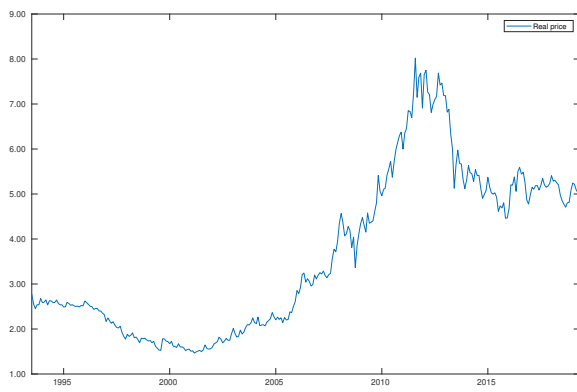
NOTES: The data generating process is from (3.1), (3.2), and (3.3) with sample size 200 $r_0 = 0.01 + 1.8/\sqrt{T}$. Power calculations are based on 2,000 replications. Empirical probabilities of rejection at nominal 5% significance level. R test uses QS kernel with a bandwidth of 10. S test uses Bartlett kernel with a bandwidth of 6.

Table B-11: Finite-sample rejection rates of the co-bubble tests under different lead/lag values

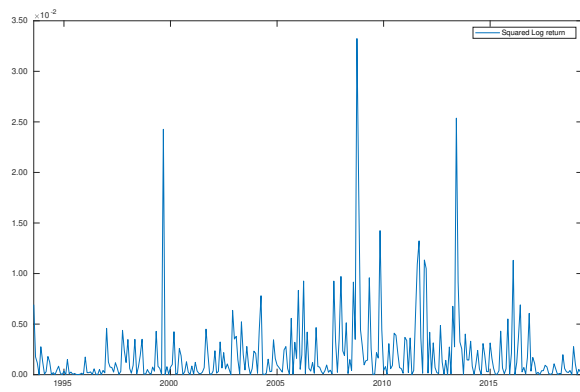
		T = 200															
$\beta_{x,t}$	τ_z	-6		-2		-1		0		1		2		6		\hat{i}	
		R	S	R	S	R	S	R	S	R	S	R	S	R	S	R	S
	0.80	0.510	0.564	0.109	0.101	0.061	0.062	0.049	0.059	0.063	0.078	0.110	0.145	0.669	0.827	0.049	0.059
	0.85	0.552	0.559	0.111	0.102	0.065	0.065	0.049	0.058	0.061	0.084	0.114	0.161	0.669	0.824	0.049	0.058
	0.90	0.565	0.565	0.113	0.099	0.061	0.061	0.048	0.054	0.059	0.078	0.106	0.162	0.643	0.803	0.048	0.054
	0.80	0.807	0.930	0.231	0.216	0.090	0.070	0.049	0.059	0.090	0.109	0.266	0.377	0.935	0.993	0.049	0.059
	0.85	0.844	0.940	0.252	0.217	0.086	0.076	0.049	0.058	0.086	0.124	0.267	0.387	0.930	0.992	0.049	0.058
	0.90	0.872	0.954	0.250	0.218	0.085	0.071	0.048	0.054	0.082	0.123	0.256	0.395	0.916	0.992	0.048	0.054
	0.8	0.922	0.991	0.420	0.429	0.140	0.097	0.049	0.059	0.137	0.188	0.527	0.720	0.978	1.000	0.049	0.059
	0.85	0.938	0.994	0.453	0.431	0.151	0.105	0.049	0.058	0.140	0.205	0.532	0.749	0.977	1.000	0.049	0.058
	0.90	0.957	0.995	0.472	0.417	0.141	0.098	0.048	0.054	0.127	0.199	0.519	0.765	0.973	1.000	0.048	0.054

		T = 400															
$\beta_{x,t}$	τ_z	-6		-2		-1		0		1		2		6		\hat{i}	
		R	S	R	S	R	S	R	S	R	S	R	S	R	S	R	S
	0.80	0.579	0.707	0.120	0.116	0.057	0.050	0.045	0.047	0.061	0.068	0.127	0.160	0.711	0.873	0.045	0.047
	0.85	0.624	0.724	0.132	0.117	0.061	0.051	0.046	0.047	0.066	0.067	0.132	0.164	0.715	0.890	0.046	0.047
	0.90	0.644	0.722	0.125	0.118	0.053	0.058	0.045	0.046	0.057	0.068	0.115	0.160	0.702	0.899	0.045	0.046
	0.80	0.846	0.965	0.290	0.312	0.098	0.083	0.045	0.047	0.102	0.118	0.314	0.441	0.927	0.996	0.045	0.047
	0.85	0.880	0.972	0.323	0.317	0.110	0.082	0.046	0.047	0.106	0.118	0.305	0.449	0.944	0.997	0.046	0.047
	0.90	0.904	0.971	0.320	0.298	0.096	0.080	0.045	0.046	0.089	0.113	0.284	0.441	0.951	0.999	0.045	0.046
	0.80	0.927	0.994	0.492	0.546	0.195	0.164	0.045	0.047	0.187	0.241	0.576	0.754	0.979	1.000	0.045	0.047
	0.85	0.948	0.997	0.532	0.576	0.216	0.169	0.046	0.047	0.189	0.245	0.588	0.775	0.988	1.000	0.046	0.047
	0.90	0.961	0.996	0.548	0.566	0.185	0.144	0.045	0.046	0.160	0.225	0.567	0.804	0.985	1.000	0.045	0.046

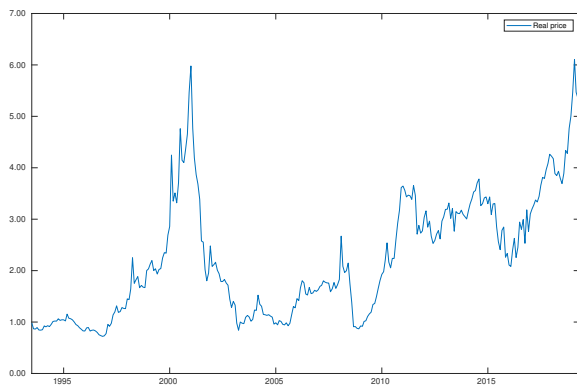
NOTES: The data generating process is from (3.1) to (3.3) with sample size of {200, 400}, $c_x = 0.4$ and $r_0 = 0.01 + 1.8/\sqrt{T}$. Power calculations are based on 2,000 replications. Empirical probabilities of rejection at nominal 5% significance level. The true lead/lag i is 0; results are given for the estimated lead/lag \hat{i} and for tests using different fitted lead/lag values j .



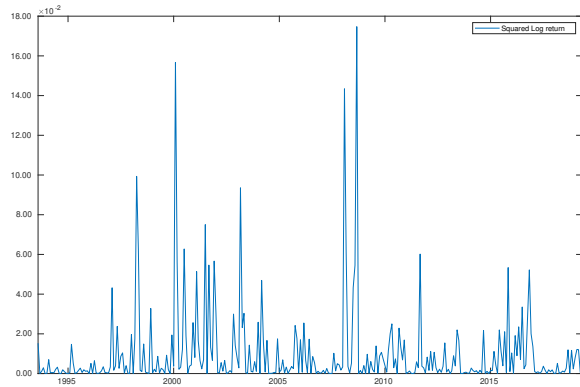
(a) Gold real price



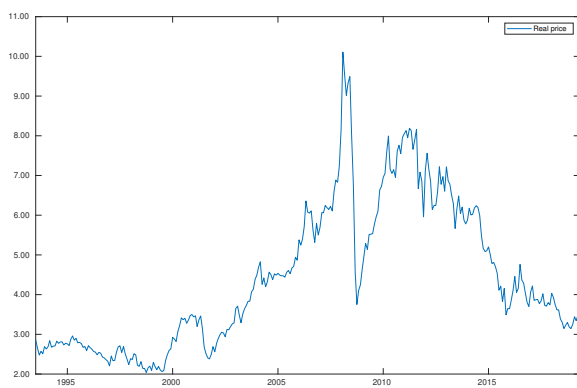
(b) Gold squared log return



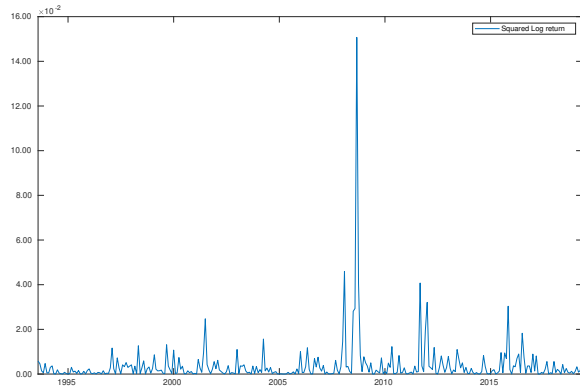
(c) Palladium real price



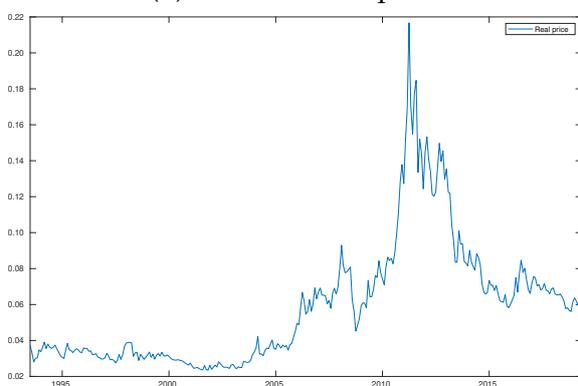
(d) Palladium squared log return



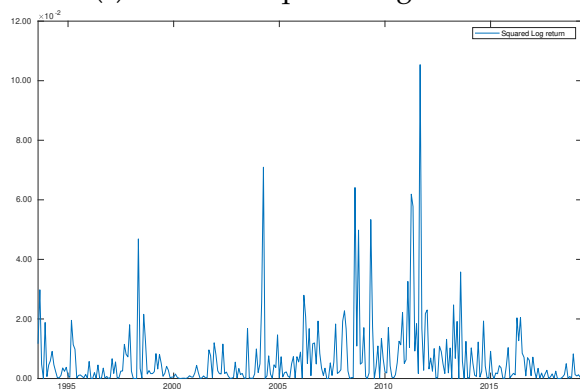
(e) Platinum real price



(f) Platinum squared log return



(g) Silver real price



(h) Silver squared log return

Figure B-5: Precious metal spot prices and their squared log returns.

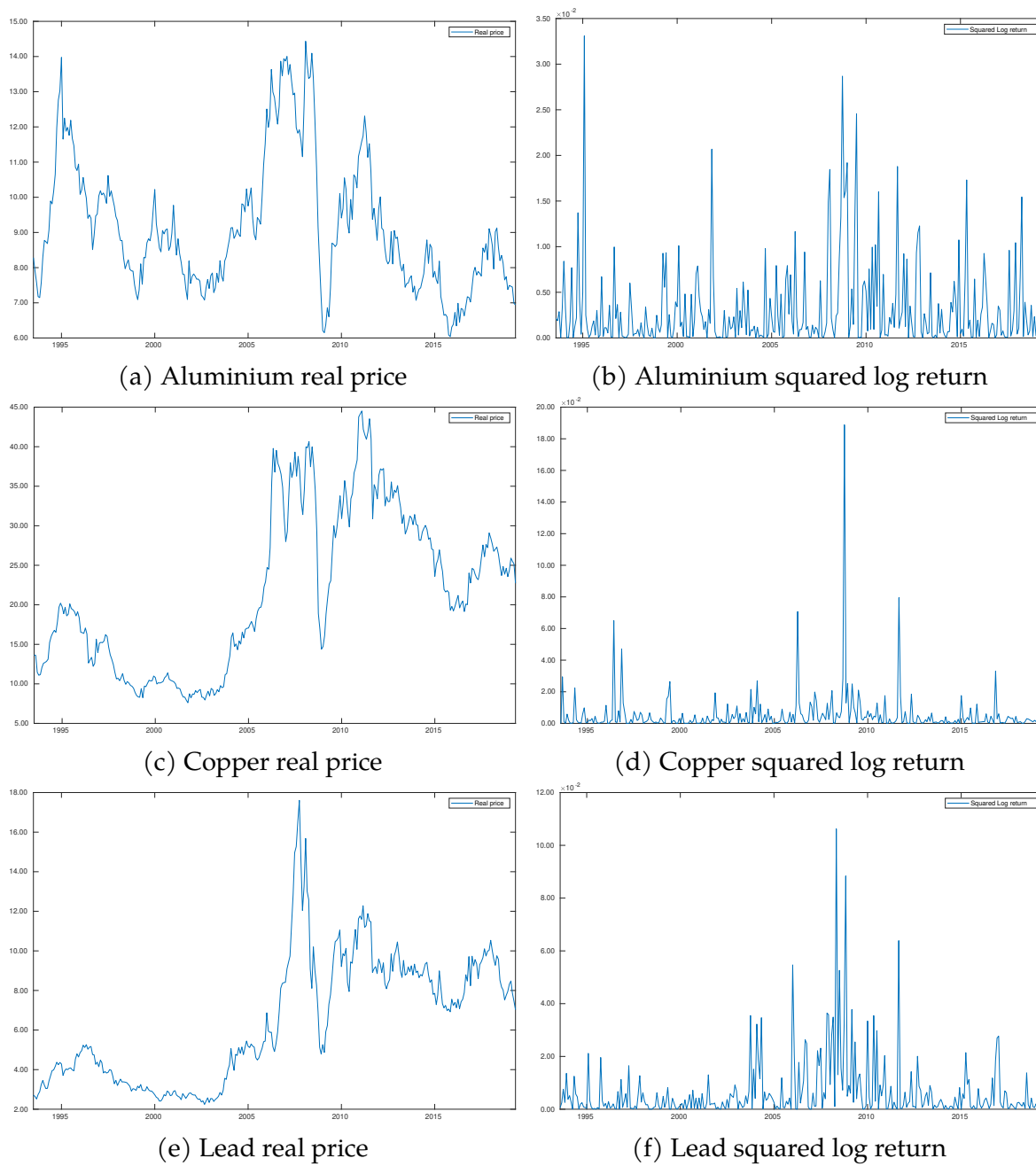


Figure B-6: Non-precious metal spot prices and their squared log returns.

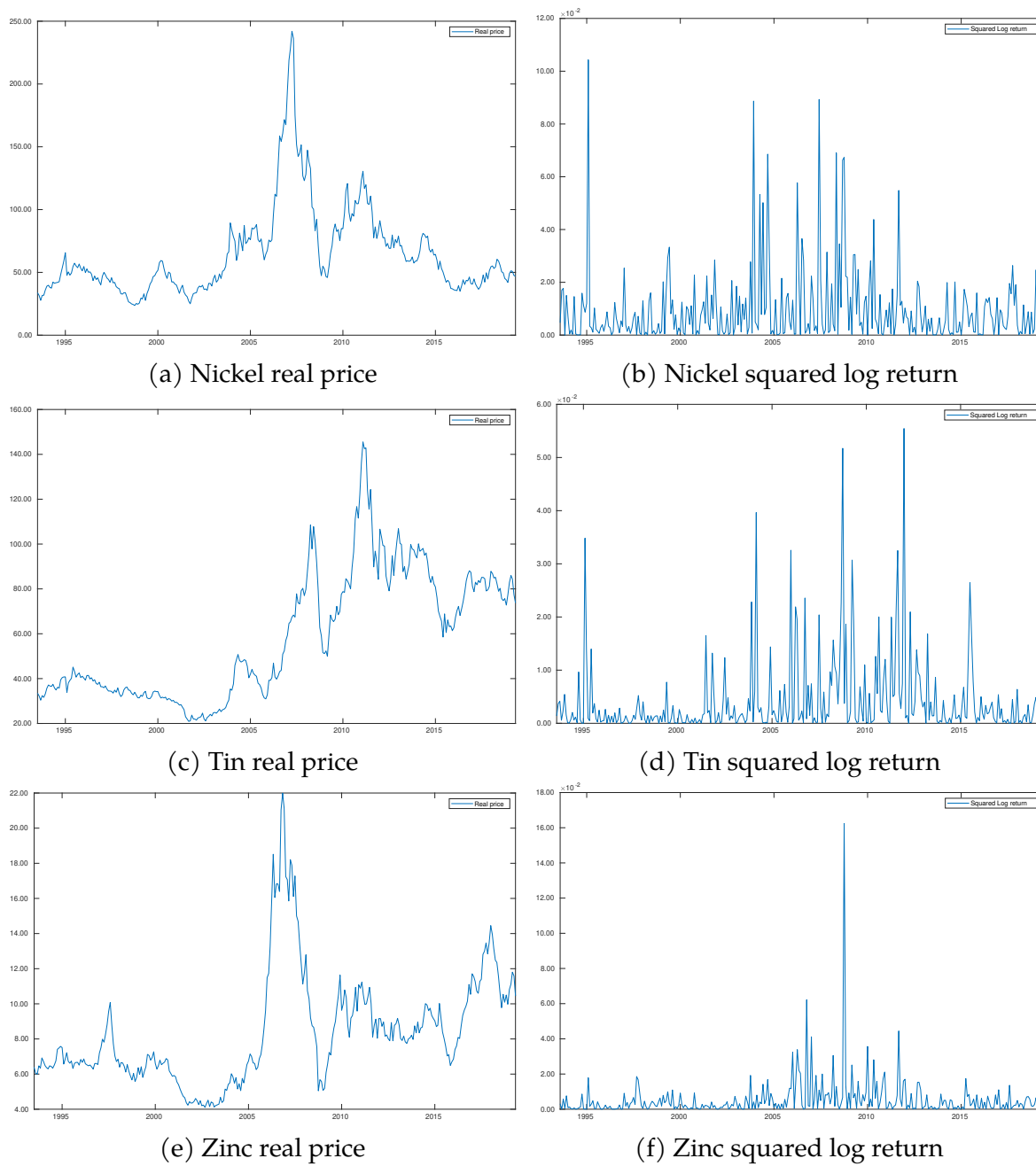


Figure B-7: Non-precious metal spot prices and their squared log returns. (Continued)

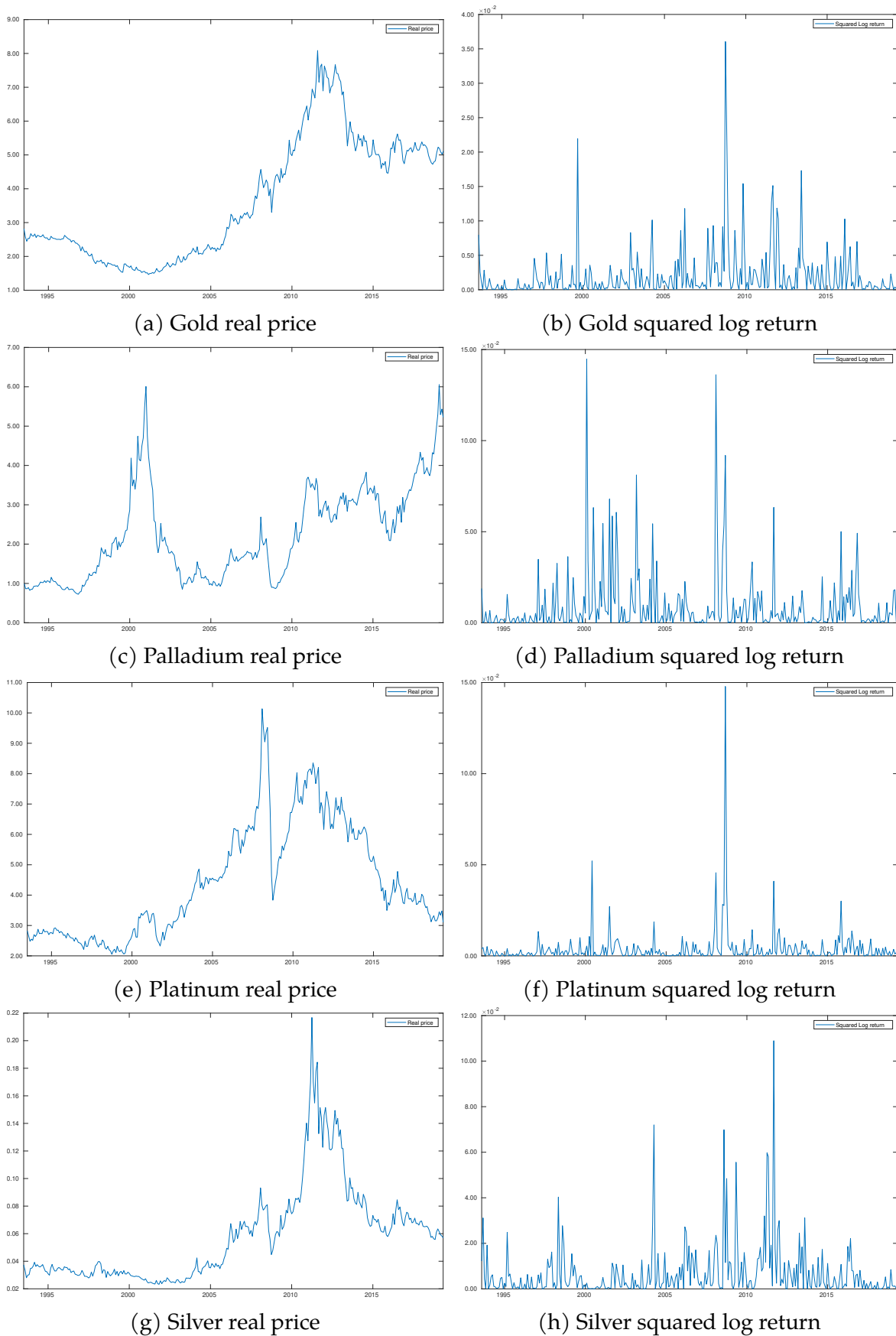


Figure B-8: Precious metal futures prices and their squared log returns.

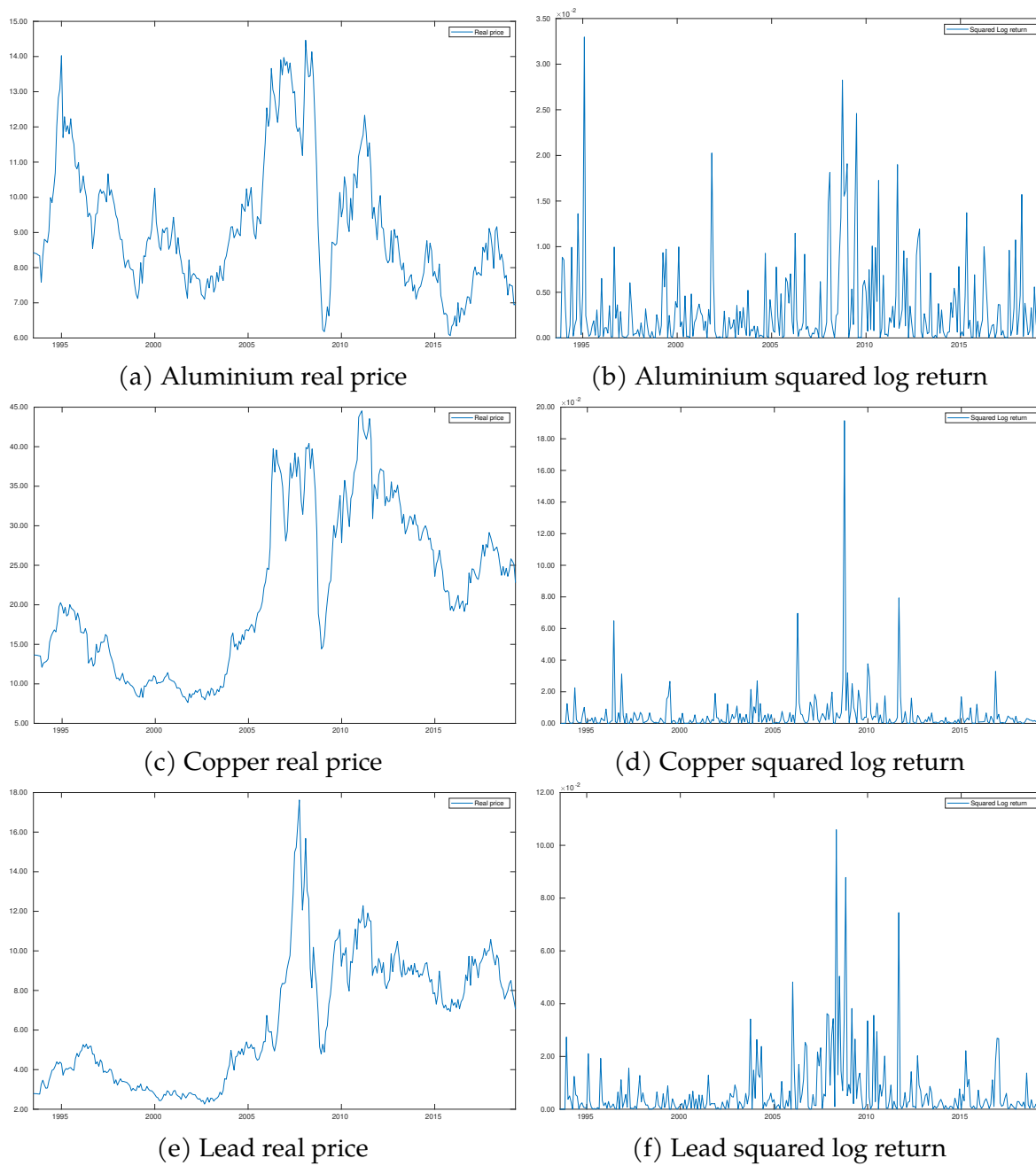


Figure B-9: Non-precious metal futures prices and their squared log returns.

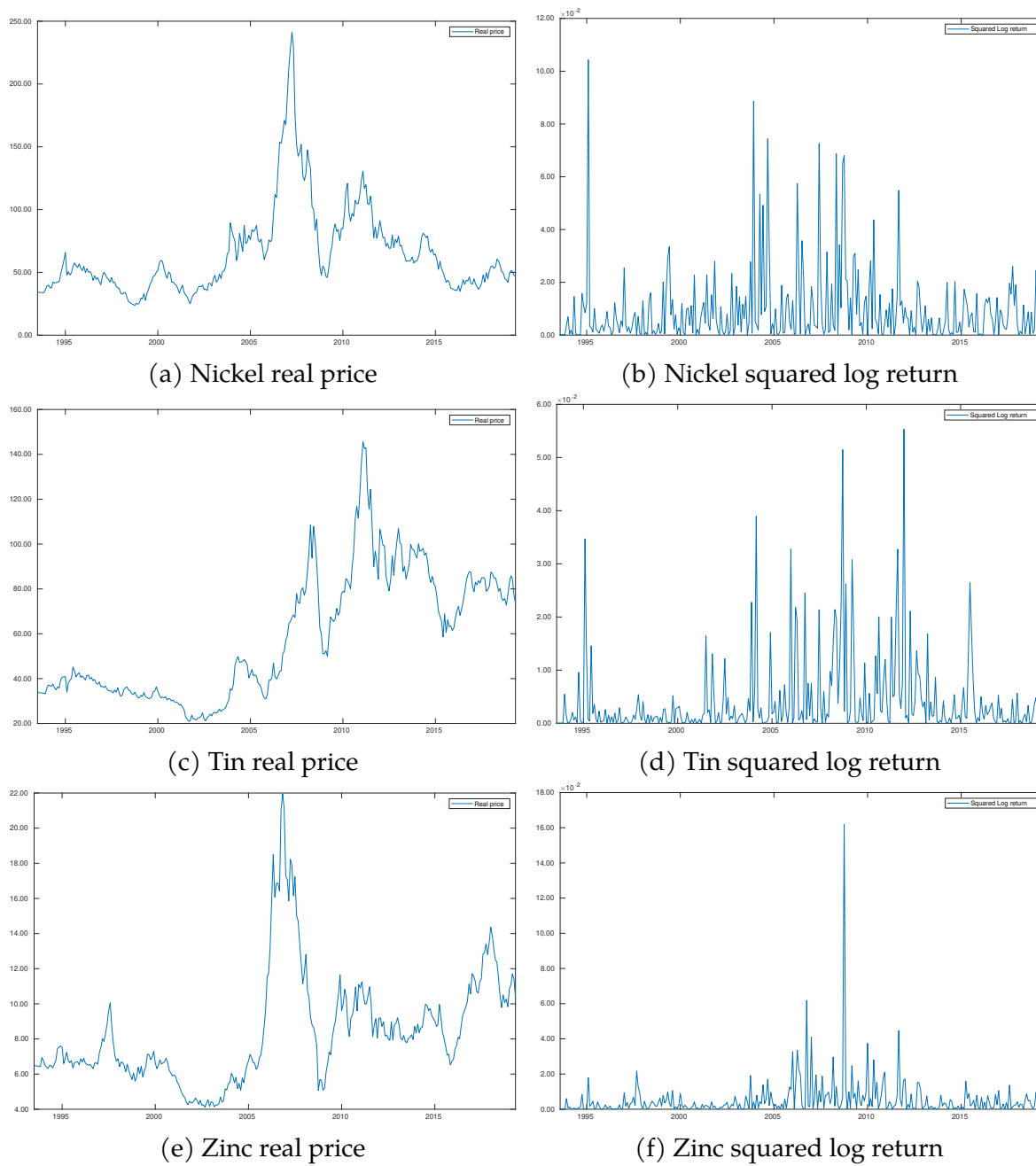


Figure B-10: Non-precious metal futures prices and their squared log returns. (Continued)

Table B-12: The descriptive statistics of metal prices

Precious metals								
	Obs	Mean	Median	Max	Min	S.D	I	W
Gold (S)	311	3.646	3.040	8.021	1.463	1.783	0.000	0.035
Palladium (S)	311	2.218	1.963	6.104	0.721	1.180	0.000	0.040
Platinum (S)	311	4.416	3.927	10.109	2.039	1.813	0.000	0.082
Silver (S)	311	0.059	0.055	0.217	0.023	0.035	0.000	0.034
Gold (F)	311	3.647	3.040	8.087	1.465	1.783	0.000	0.028
Palladium (F)	311	2.223	1.935	6.056	0.725	1.175	0.000	0.024
Platinum (F)	311	4.420	3.957	10.136	2.052	1.825	0.000	0.086
Silver (F)	311	0.059	0.054	0.217	0.023	0.035	0.000	0.041
Non-ferrous metals								
	Obs	Mean	Median	Max	Min	S.D	I	W
Aluminium (S)	311	9.163	8.778	14.434	6.038	1.888	0.140	0.309
Copper (S)	311	21.689	19.792	44.523	7.606	10.103	0.000	0.008
Lead (S)	311	6.432	5.437	17.606	2.244	3.202	0.000	0.021
Nickel (S)	311	64.904	53.114	241.982	23.630	36.227	0.000	0.030
Tin (S)	311	58.595	48.087	145.540	20.926	28.292	0.000	0.062
Zinc (S)	311	8.381	7.592	21.990	4.104	3.202	0.000	0.002
Aluminium (F)	311	9.196	8.804	14.463	6.068	1.884	0.143	0.317
Copper (F)	311	21.691	19.821	44.536	7.640	10.071	0.000	0.006
Lead (F)	311	6.441	5.406	17.625	2.259	3.198	0.000	0.018
Nickel (F)	311	64.904	53.135	241.253	23.697	35.906	0.000	0.023
Tin (F)	311	58.625	47.785	145.598	20.943	28.242	0.000	0.072
Zinc (F)	311	8.395	7.605	21.950	4.118	3.191	0.000	0.002

NOTES: Cells in the last two columns of the table display p-values corresponding to bootstrap *PSY* tests, with *I* and *W* denoting the test employing an *IID* bootstrap and a wild bootstrap, respectively. (S) denotes for spot price and (F) for futures price.

Table B-13: *PSY* date-stamping of explosive periods for metal prices

	Spot Prices			Futures Prices		
	Precious metals					
Gold	07/03–06/04	09/05–09/08	01/09–04/13	07/03–03/04	09/05–09/08	12/08–04/13
Palladium	03/98–07/98	12/98–05/99	07/99–05/01	01/98–09/98	12/98–05/01	12/10–01/11
Platinum	02/04–03/04	01/06–08/06	01/07–08/08	02/04–03/04	01/06–09/06	01/07–08/08
Silver	01/06–07/07	09/07–07/08	09/10–11/11	01/06–05/06	09/07–07/08	09/10–11/11
Non-ferrous metals						
Copper	02/04–03/04	11/04–03/05	06/05–12/06	06/05–11/06	-	-
Lead	12/03–03/04	11/04–04/05	10/06–04/08	12/03–02/04	11/04–12/04	10/06–04/08
Nickel	07/06–05/07	-	-	07/06–05/07	-	-
Tin	02/04–10/04	01/07–08/08	09/10–05/11	07/01–05/02	01/07–08/08	-
Zinc	07/97–08/97	12/04–03/05	05/05–02/07	07/97–08/97	12/04–03/05	05/05–12/06

NOTES: Cells in the table display date ranges (in MM/YY format) for positively explosive periods, which are identified by using an *IID* bootstrap *PSY* date stamping procedure.

Table B-14: Rejection rates of co-bubble tests to metal prices

Pair of Metals		Spot				Futures			
y_t	x_t	\hat{i}	\tilde{R}	\tilde{S}	$\tilde{G}\tilde{S}$	\hat{i}	\tilde{R}	\tilde{S}	$\tilde{G}\tilde{S}$
Palladium	Gold	-9	1.20%	0.64%	7.41%	-9	1.28%	0.68%	7.21%
Platinum	Gold	-12*	1.05%	4.48%	4.01%	-12*	1.04%	4.28%	3.81%
Silver	Gold	0	2.35%	0.20%	2.20%	0	2.32%	0.20%	1.80%
Copper	Gold	-8	10.26%	11.60%	33.67%	-8	10.64%	11.72%	33.47%
Lead	Gold	-7	20.21%	40.52%	7.62%	-7	20.28%	41.04%	7.21%
Nickel	Gold	-12	3.85%	5.36%	16.03%	-12	3.76%	5.40%	15.63%
Tin	Gold	0	37.37%	38.76%	15.63%	0	39.84%	40.68%	15.63%
Zinc	Gold	-12	32.22%	26.72%	21.04%	-12	32.88%	26.76%	20.44%
Gold	Palladium	-12	1.15%	0.32%	0.60%	-12	1.24%	0.36%	0.60%
Platinum	Palladium	0	0.00%	0.12%	0.20%	0	0.00%	0.16%	0.20%
Silver	Palladium	0	0.55%	1.92%	1.60%	0	0.72%	2.08%	1.60%
Copper	Palladium	0	0.20%	0.72%	0.60%	0	0.16%	0.84%	0.60%
Lead	Palladium	-4	0.25%	0.24%	0.00%	-4	0.36%	0.24%	0.00%
Nickel	Palladium	12*	0.15%	0.88%	10.22%	12*	0.16%	0.88%	9.42%
Tin	Palladium	0	0.75%	0.44%	0.20%	0	0.80%	0.56%	0.20%
Zinc	Palladium	-4	2.55%	6.88%	19.24%	-4	2.84%	7.08%	19.04%
Gold	Platinum	12*	0.90%	0.04%	5.21%	12*	0.92%	0.08%	4.01%
Palladium	Platinum	-12	0.30%	0.00%	0.80%	-12	0.32%	0.00%	0.80%
Silver	Platinum	0	0.55%	0.00%	4.81%	0	0.60%	0.00%	4.61%
Copper	Platinum	0	4.05%	0.24%	2.81%	0	4.08%	0.20%	3.01%
Lead	Platinum	0	1.80%	0.08%	5.81%	0	1.56%	0.08%	6.61%
Nickel	Platinum	-11	22.26%	24.84%	34.67%	-11	20.92%	25.44%	31.46%
Tin	Platinum	2	0.85%	0.00%	1.80%	2	0.64%	0.00%	2.61%
Zinc	Platinum	-4	18.11%	25.76%	45.09%	-4	19.80%	25.96%	50.30%
Gold	Silver	0	0.75%	0.00%	2.61%	0	0.76%	0.00%	2.81%
Palladium	Silver	-7	1.20%	0.08%	0.20%	-7	1.12%	0.08%	0.00%
Platinum	Silver	0	1.15%	0.32%	2.20%	0	1.04%	0.32%	2.00%
Copper	Silver	0	5.90%	3.80%	15.23%	0	6.48%	3.84%	13.83%
Lead	Silver	0	1.00%	13.64%	21.04%	0	1.00%	13.44%	20.44%
Nickel	Silver	-12	7.55%	9.24%	29.26%	-12	7.72%	9.16%	29.26%
Tin	Silver	0	0.55%	0.32%	35.47%	0	0.64%	0.28%	31.06%
Zinc	Silver	-3	14.31%	31.48%	19.44%	-3	14.80%	32.56%	19.04%
Gold	Copper	8	0.50%	0.12%	4.21%	8	0.40%	0.12%	4.61%
Palladium	Copper	-12	0.10%	0.00%	0.80%	-12	0.08%	0.00%	0.80%
Platinum	Copper	0	5.10%	0.80%	1.00%	0	5.08%	0.84%	1.20%
Silver	Copper	0	5.35%	1.24%	13.63%	0	5.32%	1.40%	13.83%

NOTES: Gray cells indicate values of p-value ≥ 0.025 , which means the co-explosive bubble occurs at that corresponding lag/lead.

Table B-15: Rejection rates of co-bubble tests to metal prices (Continued)

Pair of Metals		Spot				Futures			
y_t	x_t	\hat{i}	\tilde{R}	\tilde{S}	$\tilde{G}S$	\hat{i}	\tilde{R}	\tilde{S}	$\tilde{G}S$
Lead	Copper	0	4.45%	6.80%	64.73%	0	4.68%	6.72%	66.13%
Nickel	Copper	-1	0.90%	0.08%	11.82%	-1	0.96%	0.08%	12.02%
Tin	Copper	1	0.90%	0.08%	7.62%	1	1.00%	0.08%	8.22%
Zinc	Copper	0	40.57%	1.20%	4.21%	0	39.64%	1.44%	3.81%
Gold	Lead	7	7.40%	4.76%	9.02%	7	7.36%	5.12%	8.62%
Palladium	Lead	-9	0.15%	0.04%	0.40%	-9	0.28%	0.04%	0.40%
Platinum	Lead	0	3.40%	0.32%	1.00%	0	3.52%	0.32%	1.40%
Silver	Lead	0	24.36%	4.36%	29.46%	0	24.72%	4.12%	28.46%
Copper	Lead	0	37.82%	3.32%	10.42%	0	38.52%	3.04%	10.22%
Nickel	Lead	-5	2.95%	0.08%	0.80%	-5	2.80%	0.08%	0.60%
Tin	Lead	2	12.21%	17.08%	18.24%	2	11.48%	17.76%	17.64%
Zinc	Lead	-9	44.32%	16.60%	24.45%	-9	42.12%	16.84%	24.65%
Gold	Nickel	12	0.00%	0.00%	0.00%	12	0.00%	0.00%	0.00%
Palladium	Nickel	-12*	0.65%	0.28%	5.81%	-12*	0.48%	0.32%	6.01%
Platinum	Nickel	11	0.05%	0.48%	1.60%	11	0.08%	0.52%	1.40%
Silver	Nickel	12	0.10%	0.00%	1.60%	12	0.08%	0.00%	1.60%
Copper	Nickel	1	0.00%	0.00%	0.00%	1	0.00%	0.00%	0.00%
Lead	Nickel	5	0.00%	0.00%	0.00%	5	0.08%	0.00%	0.00%
Tin	Nickel	12	0.00%	0.00%	0.00%	12	0.00%	0.00%	0.00%
Zinc	Nickel	-3	2.55%	0.12%	5.61%	-3	2.52%	0.12%	5.81%
Gold	Tin	0	2.95%	24.72%	24.85%	0	3.08%	24.92%	25.85%
Palladium	Tin	-5	0.85%	0.16%	2.00%	-5	0.84%	0.24%	2.00%
Platinum	Tin	-2	0.75%	0.12%	1.20%	-2	0.64%	0.08%	1.20%
Silver	Tin	0	19.86%	3.80%	51.70%	0	18.76%	3.96%	50.90%
Copper	Tin	-1	6.55%	1.00%	9.42%	-1	7.24%	0.96%	8.82%
Lead	Tin	-2	19.31%	48.76%	60.52%	-2	19.32%	49.00%	63.13%
Nickel	Tin	-11	4.70%	3.56%	18.44%	-11	4.76%	3.52%	17.64%
Zinc	Tin	-12	54.03%	22.44%	31.06%	-12	53.48%	22.64%	30.26%
Gold	Zinc	12	0.00%	0.00%	0.40%	12	0.04%	0.00%	0.40%
Palladium	Zinc	-12	0.25%	0.00%	0.60%	-12	0.16%	0.00%	0.60%
Platinum	Zinc	4	0.15%	0.12%	0.00%	4	0.16%	0.12%	0.00%
Silver	Zinc	0	0.05%	1.16%	1.80%	0	0.12%	1.28%	1.60%
Copper	Zinc	0	0.15%	0.76%	0.20%	0	0.20%	0.88%	0.20%
Lead	Zinc	9	0.10%	0.00%	1.40%	9	0.04%	0.00%	1.40%
Nickel	Zinc	3	3.15%	0.08%	0.20%	3	3.00%	0.08%	0.20%
Tin	Zinc	12	0.00%	0.04%	0.60%	11	0.00%	0.04%	0.60%

NOTES: Gray cells indicate values of p-value ≥ 0.025 , which means the co-explosive bubble occurs at that corresponding lag/lead.

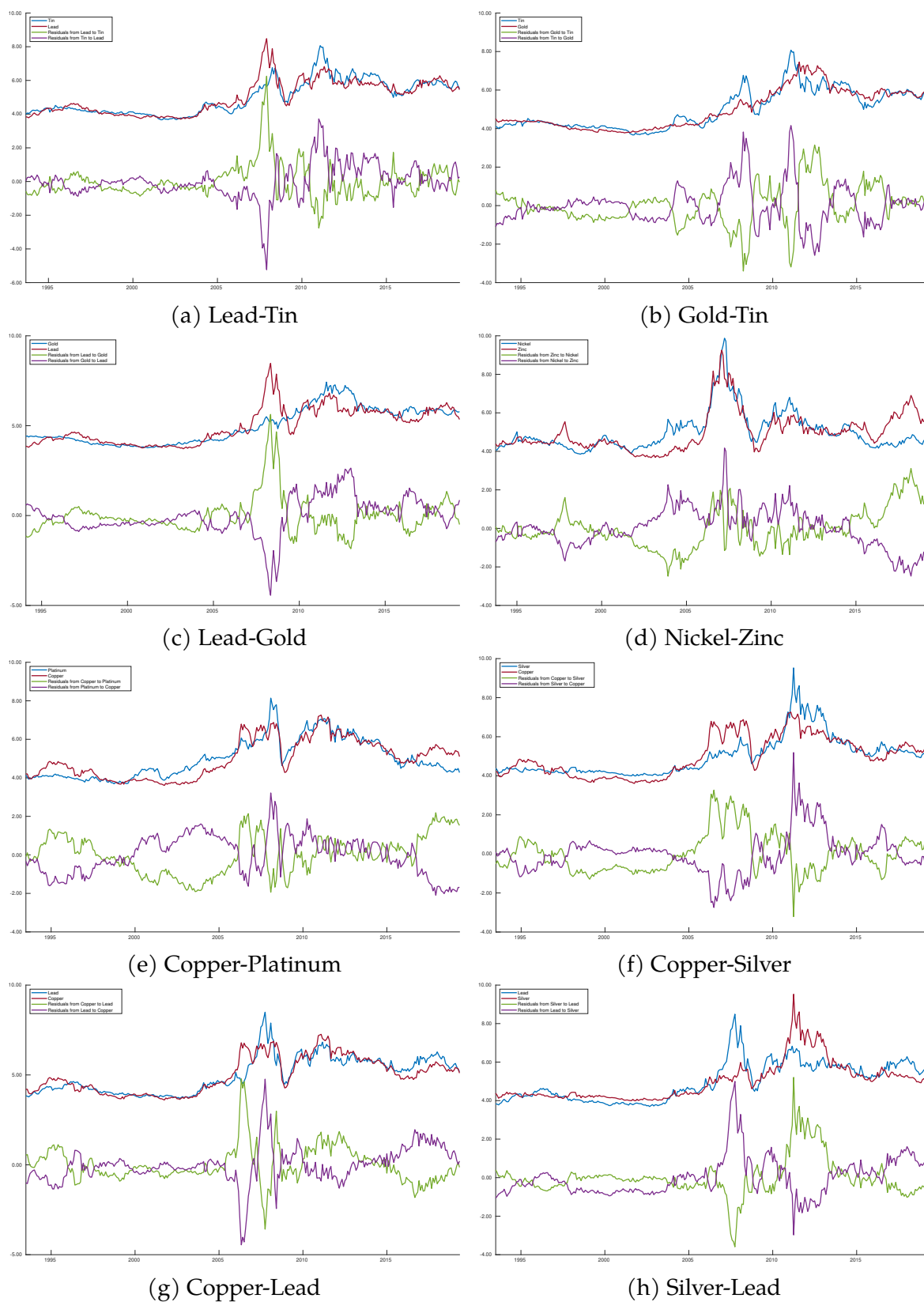


Figure B-11: Co-explosive bubble pairs of spot metal prices and full sample estimated residuals

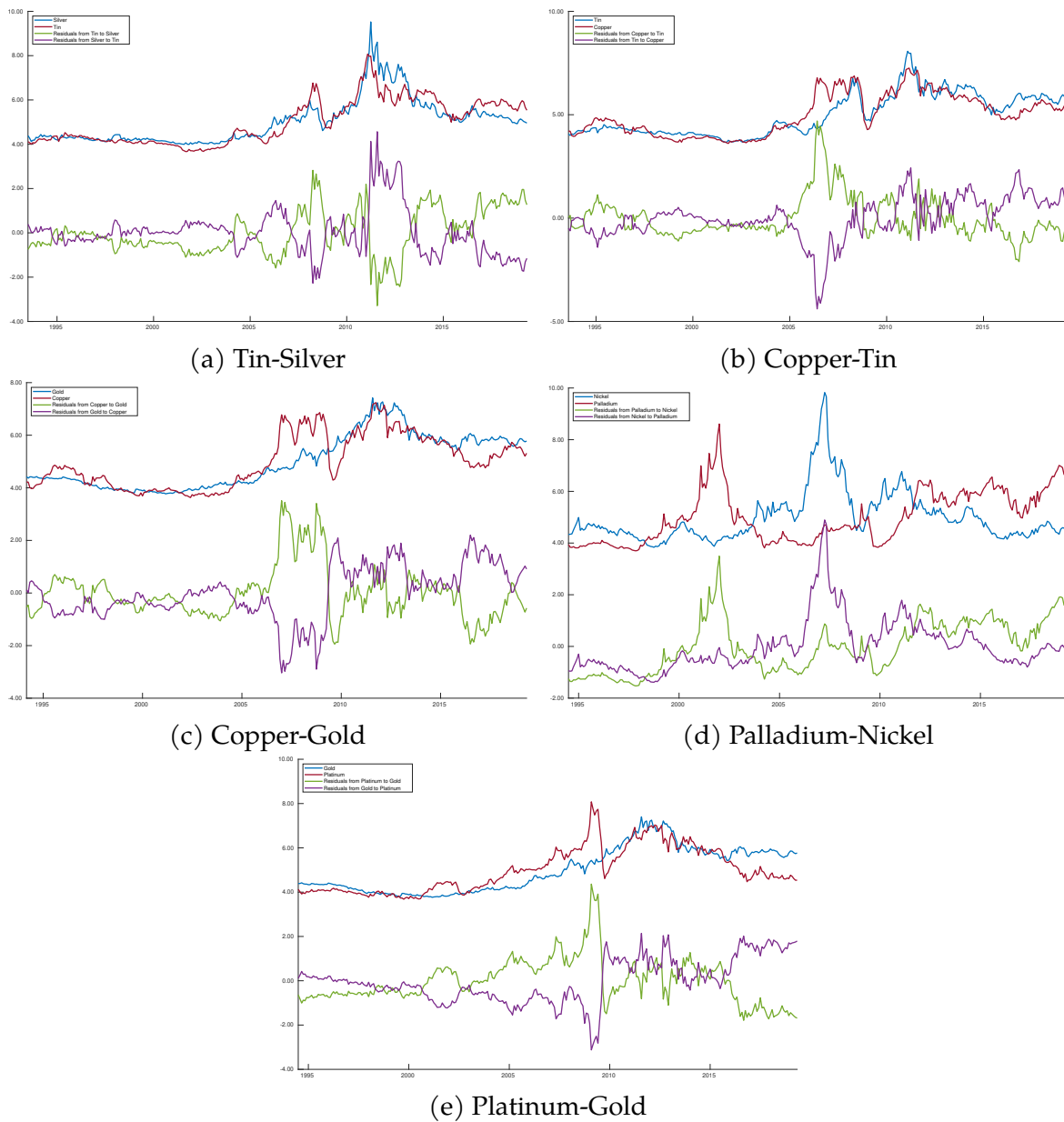


Figure B-12: Co-explosive bubble pairs of spot metal prices and full sample estimated residuals (Continued)

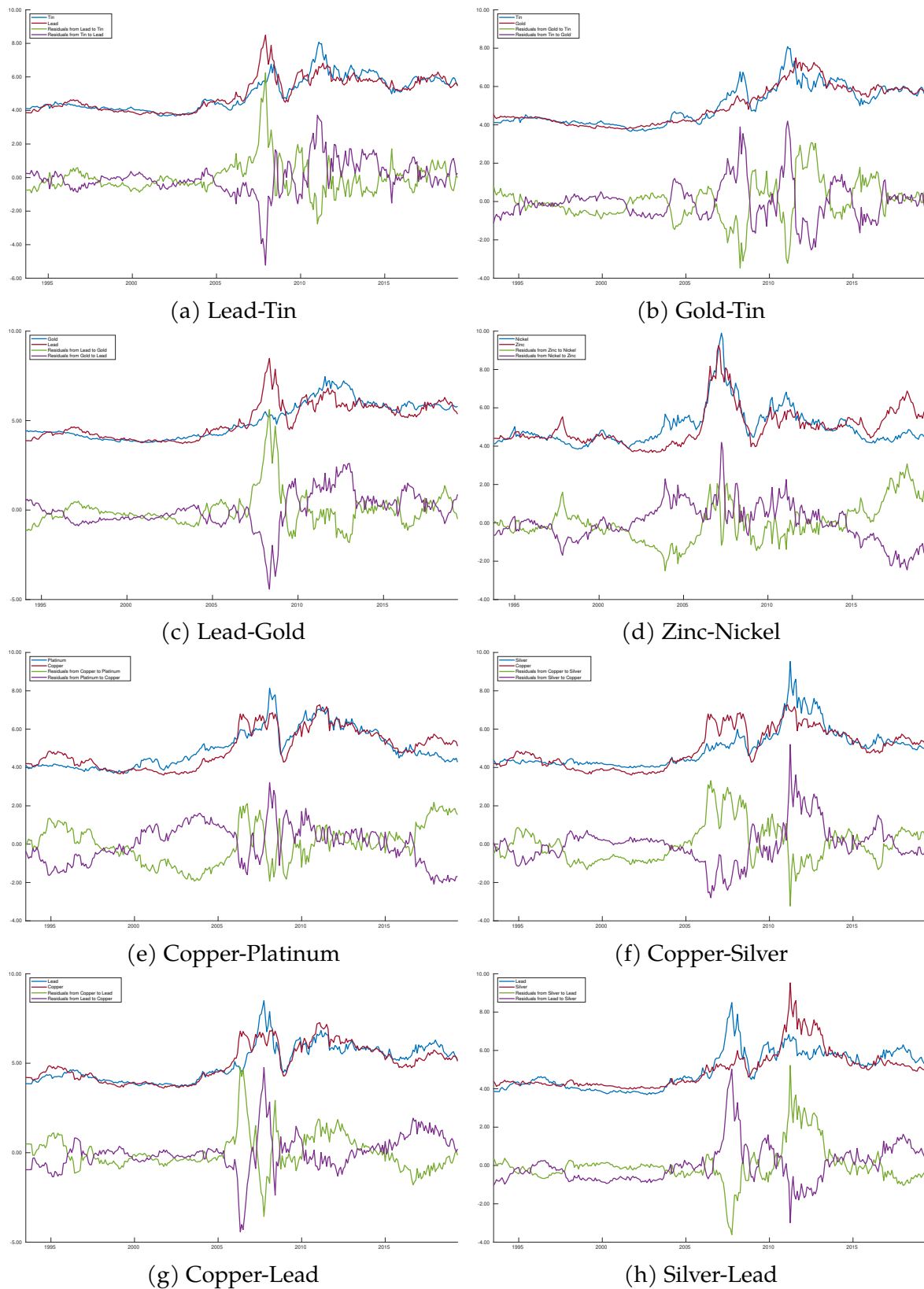


Figure B-13: Co-explosive bubble pairs of futures metal prices and full sample estimated residuals

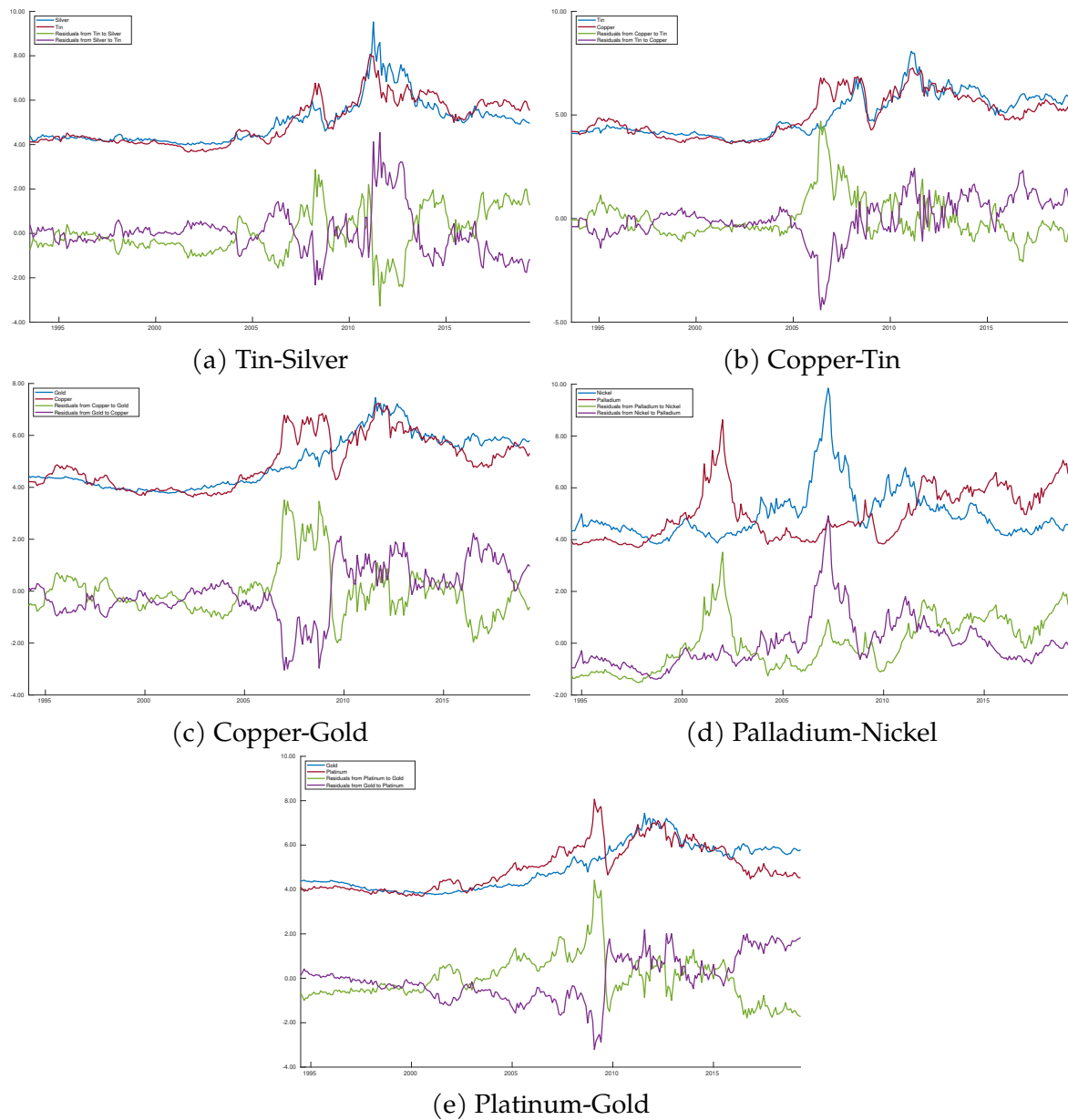


Figure B-14: Co-explosive bubble pairs of futures metal prices and full sample estimated residuals (Continued)

Appendix C: Tables and Figures of Chapter 4

Table C-1: Finite sample size at 5% significance level of one-sided predictability tests: u_t, v_t is N.i.i.d, no bubble in return

δ	T	c = 0			c = -5			c = -10		
		t_{zx}	Bonf. t	Bonf. Q	t_{zx}	Bonf. t	Bonf. Q	t_{zx}	Bonf. t	Bonf. Q
-0.95	100	0.126	0.054	0.069	0.105	0.047	0.059	0.089	0.050	0.057
	250	0.111	0.050	0.048	0.106	0.044	0.046	0.092	0.046	0.041
	500	0.115	0.052	0.045	0.104	0.044	0.040	0.095	0.045	0.041
	1000	0.107	0.052	0.041	0.104	0.041	0.036	0.094	0.048	0.038
-0.5	100	0.125	0.055	0.062	0.098	0.035	0.058	0.092	0.040	0.058
	250	0.111	0.051	0.053	0.093	0.034	0.050	0.085	0.038	0.048
	500	0.105	0.052	0.050	0.091	0.034	0.049	0.080	0.033	0.042
	1000	0.108	0.054	0.049	0.085	0.028	0.045	0.082	0.034	0.044
0	100	0.062	0.051	0.051	0.062	0.045	0.045	0.062	0.047	0.046
	250	0.053	0.046	0.048	0.058	0.048	0.049	0.057	0.049	0.047
	500	0.056	0.050	0.051	0.056	0.050	0.050	0.059	0.054	0.054
	1000	0.047	0.048	0.047	0.053	0.051	0.051	0.052	0.049	0.049
0.5	100	0.009	0.023	0.015	0.030	0.046	0.014	0.037	0.050	0.017
	250	0.007	0.019	0.018	0.021	0.038	0.015	0.035	0.049	0.017
	500	0.006	0.021	0.019	0.025	0.043	0.018	0.033	0.049	0.018
	1000	0.007	0.020	0.019	0.022	0.039	0.016	0.030	0.047	0.016
0.95	100	0.000	0.005	0.005	0.007	0.031	0.009	0.014	0.049	0.017
	250	0.001	0.005	0.011	0.009	0.035	0.014	0.016	0.045	0.016
	500	0.001	0.004	0.012	0.008	0.035	0.016	0.017	0.049	0.019
	1000	0.001	0.004	0.011	0.010	0.036	0.019	0.015	0.044	0.017

δ	T	c = -20			c = -50			c = -100		
		t_{zx}	Bonf. t	Bonf. Q	t_{zx}	Bonf. t	Bonf. Q	t_{zx}	Bonf. t	Bonf. Q
-0.95	100	0.071	0.050	0.060	0.051	0.046	0.125	0.048	0.043	0.454
	250	0.079	0.051	0.040	0.058	0.048	0.030	0.052	0.050	0.048
	500	0.079	0.051	0.035	0.067	0.053	0.021	0.057	0.050	0.011
	1000	0.081	0.049	0.031	0.069	0.051	0.019	0.060	0.052	0.006
-0.5	100	0.073	0.043	0.050	0.064	0.049	0.082	0.061	0.048	0.358
	250	0.075	0.047	0.044	0.063	0.049	0.032	0.059	0.052	0.039
	500	0.069	0.042	0.039	0.062	0.046	0.028	0.052	0.044	0.016
	1000	0.071	0.043	0.040	0.060	0.045	0.027	0.055	0.047	0.015
0	100	0.065	0.049	0.047	0.062	0.051	0.048	0.057	0.051	0.062
	250	0.058	0.046	0.045	0.057	0.052	0.050	0.058	0.050	0.050
	500	0.054	0.051	0.051	0.052	0.050	0.048	0.053	0.051	0.049
	1000	0.051	0.048	0.048	0.051	0.048	0.047	0.054	0.051	0.050
0.5	100	0.041	0.050	0.025	0.046	0.051	0.057	0.048	0.054	0.117
	250	0.037	0.046	0.021	0.042	0.047	0.052	0.041	0.047	0.153
	500	0.038	0.050	0.022	0.042	0.049	0.041	0.043	0.048	0.115
	1000	0.036	0.047	0.019	0.043	0.052	0.033	0.043	0.050	0.080
0.95	100	0.023	0.048	0.040	0.032	0.054	0.157	0.037	0.061	0.208
	250	0.021	0.048	0.033	0.029	0.049	0.152	0.035	0.053	0.320
	500	0.026	0.050	0.030	0.031	0.052	0.109	0.033	0.049	0.291
	1000	0.026	0.052	0.024	0.035	0.053	0.071	0.034	0.047	0.222

Notes: t_{zx} , *Bonf.t*, and *Bonf.Q* correspond to the test statistics of IVX test, Bonferroni-t test and Bonferroni-Q test. The data generating process is from (4.1) to (4.7).

Table C-2: Finite sample size at 5% significance level of one-sided predictability tests: u_t, v_t is N.i.i.d, bubble in return with $\tau_1 = 0.9, \tau_2 = 1, c_{bub} = 0.01$

δ	T	c = 0			c = -5			c = -10		
		t_{zx}	Bonf. t	Bonf. Q	t_{zx}	Bonf. t	Bonf. Q	t_{zx}	Bonf. t	Bonf. Q
-0.95	100	0.133	0.056	0.074	0.104	0.040	0.061	0.091	0.049	0.059
	250	0.121	0.054	0.059	0.111	0.040	0.048	0.098	0.045	0.050
	500	0.131	0.064	0.063	0.116	0.042	0.049	0.097	0.045	0.044
	1000	0.145	0.087	0.089	0.120	0.045	0.059	0.102	0.050	0.049
-0.5	100	0.127	0.055	0.064	0.101	0.037	0.061	0.086	0.041	0.059
	250	0.124	0.062	0.066	0.094	0.034	0.054	0.084	0.037	0.049
	500	0.121	0.065	0.066	0.089	0.035	0.051	0.081	0.036	0.046
	1000	0.139	0.087	0.086	0.102	0.045	0.060	0.083	0.038	0.052
0	100	0.064	0.051	0.051	0.066	0.051	0.050	0.065	0.051	0.050
	250	0.057	0.049	0.050	0.063	0.053	0.053	0.055	0.046	0.046
	500	0.065	0.065	0.066	0.063	0.058	0.057	0.059	0.055	0.055
	1000	0.072	0.077	0.077	0.068	0.066	0.065	0.064	0.062	0.062
0.5	100	0.013	0.029	0.020	0.031	0.045	0.016	0.034	0.047	0.017
	250	0.013	0.029	0.024	0.030	0.048	0.021	0.036	0.052	0.019
	500	0.013	0.032	0.025	0.027	0.046	0.020	0.036	0.050	0.021
	1000	0.018	0.039	0.037	0.038	0.055	0.029	0.041	0.058	0.026
0.95	100	0.002	0.010	0.010	0.010	0.035	0.010	0.019	0.050	0.015
	250	0.001	0.008	0.015	0.011	0.036	0.014	0.020	0.052	0.019
	500	0.002	0.008	0.021	0.013	0.040	0.017	0.022	0.052	0.018
	1000	0.004	0.014	0.029	0.021	0.048	0.022	0.029	0.059	0.027

δ	T	c = -20			c = -50			c = -100		
		t_{zx}	Bonf. t	Bonf. Q	t_{zx}	Bonf. t	Bonf. Q	t_{zx}	Bonf. t	Bonf. Q
-0.95	100	0.074	0.050	0.057	0.054	0.045	0.119	0.052	0.043	0.460
	250	0.079	0.053	0.042	0.060	0.050	0.034	0.054	0.049	0.051
	500	0.082	0.051	0.037	0.065	0.051	0.020	0.057	0.050	0.013
	1000	0.089	0.059	0.041	0.068	0.051	0.020	0.056	0.050	0.006
-0.5	100	0.072	0.043	0.048	0.058	0.048	0.077	0.057	0.045	0.339
	250	0.072	0.044	0.043	0.068	0.054	0.037	0.056	0.046	0.037
	500	0.076	0.048	0.043	0.063	0.049	0.030	0.057	0.049	0.018
	1000	0.071	0.049	0.046	0.062	0.050	0.030	0.060	0.053	0.018
0	100	0.063	0.049	0.049	0.063	0.055	0.053	0.059	0.052	0.067
	250	0.057	0.049	0.047	0.057	0.051	0.049	0.057	0.052	0.049
	500	0.058	0.052	0.053	0.057	0.053	0.052	0.053	0.048	0.047
	1000	0.060	0.059	0.060	0.056	0.054	0.053	0.053	0.050	0.049
0.5	100	0.045	0.054	0.023	0.047	0.053	0.056	0.054	0.057	0.112
	250	0.041	0.053	0.025	0.047	0.053	0.055	0.044	0.048	0.142
	500	0.041	0.053	0.024	0.044	0.051	0.040	0.043	0.050	0.113
	1000	0.046	0.060	0.026	0.047	0.057	0.038	0.045	0.053	0.080
0.95	100	0.026	0.052	0.035	0.030	0.050	0.133	0.038	0.059	0.198
	250	0.027	0.053	0.029	0.031	0.051	0.134	0.032	0.051	0.292
	500	0.026	0.050	0.025	0.035	0.054	0.100	0.033	0.049	0.262
	1000	0.035	0.057	0.025	0.036	0.056	0.057	0.034	0.048	0.187

Notes: t_{zx} , *Bonf.t*, and *Bonf.Q* correspond to the test statistics of IVX test, Bonferroni-t test and Bonferroni-Q test. The data generating process is from (4.1) to (4.7).

Table C-3: Finite sample size at 5% significance level of one-sided predictability tests: u_t, v_t is N.i.i.d, bubble in return with $\tau_1 = 0.9, \tau_2 = 1, c_{bub} = 0.05$

δ	T	c = 0			c = -5			c = -10		
		t_{zx}	Bonf. t	Bonf. Q	t_{zx}	Bonf. t	Bonf. Q	t_{zx}	Bonf. t	Bonf. Q
-0.95	100	0.127	0.062	0.078	0.106	0.041	0.063	0.092	0.050	0.061
	250	0.150	0.083	0.097	0.130	0.053	0.071	0.104	0.055	0.056
	500	0.227	0.205	0.209	0.182	0.103	0.146	0.150	0.093	0.113
	1000	0.354	0.410	0.404	0.293	0.313	0.345	0.251	0.271	0.307
-0.5	100	0.128	0.062	0.074	0.099	0.038	0.062	0.092	0.040	0.061
	250	0.135	0.083	0.089	0.108	0.045	0.068	0.094	0.044	0.060
	500	0.199	0.179	0.182	0.151	0.106	0.133	0.123	0.088	0.110
	1000	0.330	0.383	0.381	0.277	0.309	0.328	0.242	0.289	0.310
0	100	0.069	0.059	0.061	0.069	0.057	0.057	0.065	0.052	0.053
	250	0.080	0.080	0.082	0.070	0.067	0.068	0.067	0.065	0.066
	500	0.142	0.168	0.169	0.122	0.135	0.136	0.106	0.120	0.120
	1000	0.283	0.363	0.363	0.253	0.336	0.336	0.215	0.299	0.300
0.5	100	0.013	0.029	0.023	0.033	0.049	0.018	0.040	0.052	0.018
	250	0.024	0.048	0.041	0.042	0.062	0.033	0.046	0.065	0.030
	500	0.066	0.121	0.120	0.087	0.125	0.090	0.079	0.111	0.073
	1000	0.228	0.327	0.334	0.226	0.307	0.285	0.199	0.290	0.259
0.95	100	0.003	0.013	0.014	0.013	0.044	0.015	0.019	0.052	0.018
	250	0.005	0.024	0.038	0.020	0.048	0.025	0.026	0.060	0.028
	500	0.030	0.075	0.110	0.062	0.107	0.086	0.058	0.106	0.069
	1000	0.171	0.299	0.330	0.192	0.282	0.264	0.185	0.280	0.246

δ	T	c = -20			c = -50			c = -100		
		t_{zx}	Bonf. t	Bonf. Q	t_{zx}	Bonf. t	Bonf. Q	t_{zx}	Bonf. t	Bonf. Q
-0.95	100	0.073	0.049	0.060	0.056	0.051	0.122	0.045	0.037	0.448
	250	0.089	0.058	0.047	0.059	0.050	0.034	0.051	0.051	0.047
	500	0.115	0.094	0.085	0.078	0.077	0.040	0.060	0.069	0.020
	1000	0.209	0.262	0.271	0.152	0.244	0.197	0.099	0.199	0.107
-0.5	100	0.077	0.050	0.053	0.063	0.048	0.079	0.057	0.047	0.351
	250	0.075	0.049	0.049	0.064	0.053	0.036	0.054	0.048	0.037
	500	0.108	0.092	0.092	0.072	0.075	0.051	0.063	0.068	0.029
	1000	0.198	0.270	0.276	0.140	0.236	0.213	0.097	0.199	0.146
0	100	0.059	0.050	0.048	0.064	0.052	0.050	0.063	0.056	0.064
	250	0.066	0.060	0.059	0.061	0.058	0.056	0.056	0.052	0.053
	500	0.086	0.098	0.099	0.071	0.087	0.085	0.054	0.065	0.065
	1000	0.192	0.285	0.286	0.128	0.236	0.234	0.095	0.197	0.196
0.5	100	0.046	0.055	0.024	0.047	0.052	0.058	0.047	0.054	0.112
	250	0.048	0.062	0.031	0.043	0.052	0.054	0.044	0.053	0.144
	500	0.070	0.099	0.065	0.058	0.081	0.065	0.048	0.069	0.127
	1000	0.180	0.277	0.242	0.130	0.239	0.212	0.084	0.184	0.203
0.95	100	0.028	0.057	0.038	0.031	0.054	0.141	0.036	0.061	0.191
	250	0.029	0.058	0.036	0.033	0.055	0.133	0.029	0.049	0.298
	500	0.055	0.098	0.064	0.046	0.079	0.114	0.037	0.064	0.258
	1000	0.159	0.270	0.226	0.118	0.228	0.209	0.077	0.190	0.258

Notes: t_{zx} , *Bonf.t*, and *Bonf.Q* correspond to the test statistics of IVX test, Bonferroni-t test and Bonferroni-Q test. The data generating process is from (4.1) to (4.7).

Table C-4: Finite sample size at 5% significance level of one-sided predictability tests: u_t, v_t is N.i.i.d, bubble in return with $\tau_1 = 0.9, \tau_2 = 1, c_{bub} = 0.1$

δ	T	c = 0			c = -5			c = -10		
		t_{zx}	Bonf. t	Bonf. Q	t_{zx}	Bonf. t	Bonf. Q	t_{zx}	Bonf. t	Bonf. Q
-0.95	100	0.140	0.074	0.096	0.117	0.048	0.072	0.095	0.046	0.065
	250	0.210	0.185	0.192	0.160	0.090	0.132	0.133	0.087	0.108
	500	0.316	0.392	0.389	0.251	0.293	0.328	0.212	0.257	0.291
	1000	0.354	0.454	0.451	0.320	0.433	0.440	0.277	0.399	0.409
-0.5	100	0.146	0.079	0.090	0.102	0.043	0.070	0.090	0.043	0.061
	250	0.194	0.175	0.182	0.146	0.104	0.137	0.121	0.086	0.110
	500	0.289	0.379	0.376	0.240	0.306	0.325	0.194	0.266	0.286
	1000	0.347	0.450	0.449	0.308	0.422	0.428	0.277	0.412	0.418
0	100	0.073	0.064	0.065	0.073	0.061	0.060	0.069	0.059	0.058
	250	0.129	0.153	0.155	0.112	0.129	0.128	0.096	0.113	0.113
	500	0.254	0.357	0.359	0.217	0.315	0.316	0.182	0.289	0.289
	1000	0.341	0.458	0.458	0.307	0.428	0.428	0.272	0.420	0.421
0.5	100	0.018	0.039	0.030	0.041	0.062	0.027	0.045	0.061	0.025
	250	0.060	0.111	0.105	0.075	0.118	0.078	0.071	0.107	0.069
	500	0.209	0.324	0.327	0.187	0.295	0.272	0.167	0.278	0.249
	1000	0.323	0.439	0.441	0.296	0.420	0.415	0.272	0.407	0.398
0.95	100	0.004	0.019	0.022	0.017	0.047	0.019	0.023	0.058	0.022
	250	0.029	0.084	0.106	0.057	0.104	0.071	0.049	0.099	0.059
	500	0.160	0.285	0.309	0.175	0.283	0.259	0.156	0.272	0.231
	1000	0.315	0.439	0.443	0.280	0.410	0.398	0.267	0.414	0.396

δ	T	c = -20			c = -50			c = -100		
		t_{zx}	Bonf. t	Bonf. Q	t_{zx}	Bonf. t	Bonf. Q	t_{zx}	Bonf. t	Bonf. Q
-0.95	100	0.073	0.055	0.062	0.062	0.056	0.130	0.050	0.044	0.453
	250	0.106	0.090	0.083	0.064	0.074	0.048	0.050	0.060	0.055
	500	0.170	0.251	0.257	0.113	0.228	0.179	0.068	0.180	0.101
	1000	0.249	0.395	0.400	0.177	0.368	0.354	0.118	0.331	0.284
-0.5	100	0.081	0.051	0.059	0.065	0.050	0.084	0.057	0.048	0.339
	250	0.094	0.085	0.088	0.068	0.075	0.054	0.052	0.060	0.044
	500	0.159	0.246	0.251	0.107	0.223	0.197	0.064	0.175	0.127
	1000	0.237	0.393	0.398	0.176	0.375	0.368	0.109	0.329	0.306
0	100	0.067	0.056	0.054	0.058	0.052	0.052	0.060	0.053	0.065
	250	0.075	0.092	0.090	0.059	0.074	0.072	0.050	0.062	0.062
	500	0.157	0.268	0.268	0.096	0.219	0.217	0.062	0.173	0.173
	1000	0.233	0.394	0.395	0.171	0.364	0.362	0.114	0.326	0.326
0.5	100	0.044	0.059	0.027	0.049	0.054	0.058	0.049	0.055	0.112
	250	0.064	0.099	0.061	0.050	0.077	0.073	0.039	0.060	0.144
	500	0.136	0.258	0.226	0.095	0.216	0.200	0.060	0.182	0.211
	1000	0.238	0.397	0.385	0.173	0.360	0.353	0.110	0.331	0.333
0.95	100	0.029	0.058	0.039	0.033	0.056	0.129	0.039	0.064	0.199
	250	0.048	0.095	0.065	0.037	0.075	0.139	0.029	0.065	0.294
	500	0.130	0.253	0.215	0.089	0.217	0.206	0.052	0.173	0.263
	1000	0.228	0.396	0.378	0.164	0.361	0.342	0.109	0.320	0.331

Notes: t_{zx} , *Bonf.t*, and *Bonf.Q* correspond to the test statistics of IVX test, Bonferroni-t test and Bonferroni-Q test. The data generating process is from (4.1) to (4.7).

Table C-5: Finite sample size at 5% significance level of one-sided predictability tests: u_t, v_t is N.i.i.d, bubble in return with $\tau_1 = 0.7, \tau_2 = 1, c_{bub} = 0.01$

δ	T	c = 0			c = -5			c = -10		
		t_{zx}	Bonf. t	Bonf. Q	t_{zx}	Bonf. t	Bonf. Q	t_{zx}	Bonf. t	Bonf. Q
-0.95	100	0.135	0.058	0.075	0.115	0.038	0.066	0.093	0.044	0.061
	250	0.145	0.074	0.077	0.113	0.042	0.057	0.096	0.043	0.049
	500	0.189	0.128	0.136	0.148	0.057	0.082	0.120	0.057	0.066
	1000	0.319	0.311	0.309	0.246	0.159	0.205	0.199	0.124	0.165
-0.5	100	0.131	0.063	0.072	0.101	0.041	0.065	0.086	0.038	0.056
	250	0.128	0.071	0.076	0.097	0.042	0.058	0.085	0.037	0.053
	500	0.164	0.116	0.119	0.118	0.059	0.081	0.095	0.049	0.067
	1000	0.287	0.275	0.275	0.220	0.174	0.203	0.186	0.145	0.174
0	100	0.068	0.059	0.059	0.065	0.049	0.048	0.064	0.048	0.047
	250	0.074	0.071	0.073	0.069	0.061	0.060	0.064	0.057	0.058
	500	0.099	0.108	0.109	0.084	0.081	0.081	0.077	0.075	0.076
	1000	0.212	0.248	0.247	0.178	0.187	0.187	0.152	0.163	0.163
0.5	100	0.014	0.031	0.021	0.034	0.048	0.018	0.044	0.056	0.023
	250	0.022	0.042	0.035	0.033	0.050	0.024	0.042	0.055	0.024
	500	0.036	0.065	0.061	0.055	0.073	0.044	0.050	0.069	0.035
	1000	0.125	0.184	0.184	0.150	0.182	0.152	0.122	0.154	0.113
0.95	100	0.002	0.011	0.010	0.014	0.040	0.010	0.022	0.052	0.013
	250	0.004	0.017	0.023	0.020	0.046	0.018	0.023	0.049	0.015
	500	0.010	0.034	0.050	0.039	0.069	0.036	0.037	0.065	0.027
	1000	0.075	0.147	0.181	0.112	0.150	0.127	0.102	0.145	0.101

δ	T	c = -20			c = -50			c = -100		
		t_{zx}	Bonf. t	Bonf. Q	t_{zx}	Bonf. t	Bonf. Q	t_{zx}	Bonf. t	Bonf. Q
-0.95	100	0.077	0.051	0.059	0.060	0.050	0.124	0.051	0.041	0.447
	250	0.078	0.049	0.041	0.062	0.050	0.032	0.050	0.046	0.044
	500	0.091	0.061	0.046	0.068	0.056	0.026	0.058	0.051	0.013
	1000	0.152	0.121	0.115	0.090	0.091	0.051	0.069	0.070	0.015
-0.5	100	0.074	0.046	0.051	0.067	0.052	0.077	0.059	0.046	0.324
	250	0.076	0.048	0.046	0.064	0.050	0.037	0.059	0.051	0.038
	500	0.081	0.056	0.057	0.064	0.052	0.033	0.058	0.050	0.020
	1000	0.127	0.109	0.113	0.088	0.090	0.067	0.071	0.074	0.030
0	100	0.065	0.051	0.049	0.059	0.048	0.047	0.064	0.054	0.064
	250	0.058	0.050	0.050	0.056	0.052	0.050	0.054	0.050	0.049
	500	0.067	0.066	0.066	0.064	0.064	0.062	0.059	0.055	0.054
	1000	0.107	0.124	0.123	0.081	0.094	0.093	0.065	0.077	0.075
0.5	100	0.047	0.055	0.027	0.049	0.052	0.052	0.052	0.056	0.103
	250	0.044	0.052	0.028	0.050	0.054	0.052	0.048	0.052	0.138
	500	0.045	0.057	0.028	0.047	0.053	0.044	0.045	0.053	0.104
	1000	0.097	0.125	0.085	0.069	0.091	0.068	0.053	0.067	0.091
0.95	100	0.028	0.050	0.028	0.033	0.049	0.115	0.044	0.062	0.183
	250	0.029	0.051	0.025	0.032	0.051	0.105	0.038	0.054	0.268
	500	0.037	0.061	0.029	0.037	0.054	0.074	0.035	0.051	0.221
	1000	0.082	0.115	0.077	0.054	0.084	0.071	0.049	0.069	0.173

Notes: t_{zx} , *Bonf.t*, and *Bonf.Q* correspond to the test statistics of IVX test, Bonferroni-t test and Bonferroni-Q test. The data generating process is from (4.1) to (4.7).

Table C-6: Finite sample size at 5% significance level of one-sided predictability tests: u_t, v_t is N.i.i.d, bubble in return with $\tau_1 = 0.7, \tau_2 = 1, c_{bub} = 0.05$

δ	T	c = 0			c = -5			c = -10		
		t_{zx}	Bonf. t	Bonf. Q	t_{zx}	Bonf. t	Bonf. Q	t_{zx}	Bonf. t	Bonf. Q
-0.95	100	0.192	0.120	0.145	0.143	0.062	0.102	0.109	0.054	0.081
	250	0.340	0.370	0.369	0.271	0.255	0.294	0.207	0.204	0.243
	500	0.401	0.469	0.466	0.345	0.423	0.434	0.302	0.384	0.401
	1000	0.437	0.483	0.483	0.393	0.468	0.470	0.353	0.440	0.444
-0.5	100	0.176	0.114	0.129	0.121	0.061	0.091	0.099	0.053	0.076
	250	0.312	0.338	0.339	0.243	0.254	0.277	0.195	0.218	0.243
	500	0.383	0.449	0.449	0.340	0.411	0.417	0.298	0.397	0.406
	1000	0.420	0.485	0.485	0.374	0.452	0.455	0.341	0.437	0.442
0	100	0.101	0.101	0.103	0.091	0.086	0.084	0.080	0.071	0.071
	250	0.254	0.319	0.320	0.215	0.269	0.269	0.170	0.231	0.230
	500	0.367	0.453	0.453	0.334	0.426	0.426	0.291	0.404	0.405
	1000	0.411	0.473	0.473	0.380	0.452	0.452	0.347	0.449	0.449
0.5	100	0.037	0.071	0.061	0.058	0.080	0.043	0.051	0.067	0.034
	250	0.192	0.284	0.283	0.176	0.248	0.215	0.155	0.224	0.187
	500	0.344	0.438	0.440	0.315	0.409	0.402	0.274	0.396	0.381
	1000	0.406	0.469	0.470	0.388	0.458	0.457	0.347	0.451	0.447
0.95	100	0.013	0.048	0.047	0.033	0.067	0.027	0.033	0.068	0.025
	250	0.141	0.246	0.266	0.155	0.230	0.195	0.134	0.217	0.171
	500	0.327	0.425	0.430	0.303	0.399	0.384	0.272	0.388	0.368
	1000	0.390	0.460	0.461	0.373	0.458	0.454	0.339	0.439	0.431

δ	T	c = -20			c = -50			c = -100		
		t_{zx}	Bonf. t	Bonf. Q	t_{zx}	Bonf. t	Bonf. Q	t_{zx}	Bonf. t	Bonf. Q
-0.95	100	0.084	0.060	0.065	0.061	0.052	0.123	0.051	0.043	0.432
	250	0.144	0.175	0.178	0.078	0.129	0.092	0.052	0.092	0.068
	500	0.241	0.369	0.373	0.140	0.309	0.282	0.081	0.251	0.187
	1000	0.305	0.434	0.436	0.202	0.381	0.371	0.137	0.345	0.310
-0.5	100	0.081	0.056	0.062	0.061	0.050	0.073	0.054	0.049	0.321
	250	0.144	0.191	0.196	0.078	0.134	0.113	0.053	0.090	0.069
	500	0.241	0.373	0.377	0.146	0.320	0.305	0.083	0.253	0.217
	1000	0.297	0.425	0.428	0.203	0.385	0.380	0.132	0.342	0.323
0	100	0.072	0.065	0.063	0.061	0.057	0.053	0.060	0.050	0.061
	250	0.128	0.192	0.191	0.070	0.133	0.131	0.051	0.092	0.091
	500	0.237	0.383	0.382	0.138	0.311	0.310	0.084	0.256	0.256
	1000	0.296	0.427	0.426	0.201	0.389	0.388	0.129	0.339	0.338
0.5	100	0.047	0.062	0.033	0.050	0.054	0.053	0.049	0.056	0.100
	250	0.111	0.189	0.152	0.064	0.131	0.119	0.038	0.088	0.142
	500	0.216	0.363	0.348	0.138	0.314	0.301	0.076	0.242	0.257
	1000	0.294	0.427	0.422	0.194	0.385	0.378	0.121	0.338	0.339
0.95	100	0.037	0.064	0.040	0.032	0.053	0.107	0.039	0.059	0.183
	250	0.094	0.182	0.140	0.054	0.131	0.152	0.032	0.093	0.248
	500	0.214	0.362	0.336	0.130	0.305	0.287	0.075	0.243	0.269
	1000	0.291	0.423	0.411	0.194	0.377	0.365	0.131	0.340	0.348

Notes: t_{zx} , *Bonf.t*, and *Bonf.Q* correspond to the test statistics of IVX test, Bonferroni-t test and Bonferroni-Q test. The data generating process is from (4.1) to (4.7).

Table C-7: Finite sample size at 5% significance level of one-sided predictability tests: u_t, v_t is N.i.i.d, bubble in return with $\tau_1 = 0.7, \tau_2 = 1, c_{bub} = 0.1$

δ	T	c = 0			c = -5			c = -10		
		t_{zx}	Bonf. t	Bonf. Q	t_{zx}	Bonf. t	Bonf. Q	t_{zx}	Bonf. t	Bonf. Q
-0.95	100	0.283	0.281	0.296	0.197	0.151	0.208	0.154	0.127	0.164
	250	0.362	0.449	0.449	0.301	0.402	0.411	0.251	0.373	0.386
	500	0.411	0.478	0.476	0.360	0.451	0.453	0.315	0.423	0.428
	1000	0.421	0.478	0.478	0.396	0.472	0.474	0.357	0.456	0.459
-0.5	100	0.259	0.262	0.273	0.191	0.174	0.208	0.143	0.137	0.165
	250	0.345	0.445	0.444	0.283	0.391	0.397	0.243	0.371	0.381
	500	0.394	0.465	0.465	0.351	0.446	0.448	0.309	0.421	0.424
	1000	0.426	0.486	0.486	0.384	0.463	0.463	0.352	0.448	0.450
0	100	0.194	0.242	0.243	0.147	0.184	0.183	0.119	0.155	0.152
	250	0.338	0.444	0.444	0.282	0.399	0.398	0.232	0.376	0.375
	500	0.390	0.474	0.474	0.348	0.444	0.444	0.305	0.431	0.431
	1000	0.417	0.477	0.477	0.382	0.465	0.465	0.348	0.451	0.451
0.5	100	0.121	0.203	0.191	0.116	0.169	0.127	0.097	0.154	0.109
	250	0.315	0.423	0.428	0.268	0.383	0.378	0.232	0.372	0.361
	500	0.387	0.465	0.465	0.337	0.434	0.432	0.309	0.428	0.425
	1000	0.414	0.475	0.476	0.376	0.456	0.455	0.345	0.449	0.448
0.95	100	0.081	0.174	0.172	0.091	0.154	0.105	0.079	0.147	0.092
	250	0.289	0.406	0.409	0.260	0.385	0.371	0.219	0.359	0.340
	500	0.381	0.463	0.466	0.341	0.439	0.435	0.309	0.428	0.422
	1000	0.415	0.472	0.473	0.374	0.456	0.454	0.341	0.446	0.444

δ	T	c = -20			c = -50			c = -100		
		t_{zx}	Bonf. t	Bonf. Q	t_{zx}	Bonf. t	Bonf. Q	t_{zx}	Bonf. t	Bonf. Q
-0.95	100	0.102	0.113	0.127	0.055	0.073	0.126	0.040	0.047	0.425
	250	0.180	0.335	0.341	0.093	0.275	0.254	0.041	0.190	0.154
	500	0.260	0.404	0.408	0.156	0.360	0.353	0.093	0.298	0.273
	1000	0.304	0.438	0.441	0.207	0.396	0.391	0.132	0.352	0.337
-0.5	100	0.094	0.110	0.121	0.058	0.077	0.098	0.038	0.050	0.305
	250	0.180	0.340	0.345	0.084	0.270	0.261	0.039	0.191	0.176
	500	0.252	0.397	0.399	0.147	0.349	0.345	0.085	0.290	0.278
	1000	0.311	0.446	0.448	0.201	0.391	0.388	0.132	0.368	0.361
0	100	0.086	0.123	0.119	0.052	0.079	0.073	0.042	0.057	0.060
	250	0.175	0.342	0.340	0.082	0.272	0.269	0.041	0.191	0.192
	500	0.251	0.403	0.403	0.149	0.350	0.348	0.086	0.285	0.286
	1000	0.302	0.436	0.436	0.212	0.402	0.402	0.135	0.349	0.349
0.5	100	0.066	0.115	0.074	0.041	0.073	0.067	0.035	0.059	0.102
	250	0.169	0.342	0.329	0.082	0.268	0.258	0.035	0.188	0.199
	500	0.244	0.401	0.396	0.152	0.350	0.345	0.091	0.295	0.299
	1000	0.293	0.428	0.425	0.202	0.398	0.396	0.130	0.347	0.350
0.95	100	0.055	0.117	0.074	0.033	0.078	0.109	0.026	0.058	0.164
	250	0.171	0.342	0.320	0.080	0.262	0.244	0.038	0.188	0.217
	500	0.247	0.407	0.398	0.137	0.337	0.333	0.086	0.285	0.290
	1000	0.296	0.438	0.434	0.211	0.395	0.390	0.136	0.355	0.357

Notes: t_{zx} , *Bonf.t*, and *Bonf.Q* correspond to the test statistics of IVX test, Bonferroni-t test and Bonferroni-Q test. The data generating process is from (4.1) to (4.7).

Table C-8: Finite sample size at 5% significance level of one-sided predictability tests: u_t, v_t is i.i.d from t-distribution with the degree of freedom = 5, no bubble in return

δ	T	c = 0			c = -5			c = -10		
		t_{zx}	Bonf. t	Bonf. Q	t_{zx}	Bonf. t	Bonf. Q	t_{zx}	Bonf. t	Bonf. Q
-0.95	100	0.121	0.051	0.063	0.107	0.047	0.064	0.089	0.050	0.059
	250	0.111	0.052	0.047	0.105	0.043	0.045	0.092	0.045	0.044
	500	0.110	0.054	0.046	0.100	0.040	0.043	0.094	0.047	0.043
	1000	0.112	0.052	0.043	0.101	0.044	0.040	0.100	0.049	0.040
-0.5	100	0.129	0.055	0.063	0.101	0.037	0.063	0.082	0.035	0.052
	250	0.114	0.049	0.051	0.090	0.032	0.050	0.086	0.036	0.047
	500	0.106	0.053	0.051	0.091	0.031	0.047	0.081	0.033	0.042
	1000	0.101	0.052	0.048	0.086	0.031	0.042	0.081	0.034	0.043
0	100	0.060	0.047	0.048	0.063	0.050	0.049	0.062	0.048	0.048
	250	0.059	0.051	0.052	0.055	0.045	0.045	0.059	0.053	0.052
	500	0.055	0.050	0.051	0.053	0.050	0.049	0.054	0.048	0.048
	1000	0.051	0.048	0.049	0.053	0.048	0.048	0.051	0.049	0.049
0.5	100	0.008	0.020	0.014	0.026	0.043	0.013	0.035	0.049	0.016
	250	0.007	0.020	0.018	0.023	0.043	0.015	0.030	0.043	0.016
	500	0.008	0.019	0.019	0.023	0.041	0.015	0.027	0.042	0.015
	1000	0.008	0.020	0.019	0.025	0.043	0.018	0.031	0.047	0.015
0.95	100	0.001	0.005	0.006	0.006	0.032	0.010	0.013	0.046	0.017
	250	0.001	0.005	0.008	0.008	0.035	0.013	0.017	0.049	0.020
	500	0.001	0.005	0.012	0.010	0.036	0.017	0.018	0.051	0.019
	1000	0.001	0.005	0.014	0.010	0.037	0.018	0.017	0.044	0.019

δ	T	c = -20			c = -50			c = -100		
		t_{zx}	Bonf. t	Bonf. Q	t_{zx}	Bonf. t	Bonf. Q	t_{zx}	Bonf. t	Bonf. Q
-0.95	100	0.073	0.050	0.063	0.051	0.045	0.140	0.047	0.040	0.517
	250	0.077	0.049	0.040	0.062	0.048	0.037	0.053	0.045	0.059
	500	0.087	0.054	0.038	0.069	0.054	0.026	0.057	0.049	0.014
	1000	0.086	0.051	0.036	0.070	0.052	0.020	0.059	0.051	0.006
-0.5	100	0.072	0.044	0.053	0.062	0.046	0.090	0.056	0.045	0.390
	250	0.071	0.044	0.041	0.064	0.051	0.040	0.061	0.050	0.046
	500	0.073	0.045	0.042	0.060	0.045	0.027	0.060	0.050	0.021
	1000	0.071	0.045	0.041	0.058	0.044	0.027	0.062	0.053	0.019
0	100	0.062	0.049	0.048	0.061	0.049	0.048	0.059	0.051	0.067
	250	0.060	0.050	0.050	0.058	0.050	0.049	0.059	0.054	0.051
	500	0.059	0.050	0.051	0.054	0.049	0.048	0.052	0.051	0.049
	1000	0.052	0.049	0.049	0.049	0.048	0.048	0.049	0.049	0.047
0.5	100	0.043	0.050	0.023	0.046	0.053	0.055	0.052	0.057	0.107
	250	0.040	0.049	0.020	0.045	0.052	0.053	0.047	0.055	0.132
	500	0.036	0.048	0.019	0.038	0.047	0.040	0.043	0.049	0.104
	1000	0.038	0.051	0.020	0.043	0.049	0.033	0.045	0.051	0.079
0.95	100	0.021	0.048	0.045	0.031	0.052	0.131	0.036	0.058	0.163
	250	0.022	0.049	0.042	0.031	0.052	0.132	0.034	0.049	0.268
	500	0.024	0.049	0.033	0.030	0.049	0.099	0.037	0.054	0.247
	1000	0.024	0.050	0.024	0.031	0.050	0.067	0.034	0.048	0.187

Notes: t_{zx} , *Bonf.t*, and *Bonf.Q* correspond to the test statistics of IVX test, Bonferroni-t test and Bonferroni-Q test. The data generating process is from (4.1) to (4.7).

Table C-9: Finite sample size at 5% significance level of one-sided predictability tests: u_t, v_t is i.i.d from t-distribution with the degree of freedom = 5, bubble in return with $\tau_1 = 0.9, \tau_2 = 1, c_{bub} = 0.01$

δ	T	c = 0			c = -5			c = -10		
		t_{zx}	Bonf. t	Bonf. Q	t_{zx}	Bonf. t	Bonf. Q	t_{zx}	Bonf. t	Bonf. Q
-0.95	100	0.127	0.052	0.068	0.103	0.044	0.061	0.087	0.047	0.057
	250	0.118	0.055	0.057	0.109	0.043	0.051	0.098	0.048	0.048
	500	0.121	0.060	0.054	0.111	0.045	0.049	0.096	0.046	0.043
	1000	0.138	0.072	0.074	0.119	0.044	0.052	0.100	0.048	0.044
-0.5	100	0.133	0.060	0.072	0.100	0.036	0.061	0.084	0.033	0.051
	250	0.117	0.058	0.058	0.092	0.033	0.050	0.084	0.035	0.048
	500	0.119	0.064	0.065	0.093	0.037	0.053	0.081	0.041	0.048
	1000	0.125	0.075	0.076	0.096	0.042	0.056	0.089	0.040	0.053
0	100	0.063	0.052	0.053	0.066	0.052	0.050	0.065	0.049	0.047
	250	0.059	0.051	0.053	0.059	0.051	0.052	0.059	0.050	0.049
	500	0.058	0.057	0.057	0.060	0.056	0.056	0.060	0.054	0.054
	1000	0.068	0.071	0.071	0.059	0.057	0.057	0.060	0.059	0.058
0.5	100	0.010	0.026	0.017	0.031	0.046	0.015	0.035	0.047	0.017
	250	0.009	0.023	0.020	0.029	0.050	0.020	0.033	0.049	0.019
	500	0.011	0.027	0.023	0.028	0.044	0.019	0.033	0.050	0.019
	1000	0.014	0.033	0.029	0.035	0.053	0.025	0.039	0.056	0.025
0.95	100	0.001	0.006	0.007	0.008	0.034	0.009	0.017	0.044	0.013
	250	0.001	0.007	0.014	0.013	0.039	0.015	0.019	0.049	0.016
	500	0.001	0.006	0.014	0.012	0.038	0.016	0.021	0.049	0.019
	1000	0.002	0.009	0.022	0.019	0.044	0.021	0.025	0.053	0.023

δ	T	c = -20			c = -50			c = -100		
		t_{zx}	Bonf. t	Bonf. Q	t_{zx}	Bonf. t	Bonf. Q	t_{zx}	Bonf. t	Bonf. Q
-0.95	100	0.070	0.050	0.059	0.055	0.047	0.141	0.043	0.037	0.519
	250	0.079	0.048	0.043	0.061	0.048	0.036	0.053	0.048	0.060
	500	0.085	0.053	0.039	0.060	0.049	0.025	0.054	0.048	0.016
	1000	0.084	0.051	0.036	0.070	0.055	0.022	0.056	0.048	0.006
-0.5	100	0.071	0.043	0.049	0.062	0.048	0.089	0.055	0.044	0.395
	250	0.072	0.044	0.043	0.063	0.045	0.037	0.053	0.045	0.042
	500	0.076	0.046	0.044	0.066	0.050	0.033	0.059	0.050	0.021
	1000	0.077	0.051	0.048	0.063	0.050	0.031	0.057	0.051	0.019
0	100	0.064	0.049	0.049	0.058	0.050	0.046	0.057	0.047	0.059
	250	0.056	0.047	0.046	0.060	0.053	0.051	0.057	0.052	0.050
	500	0.057	0.053	0.053	0.052	0.048	0.046	0.050	0.050	0.048
	1000	0.061	0.058	0.059	0.057	0.053	0.052	0.053	0.052	0.050
0.5	100	0.044	0.051	0.026	0.047	0.049	0.054	0.053	0.056	0.105
	250	0.043	0.052	0.026	0.045	0.055	0.056	0.048	0.051	0.128
	500	0.040	0.052	0.023	0.045	0.053	0.043	0.048	0.054	0.106
	1000	0.041	0.054	0.023	0.046	0.056	0.036	0.044	0.051	0.070
0.95	100	0.021	0.045	0.038	0.032	0.048	0.124	0.041	0.062	0.168
	250	0.025	0.048	0.035	0.028	0.050	0.125	0.033	0.050	0.244
	500	0.027	0.050	0.028	0.034	0.053	0.088	0.036	0.051	0.228
	1000	0.031	0.052	0.024	0.036	0.053	0.063	0.038	0.053	0.174

Notes: t_{zx} , *Bonf.t*, and *Bonf.Q* correspond to the test statistics of IVX test, Bonferroni-t test and Bonferroni-Q test. The data generating process is from (4.1) to (4.7).

Table C-10: Finite sample size at 5% significance level of one-sided predictability tests: u_t, v_t is i.i.d from t-distribution with the degree of freedom = 5, bubble in return with $\tau_1 = 0.9, \tau_2 = 1, c_{bub} = 0.05$

δ	T	c = 0			c = -5			c = -10		
		t_{zx}	Bonf. t	Bonf. Q	t_{zx}	Bonf. t	Bonf. Q	t_{zx}	Bonf. t	Bonf. Q
-0.95	100	0.128	0.059	0.075	0.105	0.042	0.061	0.091	0.049	0.057
	250	0.130	0.077	0.077	0.117	0.047	0.061	0.103	0.052	0.057
	500	0.212	0.184	0.189	0.158	0.082	0.119	0.137	0.079	0.099
	1000	0.336	0.389	0.380	0.281	0.274	0.315	0.234	0.237	0.277
-0.5	100	0.130	0.061	0.069	0.099	0.034	0.059	0.088	0.037	0.056
	250	0.137	0.077	0.083	0.096	0.039	0.061	0.087	0.039	0.055
	500	0.189	0.155	0.162	0.137	0.086	0.114	0.115	0.070	0.094
	1000	0.317	0.365	0.362	0.258	0.276	0.299	0.220	0.246	0.271
0	100	0.068	0.058	0.059	0.066	0.054	0.053	0.063	0.051	0.049
	250	0.067	0.065	0.066	0.067	0.062	0.061	0.061	0.056	0.055
	500	0.120	0.141	0.143	0.102	0.109	0.109	0.092	0.100	0.101
	1000	0.269	0.342	0.343	0.227	0.293	0.293	0.210	0.277	0.278
0.5	100	0.012	0.026	0.017	0.032	0.046	0.018	0.042	0.053	0.021
	250	0.015	0.034	0.030	0.037	0.058	0.027	0.037	0.054	0.023
	500	0.045	0.090	0.088	0.067	0.100	0.067	0.065	0.093	0.055
	1000	0.199	0.293	0.295	0.207	0.281	0.252	0.189	0.272	0.236
0.95	100	0.002	0.010	0.010	0.013	0.040	0.014	0.016	0.049	0.017
	250	0.003	0.014	0.027	0.019	0.048	0.023	0.022	0.056	0.023
	500	0.017	0.053	0.084	0.046	0.087	0.065	0.048	0.089	0.056
	1000	0.137	0.240	0.287	0.179	0.263	0.238	0.162	0.251	0.214

δ	T	c = -20			c = -50			c = -100		
		t_{zx}	Bonf. t	Bonf. Q	t_{zx}	Bonf. t	Bonf. Q	t_{zx}	Bonf. t	Bonf. Q
-0.95	100	0.072	0.048	0.063	0.058	0.051	0.146	0.045	0.038	0.503
	250	0.084	0.055	0.046	0.066	0.055	0.040	0.053	0.051	0.056
	500	0.107	0.084	0.069	0.077	0.072	0.039	0.061	0.064	0.021
	1000	0.199	0.234	0.242	0.137	0.204	0.162	0.088	0.163	0.077
-0.5	100	0.071	0.044	0.053	0.066	0.048	0.091	0.055	0.046	0.386
	250	0.072	0.045	0.044	0.068	0.054	0.043	0.058	0.050	0.041
	500	0.095	0.077	0.075	0.070	0.067	0.048	0.059	0.060	0.028
	1000	0.189	0.243	0.247	0.137	0.213	0.188	0.087	0.166	0.114
0	100	0.064	0.054	0.052	0.058	0.050	0.048	0.061	0.055	0.069
	250	0.065	0.057	0.057	0.060	0.057	0.055	0.053	0.050	0.051
	500	0.080	0.092	0.091	0.069	0.076	0.074	0.054	0.063	0.062
	1000	0.178	0.255	0.255	0.127	0.210	0.209	0.081	0.164	0.164
0.5	100	0.041	0.050	0.026	0.048	0.053	0.055	0.053	0.057	0.101
	250	0.041	0.055	0.025	0.045	0.053	0.054	0.047	0.055	0.126
	500	0.067	0.093	0.053	0.050	0.068	0.055	0.044	0.061	0.107
	1000	0.160	0.253	0.211	0.119	0.212	0.179	0.081	0.170	0.179
0.95	100	0.023	0.050	0.042	0.030	0.051	0.118	0.036	0.054	0.166
	250	0.027	0.056	0.034	0.031	0.051	0.123	0.033	0.053	0.244
	500	0.046	0.079	0.054	0.043	0.070	0.106	0.037	0.062	0.230
	1000	0.151	0.245	0.201	0.105	0.203	0.191	0.072	0.165	0.230

Notes: t_{zx} , *Bonf.t*, and *Bonf.Q* correspond to the test statistics of IVX test, Bonferroni-t test and Bonferroni-Q test. The data generating process is from (4.1) to (4.7).

Table C-11: Finite sample size at 5% significance level of one-sided predictability tests: u_t, v_t is i.i.d from t-distribution with the degree of freedom = 5, bubble in return with $\tau_1 = 0.9, \tau_2 = 1, c_{bub} = 0.1$

δ	T	c = 0			c = -5			c = -10		
		t_{zx}	Bonf. t	Bonf. Q	t_{zx}	Bonf. t	Bonf. Q	t_{zx}	Bonf. t	Bonf. Q
-0.95	100	0.132	0.067	0.084	0.103	0.041	0.064	0.093	0.051	0.065
	250	0.186	0.165	0.174	0.153	0.079	0.117	0.117	0.071	0.089
	500	0.304	0.376	0.372	0.250	0.273	0.313	0.210	0.238	0.275
	1000	0.367	0.459	0.457	0.320	0.420	0.433	0.279	0.387	0.400
-0.5	100	0.137	0.069	0.082	0.104	0.041	0.070	0.092	0.043	0.065
	250	0.181	0.153	0.160	0.126	0.077	0.104	0.108	0.070	0.091
	500	0.280	0.350	0.347	0.233	0.279	0.301	0.190	0.248	0.272
	1000	0.352	0.456	0.454	0.307	0.417	0.423	0.275	0.397	0.407
0	100	0.073	0.064	0.065	0.072	0.061	0.061	0.063	0.054	0.053
	250	0.115	0.138	0.138	0.098	0.107	0.108	0.084	0.094	0.092
	500	0.240	0.338	0.339	0.210	0.293	0.293	0.173	0.267	0.267
	1000	0.332	0.448	0.448	0.298	0.419	0.419	0.266	0.404	0.404
0.5	100	0.015	0.032	0.021	0.032	0.051	0.020	0.039	0.055	0.022
	250	0.039	0.083	0.075	0.062	0.097	0.060	0.061	0.092	0.056
	500	0.178	0.291	0.295	0.174	0.278	0.246	0.152	0.255	0.221
	1000	0.324	0.436	0.437	0.293	0.412	0.406	0.263	0.398	0.385
0.95	100	0.003	0.013	0.017	0.013	0.044	0.014	0.018	0.052	0.018
	250	0.017	0.057	0.080	0.037	0.081	0.054	0.042	0.086	0.051
	500	0.139	0.258	0.288	0.162	0.257	0.232	0.145	0.251	0.210
	1000	0.294	0.425	0.430	0.282	0.408	0.396	0.259	0.405	0.384

δ	T	c = -20			c = -50			c = -100		
		t_{zx}	Bonf. t	Bonf. Q	t_{zx}	Bonf. t	Bonf. Q	t_{zx}	Bonf. t	Bonf. Q
-0.95	100	0.070	0.047	0.061	0.054	0.048	0.141	0.047	0.039	0.503
	250	0.093	0.073	0.067	0.064	0.064	0.048	0.051	0.057	0.060
	500	0.167	0.225	0.231	0.112	0.204	0.163	0.067	0.156	0.087
	1000	0.243	0.382	0.387	0.175	0.349	0.330	0.110	0.314	0.263
-0.5	100	0.076	0.048	0.056	0.067	0.053	0.094	0.059	0.047	0.389
	250	0.088	0.073	0.072	0.066	0.065	0.051	0.055	0.058	0.048
	500	0.154	0.230	0.237	0.104	0.202	0.177	0.062	0.148	0.106
	1000	0.234	0.383	0.387	0.180	0.362	0.353	0.116	0.315	0.287
0	100	0.062	0.052	0.051	0.062	0.054	0.053	0.060	0.056	0.065
	250	0.072	0.082	0.080	0.058	0.068	0.065	0.054	0.059	0.058
	500	0.143	0.249	0.249	0.096	0.205	0.204	0.060	0.156	0.155
	1000	0.233	0.395	0.395	0.175	0.363	0.362	0.104	0.309	0.309
0.5	100	0.040	0.050	0.025	0.048	0.056	0.060	0.050	0.054	0.100
	250	0.056	0.083	0.049	0.048	0.067	0.069	0.044	0.062	0.135
	500	0.130	0.236	0.201	0.090	0.192	0.173	0.051	0.148	0.175
	1000	0.234	0.393	0.378	0.173	0.363	0.350	0.107	0.309	0.311
0.95	100	0.025	0.052	0.040	0.030	0.052	0.127	0.033	0.053	0.165
	250	0.043	0.082	0.056	0.037	0.069	0.125	0.032	0.059	0.242
	500	0.117	0.225	0.182	0.082	0.194	0.187	0.048	0.154	0.239
	1000	0.225	0.394	0.369	0.169	0.361	0.338	0.106	0.313	0.326

Notes: t_{zx} , *Bonf.t*, and *Bonf.Q* correspond to the test statistics of IVX test, Bonferroni-t test and Bonferroni-Q test. The data generating process is from (4.1) to (4.7).

Table C-12: Finite sample size at 5% significance level of one-sided predictability tests: u_t, v_t is i.i.d from t-distribution with the degree of freedom = 5, bubble in return with $\tau_1 = 0.7, \tau_2 = 1, c_{bub} = 0.01$

δ	T	c = 0			c = -5			c = -10		
		t_{zx}	Bonf. t	Bonf. Q	t_{zx}	Bonf. t	Bonf. Q	t_{zx}	Bonf. t	Bonf. Q
-0.95	100	0.131	0.061	0.071	0.108	0.042	0.064	0.095	0.048	0.063
	250	0.132	0.064	0.065	0.118	0.042	0.056	0.097	0.049	0.049
	500	0.180	0.109	0.116	0.136	0.047	0.070	0.103	0.047	0.056
	1000	0.308	0.289	0.290	0.229	0.134	0.186	0.180	0.111	0.143
-0.5	100	0.131	0.059	0.067	0.095	0.036	0.059	0.080	0.036	0.054
	250	0.124	0.066	0.069	0.099	0.038	0.057	0.090	0.041	0.055
	500	0.156	0.101	0.108	0.112	0.053	0.075	0.095	0.045	0.061
	1000	0.257	0.238	0.235	0.195	0.142	0.172	0.153	0.109	0.138
0	100	0.067	0.058	0.060	0.066	0.051	0.052	0.066	0.050	0.049
	250	0.066	0.067	0.068	0.066	0.059	0.059	0.059	0.049	0.050
	500	0.087	0.095	0.096	0.077	0.074	0.073	0.070	0.066	0.066
	1000	0.182	0.210	0.211	0.158	0.166	0.166	0.131	0.138	0.139
0.5	100	0.010	0.022	0.015	0.032	0.044	0.016	0.040	0.052	0.019
	250	0.013	0.032	0.027	0.032	0.048	0.020	0.042	0.056	0.024
	500	0.023	0.052	0.050	0.047	0.068	0.036	0.048	0.064	0.030
	1000	0.098	0.155	0.153	0.119	0.149	0.112	0.107	0.136	0.094
0.95	100	0.001	0.008	0.007	0.012	0.037	0.010	0.019	0.045	0.015
	250	0.002	0.010	0.018	0.018	0.044	0.016	0.022	0.049	0.015
	500	0.006	0.023	0.039	0.025	0.051	0.025	0.030	0.056	0.023
	1000	0.049	0.105	0.151	0.089	0.126	0.099	0.088	0.126	0.081

δ	T	c = -20			c = -50			c = -100		
		t_{zx}	Bonf. t	Bonf. Q	t_{zx}	Bonf. t	Bonf. Q	t_{zx}	Bonf. t	Bonf. Q
-0.95	100	0.079	0.052	0.064	0.058	0.047	0.135	0.049	0.040	0.504
	250	0.082	0.050	0.042	0.060	0.048	0.036	0.054	0.048	0.057
	500	0.089	0.056	0.046	0.067	0.052	0.025	0.057	0.053	0.015
	1000	0.133	0.104	0.098	0.088	0.080	0.041	0.065	0.066	0.013
-0.5	100	0.074	0.047	0.054	0.065	0.047	0.090	0.059	0.047	0.384
	250	0.071	0.046	0.044	0.063	0.048	0.036	0.062	0.054	0.046
	500	0.071	0.047	0.046	0.064	0.054	0.036	0.058	0.053	0.022
	1000	0.120	0.098	0.101	0.083	0.080	0.059	0.064	0.065	0.028
0	100	0.062	0.048	0.047	0.060	0.050	0.048	0.061	0.051	0.066
	250	0.060	0.053	0.051	0.054	0.046	0.045	0.057	0.051	0.049
	500	0.065	0.060	0.061	0.058	0.057	0.055	0.054	0.052	0.051
	1000	0.103	0.111	0.110	0.074	0.083	0.081	0.063	0.067	0.065
0.5	100	0.040	0.048	0.024	0.045	0.051	0.055	0.055	0.058	0.099
	250	0.041	0.054	0.024	0.045	0.051	0.051	0.048	0.052	0.120
	500	0.045	0.057	0.029	0.045	0.053	0.044	0.046	0.054	0.096
	1000	0.084	0.108	0.068	0.059	0.076	0.057	0.053	0.066	0.083
0.95	100	0.026	0.052	0.033	0.034	0.049	0.109	0.039	0.057	0.165
	250	0.028	0.048	0.028	0.034	0.051	0.098	0.037	0.055	0.234
	500	0.034	0.056	0.028	0.039	0.055	0.080	0.037	0.052	0.209
	1000	0.069	0.102	0.059	0.049	0.075	0.073	0.047	0.065	0.162

Notes: t_{zx} , Bonf.t, and Bonf.Q correspond to the test statistics of IVX test, Bonferroni-t test and Bonferroni-Q test. .

Table C-13: Finite sample size at 5% significance level of one-sided predictability tests: u_t, v_t is i.i.d from t-distribution with the degree of freedom = 5, bubble in return with $\tau_1 = 0.7, \tau_2 = 1, c_{bub} = 0.05$

δ	T	c = 0			c = -5			c = -10		
		t_{zx}	Bonf. t	Bonf. Q	t_{zx}	Bonf. t	Bonf. Q	t_{zx}	Bonf. t	Bonf. Q
-0.95	100	0.177	0.106	0.128	0.130	0.049	0.088	0.105	0.057	0.072
	250	0.330	0.352	0.353	0.253	0.215	0.267	0.193	0.168	0.216
	500	0.407	0.467	0.464	0.348	0.414	0.424	0.305	0.383	0.402
	1000	0.439	0.484	0.484	0.389	0.455	0.461	0.364	0.441	0.449
-0.5	100	0.162	0.100	0.115	0.111	0.051	0.079	0.091	0.047	0.071
	250	0.298	0.316	0.317	0.235	0.228	0.258	0.185	0.189	0.217
	500	0.382	0.453	0.452	0.340	0.413	0.421	0.297	0.390	0.400
	1000	0.415	0.473	0.473	0.387	0.455	0.458	0.342	0.434	0.438
0	100	0.094	0.090	0.091	0.081	0.074	0.073	0.072	0.060	0.059
	250	0.238	0.295	0.296	0.185	0.226	0.227	0.158	0.210	0.209
	500	0.367	0.441	0.442	0.323	0.411	0.411	0.282	0.390	0.391
	1000	0.405	0.473	0.473	0.382	0.460	0.460	0.343	0.442	0.442
0.5	100	0.029	0.059	0.044	0.048	0.066	0.032	0.046	0.063	0.029
	250	0.159	0.246	0.244	0.164	0.225	0.190	0.134	0.201	0.158
	500	0.336	0.426	0.428	0.308	0.399	0.388	0.271	0.388	0.372
	1000	0.396	0.462	0.464	0.376	0.456	0.453	0.348	0.445	0.441
0.95	100	0.007	0.029	0.030	0.023	0.059	0.025	0.027	0.062	0.022
	250	0.114	0.216	0.243	0.137	0.210	0.174	0.119	0.197	0.148
	500	0.309	0.405	0.414	0.299	0.393	0.378	0.263	0.381	0.356
	1000	0.397	0.461	0.463	0.367	0.445	0.439	0.334	0.431	0.421

δ	T	c = -20			c = -50			c = -100		
		t_{zx}	Bonf. t	Bonf. Q	t_{zx}	Bonf. t	Bonf. Q	t_{zx}	Bonf. t	Bonf. Q
-0.95	100	0.075	0.053	0.065	0.057	0.049	0.137	0.050	0.043	0.511
	250	0.139	0.153	0.155	0.081	0.122	0.090	0.050	0.079	0.072
	500	0.233	0.337	0.342	0.145	0.304	0.270	0.086	0.242	0.168
	1000	0.304	0.427	0.427	0.210	0.385	0.371	0.126	0.334	0.295
-0.5	100	0.076	0.053	0.060	0.061	0.051	0.088	0.056	0.047	0.373
	250	0.131	0.162	0.168	0.079	0.121	0.102	0.051	0.081	0.061
	500	0.240	0.361	0.364	0.146	0.301	0.283	0.084	0.242	0.201
	1000	0.302	0.433	0.436	0.204	0.385	0.378	0.134	0.336	0.312
0	100	0.065	0.057	0.056	0.065	0.056	0.052	0.055	0.048	0.060
	250	0.116	0.169	0.168	0.073	0.124	0.121	0.052	0.088	0.085
	500	0.226	0.355	0.355	0.135	0.299	0.299	0.080	0.235	0.236
	1000	0.300	0.437	0.437	0.205	0.383	0.383	0.125	0.329	0.328
0.5	100	0.047	0.059	0.030	0.043	0.052	0.051	0.053	0.061	0.100
	250	0.105	0.172	0.130	0.063	0.120	0.105	0.044	0.086	0.138
	500	0.219	0.357	0.338	0.127	0.286	0.273	0.077	0.226	0.237
	1000	0.293	0.420	0.411	0.194	0.372	0.363	0.128	0.329	0.331
0.95	100	0.027	0.053	0.038	0.031	0.054	0.118	0.036	0.055	0.158
	250	0.086	0.157	0.121	0.046	0.109	0.128	0.034	0.083	0.221
	500	0.216	0.354	0.322	0.126	0.289	0.267	0.076	0.234	0.269
	1000	0.290	0.422	0.408	0.193	0.376	0.361	0.124	0.333	0.335

Notes: t_{zx} , Bonf.t, and Bonf.Q correspond to the test statistics of IVX test, Bonferroni-t test and Bonferroni-Q test. The data generating process is from (4.1) to (4.7).

Table C-14: Finite sample size at 5% significance level of one-sided predictability tests: u_t, v_t is i.i.d from t-distribution with the degree of freedom = 5, bubble in return with $\tau_1 = 0.7, \tau_2 = 1, c_{bub} = 0.1$

δ	T	c = 0			c = -5			c = -10		
		t_{zx}	Bonf. t	Bonf. Q	t_{zx}	Bonf. t	Bonf. Q	t_{zx}	Bonf. t	Bonf. Q
-0.95	100	0.276	0.261	0.279	0.196	0.136	0.199	0.146	0.114	0.157
	250	0.361	0.445	0.444	0.299	0.391	0.402	0.246	0.364	0.380
	500	0.399	0.471	0.470	0.365	0.444	0.448	0.316	0.426	0.433
	1000	0.429	0.488	0.488	0.387	0.462	0.464	0.351	0.451	0.454
-0.5	100	0.245	0.235	0.245	0.176	0.148	0.186	0.138	0.119	0.149
	250	0.345	0.449	0.446	0.299	0.403	0.411	0.234	0.356	0.367
	500	0.399	0.476	0.475	0.352	0.444	0.447	0.313	0.431	0.435
	1000	0.426	0.487	0.486	0.386	0.465	0.466	0.346	0.449	0.451
0	100	0.169	0.212	0.213	0.146	0.172	0.172	0.109	0.133	0.129
	250	0.331	0.438	0.438	0.287	0.402	0.403	0.233	0.371	0.369
	500	0.387	0.464	0.464	0.353	0.441	0.441	0.312	0.421	0.421
	1000	0.423	0.479	0.479	0.387	0.470	0.469	0.350	0.451	0.451
0.5	100	0.098	0.166	0.152	0.108	0.156	0.112	0.085	0.134	0.086
	250	0.314	0.426	0.429	0.270	0.391	0.380	0.226	0.374	0.359
	500	0.387	0.469	0.470	0.346	0.445	0.442	0.304	0.431	0.426
	1000	0.417	0.473	0.474	0.380	0.462	0.460	0.346	0.446	0.443
0.95	100	0.056	0.140	0.145	0.078	0.139	0.091	0.065	0.127	0.076
	250	0.286	0.403	0.408	0.263	0.382	0.365	0.217	0.360	0.335
	500	0.376	0.457	0.460	0.342	0.434	0.430	0.296	0.422	0.413
	1000	0.402	0.459	0.461	0.385	0.466	0.464	0.355	0.451	0.448

δ	T	c = -20			c = -50			c = -100		
		t_{zx}	Bonf. t	Bonf. Q	t_{zx}	Bonf. t	Bonf. Q	t_{zx}	Bonf. t	Bonf. Q
-0.95	100	0.097	0.097	0.111	0.053	0.069	0.145	0.038	0.043	0.502
	250	0.180	0.330	0.336	0.090	0.267	0.248	0.046	0.184	0.154
	500	0.256	0.401	0.405	0.157	0.350	0.341	0.088	0.286	0.255
	1000	0.298	0.435	0.437	0.207	0.396	0.392	0.129	0.345	0.331
-0.5	100	0.087	0.089	0.101	0.061	0.072	0.105	0.045	0.050	0.371
	250	0.169	0.319	0.325	0.085	0.262	0.254	0.042	0.183	0.165
	500	0.250	0.396	0.399	0.151	0.348	0.343	0.085	0.285	0.271
	1000	0.303	0.438	0.440	0.202	0.393	0.390	0.133	0.346	0.338
0	100	0.081	0.107	0.102	0.053	0.070	0.065	0.042	0.052	0.058
	250	0.168	0.337	0.336	0.082	0.264	0.261	0.040	0.177	0.177
	500	0.251	0.398	0.398	0.147	0.348	0.347	0.083	0.291	0.290
	1000	0.302	0.438	0.439	0.194	0.396	0.396	0.129	0.349	0.349
0.5	100	0.064	0.108	0.064	0.043	0.069	0.060	0.035	0.055	0.091
	250	0.165	0.332	0.313	0.084	0.264	0.249	0.038	0.179	0.181
	500	0.248	0.398	0.392	0.145	0.351	0.345	0.081	0.289	0.292
	1000	0.304	0.438	0.435	0.200	0.396	0.392	0.128	0.348	0.348
0.95	100	0.050	0.103	0.064	0.027	0.065	0.106	0.025	0.053	0.152
	250	0.152	0.322	0.289	0.077	0.256	0.237	0.035	0.180	0.194
	500	0.240	0.391	0.380	0.150	0.349	0.337	0.089	0.287	0.291
	1000	0.296	0.431	0.425	0.197	0.384	0.376	0.129	0.349	0.350

Notes: t_{zx} , *Bonf.t*, and *Bonf.Q* correspond to the test statistics of IVX test, Bonferroni-t test and Bonferroni-Q test. The data generating process is from (4.1) to (4.7).

Table C-15: Finite sample size at 5% significance level of one-sided predictability tests: u_t, v_t is N.i.i.d, collapsing bubble in return with $\tau_1 = 0.6, \tau_2 = 0.9, c_{bub} = 0.01$

δ	T	c = 0			c = -5			c = -10		
		t_{zx}	Bonf. t	Bonf. Q	t_{zx}	Bonf. t	Bonf. Q	t_{zx}	Bonf. t	Bonf. Q
-0.95	100	0.120	0.048	0.059	0.103	0.035	0.055	0.089	0.039	0.055
	250	0.100	0.038	0.039	0.094	0.029	0.042	0.091	0.040	0.044
	500	0.097	0.043	0.038	0.093	0.031	0.042	0.078	0.033	0.036
	1000	0.089	0.038	0.034	0.088	0.033	0.047	0.077	0.036	0.041
-0.5	100	0.107	0.043	0.053	0.091	0.034	0.055	0.079	0.035	0.050
	250	0.089	0.039	0.043	0.080	0.031	0.045	0.074	0.033	0.045
	500	0.087	0.037	0.041	0.073	0.033	0.045	0.068	0.035	0.045
	1000	0.069	0.035	0.036	0.065	0.034	0.044	0.063	0.033	0.044
0	100	0.051	0.035	0.035	0.056	0.043	0.043	0.063	0.048	0.047
	250	0.046	0.034	0.036	0.051	0.042	0.043	0.058	0.047	0.047
	500	0.043	0.033	0.034	0.050	0.045	0.045	0.054	0.045	0.045
	1000	0.036	0.026	0.027	0.046	0.040	0.040	0.051	0.047	0.047
0.5	100	0.010	0.016	0.010	0.030	0.038	0.016	0.041	0.048	0.019
	250	0.009	0.014	0.012	0.027	0.036	0.015	0.038	0.045	0.020
	500	0.009	0.013	0.011	0.028	0.035	0.018	0.038	0.046	0.022
	1000	0.009	0.010	0.010	0.028	0.031	0.022	0.038	0.041	0.026
0.95	100	0.002	0.006	0.002	0.012	0.032	0.007	0.022	0.046	0.010
	250	0.002	0.005	0.003	0.012	0.029	0.007	0.024	0.043	0.010
	500	0.002	0.005	0.002	0.011	0.027	0.008	0.020	0.036	0.009
	1000	0.002	0.003	0.002	0.014	0.025	0.008	0.026	0.038	0.012

δ	T	c = -20			c = -50			c = -100		
		t_{zx}	Bonf. t	Bonf. Q	t_{zx}	Bonf. t	Bonf. Q	t_{zx}	Bonf. t	Bonf. Q
-0.95	100	0.075	0.045	0.054	0.056	0.047	0.105	0.055	0.047	0.422
	250	0.071	0.045	0.036	0.062	0.047	0.032	0.052	0.048	0.041
	500	0.073	0.043	0.034	0.060	0.046	0.021	0.054	0.048	0.014
	1000	0.069	0.046	0.044	0.065	0.053	0.032	0.059	0.052	0.015
-0.5	100	0.072	0.042	0.048	0.064	0.046	0.069	0.058	0.049	0.306
	250	0.071	0.043	0.042	0.059	0.046	0.032	0.057	0.048	0.035
	500	0.066	0.046	0.044	0.062	0.051	0.035	0.057	0.049	0.024
	1000	0.062	0.043	0.044	0.057	0.050	0.040	0.058	0.053	0.030
0	100	0.057	0.044	0.043	0.063	0.052	0.052	0.057	0.048	0.060
	250	0.056	0.052	0.051	0.056	0.050	0.049	0.060	0.055	0.053
	500	0.055	0.049	0.048	0.055	0.050	0.049	0.052	0.050	0.050
	1000	0.053	0.047	0.047	0.051	0.049	0.047	0.054	0.052	0.051
0.5	100	0.044	0.046	0.027	0.054	0.056	0.053	0.052	0.057	0.092
	250	0.041	0.047	0.025	0.047	0.051	0.048	0.045	0.049	0.115
	500	0.042	0.046	0.027	0.045	0.047	0.039	0.046	0.048	0.087
	1000	0.043	0.045	0.027	0.049	0.050	0.035	0.046	0.049	0.061
0.95	100	0.030	0.047	0.024	0.037	0.052	0.099	0.047	0.060	0.157
	250	0.026	0.044	0.017	0.037	0.049	0.088	0.038	0.052	0.237
	500	0.027	0.042	0.015	0.032	0.041	0.050	0.040	0.049	0.160
	1000	0.032	0.041	0.014	0.042	0.049	0.031	0.044	0.048	0.088

Notes: t_{zx} , *Bonf.t*, and *Bonf.Q* correspond to the test statistics of IVX test, Bonferroni-t test and Bonferroni-Q test. The data generating process is from (4.1) to (4.7).

Table C-16: Finite sample size at 5% significance level of one-sided predictability tests: u_t, v_t is N.i.i.d, collapsing bubble in return with $\tau_1 = 0.6, \tau_2 = 0.9, c_{bub} = 0.05$

δ	T	c = 0			c = -5			c = -10		
		t_{zx}	Bonf. t	Bonf. Q	t_{zx}	Bonf. t	Bonf. Q	t_{zx}	Bonf. t	Bonf. Q
-0.95	100	0.102	0.037	0.044	0.096	0.031	0.052	0.087	0.036	0.050
	250	0.064	0.021	0.024	0.063	0.023	0.033	0.061	0.027	0.036
	500	0.227	0.259	0.263	0.204	0.213	0.227	0.170	0.181	0.197
	1000	0.401	0.456	0.456	0.352	0.411	0.418	0.318	0.381	0.388
-0.5	100	0.091	0.038	0.046	0.082	0.030	0.046	0.076	0.036	0.052
	250	0.050	0.020	0.020	0.052	0.025	0.033	0.053	0.030	0.037
	500	0.220	0.256	0.259	0.195	0.215	0.223	0.164	0.188	0.197
	1000	0.380	0.438	0.438	0.359	0.418	0.420	0.325	0.394	0.398
0	100	0.049	0.034	0.034	0.062	0.042	0.042	0.059	0.042	0.042
	250	0.030	0.016	0.016	0.040	0.027	0.027	0.047	0.035	0.034
	500	0.196	0.240	0.241	0.180	0.215	0.215	0.159	0.193	0.194
	1000	0.371	0.441	0.441	0.342	0.408	0.408	0.317	0.395	0.395
0.5	100	0.013	0.015	0.010	0.031	0.033	0.015	0.046	0.046	0.024
	250	0.010	0.007	0.006	0.027	0.023	0.017	0.037	0.033	0.023
	500	0.168	0.224	0.228	0.171	0.206	0.198	0.158	0.197	0.187
	1000	0.370	0.437	0.439	0.334	0.403	0.402	0.307	0.378	0.375
0.95	100	0.004	0.007	0.002	0.015	0.028	0.007	0.027	0.041	0.010
	250	0.004	0.003	0.002	0.018	0.017	0.008	0.030	0.031	0.015
	500	0.153	0.208	0.213	0.162	0.195	0.181	0.151	0.186	0.169
	1000	0.352	0.433	0.437	0.325	0.404	0.399	0.296	0.373	0.367

δ	T	c = -20			c = -50			c = -100		
		t_{zx}	Bonf. t	Bonf. Q	t_{zx}	Bonf. t	Bonf. Q	t_{zx}	Bonf. t	Bonf. Q
-0.95	100	0.072	0.045	0.051	0.056	0.044	0.095	0.055	0.046	0.389
	250	0.064	0.037	0.037	0.064	0.050	0.037	0.055	0.047	0.038
	500	0.139	0.157	0.166	0.089	0.119	0.106	0.062	0.089	0.065
	1000	0.273	0.357	0.362	0.183	0.298	0.289	0.116	0.244	0.216
-0.5	100	0.071	0.041	0.047	0.067	0.050	0.072	0.056	0.046	0.259
	250	0.055	0.035	0.038	0.060	0.048	0.040	0.058	0.049	0.038
	500	0.128	0.153	0.160	0.083	0.114	0.107	0.064	0.091	0.077
	1000	0.274	0.366	0.370	0.177	0.299	0.294	0.111	0.237	0.222
0	100	0.064	0.049	0.048	0.060	0.052	0.049	0.059	0.052	0.064
	250	0.048	0.039	0.038	0.054	0.045	0.043	0.052	0.046	0.045
	500	0.128	0.163	0.162	0.086	0.115	0.114	0.060	0.087	0.085
	1000	0.261	0.355	0.354	0.174	0.292	0.291	0.108	0.236	0.237
0.5	100	0.050	0.048	0.027	0.055	0.050	0.050	0.055	0.055	0.086
	250	0.046	0.041	0.030	0.050	0.045	0.043	0.051	0.049	0.072
	500	0.128	0.163	0.155	0.082	0.118	0.111	0.056	0.081	0.090
	1000	0.265	0.361	0.356	0.176	0.290	0.286	0.110	0.229	0.232
0.95	100	0.030	0.042	0.018	0.042	0.052	0.076	0.041	0.052	0.151
	250	0.042	0.040	0.023	0.047	0.043	0.047	0.048	0.047	0.111
	500	0.125	0.164	0.146	0.084	0.121	0.110	0.054	0.080	0.094
	1000	0.253	0.350	0.340	0.181	0.303	0.294	0.105	0.229	0.232

Notes: t_{zx} , *Bonf.t*, and *Bonf.Q* correspond to the test statistics of IVX test, Bonferroni-t test and Bonferroni-Q test. The data generating process is from (4.1) to (4.7).

Table C-17: Finite sample size at 5% significance level of one-sided predictability tests: u_t, v_t is N.i.i.d, collapsing bubble in return with $\tau_1 = 0.6, \tau_2 = 0.9, c_{bub} = 0.1$

δ	T	c = 0			c = -5			c = -10		
		t_{zx}	Bonf. t	Bonf. Q	t_{zx}	Bonf. t	Bonf. Q	t_{zx}	Bonf. t	Bonf. Q
-0.95	100	0.076	0.024	0.029	0.076	0.026	0.040	0.077	0.031	0.042
	250	0.181	0.221	0.221	0.150	0.173	0.184	0.129	0.152	0.163
	500	0.357	0.432	0.431	0.321	0.401	0.406	0.280	0.373	0.380
	1000	0.403	0.473	0.473	0.367	0.442	0.443	0.337	0.431	0.433
-0.5	100	0.066	0.023	0.027	0.066	0.025	0.037	0.065	0.028	0.037
	250	0.160	0.202	0.203	0.156	0.183	0.188	0.130	0.155	0.162
	500	0.346	0.426	0.426	0.326	0.407	0.409	0.278	0.375	0.379
	1000	0.392	0.457	0.457	0.368	0.449	0.450	0.345	0.439	0.441
0	100	0.035	0.018	0.018	0.048	0.028	0.028	0.052	0.033	0.033
	250	0.149	0.202	0.203	0.132	0.169	0.168	0.122	0.158	0.157
	500	0.334	0.424	0.425	0.317	0.399	0.399	0.277	0.377	0.376
	1000	0.393	0.463	0.463	0.361	0.446	0.446	0.335	0.433	0.433
0.5	100	0.013	0.009	0.007	0.032	0.026	0.016	0.040	0.033	0.018
	250	0.129	0.183	0.186	0.132	0.171	0.164	0.119	0.158	0.149
	500	0.329	0.411	0.412	0.302	0.389	0.388	0.274	0.373	0.370
	1000	0.398	0.470	0.470	0.362	0.447	0.445	0.333	0.431	0.429
0.95	100	0.004	0.003	0.001	0.016	0.019	0.006	0.030	0.031	0.011
	250	0.116	0.168	0.171	0.126	0.164	0.153	0.113	0.154	0.140
	500	0.330	0.415	0.416	0.297	0.382	0.379	0.269	0.370	0.364
	1000	0.391	0.465	0.465	0.362	0.443	0.441	0.331	0.432	0.428

δ	T	c = -20			c = -50			c = -100		
		t_{zx}	Bonf. t	Bonf. Q	t_{zx}	Bonf. t	Bonf. Q	t_{zx}	Bonf. t	Bonf. Q
-0.95	100	0.071	0.040	0.046	0.064	0.046	0.076	0.060	0.046	0.297
	250	0.108	0.133	0.139	0.068	0.098	0.091	0.043	0.071	0.060
	500	0.235	0.345	0.349	0.136	0.275	0.268	0.078	0.208	0.189
	1000	0.291	0.410	0.413	0.199	0.368	0.362	0.124	0.320	0.303
-0.5	100	0.067	0.039	0.044	0.063	0.048	0.057	0.057	0.046	0.186
	250	0.103	0.132	0.136	0.066	0.096	0.091	0.045	0.074	0.066
	500	0.227	0.343	0.345	0.134	0.274	0.270	0.074	0.207	0.199
	1000	0.296	0.416	0.417	0.201	0.369	0.366	0.126	0.322	0.315
0	100	0.059	0.039	0.037	0.063	0.048	0.047	0.062	0.050	0.063
	250	0.100	0.134	0.132	0.065	0.098	0.096	0.043	0.068	0.067
	500	0.222	0.337	0.337	0.132	0.271	0.270	0.075	0.205	0.204
	1000	0.289	0.417	0.417	0.196	0.370	0.369	0.123	0.321	0.321
0.5	100	0.047	0.037	0.025	0.059	0.050	0.048	0.069	0.061	0.069
	250	0.097	0.132	0.125	0.063	0.096	0.091	0.043	0.069	0.074
	500	0.214	0.336	0.332	0.134	0.269	0.267	0.071	0.205	0.210
	1000	0.286	0.416	0.413	0.192	0.369	0.366	0.115	0.306	0.309
0.95	100	0.038	0.036	0.022	0.051	0.048	0.057	0.057	0.058	0.110
	250	0.093	0.131	0.116	0.062	0.093	0.091	0.039	0.067	0.080
	500	0.222	0.337	0.329	0.125	0.268	0.262	0.072	0.200	0.208
	1000	0.283	0.408	0.404	0.189	0.358	0.353	0.122	0.321	0.322

Notes: t_{zx} , *Bonf.t*, and *Bonf.Q* correspond to the test statistics of IVX test, Bonferroni-t test and Bonferroni-Q test. The data generating process is from (4.1) to (4.7).

Table C-18: Finite sample size at 5% significance level of one-sided predictability tests: u_t, v_t is N.i.i.d, collapsing bubble in return with $\tau_1 = 0.6, \tau_2 = 0.9, c_{bub} = 0.2$

δ	T	c = 0			c = -5			c = -10		
		t_{zx}	Bonf. t	Bonf. Q	t_{zx}	Bonf. t	Bonf. Q	t_{zx}	Bonf. t	Bonf. Q
-0.95	100	0.058	0.031	0.034	0.064	0.039	0.047	0.065	0.044	0.051
	250	0.316	0.427	0.427	0.268	0.382	0.384	0.233	0.347	0.352
	500	0.376	0.456	0.457	0.336	0.430	0.432	0.303	0.418	0.421
	1000	0.400	0.464	0.465	0.362	0.450	0.451	0.349	0.452	0.453
-0.5	100	0.050	0.029	0.031	0.062	0.041	0.047	0.065	0.044	0.050
	250	0.293	0.412	0.412	0.263	0.372	0.373	0.223	0.345	0.347
	500	0.367	0.454	0.454	0.331	0.428	0.429	0.302	0.414	0.415
	1000	0.402	0.472	0.472	0.377	0.459	0.459	0.347	0.452	0.454
0	100	0.038	0.025	0.025	0.054	0.041	0.040	0.062	0.050	0.050
	250	0.295	0.412	0.412	0.261	0.371	0.370	0.220	0.344	0.343
	500	0.366	0.455	0.455	0.328	0.429	0.429	0.292	0.411	0.411
	1000	0.397	0.474	0.474	0.369	0.454	0.454	0.344	0.446	0.446
0.5	100	0.029	0.021	0.022	0.050	0.042	0.038	0.058	0.049	0.043
	250	0.290	0.410	0.411	0.253	0.361	0.360	0.221	0.344	0.341
	500	0.369	0.462	0.462	0.337	0.426	0.425	0.298	0.415	0.414
	1000	0.389	0.467	0.467	0.370	0.461	0.460	0.347	0.449	0.449
0.95	100	0.023	0.018	0.017	0.044	0.037	0.029	0.049	0.043	0.033
	250	0.291	0.413	0.414	0.255	0.367	0.364	0.221	0.345	0.339
	500	0.351	0.443	0.443	0.331	0.430	0.428	0.302	0.416	0.413
	1000	0.400	0.474	0.475	0.371	0.460	0.458	0.341	0.447	0.446

δ	T	c = -20			c = -50			c = -100		
		t_{zx}	Bonf. t	Bonf. Q	t_{zx}	Bonf. t	Bonf. Q	t_{zx}	Bonf. t	Bonf. Q
-0.95	100	0.063	0.046	0.050	0.062	0.054	0.060	0.056	0.052	0.135
	250	0.172	0.311	0.314	0.085	0.228	0.225	0.034	0.149	0.143
	500	0.243	0.387	0.390	0.150	0.335	0.332	0.079	0.267	0.258
	1000	0.299	0.435	0.436	0.198	0.389	0.387	0.128	0.347	0.341
-0.5	100	0.061	0.046	0.048	0.061	0.051	0.053	0.055	0.049	0.094
	250	0.169	0.309	0.311	0.084	0.232	0.230	0.033	0.149	0.145
	500	0.246	0.390	0.391	0.148	0.336	0.335	0.074	0.267	0.264
	1000	0.287	0.423	0.424	0.204	0.392	0.391	0.134	0.345	0.341
0	100	0.065	0.055	0.055	0.061	0.055	0.052	0.051	0.048	0.059
	250	0.170	0.307	0.306	0.083	0.229	0.228	0.032	0.153	0.153
	500	0.235	0.384	0.383	0.138	0.325	0.324	0.080	0.273	0.274
	1000	0.284	0.422	0.422	0.197	0.392	0.392	0.129	0.344	0.343
0.5	100	0.057	0.049	0.042	0.058	0.051	0.048	0.056	0.054	0.052
	250	0.169	0.316	0.310	0.077	0.225	0.221	0.033	0.146	0.147
	500	0.240	0.386	0.385	0.142	0.330	0.329	0.084	0.266	0.271
	1000	0.295	0.438	0.436	0.201	0.391	0.390	0.124	0.341	0.342
0.95	100	0.057	0.049	0.040	0.059	0.053	0.051	0.056	0.058	0.060
	250	0.164	0.301	0.294	0.079	0.228	0.223	0.033	0.147	0.152
	500	0.245	0.392	0.388	0.144	0.324	0.322	0.078	0.271	0.276
	1000	0.297	0.428	0.426	0.198	0.387	0.384	0.126	0.344	0.346

Notes: t_{zx} , *Bonf.t*, and *Bonf.Q* correspond to the test statistics of IVX test, Bonferroni-t test and Bonferroni-Q test. The data generating process is from (4.1) to (4.7).

Table C-19: Finite sample size at 5% significance level of one-sided predictability tests: u_t, v_t is N.i.i.d, collapsing bubble in return with $\tau_1 = 0.4, \tau_2 = 0.7, c_{bub} = 0.01$

δ	T	c = 0			c = -5			c = -10		
		t_{zx}	Bonf. t	Bonf. Q	t_{zx}	Bonf. t	Bonf. Q	t_{zx}	Bonf. t	Bonf. Q
-0.95	100	0.112	0.042	0.054	0.102	0.038	0.058	0.087	0.041	0.053
	250	0.100	0.044	0.039	0.095	0.035	0.042	0.094	0.041	0.045
	500	0.097	0.038	0.037	0.090	0.031	0.039	0.083	0.037	0.041
	1000	0.086	0.034	0.034	0.082	0.034	0.043	0.081	0.040	0.047
-0.5	100	0.100	0.041	0.048	0.085	0.032	0.050	0.075	0.033	0.050
	250	0.091	0.039	0.044	0.077	0.032	0.047	0.075	0.033	0.045
	500	0.079	0.033	0.036	0.073	0.032	0.044	0.071	0.033	0.043
	1000	0.070	0.030	0.033	0.069	0.036	0.044	0.063	0.034	0.045
0	100	0.055	0.038	0.039	0.058	0.040	0.040	0.063	0.045	0.045
	250	0.045	0.033	0.034	0.050	0.040	0.040	0.055	0.045	0.045
	500	0.040	0.031	0.032	0.047	0.039	0.040	0.054	0.045	0.045
	1000	0.035	0.027	0.027	0.046	0.042	0.041	0.050	0.044	0.045
0.5	100	0.010	0.016	0.010	0.028	0.034	0.013	0.037	0.046	0.018
	250	0.008	0.014	0.011	0.029	0.040	0.019	0.035	0.045	0.021
	500	0.010	0.014	0.012	0.024	0.032	0.016	0.035	0.042	0.022
	1000	0.009	0.010	0.009	0.025	0.029	0.018	0.037	0.038	0.024
0.95	100	0.001	0.004	0.001	0.010	0.029	0.005	0.021	0.043	0.010
	250	0.001	0.002	0.002	0.013	0.032	0.007	0.020	0.040	0.012
	500	0.001	0.004	0.002	0.014	0.030	0.007	0.022	0.040	0.010
	1000	0.001	0.002	0.001	0.013	0.023	0.007	0.025	0.037	0.011

δ	T	c = -20			c = -50			c = -100		
		t_{zx}	Bonf. t	Bonf. Q	t_{zx}	Bonf. t	Bonf. Q	t_{zx}	Bonf. t	Bonf. Q
-0.95	100	0.081	0.049	0.055	0.058	0.049	0.105	0.052	0.043	0.424
	250	0.076	0.046	0.039	0.066	0.050	0.034	0.048	0.043	0.039
	500	0.078	0.044	0.034	0.065	0.050	0.023	0.054	0.047	0.015
	1000	0.071	0.045	0.040	0.064	0.051	0.033	0.056	0.052	0.019
-0.5	100	0.073	0.043	0.050	0.061	0.046	0.067	0.059	0.045	0.302
	250	0.068	0.043	0.041	0.062	0.048	0.035	0.052	0.046	0.036
	500	0.066	0.042	0.043	0.058	0.047	0.034	0.055	0.046	0.022
	1000	0.059	0.041	0.043	0.063	0.051	0.040	0.058	0.052	0.027
0	100	0.061	0.048	0.047	0.061	0.051	0.048	0.063	0.057	0.066
	250	0.058	0.047	0.048	0.057	0.049	0.048	0.052	0.046	0.046
	500	0.053	0.048	0.047	0.055	0.050	0.048	0.056	0.052	0.050
	1000	0.054	0.049	0.050	0.052	0.049	0.048	0.052	0.048	0.048
0.5	100	0.047	0.049	0.026	0.048	0.048	0.047	0.053	0.055	0.093
	250	0.042	0.047	0.024	0.052	0.051	0.051	0.049	0.054	0.117
	500	0.040	0.043	0.024	0.047	0.050	0.042	0.049	0.052	0.087
	1000	0.044	0.045	0.029	0.044	0.046	0.034	0.047	0.049	0.056
0.95	100	0.029	0.046	0.025	0.039	0.053	0.094	0.042	0.059	0.169
	250	0.028	0.044	0.020	0.036	0.050	0.085	0.036	0.047	0.229
	500	0.030	0.045	0.017	0.035	0.046	0.051	0.039	0.049	0.169
	1000	0.036	0.044	0.016	0.037	0.043	0.028	0.041	0.047	0.086

Notes: t_{zx} , *Bonf.t*, and *Bonf.Q* correspond to the test statistics of IVX test, Bonferroni-t test and Bonferroni-Q test. The data generating process is from (4.1) to (4.7).

Table C-20: Finite sample size at 5% significance level of one-sided predictability tests: u_t, v_t is N.i.i.d, collapsing bubble in return with $\tau_1 = 0.4, \tau_2 = 0.7, c_{bub} = 0.05$

δ	T	c = 0			c = -5			c = -10		
		t_{zx}	Bonf. t	Bonf. Q	t_{zx}	Bonf. t	Bonf. Q	t_{zx}	Bonf. t	Bonf. Q
-0.95	100	0.108	0.039	0.046	0.095	0.032	0.050	0.083	0.036	0.052
	250	0.065	0.021	0.023	0.069	0.028	0.038	0.060	0.028	0.037
	500	0.195	0.188	0.188	0.188	0.194	0.209	0.178	0.187	0.203
	1000	0.347	0.392	0.394	0.335	0.389	0.395	0.324	0.391	0.399
-0.5	100	0.090	0.036	0.042	0.086	0.036	0.055	0.082	0.036	0.050
	250	0.051	0.021	0.022	0.055	0.027	0.036	0.060	0.032	0.039
	500	0.180	0.178	0.179	0.179	0.194	0.202	0.166	0.184	0.192
	1000	0.340	0.391	0.392	0.333	0.396	0.400	0.326	0.398	0.404
0	100	0.049	0.031	0.031	0.061	0.043	0.042	0.060	0.045	0.044
	250	0.025	0.013	0.014	0.042	0.030	0.030	0.046	0.033	0.034
	500	0.159	0.172	0.172	0.170	0.204	0.204	0.164	0.195	0.196
	1000	0.328	0.390	0.391	0.323	0.390	0.390	0.310	0.385	0.385
0.5	100	0.010	0.012	0.008	0.028	0.030	0.014	0.041	0.042	0.019
	250	0.009	0.006	0.007	0.026	0.022	0.016	0.035	0.030	0.021
	500	0.135	0.149	0.153	0.160	0.192	0.184	0.150	0.186	0.176
	1000	0.312	0.378	0.378	0.313	0.385	0.383	0.298	0.384	0.381
0.95	100	0.002	0.003	0.001	0.015	0.028	0.005	0.025	0.040	0.010
	250	0.004	0.002	0.002	0.017	0.018	0.008	0.028	0.029	0.012
	500	0.117	0.135	0.139	0.147	0.178	0.165	0.140	0.172	0.155
	1000	0.299	0.366	0.371	0.323	0.394	0.388	0.307	0.385	0.378

δ	T	c = -20			c = -50			c = -100		
		t_{zx}	Bonf. t	Bonf. Q	t_{zx}	Bonf. t	Bonf. Q	t_{zx}	Bonf. t	Bonf. Q
-0.95	100	0.077	0.045	0.051	0.063	0.049	0.091	0.051	0.041	0.392
	250	0.068	0.042	0.043	0.064	0.051	0.038	0.059	0.050	0.037
	500	0.136	0.153	0.163	0.087	0.118	0.105	0.062	0.095	0.069
	1000	0.268	0.346	0.350	0.179	0.300	0.292	0.112	0.245	0.216
-0.5	100	0.076	0.046	0.052	0.069	0.051	0.068	0.062	0.051	0.270
	250	0.056	0.035	0.039	0.057	0.047	0.039	0.055	0.046	0.036
	500	0.130	0.153	0.159	0.081	0.111	0.107	0.060	0.091	0.079
	1000	0.272	0.353	0.357	0.185	0.310	0.305	0.108	0.239	0.225
0	100	0.061	0.046	0.045	0.064	0.053	0.052	0.062	0.052	0.064
	250	0.053	0.039	0.039	0.054	0.048	0.045	0.058	0.053	0.053
	500	0.131	0.164	0.163	0.085	0.118	0.117	0.056	0.084	0.082
	1000	0.274	0.368	0.368	0.175	0.301	0.299	0.098	0.232	0.231
0.5	100	0.046	0.047	0.026	0.057	0.052	0.046	0.058	0.055	0.082
	250	0.043	0.038	0.029	0.053	0.047	0.044	0.053	0.051	0.070
	500	0.119	0.152	0.143	0.083	0.119	0.115	0.056	0.086	0.094
	1000	0.263	0.359	0.353	0.168	0.294	0.288	0.099	0.229	0.233
0.95	100	0.033	0.044	0.020	0.044	0.052	0.089	0.046	0.057	0.154
	250	0.038	0.038	0.020	0.048	0.045	0.047	0.046	0.046	0.110
	500	0.123	0.158	0.139	0.082	0.117	0.108	0.054	0.089	0.100
	1000	0.264	0.358	0.346	0.174	0.291	0.280	0.099	0.229	0.234

Notes: t_{zx} , *Bonf.t*, and *Bonf.Q* correspond to the test statistics of IVX test, Bonferroni-t test and Bonferroni-Q test. The data generating process is from (4.1) to (4.7).

Table C-21: Finite sample size at 5% significance level of one-sided predictability tests: u_t, v_t is N.i.i.d, collapsing bubble in return with $\tau_1 = 0.4, \tau_2 = 0.7, c_{bub} = 0.1$

δ	T	c = 0			c = -5			c = -10		
		t_{zx}	Bonf. t	Bonf. Q	t_{zx}	Bonf. t	Bonf. Q	t_{zx}	Bonf. t	Bonf. Q
-0.95	100	0.071	0.024	0.026	0.072	0.023	0.034	0.071	0.031	0.041
	250	0.141	0.144	0.144	0.147	0.164	0.176	0.135	0.151	0.164
	500	0.306	0.372	0.372	0.293	0.372	0.376	0.285	0.374	0.379
	1000	0.357	0.428	0.430	0.364	0.442	0.445	0.342	0.428	0.432
-0.5	100	0.063	0.021	0.026	0.068	0.026	0.037	0.067	0.027	0.039
	250	0.128	0.139	0.141	0.137	0.161	0.168	0.122	0.147	0.155
	500	0.296	0.375	0.376	0.297	0.381	0.384	0.272	0.367	0.369
	1000	0.356	0.430	0.431	0.360	0.447	0.448	0.331	0.423	0.425
0	100	0.034	0.017	0.018	0.046	0.026	0.027	0.058	0.038	0.038
	250	0.114	0.129	0.130	0.130	0.162	0.161	0.123	0.153	0.153
	500	0.296	0.374	0.375	0.297	0.381	0.381	0.272	0.369	0.368
	1000	0.351	0.432	0.432	0.350	0.436	0.436	0.338	0.435	0.435
0.5	100	0.012	0.007	0.005	0.028	0.022	0.013	0.042	0.035	0.019
	250	0.100	0.119	0.122	0.124	0.161	0.154	0.118	0.155	0.147
	500	0.284	0.369	0.370	0.295	0.388	0.385	0.269	0.367	0.363
	1000	0.352	0.433	0.434	0.351	0.445	0.444	0.329	0.424	0.422
0.95	100	0.002	0.001	0.001	0.016	0.018	0.005	0.032	0.033	0.012
	250	0.085	0.103	0.106	0.114	0.151	0.140	0.114	0.155	0.138
	500	0.272	0.359	0.360	0.276	0.375	0.372	0.263	0.362	0.353
	1000	0.351	0.433	0.432	0.344	0.435	0.433	0.327	0.423	0.420

δ	T	c = -20			c = -50			c = -100		
		t_{zx}	Bonf. t	Bonf. Q	t_{zx}	Bonf. t	Bonf. Q	t_{zx}	Bonf. t	Bonf. Q
-0.95	100	0.068	0.037	0.042	0.065	0.049	0.078	0.056	0.047	0.298
	250	0.103	0.126	0.133	0.067	0.098	0.090	0.042	0.072	0.061
	500	0.237	0.345	0.352	0.133	0.280	0.273	0.065	0.199	0.182
	1000	0.290	0.409	0.412	0.193	0.360	0.356	0.113	0.317	0.304
-0.5	100	0.064	0.036	0.042	0.065	0.047	0.059	0.066	0.050	0.189
	250	0.108	0.136	0.140	0.066	0.097	0.093	0.038	0.067	0.061
	500	0.226	0.337	0.340	0.134	0.277	0.273	0.061	0.199	0.190
	1000	0.283	0.405	0.407	0.197	0.370	0.369	0.121	0.325	0.318
0	100	0.060	0.042	0.042	0.060	0.046	0.044	0.066	0.054	0.066
	250	0.101	0.134	0.132	0.064	0.099	0.096	0.045	0.072	0.071
	500	0.226	0.344	0.345	0.130	0.266	0.265	0.063	0.200	0.201
	1000	0.288	0.408	0.408	0.196	0.364	0.363	0.114	0.319	0.319
0.5	100	0.048	0.039	0.026	0.060	0.050	0.046	0.066	0.061	0.067
	250	0.096	0.133	0.124	0.063	0.094	0.090	0.040	0.069	0.074
	500	0.225	0.341	0.337	0.127	0.265	0.263	0.058	0.197	0.202
	1000	0.293	0.417	0.415	0.189	0.363	0.360	0.113	0.313	0.316
0.95	100	0.041	0.040	0.020	0.052	0.050	0.055	0.057	0.058	0.098
	250	0.098	0.134	0.121	0.060	0.097	0.092	0.042	0.075	0.086
	500	0.220	0.339	0.329	0.127	0.270	0.264	0.059	0.191	0.199
	1000	0.286	0.406	0.400	0.194	0.364	0.358	0.108	0.305	0.308

Notes: t_{zx} , *Bonf.t*, and *Bonf.Q* correspond to the test statistics of IVX test, Bonferroni-t test and Bonferroni-Q test. The data generating process is from (4.1) to (4.7).

Table C-22: Finite sample size at 5% significance level of one-sided predictability tests: u_t, v_t is N.i.i.d, collapsing bubble in return with $\tau_1 = 0.4, \tau_2 = 0.7, c_{bub} = 0.2$

δ	T	c = 0			c = -5			c = -10		
		t_{zx}	Bonf. t	Bonf. Q	t_{zx}	Bonf. t	Bonf. Q	t_{zx}	Bonf. t	Bonf. Q
-0.95	100	0.057	0.028	0.033	0.064	0.041	0.049	0.068	0.046	0.055
	250	0.247	0.345	0.346	0.255	0.367	0.369	0.221	0.339	0.343
	500	0.323	0.416	0.416	0.313	0.420	0.422	0.302	0.417	0.420
	1000	0.359	0.447	0.447	0.362	0.457	0.458	0.342	0.445	0.446
-0.5	100	0.049	0.029	0.031	0.059	0.040	0.045	0.066	0.047	0.051
	250	0.242	0.344	0.345	0.245	0.360	0.361	0.221	0.340	0.342
	500	0.320	0.417	0.417	0.316	0.423	0.424	0.292	0.410	0.411
	1000	0.370	0.451	0.451	0.354	0.450	0.451	0.343	0.448	0.449
0	100	0.036	0.021	0.021	0.058	0.043	0.042	0.062	0.048	0.047
	250	0.233	0.342	0.343	0.238	0.353	0.353	0.221	0.341	0.340
	500	0.312	0.412	0.412	0.321	0.422	0.423	0.294	0.412	0.412
	1000	0.365	0.453	0.454	0.365	0.453	0.453	0.342	0.450	0.449
0.5	100	0.025	0.016	0.016	0.047	0.038	0.034	0.056	0.046	0.041
	250	0.235	0.343	0.343	0.232	0.346	0.345	0.211	0.340	0.337
	500	0.310	0.410	0.410	0.312	0.417	0.416	0.297	0.413	0.411
	1000	0.360	0.446	0.446	0.355	0.443	0.442	0.331	0.434	0.432
0.95	100	0.019	0.014	0.012	0.043	0.037	0.030	0.052	0.046	0.037
	250	0.223	0.333	0.336	0.235	0.350	0.347	0.212	0.338	0.332
	500	0.309	0.408	0.409	0.310	0.415	0.413	0.293	0.422	0.419
	1000	0.350	0.436	0.437	0.349	0.444	0.443	0.337	0.445	0.443

δ	T	c = -20			c = -50			c = -100		
		t_{zx}	Bonf. t	Bonf. Q	t_{zx}	Bonf. t	Bonf. Q	t_{zx}	Bonf. t	Bonf. Q
-0.95	100	0.067	0.049	0.053	0.060	0.053	0.059	0.053	0.050	0.131
	250	0.172	0.308	0.312	0.074	0.223	0.220	0.025	0.150	0.143
	500	0.246	0.390	0.392	0.149	0.344	0.341	0.064	0.267	0.258
	1000	0.298	0.426	0.428	0.210	0.393	0.391	0.120	0.337	0.330
-0.5	100	0.064	0.049	0.052	0.060	0.054	0.053	0.054	0.051	0.093
	250	0.170	0.305	0.306	0.078	0.230	0.228	0.026	0.151	0.147
	500	0.247	0.384	0.385	0.143	0.331	0.329	0.062	0.267	0.262
	1000	0.295	0.425	0.426	0.198	0.384	0.383	0.116	0.342	0.340
0	100	0.065	0.053	0.050	0.063	0.056	0.054	0.055	0.053	0.060
	250	0.168	0.303	0.301	0.074	0.228	0.226	0.024	0.149	0.151
	500	0.249	0.392	0.391	0.145	0.333	0.332	0.066	0.266	0.265
	1000	0.294	0.431	0.431	0.193	0.390	0.389	0.116	0.349	0.349
0.5	100	0.057	0.048	0.041	0.055	0.050	0.045	0.055	0.053	0.054
	250	0.166	0.304	0.301	0.080	0.237	0.235	0.021	0.151	0.153
	500	0.243	0.380	0.378	0.141	0.332	0.331	0.066	0.264	0.266
	1000	0.300	0.431	0.430	0.201	0.385	0.383	0.112	0.344	0.345
0.95	100	0.058	0.050	0.041	0.054	0.051	0.048	0.052	0.052	0.057
	250	0.164	0.306	0.299	0.078	0.232	0.227	0.020	0.147	0.152
	500	0.244	0.391	0.386	0.143	0.330	0.327	0.067	0.264	0.269
	1000	0.293	0.428	0.427	0.202	0.387	0.384	0.122	0.350	0.351

Notes: t_{zx} , *Bonf.t*, and *Bonf.Q* correspond to the test statistics of IVX test, Bonferroni-t test and Bonferroni-Q test. The data generating process is from (4.1) to (4.7).

Table C-23: Finite sample size at 5% significance level of one-sided predictability tests: u_t, v_t is N.i.i.d, collapsing bubble in return with $\tau_1 = 0.1, \tau_2 = 0.4, c_{bub} = 0.01$

δ	T	c = 0			c = -5			c = -10		
		t_{zx}	Bonf. t	Bonf. Q	t_{zx}	Bonf. t	Bonf. Q	t_{zx}	Bonf. t	Bonf. Q
-0.95	100	0.114	0.048	0.049	0.100	0.035	0.054	0.090	0.040	0.052
	250	0.098	0.046	0.040	0.094	0.031	0.042	0.089	0.041	0.045
	500	0.097	0.040	0.039	0.090	0.031	0.039	0.089	0.038	0.042
	1000	0.087	0.034	0.032	0.088	0.032	0.045	0.081	0.037	0.046
-0.5	100	0.105	0.044	0.049	0.084	0.032	0.051	0.081	0.036	0.052
	250	0.095	0.039	0.043	0.084	0.035	0.048	0.076	0.036	0.047
	500	0.085	0.039	0.040	0.076	0.030	0.043	0.068	0.034	0.045
	1000	0.074	0.034	0.036	0.065	0.033	0.043	0.065	0.036	0.048
0	100	0.052	0.037	0.037	0.058	0.042	0.042	0.065	0.048	0.046
	250	0.046	0.036	0.037	0.053	0.043	0.043	0.052	0.042	0.042
	500	0.042	0.034	0.035	0.049	0.044	0.045	0.051	0.044	0.043
	1000	0.038	0.031	0.031	0.047	0.042	0.042	0.051	0.046	0.047
0.5	100	0.009	0.013	0.011	0.028	0.034	0.013	0.037	0.044	0.018
	250	0.009	0.015	0.012	0.026	0.034	0.015	0.036	0.044	0.019
	500	0.007	0.011	0.010	0.027	0.035	0.016	0.032	0.039	0.017
	1000	0.010	0.011	0.012	0.027	0.031	0.021	0.037	0.043	0.025
0.95	100	0.000	0.002	0.001	0.011	0.029	0.005	0.019	0.043	0.009
	250	0.001	0.003	0.002	0.011	0.029	0.006	0.021	0.038	0.010
	500	0.000	0.002	0.001	0.012	0.025	0.007	0.021	0.038	0.009
	1000	0.002	0.003	0.003	0.015	0.028	0.007	0.024	0.037	0.011

δ	T	c = -20			c = -50			c = -100		
		t_{zx}	Bonf. t	Bonf. Q	t_{zx}	Bonf. t	Bonf. Q	t_{zx}	Bonf. t	Bonf. Q
-0.95	100	0.080	0.048	0.056	0.057	0.046	0.111	0.054	0.044	0.430
	250	0.076	0.046	0.037	0.068	0.053	0.035	0.056	0.051	0.044
	500	0.074	0.044	0.036	0.062	0.047	0.025	0.055	0.048	0.016
	1000	0.071	0.047	0.042	0.063	0.051	0.030	0.056	0.049	0.015
-0.5	100	0.076	0.044	0.050	0.067	0.054	0.074	0.059	0.044	0.301
	250	0.068	0.042	0.041	0.059	0.045	0.034	0.057	0.048	0.037
	500	0.065	0.042	0.042	0.058	0.045	0.031	0.059	0.053	0.025
	1000	0.063	0.043	0.043	0.058	0.049	0.037	0.054	0.046	0.024
0	100	0.058	0.045	0.043	0.058	0.050	0.049	0.055	0.047	0.059
	250	0.061	0.052	0.051	0.060	0.052	0.050	0.056	0.052	0.050
	500	0.055	0.047	0.047	0.052	0.048	0.047	0.052	0.050	0.049
	1000	0.050	0.044	0.044	0.051	0.049	0.049	0.052	0.049	0.048
0.5	100	0.047	0.050	0.025	0.046	0.048	0.047	0.053	0.058	0.094
	250	0.040	0.047	0.023	0.049	0.051	0.050	0.048	0.051	0.109
	500	0.042	0.047	0.024	0.045	0.049	0.041	0.048	0.051	0.086
	1000	0.039	0.041	0.025	0.044	0.046	0.037	0.047	0.048	0.060
0.95	100	0.030	0.048	0.022	0.037	0.049	0.095	0.042	0.054	0.168
	250	0.028	0.044	0.020	0.035	0.050	0.088	0.039	0.053	0.236
	500	0.029	0.043	0.017	0.040	0.050	0.050	0.041	0.051	0.173
	1000	0.031	0.041	0.015	0.035	0.043	0.027	0.046	0.051	0.091

Notes: t_{zx} , *Bonf.t*, and *Bonf.Q* correspond to the test statistics of IVX test, Bonferroni-t test and Bonferroni-Q test. The data generating process is from (4.1) to (4.7).

Table C-24: Finite sample size at 5% significance level of one-sided predictability tests: u_t, v_t is N.i.i.d, collapsing bubble in return with $\tau_1 = 0.1, \tau_2 = 0.4, c_{bub} = 0.05$

δ	T	c = 0			c = -5			c = -10		
		t_{zx}	Bonf. t	Bonf. Q	t_{zx}	Bonf. t	Bonf. Q	t_{zx}	Bonf. t	Bonf. Q
-0.95	100	0.059	0.031	0.035	0.068	0.043	0.051	0.072	0.048	0.055
	250	0.285	0.390	0.389	0.264	0.372	0.376	0.221	0.340	0.344
	500	0.361	0.456	0.455	0.334	0.424	0.426	0.302	0.415	0.418
	1000	0.401	0.469	0.468	0.378	0.457	0.458	0.340	0.441	0.443
-0.5	100	0.055	0.029	0.034	0.062	0.046	0.051	0.072	0.050	0.056
	250	0.278	0.393	0.393	0.262	0.370	0.372	0.219	0.344	0.346
	500	0.359	0.447	0.446	0.343	0.437	0.439	0.295	0.412	0.413
	1000	0.384	0.458	0.458	0.378	0.459	0.459	0.345	0.446	0.447
0	100	0.039	0.027	0.028	0.056	0.043	0.042	0.059	0.045	0.046
	250	0.273	0.386	0.386	0.252	0.360	0.360	0.223	0.337	0.336
	500	0.354	0.448	0.449	0.339	0.436	0.436	0.303	0.420	0.419
	1000	0.390	0.461	0.461	0.367	0.453	0.453	0.338	0.443	0.443
0.5	100	0.032	0.024	0.024	0.049	0.043	0.038	0.057	0.047	0.042
	250	0.276	0.393	0.395	0.260	0.372	0.369	0.218	0.344	0.340
	500	0.354	0.441	0.442	0.332	0.430	0.430	0.294	0.412	0.411
	1000	0.393	0.473	0.473	0.378	0.458	0.457	0.341	0.447	0.446
0.95	100	0.026	0.020	0.018	0.043	0.039	0.032	0.053	0.047	0.037
	250	0.259	0.381	0.384	0.247	0.354	0.351	0.217	0.341	0.336
	500	0.360	0.450	0.450	0.331	0.430	0.429	0.298	0.413	0.411
	1000	0.402	0.466	0.467	0.375	0.464	0.463	0.333	0.440	0.439

δ	T	c = -20			c = -50			c = -100		
		t_{zx}	Bonf. t	Bonf. Q	t_{zx}	Bonf. t	Bonf. Q	t_{zx}	Bonf. t	Bonf. Q
-0.95	100	0.066	0.049	0.055	0.058	0.050	0.055	0.060	0.055	0.139
	250	0.170	0.307	0.310	0.081	0.231	0.228	0.030	0.154	0.147
	500	0.249	0.395	0.396	0.146	0.330	0.328	0.074	0.270	0.261
	1000	0.297	0.421	0.423	0.207	0.398	0.396	0.125	0.351	0.343
-0.5	100	0.063	0.046	0.050	0.068	0.059	0.061	0.055	0.048	0.094
	250	0.164	0.304	0.305	0.077	0.219	0.217	0.026	0.148	0.143
	500	0.247	0.391	0.392	0.148	0.340	0.338	0.071	0.258	0.254
	1000	0.293	0.434	0.435	0.202	0.389	0.388	0.124	0.338	0.334
0	100	0.061	0.049	0.047	0.060	0.052	0.049	0.052	0.049	0.064
	250	0.169	0.297	0.295	0.080	0.226	0.224	0.030	0.150	0.149
	500	0.238	0.385	0.385	0.150	0.335	0.334	0.073	0.263	0.264
	1000	0.291	0.425	0.426	0.200	0.386	0.385	0.130	0.355	0.354
0.5	100	0.064	0.054	0.048	0.063	0.057	0.054	0.054	0.052	0.053
	250	0.164	0.307	0.302	0.079	0.220	0.216	0.028	0.147	0.150
	500	0.243	0.391	0.389	0.143	0.331	0.330	0.073	0.269	0.274
	1000	0.289	0.421	0.420	0.202	0.384	0.384	0.126	0.350	0.351
0.95	100	0.056	0.050	0.039	0.060	0.056	0.050	0.055	0.052	0.056
	250	0.159	0.299	0.291	0.080	0.225	0.220	0.026	0.147	0.151
	500	0.241	0.389	0.385	0.144	0.330	0.328	0.073	0.271	0.274
	1000	0.289	0.429	0.426	0.195	0.380	0.378	0.125	0.343	0.345

Notes: t_{zx} , *Bonf.t*, and *Bonf.Q* correspond to the test statistics of IVX test, Bonferroni-t test and Bonferroni-Q test. The data generating process is from (4.1) to (4.7).

Table C-25: Finite sample size at 5% significance level of one-sided predictability tests: u_t, v_t is N.i.i.d, collapsing bubble in return with $\tau_1 = 0.1, \tau_2 = 0.4, c_{bub} = 0.1$

δ	T	c = 0			c = -5			c = -10		
		t_{zx}	Bonf. t	Bonf. Q	t_{zx}	Bonf. t	Bonf. Q	t_{zx}	Bonf. t	Bonf. Q
-0.95	100	0.076	0.024	0.030	0.078	0.026	0.040	0.072	0.029	0.041
	250	0.159	0.174	0.178	0.160	0.178	0.191	0.133	0.152	0.165
	500	0.344	0.419	0.419	0.315	0.389	0.395	0.282	0.368	0.374
	1000	0.392	0.462	0.462	0.376	0.449	0.451	0.343	0.433	0.436
-0.5	100	0.062	0.020	0.025	0.066	0.025	0.038	0.069	0.029	0.039
	250	0.152	0.181	0.180	0.146	0.171	0.177	0.129	0.161	0.168
	500	0.331	0.407	0.408	0.318	0.399	0.402	0.273	0.366	0.369
	1000	0.385	0.458	0.458	0.369	0.446	0.448	0.338	0.435	0.437
0	100	0.035	0.021	0.020	0.050	0.026	0.027	0.056	0.034	0.035
	250	0.135	0.171	0.173	0.137	0.175	0.174	0.123	0.161	0.162
	500	0.322	0.409	0.409	0.304	0.390	0.390	0.280	0.376	0.377
	1000	0.382	0.457	0.457	0.369	0.451	0.451	0.337	0.440	0.440
0.5	100	0.011	0.007	0.005	0.027	0.020	0.010	0.042	0.032	0.019
	250	0.128	0.169	0.170	0.136	0.173	0.166	0.118	0.154	0.145
	500	0.329	0.415	0.417	0.299	0.389	0.387	0.261	0.358	0.355
	1000	0.387	0.462	0.464	0.367	0.450	0.450	0.335	0.437	0.435
0.95	100	0.004	0.002	0.002	0.017	0.016	0.004	0.033	0.033	0.011
	250	0.114	0.158	0.158	0.121	0.165	0.151	0.110	0.153	0.137
	500	0.315	0.405	0.408	0.300	0.390	0.385	0.266	0.371	0.365
	1000	0.389	0.463	0.464	0.365	0.442	0.441	0.335	0.434	0.431

δ	T	c = -20			c = -50			c = -100		
		t_{zx}	Bonf. t	Bonf. Q	t_{zx}	Bonf. t	Bonf. Q	t_{zx}	Bonf. t	Bonf. Q
-0.95	100	0.068	0.037	0.043	0.063	0.047	0.078	0.065	0.049	0.294
	250	0.105	0.128	0.136	0.062	0.094	0.086	0.044	0.071	0.062
	500	0.227	0.333	0.337	0.131	0.271	0.263	0.065	0.195	0.176
	1000	0.294	0.415	0.418	0.204	0.374	0.369	0.125	0.322	0.306
-0.5	100	0.064	0.035	0.040	0.067	0.048	0.059	0.063	0.051	0.184
	250	0.103	0.128	0.133	0.069	0.100	0.095	0.044	0.072	0.067
	500	0.223	0.338	0.340	0.133	0.272	0.269	0.072	0.207	0.195
	1000	0.290	0.412	0.414	0.208	0.379	0.376	0.118	0.315	0.309
0	100	0.058	0.039	0.038	0.063	0.049	0.047	0.064	0.052	0.066
	250	0.100	0.136	0.135	0.067	0.096	0.094	0.044	0.070	0.070
	500	0.222	0.338	0.337	0.130	0.274	0.273	0.069	0.211	0.211
	1000	0.293	0.415	0.415	0.198	0.372	0.371	0.120	0.319	0.319
0.5	100	0.045	0.038	0.026	0.057	0.049	0.045	0.062	0.054	0.068
	250	0.097	0.134	0.127	0.066	0.100	0.097	0.043	0.072	0.079
	500	0.221	0.339	0.335	0.129	0.272	0.269	0.065	0.201	0.205
	1000	0.282	0.413	0.410	0.192	0.360	0.359	0.115	0.311	0.313
0.95	100	0.043	0.040	0.021	0.047	0.045	0.056	0.057	0.059	0.108
	250	0.097	0.134	0.118	0.064	0.099	0.091	0.040	0.069	0.084
	500	0.217	0.333	0.326	0.124	0.258	0.254	0.069	0.202	0.209
	1000	0.291	0.410	0.406	0.196	0.363	0.359	0.119	0.312	0.313

Notes: t_{zx} , *Bonf.t*, and *Bonf.Q* correspond to the test statistics of IVX test, Bonferroni-t test and Bonferroni-Q test. The data generating process is from (4.1) to (4.7).

Table C-26: Finite sample size at 5% significance level of one-sided predictability tests: u_t, v_t is N.i.i.d, collapsing bubble in return with $\tau_1 = 0.1, \tau_2 = 0.4, c_{bub} = 0.2$

δ	T	c = 0			c = -5			c = -10		
		t_{zx}	Bonf. t	Bonf. Q	t_{zx}	Bonf. t	Bonf. Q	t_{zx}	Bonf. t	Bonf. Q
-0.95	100	0.059	0.031	0.035	0.068	0.043	0.051	0.072	0.048	0.055
	250	0.285	0.390	0.389	0.264	0.372	0.376	0.221	0.340	0.344
	500	0.361	0.456	0.455	0.334	0.424	0.426	0.302	0.415	0.418
	1000	0.401	0.469	0.468	0.378	0.457	0.458	0.340	0.441	0.443
-0.5	100	0.055	0.029	0.034	0.062	0.046	0.051	0.072	0.050	0.056
	250	0.278	0.393	0.393	0.262	0.370	0.372	0.219	0.344	0.346
	500	0.359	0.447	0.446	0.343	0.437	0.439	0.295	0.412	0.413
	1000	0.384	0.458	0.458	0.378	0.459	0.459	0.345	0.446	0.447
0	100	0.039	0.027	0.028	0.056	0.043	0.042	0.059	0.045	0.046
	250	0.273	0.386	0.386	0.252	0.360	0.360	0.223	0.337	0.336
	500	0.354	0.448	0.449	0.339	0.436	0.436	0.303	0.420	0.419
	1000	0.390	0.461	0.461	0.367	0.453	0.453	0.338	0.443	0.443
0.5	100	0.032	0.024	0.024	0.049	0.043	0.038	0.057	0.047	0.042
	250	0.276	0.393	0.395	0.260	0.372	0.369	0.218	0.344	0.340
	500	0.354	0.441	0.442	0.332	0.430	0.430	0.294	0.412	0.411
	1000	0.393	0.473	0.473	0.378	0.458	0.457	0.341	0.447	0.446
0.95	100	0.026	0.020	0.018	0.043	0.039	0.032	0.053	0.047	0.037
	250	0.259	0.381	0.384	0.247	0.354	0.351	0.217	0.341	0.336
	500	0.360	0.450	0.450	0.331	0.430	0.429	0.298	0.413	0.411
	1000	0.402	0.466	0.467	0.375	0.464	0.463	0.333	0.440	0.439

δ	T	c = -20			c = -50			c = -100		
		t_{zx}	Bonf. t	Bonf. Q	t_{zx}	Bonf. t	Bonf. Q	t_{zx}	Bonf. t	Bonf. Q
-0.95	100	0.066	0.049	0.055	0.058	0.050	0.055	0.060	0.055	0.139
	250	0.170	0.307	0.310	0.081	0.231	0.228	0.030	0.154	0.147
	500	0.249	0.395	0.396	0.146	0.330	0.328	0.074	0.270	0.261
	1000	0.297	0.421	0.423	0.207	0.398	0.396	0.125	0.351	0.343
-0.5	100	0.063	0.046	0.050	0.068	0.059	0.061	0.055	0.048	0.094
	250	0.164	0.304	0.305	0.077	0.219	0.217	0.026	0.148	0.143
	500	0.247	0.391	0.392	0.148	0.340	0.338	0.071	0.258	0.254
	1000	0.293	0.434	0.435	0.202	0.389	0.388	0.124	0.338	0.334
0	100	0.061	0.049	0.047	0.060	0.052	0.049	0.052	0.049	0.064
	250	0.169	0.297	0.295	0.080	0.226	0.224	0.030	0.150	0.149
	500	0.238	0.385	0.385	0.150	0.335	0.334	0.073	0.263	0.264
	1000	0.291	0.425	0.426	0.200	0.386	0.385	0.130	0.355	0.354
0.5	100	0.064	0.054	0.048	0.063	0.057	0.054	0.054	0.052	0.053
	250	0.164	0.307	0.302	0.079	0.220	0.216	0.028	0.147	0.150
	500	0.243	0.391	0.389	0.143	0.331	0.330	0.073	0.269	0.274
	1000	0.289	0.421	0.420	0.202	0.384	0.384	0.126	0.350	0.351
0.95	100	0.056	0.050	0.039	0.060	0.056	0.050	0.055	0.052	0.056
	250	0.159	0.299	0.291	0.080	0.225	0.220	0.026	0.147	0.151
	500	0.241	0.389	0.385	0.144	0.330	0.328	0.073	0.271	0.274
	1000	0.289	0.429	0.426	0.195	0.380	0.378	0.125	0.343	0.345

Notes: t_{zx} , *Bonf.t*, and *Bonf.Q* correspond to the test statistics of IVX test, Bonferroni-t test and Bonferroni-Q test. The data generating process is from (4.1) to (4.7).

Table C-27: Finite sample size at 5% significance level of one-sided predictability tests: u_t, v_t is i.i.d from t-distribution with the degree of freedom = 5, collapsing bubble in return with $\tau_1 = 0.6, \tau_2 = 0.9, c_{bub} = 0.01$

δ	T	c = 0			c = -5			c = -10		
		t_{zx}	Bonf. t	Bonf. Q	t_{zx}	Bonf. t	Bonf. Q	t_{zx}	Bonf. t	Bonf. Q
-0.95	100	0.115	0.044	0.055	0.108	0.037	0.058	0.094	0.043	0.059
	250	0.104	0.045	0.043	0.099	0.036	0.045	0.092	0.044	0.046
	500	0.099	0.041	0.037	0.093	0.031	0.040	0.084	0.037	0.039
	1000	0.100	0.042	0.041	0.089	0.034	0.044	0.084	0.039	0.043
-0.5	100	0.108	0.045	0.053	0.090	0.033	0.052	0.081	0.033	0.053
	250	0.096	0.042	0.046	0.085	0.031	0.047	0.073	0.033	0.046
	500	0.092	0.043	0.042	0.083	0.031	0.045	0.073	0.033	0.044
	1000	0.077	0.034	0.036	0.072	0.032	0.047	0.069	0.039	0.049
0	100	0.056	0.041	0.041	0.061	0.046	0.046	0.064	0.049	0.048
	250	0.049	0.038	0.038	0.057	0.048	0.048	0.059	0.048	0.047
	500	0.045	0.036	0.036	0.049	0.043	0.043	0.051	0.046	0.047
	1000	0.045	0.037	0.037	0.048	0.044	0.044	0.048	0.044	0.044
0.5	100	0.010	0.019	0.012	0.030	0.037	0.015	0.037	0.044	0.018
	250	0.007	0.016	0.013	0.026	0.038	0.015	0.034	0.041	0.018
	500	0.009	0.016	0.013	0.025	0.034	0.015	0.033	0.044	0.020
	1000	0.009	0.011	0.010	0.029	0.033	0.020	0.037	0.042	0.023
0.95	100	0.002	0.005	0.003	0.011	0.029	0.007	0.018	0.042	0.011
	250	0.001	0.006	0.002	0.011	0.031	0.009	0.017	0.040	0.013
	500	0.001	0.003	0.002	0.013	0.030	0.009	0.020	0.040	0.011
	1000	0.001	0.003	0.002	0.014	0.027	0.008	0.024	0.037	0.010

δ	T	c = -20			c = -50			c = -100		
		t_{zx}	Bonf. t	Bonf. Q	t_{zx}	Bonf. t	Bonf. Q	t_{zx}	Bonf. t	Bonf. Q
-0.95	100	0.067	0.043	0.050	0.058	0.048	0.128	0.052	0.044	0.494
	250	0.076	0.044	0.038	0.063	0.050	0.036	0.051	0.048	0.052
	500	0.072	0.044	0.035	0.062	0.048	0.026	0.057	0.050	0.017
	1000	0.074	0.046	0.041	0.065	0.052	0.030	0.059	0.052	0.016
-0.5	100	0.072	0.042	0.052	0.065	0.051	0.086	0.059	0.048	0.367
	250	0.067	0.041	0.043	0.063	0.049	0.038	0.058	0.049	0.041
	500	0.067	0.043	0.043	0.061	0.048	0.033	0.059	0.050	0.025
	1000	0.063	0.043	0.045	0.062	0.051	0.039	0.053	0.048	0.026
0	100	0.066	0.052	0.050	0.060	0.051	0.049	0.056	0.050	0.065
	250	0.060	0.048	0.047	0.057	0.050	0.048	0.056	0.050	0.051
	500	0.056	0.047	0.047	0.055	0.049	0.048	0.053	0.050	0.049
	1000	0.050	0.046	0.047	0.050	0.047	0.046	0.053	0.050	0.049
0.5	100	0.043	0.048	0.025	0.047	0.047	0.052	0.052	0.053	0.088
	250	0.041	0.046	0.024	0.049	0.053	0.054	0.048	0.053	0.113
	500	0.035	0.042	0.022	0.049	0.052	0.042	0.048	0.051	0.082
	1000	0.038	0.042	0.025	0.045	0.047	0.034	0.047	0.050	0.058
0.95	100	0.027	0.049	0.029	0.036	0.051	0.099	0.040	0.055	0.153
	250	0.027	0.046	0.024	0.033	0.048	0.095	0.037	0.051	0.213
	500	0.029	0.043	0.016	0.030	0.043	0.055	0.040	0.050	0.168
	1000	0.031	0.041	0.014	0.039	0.046	0.035	0.041	0.045	0.090

Notes: t_{zx} , *Bonf.t*, and *Bonf.Q* correspond to the test statistics of IVX test, Bonferroni-t test and Bonferroni-Q test. The data generating process is from (4.1) to (4.7).

Table C-28: Finite sample size at 5% significance level of one-sided predictability tests: u_t, v_t is i.i.d from t-distribution with the degree of freedom = 5, collapsing bubble in return with $\tau_1 = 0.6, \tau_2 = 0.9, c_{bub} = 0.05$

δ	T	c = 0			c = -5			c = -10		
		t_{zx}	Bonf. t	Bonf. Q	t_{zx}	Bonf. t	Bonf. Q	t_{zx}	Bonf. t	Bonf. Q
-0.95	100	0.108	0.040	0.054	0.099	0.035	0.055	0.086	0.038	0.050
	250	0.077	0.028	0.028	0.074	0.027	0.038	0.067	0.031	0.036
	500	0.243	0.266	0.271	0.199	0.202	0.221	0.169	0.173	0.191
	1000	0.392	0.440	0.442	0.353	0.401	0.408	0.330	0.392	0.402
-0.5	100	0.101	0.039	0.050	0.083	0.032	0.050	0.077	0.032	0.049
	250	0.059	0.025	0.026	0.057	0.027	0.035	0.057	0.028	0.037
	500	0.228	0.260	0.262	0.194	0.210	0.219	0.165	0.182	0.193
	1000	0.375	0.439	0.440	0.346	0.404	0.406	0.313	0.385	0.392
0	100	0.052	0.035	0.036	0.060	0.043	0.044	0.059	0.042	0.042
	250	0.029	0.018	0.020	0.043	0.032	0.033	0.049	0.038	0.038
	500	0.193	0.240	0.241	0.179	0.211	0.211	0.159	0.196	0.195
	1000	0.368	0.435	0.435	0.345	0.407	0.407	0.318	0.396	0.396
0.5	100	0.012	0.015	0.011	0.033	0.039	0.018	0.042	0.045	0.021
	250	0.010	0.008	0.008	0.028	0.026	0.017	0.036	0.034	0.021
	500	0.168	0.218	0.221	0.171	0.204	0.195	0.145	0.182	0.169
	1000	0.360	0.434	0.437	0.345	0.415	0.412	0.308	0.388	0.384
0.95	100	0.002	0.005	0.001	0.013	0.029	0.007	0.023	0.041	0.012
	250	0.003	0.003	0.001	0.016	0.019	0.007	0.028	0.030	0.012
	500	0.149	0.200	0.208	0.159	0.194	0.176	0.144	0.184	0.161
	1000	0.340	0.418	0.422	0.329	0.401	0.395	0.303	0.383	0.374

δ	T	c = -20			c = -50			c = -100		
		t_{zx}	Bonf. t	Bonf. Q	t_{zx}	Bonf. t	Bonf. Q	t_{zx}	Bonf. t	Bonf. Q
-0.95	100	0.069	0.041	0.055	0.059	0.047	0.118	0.050	0.040	0.465
	250	0.067	0.043	0.042	0.058	0.046	0.039	0.053	0.045	0.042
	500	0.140	0.152	0.161	0.086	0.117	0.104	0.060	0.080	0.059
	1000	0.264	0.350	0.355	0.175	0.289	0.279	0.109	0.232	0.198
-0.5	100	0.068	0.039	0.047	0.065	0.050	0.077	0.055	0.044	0.324
	250	0.064	0.042	0.044	0.056	0.044	0.037	0.051	0.045	0.039
	500	0.136	0.154	0.162	0.087	0.114	0.107	0.062	0.085	0.073
	1000	0.259	0.349	0.354	0.177	0.292	0.287	0.111	0.236	0.220
0	100	0.064	0.047	0.045	0.058	0.047	0.046	0.060	0.051	0.066
	250	0.056	0.043	0.043	0.055	0.047	0.046	0.052	0.045	0.045
	500	0.123	0.155	0.155	0.086	0.114	0.112	0.056	0.081	0.080
	1000	0.260	0.360	0.360	0.175	0.297	0.295	0.105	0.229	0.229
0.5	100	0.047	0.049	0.028	0.045	0.044	0.048	0.053	0.056	0.084
	250	0.045	0.041	0.027	0.052	0.048	0.045	0.052	0.052	0.074
	500	0.127	0.166	0.153	0.084	0.115	0.109	0.056	0.082	0.088
	1000	0.257	0.347	0.340	0.172	0.290	0.283	0.107	0.230	0.232
0.95	100	0.029	0.044	0.024	0.038	0.047	0.081	0.044	0.058	0.143
	250	0.035	0.037	0.020	0.045	0.045	0.049	0.047	0.048	0.111
	500	0.119	0.156	0.136	0.077	0.111	0.099	0.057	0.082	0.098
	1000	0.253	0.348	0.332	0.170	0.289	0.276	0.107	0.230	0.234

Notes: t_{zx} , *Bonf.t*, and *Bonf.Q* correspond to the test statistics of IVX test, Bonferroni-t test and Bonferroni-Q test. The data generating process is from (4.1) to (4.7).

Table C-29: Finite sample size at 5% significance level of one-sided predictability tests: u_t, v_t is i.i.d from t-distribution with the degree of freedom = 5, collapsing bubble in return with $\tau_1 = 0.6, \tau_2 = 0.9, c_{bub} = 0.1$

δ	T	c = 0			c = -5			c = -10		
		t_{zx}	Bonf. t	Bonf. Q	t_{zx}	Bonf. t	Bonf. Q	t_{zx}	Bonf. t	Bonf. Q
-0.95	100	0.086	0.029	0.034	0.074	0.024	0.039	0.075	0.031	0.042
	250	0.187	0.222	0.225	0.155	0.167	0.181	0.135	0.152	0.169
	500	0.353	0.437	0.438	0.325	0.401	0.408	0.280	0.366	0.377
	1000	0.404	0.474	0.474	0.369	0.447	0.450	0.342	0.438	0.442
-0.5	100	0.067	0.023	0.027	0.069	0.028	0.041	0.069	0.028	0.042
	250	0.167	0.209	0.212	0.144	0.172	0.181	0.124	0.152	0.160
	500	0.351	0.434	0.434	0.310	0.390	0.393	0.278	0.368	0.372
	1000	0.397	0.466	0.466	0.369	0.449	0.451	0.352	0.444	0.447
0	100	0.038	0.023	0.023	0.047	0.030	0.030	0.056	0.035	0.036
	250	0.145	0.197	0.198	0.136	0.172	0.173	0.118	0.156	0.155
	500	0.336	0.425	0.425	0.312	0.398	0.398	0.271	0.371	0.371
	1000	0.395	0.464	0.464	0.375	0.447	0.447	0.339	0.436	0.436
0.5	100	0.010	0.008	0.007	0.030	0.026	0.015	0.039	0.034	0.018
	250	0.118	0.172	0.175	0.135	0.172	0.162	0.122	0.156	0.146
	500	0.337	0.429	0.430	0.304	0.391	0.388	0.270	0.364	0.359
	1000	0.383	0.460	0.460	0.364	0.442	0.440	0.336	0.435	0.434
0.95	100	0.003	0.004	0.001	0.017	0.022	0.006	0.029	0.035	0.012
	250	0.109	0.163	0.164	0.122	0.162	0.145	0.113	0.152	0.132
	500	0.321	0.411	0.413	0.299	0.380	0.376	0.273	0.368	0.361
	1000	0.377	0.455	0.456	0.364	0.447	0.446	0.322	0.424	0.420

δ	T	c = -20			c = -50			c = -100		
		t_{zx}	Bonf. t	Bonf. Q	t_{zx}	Bonf. t	Bonf. Q	t_{zx}	Bonf. t	Bonf. Q
-0.95	100	0.070	0.039	0.047	0.061	0.046	0.089	0.051	0.041	0.373
	250	0.110	0.131	0.140	0.066	0.096	0.089	0.043	0.066	0.057
	500	0.231	0.339	0.344	0.135	0.275	0.268	0.074	0.197	0.177
	1000	0.292	0.418	0.421	0.197	0.367	0.361	0.120	0.308	0.289
-0.5	100	0.067	0.040	0.047	0.058	0.042	0.059	0.058	0.047	0.239
	250	0.107	0.131	0.136	0.064	0.092	0.088	0.044	0.066	0.060
	500	0.227	0.342	0.346	0.134	0.278	0.273	0.071	0.199	0.188
	1000	0.292	0.410	0.413	0.202	0.379	0.376	0.128	0.322	0.312
0	100	0.060	0.041	0.041	0.062	0.051	0.050	0.059	0.048	0.064
	250	0.095	0.129	0.130	0.060	0.092	0.089	0.043	0.069	0.067
	500	0.229	0.342	0.340	0.131	0.273	0.272	0.077	0.202	0.202
	1000	0.290	0.415	0.415	0.201	0.375	0.375	0.126	0.319	0.319
0.5	100	0.050	0.043	0.026	0.052	0.046	0.044	0.053	0.048	0.067
	250	0.099	0.137	0.126	0.060	0.090	0.086	0.043	0.068	0.072
	500	0.229	0.347	0.341	0.139	0.280	0.275	0.074	0.207	0.211
	1000	0.274	0.404	0.400	0.197	0.373	0.370	0.130	0.319	0.320
0.95	100	0.035	0.038	0.022	0.049	0.049	0.066	0.053	0.056	0.103
	250	0.092	0.132	0.112	0.062	0.092	0.085	0.044	0.068	0.079
	500	0.215	0.337	0.325	0.130	0.272	0.260	0.068	0.206	0.210
	1000	0.273	0.396	0.390	0.196	0.366	0.360	0.123	0.307	0.309

Notes: t_{zx} , *Bonf.t*, and *Bonf.Q* correspond to the test statistics of IVX test, Bonferroni-t test and Bonferroni-Q test. The data generating process is from (4.1) to (4.7).

Table C-30: Finite sample size at 5% significance level of one-sided predictability tests: u_t, v_t is i.i.d from t-distribution with the degree of freedom = 5, collapsing bubble in return with $\tau_1 = 0.6, \tau_2 = 0.9, c_{bub} = 0.2$

δ	T	c = 0			c = -5			c = -10		
		t_{zx}	Bonf. t	Bonf. Q	t_{zx}	Bonf. t	Bonf. Q	t_{zx}	Bonf. t	Bonf. Q
-0.95	100	0.068	0.035	0.040	0.068	0.042	0.052	0.074	0.047	0.057
	250	0.310	0.409	0.409	0.266	0.367	0.372	0.233	0.350	0.355
	500	0.370	0.455	0.455	0.329	0.426	0.428	0.306	0.415	0.419
	1000	0.407	0.477	0.477	0.373	0.453	0.454	0.346	0.444	0.447
-0.5	100	0.053	0.029	0.031	0.066	0.046	0.052	0.063	0.044	0.051
	250	0.302	0.415	0.415	0.268	0.372	0.374	0.221	0.345	0.348
	500	0.365	0.454	0.454	0.343	0.440	0.442	0.298	0.414	0.415
	1000	0.400	0.477	0.477	0.369	0.451	0.451	0.344	0.453	0.454
0	100	0.039	0.027	0.028	0.054	0.043	0.042	0.055	0.044	0.044
	250	0.289	0.408	0.408	0.261	0.371	0.370	0.212	0.343	0.341
	500	0.365	0.452	0.453	0.329	0.424	0.424	0.300	0.419	0.418
	1000	0.401	0.473	0.473	0.371	0.459	0.459	0.334	0.432	0.432
0.5	100	0.027	0.019	0.019	0.048	0.040	0.035	0.057	0.047	0.039
	250	0.280	0.407	0.408	0.258	0.366	0.363	0.226	0.346	0.342
	500	0.371	0.461	0.461	0.329	0.431	0.430	0.298	0.413	0.412
	1000	0.392	0.460	0.459	0.369	0.451	0.450	0.335	0.440	0.439
0.95	100	0.018	0.015	0.014	0.041	0.036	0.028	0.049	0.045	0.033
	250	0.281	0.398	0.399	0.258	0.363	0.358	0.218	0.346	0.338
	500	0.360	0.450	0.450	0.330	0.428	0.427	0.296	0.412	0.409
	1000	0.383	0.457	0.458	0.384	0.464	0.464	0.342	0.453	0.451

δ	T	c = -20			c = -50			c = -100		
		t_{zx}	Bonf. t	Bonf. Q	t_{zx}	Bonf. t	Bonf. Q	t_{zx}	Bonf. t	Bonf. Q
-0.95	100	0.064	0.045	0.049	0.062	0.053	0.063	0.050	0.047	0.173
	250	0.174	0.316	0.320	0.088	0.225	0.221	0.040	0.153	0.147
	500	0.251	0.391	0.393	0.145	0.330	0.327	0.077	0.261	0.251
	1000	0.290	0.424	0.426	0.198	0.386	0.384	0.129	0.353	0.344
-0.5	100	0.062	0.046	0.051	0.053	0.047	0.052	0.049	0.045	0.109
	250	0.169	0.307	0.310	0.083	0.226	0.222	0.037	0.148	0.146
	500	0.236	0.379	0.381	0.146	0.327	0.325	0.080	0.268	0.263
	1000	0.295	0.435	0.437	0.200	0.392	0.390	0.124	0.341	0.338
0	100	0.060	0.048	0.048	0.058	0.052	0.050	0.051	0.047	0.059
	250	0.171	0.322	0.320	0.080	0.225	0.223	0.031	0.140	0.140
	500	0.244	0.387	0.388	0.139	0.334	0.332	0.078	0.270	0.270
	1000	0.294	0.435	0.434	0.192	0.381	0.380	0.130	0.340	0.339
0.5	100	0.057	0.051	0.043	0.055	0.049	0.045	0.050	0.048	0.049
	250	0.166	0.309	0.305	0.081	0.229	0.224	0.033	0.147	0.148
	500	0.246	0.388	0.386	0.147	0.338	0.336	0.072	0.258	0.260
	1000	0.295	0.424	0.422	0.201	0.386	0.385	0.127	0.347	0.347
0.95	100	0.058	0.052	0.037	0.050	0.047	0.044	0.048	0.047	0.059
	250	0.166	0.311	0.302	0.080	0.227	0.219	0.035	0.145	0.148
	500	0.240	0.388	0.384	0.146	0.329	0.324	0.082	0.270	0.275
	1000	0.286	0.420	0.417	0.199	0.380	0.377	0.124	0.341	0.342

Notes: t_{zx} , *Bonf.t*, and *Bonf.Q* correspond to the test statistics of IVX test, Bonferroni-t test and Bonferroni-Q test. The data generating process is from (4.1) to (4.7).

Table C-31: Finite sample size at 5% significance level of one-sided predictability tests: u_t, v_t is i.i.d from t-distribution with the degree of freedom = 5, collapsing bubble in return with $\tau_1 = 0.4, \tau_2 = 0.7, c_{bub} = 0.01$

δ	T	c = 0			c = -5			c = -10		
		t_{zx}	Bonf. t	Bonf. Q	t_{zx}	Bonf. t	Bonf. Q	t_{zx}	Bonf. t	Bonf. Q
-0.95	100	0.118	0.046	0.055	0.104	0.036	0.059	0.090	0.044	0.059
	250	0.104	0.044	0.041	0.099	0.038	0.043	0.086	0.041	0.041
	500	0.102	0.039	0.040	0.099	0.035	0.044	0.087	0.035	0.037
	1000	0.097	0.041	0.040	0.094	0.035	0.043	0.083	0.041	0.045
-0.5	100	0.110	0.047	0.054	0.088	0.036	0.053	0.081	0.034	0.054
	250	0.095	0.042	0.043	0.084	0.033	0.049	0.078	0.033	0.047
	500	0.090	0.040	0.042	0.071	0.029	0.041	0.075	0.035	0.046
	1000	0.078	0.036	0.040	0.072	0.036	0.047	0.072	0.039	0.049
0	100	0.054	0.038	0.039	0.061	0.046	0.046	0.062	0.046	0.046
	250	0.046	0.038	0.037	0.056	0.048	0.048	0.060	0.047	0.048
	500	0.043	0.037	0.038	0.050	0.042	0.042	0.051	0.045	0.045
	1000	0.042	0.034	0.035	0.045	0.043	0.043	0.049	0.044	0.046
0.5	100	0.009	0.014	0.009	0.028	0.037	0.013	0.040	0.047	0.019
	250	0.009	0.017	0.014	0.027	0.039	0.017	0.035	0.045	0.019
	500	0.010	0.016	0.013	0.025	0.034	0.015	0.034	0.042	0.020
	1000	0.009	0.012	0.010	0.029	0.034	0.021	0.038	0.045	0.025
0.95	100	0.001	0.004	0.001	0.010	0.030	0.006	0.021	0.047	0.012
	250	0.001	0.003	0.002	0.011	0.030	0.006	0.017	0.038	0.010
	500	0.001	0.002	0.002	0.012	0.030	0.007	0.019	0.039	0.009
	1000	0.001	0.004	0.001	0.014	0.027	0.006	0.019	0.035	0.009

δ	T	c = -20			c = -50			c = -100		
		t_{zx}	Bonf. t	Bonf. Q	t_{zx}	Bonf. t	Bonf. Q	t_{zx}	Bonf. t	Bonf. Q
-0.95	100	0.068	0.042	0.053	0.056	0.046	0.128	0.049	0.042	0.498
	250	0.076	0.048	0.039	0.064	0.047	0.037	0.047	0.043	0.050
	500	0.078	0.050	0.036	0.062	0.046	0.024	0.060	0.052	0.018
	1000	0.072	0.046	0.039	0.065	0.050	0.030	0.057	0.049	0.015
-0.5	100	0.069	0.041	0.052	0.065	0.048	0.085	0.059	0.048	0.368
	250	0.066	0.042	0.039	0.063	0.049	0.039	0.058	0.049	0.043
	500	0.068	0.042	0.041	0.060	0.048	0.035	0.055	0.047	0.023
	1000	0.062	0.044	0.045	0.061	0.050	0.039	0.057	0.050	0.027
0	100	0.062	0.046	0.045	0.061	0.050	0.047	0.057	0.048	0.063
	250	0.057	0.047	0.048	0.058	0.051	0.049	0.059	0.054	0.054
	500	0.056	0.050	0.051	0.051	0.047	0.045	0.057	0.053	0.051
	1000	0.052	0.046	0.046	0.055	0.053	0.052	0.052	0.050	0.049
0.5	100	0.044	0.051	0.025	0.048	0.050	0.051	0.054	0.058	0.090
	250	0.042	0.049	0.024	0.044	0.049	0.048	0.046	0.051	0.111
	500	0.041	0.047	0.024	0.045	0.049	0.042	0.049	0.052	0.088
	1000	0.042	0.046	0.026	0.046	0.049	0.034	0.047	0.049	0.057
0.95	100	0.029	0.048	0.030	0.033	0.046	0.103	0.040	0.056	0.151
	250	0.028	0.048	0.021	0.033	0.047	0.095	0.037	0.052	0.212
	500	0.027	0.046	0.018	0.036	0.048	0.058	0.038	0.048	0.169
	1000	0.030	0.043	0.015	0.039	0.047	0.034	0.045	0.052	0.094

Notes: t_{zx} , *Bonf.t*, and *Bonf.Q* correspond to the test statistics of IVX test, Bonferroni-t test and Bonferroni-Q test. The data generating process is from (4.1) to (4.7).

Table C-32: Finite sample size at 5% significance level of one-sided predictability tests: u_t, v_t is i.i.d from t-distribution with the degree of freedom = 5, collapsing bubble in return with $\tau_1 = 0.4, \tau_2 = 0.7, c_{bub} = 0.05$

δ	T	c = 0			c = -5			c = -10		
		t_{zx}	Bonf. t	Bonf. Q	t_{zx}	Bonf. t	Bonf. Q	t_{zx}	Bonf. t	Bonf. Q
-0.95	100	0.107	0.038	0.049	0.095	0.033	0.053	0.083	0.038	0.051
	250	0.071	0.024	0.024	0.066	0.026	0.034	0.074	0.034	0.044
	500	0.204	0.186	0.188	0.196	0.194	0.214	0.173	0.174	0.192
	1000	0.346	0.384	0.385	0.342	0.393	0.402	0.322	0.378	0.388
-0.5	100	0.104	0.041	0.050	0.079	0.028	0.047	0.084	0.035	0.053
	250	0.061	0.026	0.027	0.059	0.026	0.035	0.058	0.031	0.039
	500	0.185	0.183	0.185	0.178	0.188	0.199	0.168	0.184	0.197
	1000	0.337	0.390	0.391	0.338	0.396	0.400	0.312	0.377	0.384
0	100	0.051	0.036	0.037	0.059	0.041	0.040	0.059	0.042	0.043
	250	0.029	0.016	0.017	0.041	0.031	0.030	0.048	0.036	0.037
	500	0.158	0.164	0.164	0.165	0.197	0.197	0.162	0.191	0.191
	1000	0.331	0.388	0.389	0.330	0.400	0.400	0.297	0.376	0.376
0.5	100	0.010	0.013	0.009	0.030	0.036	0.015	0.040	0.045	0.018
	250	0.010	0.007	0.007	0.027	0.025	0.017	0.035	0.032	0.021
	500	0.132	0.141	0.146	0.155	0.189	0.181	0.152	0.184	0.172
	1000	0.312	0.373	0.375	0.320	0.391	0.386	0.307	0.382	0.374
0.95	100	0.001	0.003	0.001	0.009	0.026	0.004	0.023	0.041	0.010
	250	0.002	0.002	0.001	0.014	0.017	0.007	0.026	0.030	0.011
	500	0.105	0.127	0.130	0.141	0.174	0.156	0.138	0.176	0.155
	1000	0.298	0.363	0.368	0.317	0.387	0.381	0.289	0.369	0.357

δ	T	c = -20			c = -50			c = -100		
		t_{zx}	Bonf. t	Bonf. Q	t_{zx}	Bonf. t	Bonf. Q	t_{zx}	Bonf. t	Bonf. Q
-0.95	100	0.070	0.044	0.053	0.059	0.046	0.119	0.052	0.042	0.462
	250	0.071	0.042	0.043	0.058	0.048	0.039	0.056	0.050	0.047
	500	0.141	0.156	0.164	0.089	0.114	0.099	0.054	0.083	0.062
	1000	0.281	0.358	0.363	0.185	0.299	0.288	0.111	0.236	0.203
-0.5	100	0.073	0.042	0.050	0.059	0.044	0.073	0.057	0.046	0.323
	250	0.061	0.039	0.040	0.054	0.043	0.037	0.056	0.049	0.042
	500	0.142	0.162	0.170	0.092	0.120	0.112	0.053	0.078	0.065
	1000	0.272	0.356	0.360	0.176	0.292	0.287	0.105	0.232	0.214
0	100	0.062	0.048	0.047	0.058	0.049	0.047	0.061	0.056	0.068
	250	0.051	0.041	0.042	0.058	0.050	0.047	0.051	0.046	0.044
	500	0.132	0.165	0.164	0.078	0.109	0.106	0.057	0.086	0.086
	1000	0.262	0.356	0.356	0.177	0.298	0.297	0.103	0.226	0.226
0.5	100	0.048	0.049	0.027	0.048	0.048	0.048	0.055	0.056	0.081
	250	0.045	0.042	0.028	0.047	0.043	0.040	0.052	0.051	0.072
	500	0.124	0.159	0.147	0.083	0.114	0.108	0.054	0.083	0.090
	1000	0.263	0.356	0.347	0.173	0.296	0.289	0.104	0.234	0.236
0.95	100	0.029	0.044	0.024	0.039	0.048	0.082	0.044	0.054	0.143
	250	0.035	0.038	0.021	0.046	0.048	0.051	0.045	0.045	0.114
	500	0.116	0.154	0.130	0.073	0.106	0.095	0.052	0.078	0.093
	1000	0.255	0.349	0.333	0.174	0.291	0.274	0.099	0.228	0.230

Notes: t_{zx} , *Bonf.t*, and *Bonf.Q* correspond to the test statistics of IVX test, Bonferroni-t test and Bonferroni-Q test. The data generating process is from (4.1) to (4.7).

Table C-33: Finite sample size at 5% significance level of one-sided predictability tests: u_t, v_t is i.i.d from t-distribution with the degree of freedom = 5, collapsing bubble in return with $\tau_1 = 0.4, \tau_2 = 0.7, c_{bub} = 0.1$

δ	T	c = 0			c = -5			c = -10		
		t_{zx}	Bonf. t	Bonf. Q	t_{zx}	Bonf. t	Bonf. Q	t_{zx}	Bonf. t	Bonf. Q
-0.95	100	0.087	0.027	0.034	0.078	0.026	0.041	0.077	0.031	0.044
	250	0.152	0.150	0.151	0.150	0.163	0.178	0.135	0.146	0.165
	500	0.312	0.383	0.384	0.303	0.381	0.387	0.289	0.376	0.384
	1000	0.365	0.437	0.438	0.358	0.437	0.441	0.345	0.434	0.439
-0.5	100	0.071	0.026	0.030	0.071	0.026	0.038	0.066	0.027	0.038
	250	0.130	0.136	0.138	0.143	0.167	0.177	0.124	0.149	0.158
	500	0.296	0.371	0.372	0.299	0.379	0.383	0.278	0.365	0.370
	1000	0.355	0.425	0.425	0.355	0.438	0.440	0.329	0.425	0.428
0	100	0.034	0.017	0.018	0.049	0.029	0.030	0.054	0.036	0.035
	250	0.115	0.129	0.129	0.126	0.161	0.161	0.122	0.155	0.155
	500	0.296	0.378	0.379	0.294	0.380	0.380	0.274	0.369	0.370
	1000	0.360	0.434	0.434	0.348	0.433	0.433	0.336	0.431	0.431
0.5	100	0.009	0.007	0.006	0.030	0.025	0.015	0.037	0.034	0.020
	250	0.087	0.109	0.111	0.121	0.155	0.145	0.113	0.151	0.139
	500	0.275	0.359	0.361	0.283	0.378	0.375	0.268	0.369	0.363
	1000	0.346	0.425	0.427	0.346	0.434	0.432	0.331	0.431	0.428
0.95	100	0.002	0.003	0.001	0.017	0.021	0.004	0.027	0.032	0.010
	250	0.079	0.101	0.103	0.109	0.145	0.131	0.108	0.147	0.126
	500	0.269	0.356	0.360	0.279	0.366	0.360	0.274	0.371	0.363
	1000	0.330	0.418	0.420	0.343	0.427	0.422	0.327	0.423	0.419

δ	T	c = -20			c = -50			c = -100		
		t_{zx}	Bonf. t	Bonf. Q	t_{zx}	Bonf. t	Bonf. Q	t_{zx}	Bonf. t	Bonf. Q
-0.95	100	0.069	0.039	0.048	0.054	0.040	0.090	0.057	0.046	0.372
	250	0.102	0.119	0.128	0.067	0.095	0.088	0.042	0.068	0.059
	500	0.229	0.335	0.339	0.137	0.278	0.271	0.066	0.197	0.177
	1000	0.297	0.415	0.417	0.201	0.370	0.364	0.120	0.319	0.301
-0.5	100	0.066	0.040	0.045	0.061	0.045	0.064	0.057	0.046	0.240
	250	0.103	0.131	0.136	0.059	0.091	0.088	0.042	0.066	0.060
	500	0.235	0.350	0.352	0.133	0.270	0.266	0.066	0.206	0.195
	1000	0.293	0.408	0.409	0.201	0.371	0.369	0.115	0.311	0.302
0	100	0.057	0.039	0.040	0.059	0.047	0.045	0.059	0.052	0.064
	250	0.096	0.130	0.129	0.058	0.091	0.089	0.039	0.067	0.067
	500	0.227	0.343	0.342	0.136	0.273	0.272	0.062	0.201	0.200
	1000	0.284	0.406	0.405	0.197	0.364	0.363	0.122	0.317	0.316
0.5	100	0.044	0.038	0.026	0.052	0.048	0.046	0.053	0.049	0.066
	250	0.090	0.127	0.118	0.063	0.096	0.093	0.038	0.066	0.070
	500	0.218	0.333	0.327	0.117	0.260	0.254	0.060	0.195	0.196
	1000	0.303	0.426	0.423	0.197	0.365	0.360	0.116	0.313	0.314
0.95	100	0.035	0.038	0.021	0.044	0.046	0.058	0.048	0.050	0.105
	250	0.087	0.123	0.105	0.058	0.089	0.084	0.036	0.061	0.075
	500	0.219	0.330	0.319	0.125	0.270	0.262	0.058	0.204	0.208
	1000	0.286	0.406	0.400	0.193	0.363	0.355	0.115	0.315	0.316

Notes: t_{zx} , *Bonf.t*, and *Bonf.Q* correspond to the test statistics of IVX test, Bonferroni-t test and Bonferroni-Q test. The data generating process is from (4.1) to (4.7).

Table C-34: Finite sample size at 5% significance level of one-sided predictability tests: u_t, v_t is i.i.d from t-distribution with the degree of freedom = 5, collapsing bubble in return with $\tau_1 = 0.4, \tau_2 = 0.7, c_{bub} = 0.2$

δ	T	c = 0			c = -5			c = -10		
		t_{zx}	Bonf. t	Bonf. Q	t_{zx}	Bonf. t	Bonf. Q	t_{zx}	Bonf. t	Bonf. Q
-0.95	100	0.058	0.030	0.033	0.072	0.045	0.053	0.068	0.044	0.054
	250	0.256	0.350	0.351	0.250	0.361	0.366	0.229	0.348	0.354
	500	0.326	0.419	0.420	0.318	0.416	0.419	0.292	0.411	0.413
	1000	0.356	0.441	0.441	0.359	0.450	0.452	0.342	0.442	0.443
-0.5	100	0.048	0.027	0.028	0.062	0.042	0.047	0.062	0.043	0.047
	250	0.244	0.348	0.349	0.246	0.356	0.358	0.222	0.339	0.340
	500	0.320	0.416	0.416	0.316	0.419	0.420	0.299	0.416	0.417
	1000	0.360	0.447	0.448	0.351	0.445	0.446	0.345	0.447	0.448
0	100	0.038	0.026	0.026	0.051	0.041	0.041	0.059	0.045	0.044
	250	0.235	0.341	0.341	0.237	0.347	0.347	0.221	0.339	0.338
	500	0.315	0.413	0.413	0.320	0.425	0.425	0.299	0.414	0.414
	1000	0.359	0.449	0.449	0.362	0.450	0.450	0.343	0.449	0.449
0.5	100	0.026	0.019	0.018	0.046	0.040	0.033	0.056	0.048	0.040
	250	0.229	0.337	0.339	0.226	0.347	0.345	0.224	0.349	0.344
	500	0.309	0.405	0.406	0.320	0.424	0.422	0.291	0.412	0.410
	1000	0.354	0.444	0.444	0.352	0.452	0.451	0.340	0.448	0.446
0.95	100	0.018	0.013	0.012	0.042	0.037	0.030	0.046	0.043	0.033
	250	0.223	0.329	0.333	0.231	0.349	0.346	0.214	0.334	0.329
	500	0.311	0.412	0.414	0.313	0.417	0.414	0.283	0.405	0.402
	1000	0.344	0.432	0.434	0.350	0.441	0.440	0.330	0.437	0.434

δ	T	c = -20			c = -50			c = -100		
		t_{zx}	Bonf. t	Bonf. Q	t_{zx}	Bonf. t	Bonf. Q	t_{zx}	Bonf. t	Bonf. Q
-0.95	100	0.072	0.052	0.057	0.055	0.050	0.060	0.049	0.044	0.164
	250	0.170	0.302	0.306	0.081	0.228	0.225	0.027	0.150	0.142
	500	0.242	0.378	0.382	0.141	0.329	0.325	0.062	0.266	0.256
	1000	0.304	0.431	0.434	0.207	0.391	0.388	0.114	0.348	0.339
-0.5	100	0.063	0.048	0.051	0.054	0.048	0.052	0.050	0.047	0.108
	250	0.172	0.306	0.310	0.077	0.228	0.226	0.028	0.150	0.148
	500	0.250	0.390	0.392	0.142	0.331	0.330	0.063	0.267	0.262
	1000	0.293	0.414	0.415	0.200	0.390	0.388	0.118	0.351	0.348
0	100	0.061	0.051	0.049	0.056	0.048	0.047	0.049	0.049	0.059
	250	0.169	0.303	0.301	0.075	0.217	0.213	0.025	0.156	0.156
	500	0.249	0.391	0.391	0.148	0.336	0.336	0.062	0.268	0.268
	1000	0.296	0.431	0.430	0.210	0.393	0.393	0.121	0.345	0.345
0.5	100	0.056	0.048	0.042	0.055	0.051	0.044	0.048	0.048	0.050
	250	0.158	0.296	0.291	0.075	0.222	0.218	0.024	0.144	0.145
	500	0.238	0.384	0.380	0.143	0.332	0.331	0.062	0.259	0.261
	1000	0.292	0.426	0.425	0.196	0.381	0.380	0.118	0.356	0.357
0.95	100	0.054	0.048	0.036	0.048	0.045	0.043	0.049	0.050	0.059
	250	0.164	0.306	0.298	0.075	0.221	0.216	0.026	0.145	0.144
	500	0.244	0.382	0.378	0.144	0.335	0.330	0.060	0.262	0.268
	1000	0.287	0.413	0.411	0.199	0.396	0.392	0.113	0.339	0.340

Notes: t_{zx} , *Bonf.t*, and *Bonf.Q* correspond to the test statistics of IVX test, Bonferroni-t test and Bonferroni-Q test. The data generating process is from (4.1) to (4.7).

Table C-35: Finite sample size at 5% significance level of one-sided predictability tests: u_t, v_t is i.i.d from t-distribution with the degree of freedom = 5, collapsing bubble in return with $\tau_1 = 0.1, \tau_2 = 0.4, c_{bub} = 0.01$

δ	T	c = 0			c = -5			c = -10		
		t_{zx}	Bonf. t	Bonf. Q	t_{zx}	Bonf. t	Bonf. Q	t_{zx}	Bonf. t	Bonf. Q
-0.95	100	0.112	0.050	0.054	0.107	0.036	0.062	0.091	0.042	0.055
	250	0.108	0.046	0.044	0.103	0.033	0.044	0.091	0.043	0.043
	500	0.098	0.042	0.036	0.102	0.037	0.044	0.090	0.041	0.044
	1000	0.100	0.041	0.037	0.096	0.035	0.045	0.083	0.040	0.044
-0.5	100	0.114	0.047	0.053	0.088	0.033	0.053	0.082	0.036	0.053
	250	0.097	0.044	0.048	0.086	0.030	0.049	0.076	0.038	0.050
	500	0.092	0.040	0.044	0.079	0.032	0.045	0.075	0.034	0.046
	1000	0.076	0.038	0.036	0.076	0.036	0.049	0.068	0.036	0.046
0	100	0.049	0.036	0.037	0.062	0.045	0.046	0.062	0.049	0.046
	250	0.049	0.043	0.044	0.055	0.046	0.046	0.053	0.043	0.043
	500	0.044	0.037	0.037	0.054	0.049	0.049	0.051	0.046	0.047
	1000	0.041	0.035	0.035	0.051	0.048	0.048	0.051	0.046	0.046
0.5	100	0.009	0.016	0.011	0.027	0.038	0.012	0.038	0.047	0.018
	250	0.007	0.016	0.015	0.023	0.035	0.014	0.035	0.044	0.020
	500	0.008	0.013	0.013	0.026	0.037	0.016	0.033	0.042	0.019
	1000	0.009	0.012	0.013	0.028	0.033	0.018	0.033	0.041	0.022
0.95	100	0.001	0.003	0.001	0.009	0.028	0.005	0.017	0.039	0.012
	250	0.001	0.003	0.002	0.009	0.029	0.005	0.019	0.044	0.011
	500	0.000	0.002	0.002	0.010	0.026	0.007	0.022	0.044	0.012
	1000	0.001	0.004	0.003	0.012	0.027	0.007	0.019	0.039	0.009

δ	T	c = -20			c = -50			c = -100		
		t_{zx}	Bonf. t	Bonf. Q	t_{zx}	Bonf. t	Bonf. Q	t_{zx}	Bonf. t	Bonf. Q
-0.95	100	0.076	0.049	0.059	0.059	0.046	0.133	0.050	0.042	0.498
	250	0.075	0.045	0.038	0.061	0.047	0.034	0.051	0.045	0.053
	500	0.074	0.045	0.037	0.069	0.053	0.028	0.060	0.051	0.018
	1000	0.083	0.051	0.046	0.065	0.051	0.030	0.059	0.051	0.017
-0.5	100	0.075	0.046	0.053	0.062	0.047	0.083	0.060	0.051	0.355
	250	0.072	0.046	0.045	0.064	0.049	0.038	0.056	0.047	0.038
	500	0.065	0.041	0.041	0.064	0.051	0.036	0.053	0.045	0.022
	1000	0.065	0.046	0.046	0.059	0.051	0.039	0.057	0.051	0.028
0	100	0.063	0.049	0.046	0.062	0.053	0.052	0.061	0.053	0.064
	250	0.061	0.049	0.049	0.055	0.048	0.046	0.058	0.051	0.049
	500	0.056	0.050	0.049	0.055	0.051	0.049	0.051	0.048	0.047
	1000	0.051	0.047	0.048	0.048	0.045	0.045	0.052	0.051	0.049
0.5	100	0.042	0.043	0.023	0.048	0.048	0.052	0.052	0.056	0.092
	250	0.038	0.044	0.022	0.046	0.051	0.047	0.047	0.049	0.110
	500	0.041	0.049	0.024	0.043	0.048	0.039	0.049	0.053	0.085
	1000	0.037	0.044	0.024	0.042	0.043	0.033	0.044	0.046	0.058
0.95	100	0.026	0.045	0.031	0.035	0.051	0.098	0.043	0.056	0.153
	250	0.027	0.045	0.026	0.036	0.053	0.088	0.039	0.051	0.198
	500	0.028	0.044	0.018	0.035	0.049	0.061	0.036	0.047	0.167
	1000	0.030	0.041	0.016	0.038	0.045	0.032	0.040	0.048	0.094

Notes: t_{zx} , *Bonf.t*, and *Bonf.Q* correspond to the test statistics of IVX test, Bonferroni-t test and Bonferroni-Q test. The data generating process is from (4.1) to (4.7).

Table C-36: Finite sample size at 5% significance level of one-sided predictability tests: u_t, v_t is i.i.d from t-distribution with the degree of freedom = 5, collapsing bubble in return with $\tau_1 = 0.1, \tau_2 = 0.4, c_{bub} = 0.05$

δ	T	c = 0			c = -5			c = -10		
		t_{zx}	Bonf. t	Bonf. Q	t_{zx}	Bonf. t	Bonf. Q	t_{zx}	Bonf. t	Bonf. Q
-0.95	100	0.109	0.044	0.049	0.102	0.035	0.058	0.086	0.038	0.054
	250	0.076	0.030	0.031	0.070	0.026	0.035	0.069	0.031	0.042
	500	0.222	0.220	0.220	0.215	0.212	0.232	0.183	0.187	0.204
	1000	0.385	0.435	0.435	0.358	0.408	0.415	0.321	0.381	0.392
-0.5	100	0.106	0.046	0.050	0.089	0.034	0.054	0.080	0.035	0.051
	250	0.060	0.022	0.025	0.061	0.029	0.038	0.061	0.029	0.040
	500	0.205	0.218	0.219	0.193	0.208	0.217	0.164	0.180	0.192
	1000	0.372	0.430	0.431	0.348	0.406	0.409	0.318	0.388	0.392
0	100	0.053	0.037	0.038	0.057	0.043	0.042	0.064	0.044	0.044
	250	0.034	0.020	0.021	0.042	0.033	0.033	0.051	0.037	0.039
	500	0.188	0.222	0.223	0.186	0.217	0.218	0.157	0.194	0.194
	1000	0.363	0.422	0.422	0.339	0.399	0.399	0.308	0.390	0.390
0.5	100	0.008	0.013	0.010	0.032	0.037	0.014	0.038	0.043	0.017
	250	0.009	0.007	0.007	0.025	0.023	0.014	0.034	0.033	0.021
	500	0.158	0.203	0.206	0.169	0.205	0.197	0.148	0.187	0.173
	1000	0.352	0.421	0.425	0.336	0.406	0.404	0.302	0.383	0.377
0.95	100	0.000	0.002	0.001	0.011	0.028	0.007	0.020	0.039	0.010
	250	0.004	0.003	0.003	0.016	0.021	0.008	0.022	0.026	0.010
	500	0.141	0.188	0.190	0.155	0.194	0.177	0.139	0.179	0.154
	1000	0.336	0.412	0.417	0.327	0.395	0.389	0.300	0.380	0.369

δ	T	c = -20			c = -50			c = -100		
		t_{zx}	Bonf. t	Bonf. Q	t_{zx}	Bonf. t	Bonf. Q	t_{zx}	Bonf. t	Bonf. Q
-0.95	100	0.071	0.043	0.058	0.062	0.049	0.121	0.053	0.044	0.466
	250	0.066	0.041	0.041	0.060	0.048	0.041	0.055	0.047	0.045
	500	0.141	0.154	0.163	0.093	0.121	0.109	0.061	0.085	0.062
	1000	0.275	0.359	0.364	0.184	0.299	0.287	0.107	0.231	0.200
-0.5	100	0.078	0.047	0.055	0.064	0.048	0.076	0.058	0.048	0.317
	250	0.063	0.038	0.043	0.053	0.041	0.037	0.052	0.046	0.039
	500	0.137	0.158	0.165	0.086	0.115	0.109	0.058	0.083	0.070
	1000	0.269	0.354	0.361	0.182	0.303	0.296	0.108	0.234	0.216
0	100	0.062	0.050	0.049	0.059	0.051	0.048	0.061	0.051	0.064
	250	0.051	0.042	0.041	0.053	0.044	0.042	0.053	0.046	0.047
	500	0.129	0.158	0.158	0.083	0.114	0.112	0.060	0.084	0.082
	1000	0.258	0.353	0.352	0.174	0.296	0.295	0.099	0.223	0.221
0.5	100	0.049	0.050	0.028	0.053	0.050	0.047	0.051	0.051	0.088
	250	0.042	0.037	0.026	0.045	0.042	0.038	0.050	0.047	0.072
	500	0.123	0.161	0.148	0.082	0.112	0.106	0.057	0.084	0.090
	1000	0.252	0.347	0.339	0.170	0.288	0.281	0.105	0.232	0.234
0.95	100	0.032	0.048	0.025	0.042	0.054	0.091	0.044	0.056	0.139
	250	0.036	0.039	0.021	0.044	0.044	0.048	0.048	0.049	0.116
	500	0.120	0.156	0.132	0.076	0.107	0.096	0.053	0.081	0.092
	1000	0.255	0.355	0.338	0.163	0.284	0.271	0.098	0.223	0.224

Notes: t_{zx} , *Bonf.t*, and *Bonf.Q* correspond to the test statistics of IVX test, Bonferroni-t test and Bonferroni-Q test. The data generating process is from (4.1) to (4.7).

Table C-37: Finite sample size at 5% significance level of one-sided predictability tests: u_t, v_t is i.i.d from t-distribution with the degree of freedom = 5, collapsing bubble in return with $\tau_1 = 0.1, \tau_2 = 0.4, c_{bub} = 0.1$

δ	T	c = 0			c = -5			c = -10		
		t_{zx}	Bonf. t	Bonf. Q	t_{zx}	Bonf. t	Bonf. Q	t_{zx}	Bonf. t	Bonf. Q
-0.95	100	0.084	0.029	0.032	0.085	0.030	0.046	0.083	0.032	0.046
	250	0.175	0.183	0.186	0.154	0.167	0.183	0.137	0.151	0.167
	500	0.344	0.416	0.415	0.317	0.396	0.402	0.289	0.373	0.381
	1000	0.390	0.460	0.459	0.372	0.450	0.453	0.339	0.434	0.437
-0.5	100	0.073	0.027	0.032	0.063	0.026	0.036	0.066	0.029	0.041
	250	0.157	0.180	0.183	0.143	0.167	0.175	0.130	0.152	0.161
	500	0.338	0.415	0.415	0.310	0.390	0.392	0.285	0.384	0.388
	1000	0.386	0.451	0.451	0.370	0.454	0.456	0.345	0.433	0.436
0	100	0.040	0.024	0.025	0.048	0.030	0.030	0.053	0.035	0.034
	250	0.133	0.168	0.170	0.138	0.170	0.170	0.126	0.160	0.161
	500	0.332	0.417	0.418	0.324	0.406	0.406	0.273	0.373	0.373
	1000	0.388	0.462	0.462	0.365	0.442	0.442	0.341	0.439	0.439
0.5	100	0.008	0.006	0.005	0.029	0.026	0.011	0.042	0.034	0.019
	250	0.120	0.167	0.168	0.132	0.171	0.163	0.113	0.152	0.142
	500	0.315	0.399	0.402	0.303	0.390	0.388	0.275	0.372	0.367
	1000	0.383	0.466	0.468	0.362	0.446	0.446	0.325	0.429	0.427
0.95	100	0.002	0.001	0.000	0.014	0.017	0.005	0.028	0.033	0.012
	250	0.105	0.154	0.155	0.125	0.164	0.145	0.115	0.157	0.137
	500	0.306	0.398	0.402	0.307	0.387	0.385	0.265	0.362	0.354
	1000	0.387	0.461	0.464	0.354	0.429	0.428	0.327	0.427	0.423

δ	T	c = -20			c = -50			c = -100		
		t_{zx}	Bonf. t	Bonf. Q	t_{zx}	Bonf. t	Bonf. Q	t_{zx}	Bonf. t	Bonf. Q
-0.95	100	0.064	0.040	0.045	0.057	0.042	0.087	0.055	0.042	0.384
	250	0.105	0.126	0.135	0.068	0.100	0.091	0.042	0.068	0.059
	500	0.225	0.326	0.333	0.140	0.275	0.266	0.073	0.208	0.186
	1000	0.292	0.408	0.412	0.199	0.377	0.372	0.116	0.312	0.296
-0.5	100	0.065	0.035	0.043	0.059	0.044	0.064	0.058	0.047	0.244
	250	0.108	0.136	0.141	0.068	0.098	0.094	0.043	0.066	0.060
	500	0.226	0.335	0.339	0.131	0.274	0.270	0.068	0.201	0.190
	1000	0.287	0.405	0.407	0.205	0.378	0.375	0.123	0.314	0.305
0	100	0.060	0.041	0.042	0.060	0.044	0.042	0.056	0.048	0.057
	250	0.101	0.134	0.132	0.063	0.096	0.093	0.043	0.069	0.067
	500	0.224	0.341	0.340	0.137	0.279	0.277	0.066	0.200	0.201
	1000	0.288	0.408	0.408	0.200	0.374	0.373	0.122	0.314	0.314
0.5	100	0.047	0.040	0.026	0.056	0.050	0.047	0.056	0.052	0.066
	250	0.096	0.131	0.121	0.063	0.092	0.087	0.041	0.068	0.071
	500	0.230	0.347	0.340	0.129	0.261	0.258	0.070	0.199	0.206
	1000	0.290	0.418	0.414	0.195	0.364	0.361	0.117	0.321	0.320
0.95	100	0.037	0.040	0.021	0.047	0.047	0.062	0.049	0.051	0.108
	250	0.094	0.133	0.115	0.057	0.088	0.082	0.038	0.063	0.076
	500	0.214	0.331	0.319	0.126	0.264	0.255	0.067	0.200	0.203
	1000	0.269	0.400	0.393	0.193	0.364	0.358	0.119	0.315	0.318

Notes: t_{zx} , *Bonf.t*, and *Bonf.Q* correspond to the test statistics of IVX test, Bonferroni-t test and Bonferroni-Q test. The data generating process is from (4.1) to (4.7).

Table C-38: Finite sample size at 5% significance level of one-sided predictability tests: u_t, v_t is i.i.d from t-distribution with the degree of freedom = 5, collapsing bubble in return with $\tau_1 = 0.1, \tau_2 = 0.4, c_{bub} = 0.2$

δ	T	c = 0			c = -5			c = -10		
		t_{zx}	Bonf. t	Bonf. Q	t_{zx}	Bonf. t	Bonf. Q	t_{zx}	Bonf. t	Bonf. Q
-0.95	100	0.067	0.036	0.039	0.072	0.045	0.055	0.069	0.043	0.054
	250	0.286	0.390	0.388	0.263	0.368	0.374	0.224	0.334	0.340
	500	0.373	0.457	0.457	0.328	0.421	0.425	0.296	0.410	0.413
	1000	0.397	0.467	0.467	0.375	0.452	0.452	0.340	0.443	0.445
-0.5	100	0.056	0.032	0.034	0.063	0.045	0.050	0.068	0.049	0.054
	250	0.279	0.387	0.386	0.267	0.369	0.371	0.220	0.338	0.341
	500	0.358	0.449	0.449	0.337	0.434	0.436	0.301	0.415	0.417
	1000	0.404	0.474	0.473	0.377	0.457	0.458	0.340	0.442	0.444
0	100	0.043	0.030	0.031	0.054	0.042	0.042	0.066	0.053	0.052
	250	0.279	0.390	0.391	0.258	0.369	0.369	0.224	0.348	0.348
	500	0.355	0.452	0.452	0.340	0.441	0.442	0.290	0.408	0.408
	1000	0.394	0.469	0.469	0.376	0.453	0.453	0.347	0.450	0.450
0.5	100	0.032	0.024	0.023	0.052	0.045	0.041	0.052	0.044	0.038
	250	0.273	0.384	0.387	0.255	0.369	0.365	0.215	0.339	0.335
	500	0.352	0.449	0.450	0.328	0.422	0.422	0.293	0.416	0.414
	1000	0.389	0.464	0.464	0.366	0.451	0.451	0.330	0.435	0.434
0.95	100	0.020	0.018	0.016	0.038	0.036	0.029	0.051	0.045	0.033
	250	0.265	0.377	0.379	0.246	0.365	0.360	0.208	0.330	0.322
	500	0.356	0.441	0.442	0.333	0.433	0.430	0.297	0.415	0.413
	1000	0.394	0.467	0.468	0.363	0.445	0.445	0.339	0.445	0.443

δ	T	c = -20			c = -50			c = -100		
		t_{zx}	Bonf. t	Bonf. Q	t_{zx}	Bonf. t	Bonf. Q	t_{zx}	Bonf. t	Bonf. Q
-0.95	100	0.066	0.050	0.057	0.059	0.052	0.061	0.054	0.047	0.166
	250	0.173	0.308	0.312	0.080	0.228	0.225	0.028	0.146	0.141
	500	0.242	0.387	0.391	0.145	0.340	0.337	0.071	0.260	0.251
	1000	0.291	0.422	0.425	0.201	0.390	0.388	0.123	0.340	0.332
-0.5	100	0.062	0.047	0.050	0.059	0.051	0.053	0.051	0.045	0.107
	250	0.165	0.293	0.295	0.083	0.233	0.230	0.028	0.147	0.145
	500	0.245	0.391	0.393	0.146	0.329	0.328	0.075	0.266	0.262
	1000	0.287	0.423	0.424	0.203	0.391	0.390	0.130	0.350	0.347
0	100	0.064	0.052	0.052	0.052	0.047	0.048	0.055	0.050	0.063
	250	0.172	0.314	0.312	0.082	0.231	0.229	0.027	0.143	0.142
	500	0.244	0.386	0.386	0.142	0.322	0.321	0.075	0.269	0.268
	1000	0.287	0.428	0.428	0.197	0.395	0.394	0.121	0.342	0.342
0.5	100	0.063	0.052	0.044	0.052	0.046	0.044	0.053	0.051	0.052
	250	0.169	0.309	0.304	0.081	0.227	0.222	0.029	0.148	0.147
	500	0.235	0.379	0.376	0.150	0.335	0.331	0.073	0.264	0.266
	1000	0.291	0.428	0.426	0.200	0.388	0.386	0.129	0.349	0.351
0.95	100	0.051	0.048	0.038	0.052	0.048	0.043	0.049	0.049	0.060
	250	0.160	0.306	0.295	0.074	0.221	0.214	0.031	0.149	0.149
	500	0.243	0.386	0.382	0.136	0.330	0.326	0.074	0.267	0.271
	1000	0.284	0.429	0.426	0.192	0.378	0.375	0.123	0.347	0.349

Notes: t_{zx} , *Bonf.t*, and *Bonf.Q* correspond to the test statistics of IVX test, Bonferroni-t test and Bonferroni-Q test. The data generating process is from (4.1) to (4.7).

Table C-39: Unit root tests for regressors

Predictor	$\hat{\pi}$	ADF	DF-GLS	PP
Dividend payout ratio (d/e)	0.9915	-4.409***	-3.946***	-4.495***
Long-term yield (lty)	0.9962	-1.223	-1.149	-1.183
Dividend yield (d/y)	0.9943	-1.796	-1.029	-1.745
Dividend-price ratio (d/p)	0.9943	-1.721	-1.030	-1.752
T-bill rate (tbl)	0.9928	-2.310	-2.236**	-2.117
Earnings-price ratio (e/p)	0.9876	-3.789***	-2.438**	-3.712***
Book-to-market value ratio (b/m)	0.9867	-2.969**	-2.936***	-2.62*
Default yield spread (dfy)	0.9741	-4.063***	-3.971***	-3.88***
Net equity expansion (ntis)	0.9817	-4.957***	-3.421***	-4.106***
Term spread (tms)	0.9614	-5.298***	-3.013***	-4.846***
Inflation rate (inf)	0.4845	-9.592***	-1.007	-21.532***
Stock variance (svar)	0.5767	-7.207***	-4.572***	-18.491***
Long-term rate of return (ltr)	0.0488	-24.615***	-8.642***	-32.064***
Default return spread (dfr)	0.5357	-2.514**	-2.307**	-20.81***

Notes: This table presents the results of four unit root tests' results for 14 predictive variables: dividend payout ratio (d/e), long-term yield (lty), dividend yield (d/y), dividend-price ratio (d/p), T-bill rate (tbl), earnings-price ratio (e/p), book-to-market value (b/m), default yield spread (dfy), net equity expansion (ntis), term spread (tms), inflation rate (inf), stock variance (svar), long-term rate of returns (ltr) and default return spread (dfr). The sample period is span from 01/1927 to 12/2021. As in [Yang et al. \(2022\)](#), $\hat{\pi}$ indicates the least square estimate of π in the AR(1) process: $x_t = s + \pi x_{t-1} + e_t$. ADF stands for the test statistic of the Augmented Dickey-Fuller test by Said and Dickey (1984). DF-GLS stands for the statistic from an ADF-type test by Elliott et al. (1996). PP represents the test statistic from the Phillips-Perron test by Phillips and Perron (1988). *, ** and *** respectively indicate rejection of the null hypothesis of a unit root (for ADF, DF-GLS, and PP tests) at 10%, 5% and 1% level.

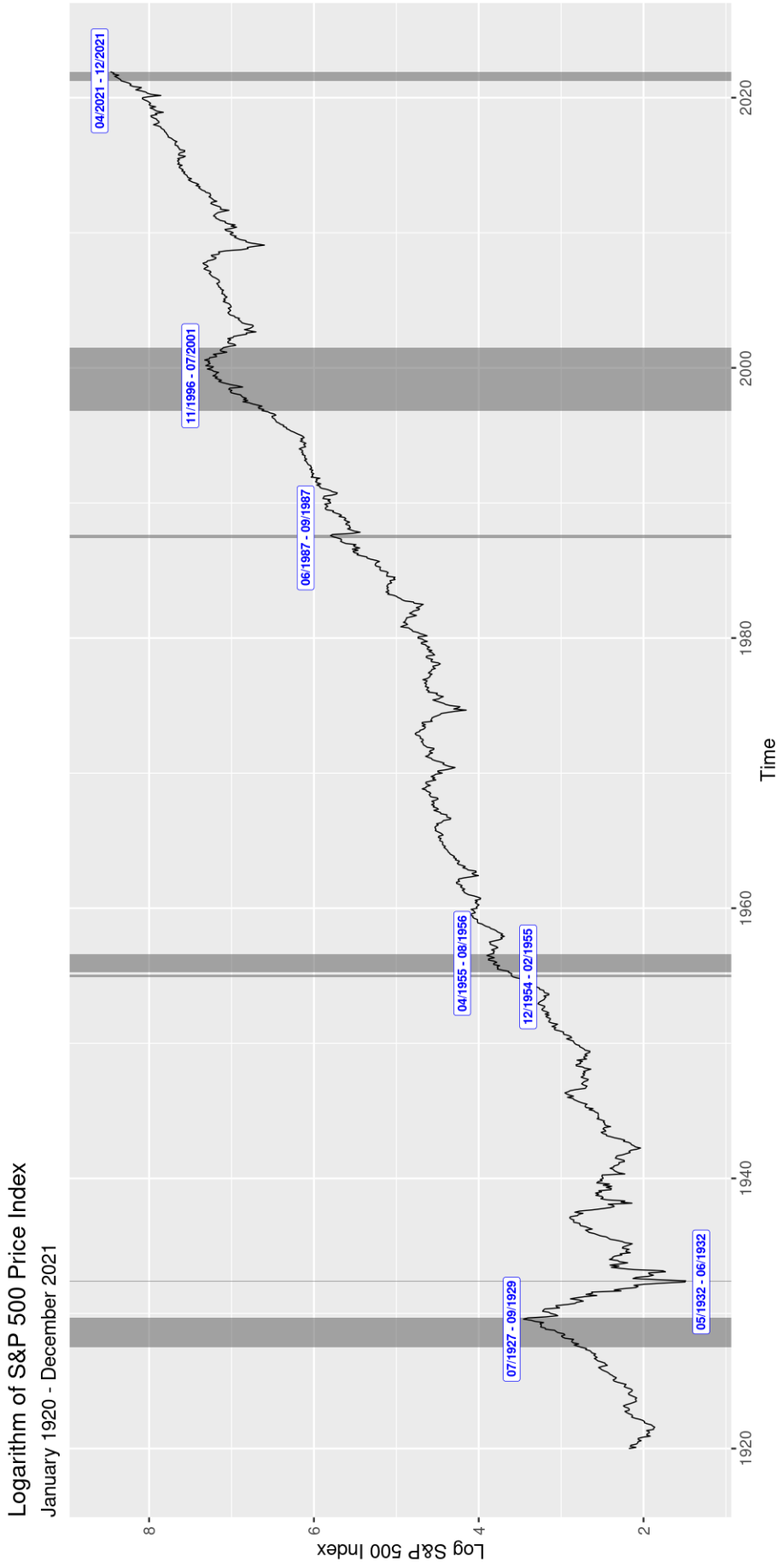


Figure C-1: Date-stamping the logarithm of monthly S&P 500 price index from 01/1920 to 12/2021

Table C-40: Empirical results for the Welch and Goyal (2008) predictive regressions

Regressor	d/e	lty	d/y	d/p	tbl	e/p	b/m
Panel A: January 1927 – December 2021							
IVX coefficient	0.000	-0.103*	0.008*	0.007	-0.108*	0.008*	0.015**
Bonf.t 90% CI	[-0.004, 0.004]	[-0.009, -0.000]	[0.001, 0.012]	[-0.005, 0.009]	[-0.012, -0.001]	[-0.001, 0.014]	[-0.001, 0.017]
Bonf.Q 90% CI	[-0.004, 0.004]	[-0.008, 0.000]	[0.000, 0.012]	[-0.003, 0.005]	[-0.012, -0.001]	[-0.005, 0.011]	[0.002, 0.020]
Panel B: October 1987 – October 1996							
IVX coefficient	-0.018	0.145	0.015	0.021	0.102	0.025*	0.041
Bonf.t 90% CI	[-0.011, 0.003]	[-0.060, 0.035]	[-0.028, 0.063]	[-0.054, 0.034]	[-0.013, 0.019]	[-0.025, 0.039]	[-0.044, 0.029]
Bonf.Q 90% CI	[-0.011, 0.002]	[-0.060, 0.033]	[-0.028, 0.064]	[-0.035, 0.018]	[-0.012, 0.020]	[-0.019, 0.058]	[-0.038, 0.027]
Panel C: October 1987 – July 2001							
IVX coefficient	-0.006	0.027	0.007	0.008	0.002	0.018*	0.017
Bonf.t 90% CI	[-0.005, 0.005]	[-0.030, 0.027]	[-0.006, 0.025]	[-0.016, 0.017]	[-0.016, 0.015]	[-0.016, 0.031]	[-0.019, 0.017]
Bonf.Q 90% CI	[-0.005, 0.005]	[-0.031, 0.024]	[-0.006, 0.024]	[-0.020, 0.010]	[-0.016, 0.015]	[-0.009, 0.029]	[-0.021, 0.013]
Panel D: October 1987 – March 2021							
IVX coefficient	0.002	-0.115	0.015*	0.016	-0.027	0.007	0.036
Bonf.t 90% CI	[-0.007, 0.011]	[-0.014, 0.004]	[0.002, 0.027]	[-0.009, 0.020]	[-0.007, 0.004]	[-0.008, 0.022]	[-0.013, 0.028]
Bonf.Q 90% CI	[-0.008, 0.011]	[-0.014, 0.004]	[0.002, 0.027]	[-0.010, 0.007]	[-0.007, 0.004]	[-0.020, 0.010]	[-0.018, 0.016]

Notes: This table shows the results of predictive regression models during full sample (01/1927-12/2021) and subsamples (10/1987-03/2021, 10/1987-10/1996, and 10/1987-07/2021). In panels, the dependent variable is the monthly S&P 500 value-weighted log excess returns (including dividends). There are fourteen lagged persistent regressors: dividend payout ratio (d/e), long-term yield (lty), dividend yield (d/y), dividend-price ratio (d/p), T-bill rate (tbl), earnings-price ratio (e/p), book-to-market value (b/m), default yield spread (dfy), net equity expansion (ntis), term spread (tms), inflation rate (inf), stock variance (svar), long-term rate of returns (ltr) and default return spread (dfr). IVX coefficient is the estimated coefficient of the predictor. *, **, and *** imply rejection of the null hypothesis at 5%, 2.5%, and 0.5% level, respectively. The 90% Bonferroni confidence intervals of Bonf.t and Bonf.Q test for the bias-corrected scaled least-squares slope coefficient are represented in the squared brackets. Bold indicates rejection of the null hypothesis of no predictability at the 10% level on two tails.

Table C-41: Empirical results for the Welch and Goyal (2008) predictive regressions (continued)

Regressor	dfy	ntis	tms	inf	svar	ltr	dfr
Panel A: January 1927 – December 2021							
IVX coefficient	0.354	-0.168**	0.151	-0.531	0.107	0.099	-0.108**
Bonf.t 90% CI	[-0.001, 0.021]	[-0.023, -0.004]	[-0.002, 0.024]	[-0.082, 0.001]	[-0.028, 0.049]	[-0.002, 0.095]	[-0.089, -0.014]
Bonf.Q 90% CI	[-0.001, 0.022]	[-0.023, -0.004]	[-0.002, 0.024]	[-0.074, 0.010]	[-0.074, 0.011]	[0.012, 0.111]	[-0.101, -0.025]
Panel B: October 1987 – October 1996							
IVX coefficient	1.718	-0.126	-0.121	-1.154	-2.123	0.098	-0.071
Bonf.t 90% CI	[-0.023, 0.063]	[-0.039, 0.016]	[-0.059, 0.019]	[-0.223, 0.082]	[-0.053, 0.157]	[-0.098, 0.210]	[-0.210, 0.100]
Bonf.Q 90% CI	[-0.024, 0.061]	[-0.037, 0.018]	[-0.053, 0.033]	[-0.162, 0.186]	[-0.171, 0.046]	[0.117, 0.459]	[-0.330, 0.033]
Panel C: October 1987 – July 2001							
IVX coefficient	0.868	0.014	0.013	-2.238*	-1.400	-0.001	-0.020
Bonf.t 90% CI	[-0.023, 0.050]	[-0.025, 0.025]	[-0.032, 0.033]	[-0.235, 0.017]	[-0.085, -0.002]	[-0.116, 0.135]	[-0.141, 0.109]
Bonf.Q 90% CI	[-0.025, 0.046]	[-0.023, 0.028]	[-0.029, 0.036]	[-0.214, 0.053]	[-0.180, -0.097]	[0.056, 0.324]	[-0.222, 0.056]
Panel D: October 1987 – March 2021							
IVX coefficient	-0.388	0.120	-0.102	0.006	-0.105	0.072	-0.074
Bonf.t 90% CI	[-0.027, 0.015]	[-0.007, 0.024]	[-0.022, 0.012]	[-0.073, 0.068]	[-0.099, 0.027]	[-0.029, 0.134]	[-0.142, 0.009]
Bonf.Q 90% CI	[-0.031, 0.013]	[-0.007, 0.024]	[-0.022, 0.011]	[-0.075, 0.067]	[-0.309, -0.187]	[-0.060, 0.108]	[-0.095, 0.059]

Notes: This table shows the results of predictive regression models during full sample (01/1927-12/2021) and subsamples (10/1987-03/2021, 10/1987-10/1996, and 10/1987-07/2021). In panels, the dependent variable is the monthly S&P 500 value-weighted log excess returns (including dividends). There are fourteen lagged persistent regressors: dividend payout ratio (d/e), long-term yield (lty), dividend yield (d/y), dividend-price ratio (d/p), T-bill rate (tbl), earnings-price ratio (e/p), book-to-market value (b/m), default yield spread (dfy), net equity expansion (ntis), term spread (tms), inflation rate (inf), stock variance (svar), long-term rate of returns (ltr) and default return spread (dfr). IVX coefficient is the estimated coefficient of the predictor. *, **, and *** imply rejection of the null hypothesis at 5%, 2.5%, and 0.5% level, respectively. The 90% Bonferroni confidence intervals of Bonf.t and Bonf.Q test for the bias-corrected scaled least-squares slope coefficient are represented in the squared brackets. Bold indicates rejection of the null hypothesis of no predictability at the 10% level on two tails.

Bibliography

- Abel, A. B., Mankiw, N. G., Summers, L. H., and Zeckhauser, R. J. (1986). Assessing Dynamic Efficiency: Theory and Evidence. Working Paper 2097, National Bureau of Economic Research.
- Allen, F. and Gale, D. (2000). Bubbles and Crises. *The Economic Journal*, 110(460):236–255.
- Andreou, E. and Ghysels, E. (2002). Detecting Multiple Breaks in Financial Market Volatility Dynamics. *Journal of Applied Econometrics*, 17(5):579–600.
- Andrews, D. W. K. (1991). Heteroskedasticity and Autocorrelation Consistent Covariance Matrix Estimation. *Econometrica*, 59(3):817–858.
- Ang, A. and Bekaert, G. (2007). Stock Return Predictability: Is it There? *The Review of Financial Studies*, 20(3):651–707.
- Astill, S., Harvey, D. I., Leybourne, S. J., Sollis, R., and Robert Taylor, A. M. (2018). Real-Time Monitoring for Explosive Financial Bubbles. *Journal of Time Series Analysis*, 39(6):863–891.
- Astill, S., Harvey, D. I., Leybourne, S. J., and Taylor, A. M. R. (2017). Tests for an End-of-sample Bubble in Financial Time Series. *Econometric Reviews*, 36(6-9):651–666.
- Astill, S., Harvey, D. I., Leybourne, S. J., Taylor, A. M. R., and Zu, Y. (2021). CUSUM-Based Monitoring for Explosive Episodes in Financial Data in the Presence of Time-Varying Volatility. *Journal of Financial Econometrics*, 21(1):187–227.

-
- Bai, J. and Perron, P. (1998). Estimating and Testing Linear Models with Multiple Structural Changes. *Econometrica*, 66(1):47–78.
- Barsky, R., Epstein, C., Lafont-Mueller, A., and Yoo, Y. (2021). What Drives Gold Prices? Technical Report 464, Chicago Fed Letter. Federal Reserve Bank of Chicago.
- Baur, D. G. and Tran, D. T. (2014). The Long-run Relationship of Gold and Silver and the Influence of Bubbles and Financial Crises. *Empirical Economics*, 47(16):1525–1541.
- Bettendorf, T. and Chen, W. (2013). Are there Bubbles in the Sterling-dollar Exchange Rate? New Evidence from Sequential ADF Tests. *Economics Letters*, 120(2):350–353.
- Bhargava, A. (1986). On the Theory of Testing for Unit Roots in Observed Time Series. *The Review of Economic Studies*, 53(3):369–384.
- Blanchard, O. J. and Watson, M. W. (1982). Bubbles, Rational Expectations and Financial Markets. Working Paper 945, National Bureau of Economic Research.
- Bohl, M. T., Kaufmann, P., and Stephan, P. M. (2013). From Hero to Zero: Evidence of Performance Reversal and Speculative Bubbles in German Renewable Energy Stocks. *Energy Economics*, 37:40–51.
- Bollerslev, T. and Zhou, H. (2002). Estimating stochastic volatility diffusion using conditional moments of integrated volatility. *Journal of Econometrics*, 109(1):33–65.
- Boswijk, H. P. and Zu, Y. (2018). Adaptive Wild Bootstrap Tests for a Unit Root With Non-stationary Volatility. *The Econometrics Journal*, 21(2):87–113.
- Boudoukh, J., Richardson, M., and Whitelaw, R. F. (2006). The Myth of Long-Horizon Predictability. *The Review of Financial Studies*, 21(4):1577–1605.
- Breitung, J. and Demetrescu, M. (2015). Instrumental Variable and Variable Addition based Inference in Predictive Regressions. *Journal of Econometrics*, 187(1):358–375.

-
- Breitung, J. and Kruse, R. (2013). When Bubbles Burst: Econometric Tests based on Structural Breaks. *Statistical Papers*, 54:911–930.
- Busetti, F. and Taylor, A. M. R. (2003). Variance Shifts, Structural Breaks, and Stationarity Tests. *Journal of Business & Economic Statistics*, 21(4):510–531.
- Campbell, J. Y. (1991). A Variance Decomposition for Stock Returns. *The Economic Journal*, 101(405):157–179.
- Campbell, J. Y., Lo, A. W., and MacKinlay, A. (1997). *The Econometrics of Financial Markets*. Princeton University Press.
- Campbell, J. Y. and Shiller, R. J. (1988a). Stock Prices, Earnings, and Expected Dividends. *The Journal of Finance*, 43(3):661–676.
- Campbell, J. Y. and Shiller, R. J. (1988b). The Dividend-Price Ratio and Expectations of Future Dividends and Discount Factors. *The Review of Financial Studies*, 1(3):195–228.
- Campbell, J. Y. and Yogo, M. (2006). Efficient Tests of Stock Return Predictability. *Journal of Financial Economics*, 81(1):27–60.
- Caspi, I., Katzke, N., and Gupta, R. (2018). Date Stamping Historical Periods of Oil Price Explosivity: 1876–2014. *Energy Economics*, 70:582–587.
- Cavaliere, G. (2005). Unit Root Tests under Time-Varying Variances. *Econometric Reviews*, 23(3):259–292.
- Cavaliere, G. and Taylor, A. M. R. (2009). Heteroskedastic Time Series with a Unit Root. *Econometric Theory*, 25(5):1228–1276.
- Cavaliere, G. and Taylor, A. R. (2007). Testing for Unit Roots in Time Series Models with Non-stationary Volatility. *Journal of Econometrics*, 140(2):919–947.
- Cavanagh, C. L., Elliott, G., and Stock, J. H. (1995). Inference in Models with Nearly Integrated Regressors. *Econometric Theory*, 11(5):1131–1147.

-
- Chang, Y. and Park, J. Y. (2002). On The Asymptotics of ADF Tests For Unit Roots. *Econometric Reviews*, 21(4):431–447.
- Chu, C.-S. J., Stinchcombe, M., and White, H. (1996). Monitoring Structural Change. *Econometrica*, 64(5):1045–1065.
- Cochrane, J. H. (1992). Explaining the Variance of Price–Dividend Ratios. *The Review of Financial Studies*, 5(2):243–280.
- Corbet, S., Lucey, B., and Yarovaya, L. (2018). Datestamping the Bitcoin and Ethereum Bubbles. *Finance Research Letters*, 26:81–88.
- Cuñado, J., Gil-Alana, L., and de Gracia, F. P. (2005). A Test for Rational Bubbles in the NASDAQ Stock Index: A Fractionally Integrated Approach. *Journal of Banking & Finance*, 29(10):2633–2654.
- de Pooter, M. and van Dijk, D. (2004). Testing for Changes in Volatility in Heteroskedastic Time Series - A Further Examination. Technical report, Erasmus University Rotterdam.
- Demetrescu, M., Georgiev, I., Rodrigues, P. M., and Taylor, A. R. (2022a). Extensions to IVX Methods of Inference for Return Predictability. *Journal of Econometrics*.
- Demetrescu, M., Georgiev, I., Rodrigues, P. M., and Taylor, A. R. (2022b). Testing for Episodic Predictability in Stock Returns. *Journal of Econometrics*, 227(1):85–113. Annals Issue: Time Series Analysis of Higher Moments and Distributions of Financial Data.
- Demetrescu, M. and Hillmann, B. (2022). Nonlinear Predictability of Stock Returns? Parametric Versus Nonparametric Inference in Predictive Regressions. *Journal of Business & Economic Statistics*, 40(1):382–397.
- Deng, Y., Girardin, E., Joyeux, R., and Shi, S. (2017). Did Bubbles Migrate from the Stock to the Housing Market in China between 2005 and 2010? *Pacific Economic Review*, 22(3):276–292.

-
- Dezhbakhsh, H. and Demirguc-Kunt, A. (1990). On the Presence of Speculative Bubbles in Stock Prices. *The Journal of Financial and Quantitative Analysis*, 25(1):101–112.
- Diba, B. T. and Grossman, H. I. (1988). Explosive Rational Bubbles in Stock Prices? *The American Economic Review*, 78(3):520–530.
- Dickey, D. A. and Fuller, W. A. (1979). Distribution of the Estimators for Autoregressive Time Series With a Unit Root. *Journal of the American Statistical Association*, 74(366):427–431.
- Elliott, G., Rothenberg, T. J., and Stock, J. H. (1996). Efficient Tests for an Autoregressive Unit Root. *Econometrica*, 64(4):813–836.
- Elliott, G. and Stock, J. H. (1994). Inference in Time Series Regression When the Order of Integration of a Regressor Is Unknown. *Econometric Theory*, 10(3/4):672–700.
- Elliott, G. and Stock, J. H. (2001). Confidence Intervals for Autoregressive Coefficients Near One. *Journal of Econometrics*, 103(1):155–181. Studies in estimation and testing.
- Engsted, T., Hviid, S. J., and Pedersen, T. Q. (2016). Explosive Bubbles in House Prices? Evidence from the OECD Countries. *Journal of International Financial Markets, Institutions and Money*, 40:14–25.
- Engsted, T. and Nielsen, B. (2012). Testing for Rational Bubbles in a Coexplosive Vector Autoregression. *The Econometrics Journal*, 15(2):226–254.
- Escobari, D., Garcia, S., and Mellado, C. (2017). Identifying Bubbles in Latin American Equity Markets: Phillips-Perron-based Tests and Linkages. *Emerging Markets Review*, 33:90–101.
- Escribano, A. and Granger, C. W. J. (1998). Investigating the Relationship Between Gold and Silver Prices. *Journal of Forecasting*, 17(2):81–107.
- Etienne, X. L., Irwin, S. H., and Garcia, P. (2014). Bubbles in Food Commodity Markets: Four Decades of Evidence. *Journal of International Money and Finance*, 42:129–155. Understanding International Commodity Price Fluctuations.

-
- Evans, G. W. (1991). Pitfalls in Testing for Explosive Bubbles in Asset Prices. *The American Economic Review*, 81(4):922–930.
- Evripidou, A. C., Harvey, D. I., Leybourne, S. J., and Sollis, R. (2022). Testing for Co-explosive Behaviour in Financial Time Series. *Oxford Bulletin of Economics and Statistics*, 84(3):624–650.
- Fama, E. F. (1965). Random Walks in Stock Market Prices. *Financial Analysts Journal*, 21(5):55–59.
- Fama, E. F. (1970). Efficient Capital Markets: A Review of Theory and Empirical Work. *The Journal of Finance*, 25(2):383–417.
- Fama, E. F. (1990a). Stock Returns, Expected Returns, and Real Activity. *The Journal of Finance*, 45(4):1089–1108.
- Fama, E. F. (1990b). Stock Returns, Expected Returns, and Real Activity. *The Journal of Finance*, 45(4):1089–1108.
- Fama, E. F. and French, K. R. (1988a). Dividend yields and expected stock returns. *Journal of Financial Economics*, 22(1):3–25.
- Fama, E. F. and French, K. R. (1988b). Permanent and Temporary Components of Stock Prices. *Journal of Political Economy*, 96(2):246–273.
- Fama, E. F. and French, K. R. (1989). Business Conditions and Expected Returns on Stocks and Bonds. *Journal of Financial Economics*, 25(1):23–49.
- Figuerola-Ferretti, I., Gilbert, C. L., and McCrorie, J. R. (2015). Testing for Mild Explosivity and Bubbles in LME Non-Ferrous Metals Prices. *Journal of Time Series Analysis*, 36(5):763–782.
- Figuerola-Ferretti, I. and McCrorie, J. R. (2016). The Shine of Precious Metals around the Global Financial Crisis. *Journal of Empirical Finance*, 38:717–738. Recent developments in financial econometrics and empirical finance.

-
- Flood, R. P. and Hodrick, R. J. (1990). On Testing for Speculative Bubbles. *Journal of Economic Perspectives*, 4(2):85–101.
- Frömmel, M. and Kruse, R. (2012). Testing for a Rational Bubble under Long Memory. *Quantitative Finance*, 12(11):1723–1732.
- Garber, P. M. (1990). Famous First Bubbles. *The Journal of Economic Perspectives*, 4(2):35–54.
- Gilbert, L. C. (2010). Speculative Influences on Commodity Futures Prices 2006–2008. UNCTAD Discussion Papers 197. United Nations Conference on Trade and Development. Url: https://unctad.org/system/files/official-document/osgdp20101_en.pdf.
- Gomez-Gonzalez, J. E., Gamboa-Arbeláez, J., Hirs-Garzón, J., and Pinchao-Rosero, A. (2018). When Bubble Meets Bubble: Contagion in OECD Countries. *The Journal of Real Estate Finance and Economics*, 56:546–566.
- Gonzalo, J. and Pitarakis, J.-Y. (2012). Regime-Specific Predictability in Predictive Regressions. *Journal of Business & Economic Statistics*, 30(2):229–241.
- Goyal, A., Welch, I., and Zafirov, A. (2021). A Comprehensive Look at the Empirical Performance of Equity Premium Prediction II. Swiss Finance Institute Research Paper Series 21-85, Swiss Finance Institute.
- Greenaway-McGrevy, R. and Phillips, P. C. (2016). Hot Property in New Zealand: Empirical Evidence of Housing Bubbles in the Metropolitan Centres. *New Zealand Economic Papers*, 50(1):88–113.
- Gregory Mankiw, N. and Shapiro, M. D. (1986). Do We Reject Too Often?: Small Sample Properties of Tests of Rational Expectations Models. *Economics Letters*, 20(2):139–145.
- Gutierrez, L. (2012). Speculative Bubbles in Agricultural Commodity Markets†. *European Review of Agricultural Economics*, 40(2):217–238.

-
- Gürkaynak, R. S. (2008). Econometric Tests of Asset Price Bubbles: Taking Stock. *Journal of Economic Surveys*, 22(1):166–186.
- Hafner, C. M. (2018). Testing for Bubbles in Cryptocurrencies with Time-Varying Volatility. *Journal of Financial Econometrics*, 18(2):233–249.
- Hamori, S. and Tokihisa, A. (1997). Testing for a Unit Root in the Presence of a Variance Shift. *Economics Letters*, 57(3):245–253.
- Harvey, D. I., Leybourne, S. J., Sollis, R., and Taylor, A. R. (2016). Tests for Explosive Financial Bubbles in the Presence of Non-stationary Volatility. *Journal of Empirical Finance*, 38:548–574. Recent developments in financial econometrics and empirical finance.
- Harvey, D. I., Leybourne, S. J., and Taylor, A. R. (2009). Unit Root Testing in Practice: Dealing with Uncertainty over the Trend and Initial Condition. *Econometric Theory*, 25(3):587–636.
- Harvey, D. I., Leybourne, S. J., and Taylor, A. R. (2012). Testing for Unit Roots in the Presence of Uncertainty over Both the Trend and Initial Condition. *Journal of Econometrics*, 169(2):188–195. Recent Advances in Nonstationary Time Series: A Festschrift in honor of Peter C.B. Phillips.
- Harvey, D. I., Leybourne, S. J., and Zu, Y. (2019). Testing Explosive Bubbles with Time-varying Volatility. *Econometric Reviews*, 38(10):1131–1151.
- Harvey, D. I., Leybourne, S. J., and Zu, Y. (2020). Sign-Based Unit Root Tests For Explosive Financial Bubbles In The Presence Of Deterministically Time-Varying Volatility. *Econometric Theory*, 36(1):122–169.
- Hodrick, R. J. (1992). Dividend Yields and Expected Stock Returns: Alternative Procedures for Inference and Measurement. *The Review of Financial Studies*, 5(3):357–386.

-
- Homm, U. and Breitung, J. (2012). Testing for Speculative Bubbles in Stock Markets: A Comparison of Alternative Methods. *Journal of Financial Econometrics*, 10(1):198–231.
- Inclán, C. and Tiao, G. C. (1994). Use of Cumulative Sums of Squares for Retrospective Detection of Changes of Variance. *Journal of the American Statistical Association*, 89(427):913–923.
- Jansson, M. and Moreira, M. J. (2006). Optimal Inference in Regression Models with Nearly Integrated Regressors. *Econometrica*, 74(3):681–714.
- Jiang, L., Phillips, P. C., and Yu, J. (2015). New Methodology for Constructing Real Estate Price Indices Applied to the Singapore Residential Market. *Journal of Banking & Finance*, 61:S121–S131. Recent Developments in Financial Econometrics and Applications.
- Keim, D. B. and Stambaugh, R. F. (1986). Predicting Returns in The Stock and Bond Markets. *Journal of Financial Economics*, 17(2):357–390.
- Kim, T.-H., Leybourne, S., and Newbold, P. (2002). Unit Root Tests with a Break in Innovation Variance. *Journal of Econometrics*, 109(2):365–387.
- Kostakis, A., Magdalinos, T., and Stamatogiannis, M. P. (2015). Robust Econometric Inference for Stock Return Predictability. *The Review of Financial Studies*, 28(5):1506–1553.
- Kurozumi, E. (2021). Asymptotic Behavior of Delay Times of Bubble Monitoring Tests. *Journal of Time Series Analysis*, 42(3):314–337.
- Kwiatkowski, D., Phillips, P. C., Schmidt, P., and Shin, Y. (1992). Testing the Null Hypothesis of Stationarity against the Alternative of a Unit Root: How Sure Are We that Economic Time Series have a Unit Root? *Journal of Econometrics*, 54(1):159–178.
- Lanne, M. (2002). Testing the Predictability of Stock Returns. *The Review of Economics and Statistics*, 84(3):407–415.

-
- Lee, J. H. (2016). Predictive Quantile Regression with Persistent Covariates: IVX-QR Approach. *Journal of Econometrics*, 192(1):105–118.
- LeRoy, S. F. and Porter, R. D. (1981). The Present-Value Relation: Tests Based on Implied Variance Bounds. *Econometrica*, 49(3):555–574.
- Lewellen, J. (2004). Predicting Returns with Financial Ratios. *Journal of Financial Economics*, 74(2):209–235.
- McMillan, D. G. and Wohar, M. E. (2011). Structural Breaks in Volatility: The Case of UK Sector Returns. *Applied Financial Economics*, 21(15):1079–1093.
- Meltzer, A. (2002). Rational and Irrational Bubbles. Keynote address for the Federal Reserve Bank of Chicago-World Bank Conference on Asset Price Bubbles. Carnegie Mellon University and the American Enterprise Institute. Url: https://kilthub.cmu.edu/articles/journal_contribution/Rational_and_Irrational_Bubbles/6707615.
- Narayan, P. K. and Smyth, R. (2005). Are OECD Stock Prices Characterized by a Random Walk? Evidence from Sequential trend break and Panel Data Models. *Applied Financial Economics*, 15(8):547–556.
- Nelson, C. R. and Kim, M. J. (1993). Predictable Stock Returns: The Role of Small Sample Bias. *The Journal of Finance*, 48(2):641–661.
- Newey, W. K. and West, K. D. (1987). A Simple, Positive Semi-Definite, Heteroskedasticity and Autocorrelation Consistent Covariance Matrix. *Econometrica*, 55(3):703–708.
- Newey, W. K. and West, K. D. (1994). Automatic Lag Selection in Covariance Matrix Estimation. *The Review of Economic Studies*, 61(4):631–653.
- Ofek, E. and Richardson, M. (2003). DotCom Mania: The Rise and Fall of Internet Stock Prices. *The Journal of Finance*, 58(3):1113–1137.

-
- Pan, W.-F. (2018). Sentiment and Asset Price Bubble in the Precious Metals Markets. *Finance Research Letters*, 26:106–111.
- Pavlidis, E., Yusupova, A., Paya, I., Peel, D., Martínez-García, E., Mack, A., and Grossman, V. (2016). Episodes of Exuberance in Housing Markets: In Search of the Smoking Gun. *The Journal of Real Estate Finance and Economics*, 53(4):419–449.
- Pedersen, T. Q. and Schütte, E. C. M. (2020). Testing for Explosive Bubbles in the Presence of Autocorrelated Innovations. *Journal of Empirical Finance*, 58:207–225.
- Phillips, P. C. and Lee, J. H. (2013). Predictive Regression under Various Degrees of Persistence and Robust Long-horizon Regression. *Journal of Econometrics*, 177(2):250–264. *Dynamic Econometric Modeling and Forecasting*.
- Phillips, P. C. and Shi, S. (2020). Chapter 2 - Real Time Monitoring of Asset Markets: Bubbles and Crises. In Vinod, H. D. and Rao, C., editors, *Financial, Macro and Micro Econometrics Using R*, volume 42 of *Handbook of Statistics*, pages 61–80. Elsevier.
- Phillips, P. C. and Shi, S.-P. (2018). Financial Bubble Implosion and Reverse Regression. *Econometric Theory*, 34(4):705–753.
- Phillips, P. C. B. and Magdalinos, T. (2008). Limit Theory for Explosively Cointegrated Systems. *Econometric Theory*, 24(4):865–887.
- Phillips, P. C. B. and Shi, S. (2019). Detecting Financial Collapse and Ballooning Sovereign Risk. *Oxford Bulletin of Economics and Statistics*, 81(6):1336–1361.
- Phillips, P. C. B., Shi, S., and Yu, J. (2015). Testing for Multiple Bubbles: Historical Episodes of Exuberance and Collapse in the S&P 500. *International Economic Review*, 56(4):1043–1078.
- Phillips, P. C. B. and Solo, V. (1992). Asymptotics for Linear Processes. *The Annals of Statistics*, 20(2):971–1001.

-
- Phillips, P. C. B., Wu, Y., and Yu, J. (2011). Explosive Behavior in the 1990s NASDAQ: When Did Exuberance Escalate Asset Values? *International Economic Review*, 52(1):201–226.
- Phillips, P. C. B. and Yu, J. (2011). Dating the Timeline of Financial Bubbles During the Subprime Crisis. *Quantitative Economics*, 2(3):455–491.
- Rapach, D. E., Strauss, J. K., and Wohar, M. E. (2008). Forecasting Stock Return Volatility in the Presence of Structural Breaks. *Frontiers of Economics and Globalization*, 3:381 – 416.
- Richardson, M. and Smith, T. (1991). Tests of Financial Models in the Presence of Overlapping Observations. *The Review of Financial Studies*, 4(2):227–254.
- Said, S. E. and Dickey, D. A. (1984). Testing for Unit Roots in Autoregressive-Moving Average Models of Unknown Order. *Biometrika*, 71(3):599–607.
- Sansó, A., Aragó, V., and Carrion, J. L. (2003). Testing for Changes in the Unconditional Variance of Financial Time Series. DEA Working Papers 5, Universitat de les Illes Balears, Departament d’Economía Aplicada.
- Sharma, S. and Escobari, D. (2018). Identifying Price Bubble Periods in the Energy Sector. *Energy Economics*, 69:418–429.
- Shi, S. (2017). Speculative Bubbles or Market Fundamentals? An Investigation of US Regional Housing Markets. *Economic Modelling*, 66:101–111.
- Shi, S., Valadkhani, A., Smyth, R., and Vahid, F. (2016). Dating the Timeline of House Price Bubbles in Australian Capital Cities. *Economic Record*, 92(299):590–605.
- Shiller, R. J. (1981). Do Stock Prices Move Too Much to be Justified by Subsequent Changes in Dividends? *The American Economic Review*, 71(3):421–436.
- Stambaugh, R. F. (1999). Predictive Regressions. *Journal of Financial Economics*, 54(3):375–421.

-
- Stock, J. H. (1991). Confidence Intervals for the Largest Autoregressive Root in U.S. Macroeconomic Time Series. *Journal of Monetary Economics*, 28(3):435–459.
- Tirole, J. (1982). On the Possibility of Speculation under Rational Expectations. *Econometrica*, 50(5):1163–1181.
- Torous, W., Valkanov, R., and Yan, S. (2004). On Predicting Stock Returns with Nearly Integrated Explanatory Variables. *The Journal of Business*, 77(4):937–966.
- Tsvetanov, D., Coakley, J., and Kellard, N. (2016). Bubbling Over! The Behaviour of Oil Futures along the Yield Curve. *Journal of Empirical Finance*, 38:516–533. Recent developments in financial econometrics and empirical finance.
- Welch, I. and Goyal, A. (2008). A Comprehensive Look at the Empirical Performance of Equity Premium Prediction. *The Review of Financial Studies*, 21(4):1455–1508.
- West, K. D. (1987). A Specification Test for Speculative Bubbles. *The Quarterly Journal of Economics*, 102(3):553–580.
- Whitehouse, E. J. (2019). Explosive Asset Price Bubble Detection with Unknown Bubble Length and Initial Condition. *Oxford Bulletin of Economics and Statistics*, 81(1):20–41.
- Xu, K. (2015). Testing for Structural Change under Non-stationary Variances. *The Econometrics Journal*, 18(2):274–305.
- Xu, K.-L. and Guo, J. (2022). A New Test for Multiple Predictive Regression*. *Journal of Financial Econometrics*. nbac030.
- Xu, K.-L. and Phillips, P. C. (2008). Adaptive Estimation of Autoregressive Models with Time-varying Variances. *Journal of Econometrics*, 142(1):265–280.
- Yang, B., Long, W., and Yang, Z. (2022). Testing Predictability of Stock Returns under Possible Bubbles. *Journal of Empirical Finance*, 68:246–260.

Yiu, M. S., Yu, J., and Jin, L. (2013). Detecting Bubbles in Hong Kong Residential Property Market. *Journal of Asian Economics*, 28:115–124. ACAES-FEG Special Issue: Econometrics of Financial Markets in Asia.

Zhao, Y., Chang, H.-L., Su, C.-W., and Nian, R. (2015). Gold Bubbles: When are They Most Likely to Occur? *Japan and the World Economy*, 34-35:17–23.

Zivot, E. and Andrews, D. W. K. (1992). Further Evidence on the Great Crash, the Oil-Price Shock, and the Unit-Root Hypothesis. *Journal of Business & Economic Statistics*, 10(3):251–270.